Understanding the Development of MLL-Rearranged Leukemias:

Developing disease models

ROSHANI SINHA

Doctoral Thesis 2016 UPF

THESIS DIRECTOR:

Dr. Anna Bigas Salvans

THESIS CO-DIRECTOR:

Dr. Cristina Porcheri

Cancer and Stem Cell Research Group

Institut Hospital del Mar d'Investigacions Mèdiques

DEDICATION

My thesis is dedicated to my Mother Shashi, Sister Pavitra, Father Gaurav and my Partner Amit. They are my biggest blessing in life and without them none of this would be possible.

And to leukemia patients and their families all over the world. I'm forever inspired to make a difference in their lives for the better.

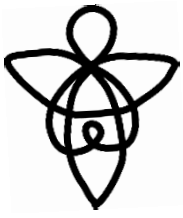

ACKNOWLEDGEMENTS

ACKNOWLEDGEMENTS

There are many people I'd like to acknowledge for the parts they have played in either my scientific or personal life especially in the past four years of my doctoral research. I am most grateful to my mother Shashi (Mimmidus), my sister Pavitra (Piyu) and my partner Amit (Gaga) for their unconditional love and support. I am equally grateful to my father Gaurav, there isn't a day that goes by when I don't miss him. I am incredibly lucky to have a family that has always been a pillar of strength for me especially these past four years that I have spent away from them. My mother and my sister are undoubtedly the two most formidable women I know. No words will ever be able to express the magnitude of love and respect I have for them. You make me want to be better every day. Without their conviction, encouragement and undying support I wouldn't have been able to pursue my doctoral research. I am also grateful to my partner Amit, for his unconditional love and support. I thank him for always standing by me, propelling me to live life to my full potential and for not only indulging my every dream in life but also nurturing them. I thank my family for sharing their love, wisdom and life with me. And, for always believing in me and my passion for my work and supporting my want of making a positive contribution to science. I'd also like to extend my gratitude to my brother-in-law Bhuwan (peekaboo) who is a part of our family now, for your positivity and light hearted spirit. Thank you to Alka (Mumma) and Laxman (Papa), the parents of my partner Amit, and to my brothers-in-law Pankaj and Paul for all your love, support and encouragement.

Thank you to my supervisors and guides Dr. Anna Bigas, Dr. Lluis Espinosa and Dr. Cristina Porcheri for your guidance and critiques. I have learnt a great many lessons in the past four years about being a good scientist so thank you for that. Cristina, I'll always remember the many lessons you have taught me, some harder to learn for me than others but I am grateful for your brutal honesty and guidance.

Thank you Dr. Antonio Garcia de Herreros, for being the tutor of my doctoral thesis. And to all the principal investigators of the Cancer department at Institut Hospital del Mar d'Investigacions Mèdiques (IMIM) for your inputs and support during department seminars and throughout my doctoral research.

I also want to thank my Master's professor in the UK, Dr. Petros and Prof. Modjtahedi. I am more grateful to you now than ever before for your encouragement during my early days of research. And, for your belief in me. Thank you for all the kind words of support and motivation that you offered to me five years ago.

I want to extend my gratitude to some dear friends of mine back home, Hasan and Sirisha. Hasan, you're my rakhi brother and I do think of you as family. You've always been a well-wisher and you are a wonderful person. I thank you for your duas. Sirisha (Ish!), you are one of my closest friends back home and I thank you for supporting me even from afar and for sharing my joys and sorrows. I cherish you both for who you are as people and for adding beautiful memories to my life.

I am happy to have made many friends during the course of my doctoral research in Barcelona, some of them I have had the great pleasure of working with. Marta Rebull and Cristina Rius, you are two of my dearest

friends, I love and adore both of you very much. I thank you for your many pick-me-ups at our little coffee breaks, and for the many moments of laughter and fun that we have shared together. Marta you're one of the kindest and most honest people I have ever had the pleasure of meeting. You are a special person and I admire and respect your generosity of spirit. Thank you for being a big part of my doctoral journey and for giving me advice that made me a better scientist but above that a better person. I wish you nothing but joy for all the new adventures in life that await you. Cris! You have always understood me and managed to lift my spirits by adding joy, spunk and laughter during some hard times I have faced here. I will miss singing backstreet boys songs really loudly and out of pitch with you and all our miriendas and long walks but I am happy just knowing that I have a true friend in you. I wish you the best in your career and much love and joy in life.

Carlos! What can I say? You're one of a kind. You're incredibly funny, humble, kind, quirky, witty and sweet. But the quality I love the most in you is your honesty. You know just how much I love and adore you. It's been a blast hanging with you. You have a friend in me for life.

Bing, Vera and Adrien, I am very happy to have met you during your short-stay in the lab. With my weak Spanish skills, I became quick friends with international students that joined the lab and I am glad that we have continued to be good friends. Bing, you and I have had many things in common based on where we both come from. You are one of the nicest people I've ever met. Thank you for your friendship. Vera and Adrien, you both are truly wonderful people too. I have loved whatever time I could spend with all three of you. I have only fond memories when I think of all three of you and I thank you for that.

A big Thank you also goes out to Eva, Irene, David, Albert and Hector for all the fun times we shared. Eva, you have always supported me and looked out for me and been a very good friend to me through my low points. For that I am always grateful. Thank you all for your kindness and support through several hard times that I have faced in a foreign land. I wish you the best in life. I am happy to have met all of you.

Erika! (I'm tempted to call you Elga), you were my first friend in Spain, even before I stepped on Spanish soil. You've been incredibly sweet to me through these years. You've seen my ups and downs in the lab and always looked out for me and taught me many things. I thank you for offering encouraging words and warm hugs to me on some difficult days and you should know that your kindness has gone a long way in helping me. You're a very good scientist and a lovely person and I can't wait to see the wonderful things you do in future.

Jessica (Jessi to me), my friendship with you has only grown with time and I have much respect for you and your work ethic. You're also one of the nicest people I know. You're patient, kind, selfless and certainly a team player. Working with you has been an absolute pleasure. I thank you for teaching me many things. I will miss having conversations with you not only about work but pretty much everything under the sun.

Cristina Ruiz, I probably haven't shared with you how much I admire you, well here's my chance! You're a lovely, strong, dependable, generous and candid person and I have so much respect for you. Your honesty has meant more to me than you know. Over the years, I have found myself never hesitating to discuss whatever is on my mind with you. Be it qualms about technicalities of an experiment or any troubles I was facing. The credit for that goes to you for making me feel

comfortable and safe to do that so thank you so much for that. You have also taught me many techniques and have also found time to give help whenever and wherever it was needed. In addition to all these things, I thank you for your kindness too.

Julia, you were the lab manager when I joined the lab four years ago and you are sorely missed in the lab by everyone, including myself. It brings a grin to my face when I think about how you would always call me 'Roshina' and I didn't correct you after the first couple of times because you were so sweet and kind and I felt bad about pointing it out. I was happy to go along with it because I didn't mind being Roshina to you. You are a warm, generous and kind hearted person and I have nothing but respect for you in my heart. Ex-members of the lab Mari, Jordi, Leonor, Teresa, Pol, Ricardo and Christos, it was a pleasure to work with you and under your guidance. Jordi and Teresa you have taught me most techniques in the lab and I am thankful to you both. I wish you both the best. Leonor, you're a really good person and I have looked up to you quite a bit. Thank you for sharing your insights with me, you're lovely. Pol, although I have never really had a chance to work directly with you, you've been a wonderful colleague and I want to thank you for helping me with the handful of western blots I did in the lab. Christos, thank you for teaching me many techniques such as FACS and performing transplantations in mice. I will always be thankful to you for that.

It's been a pleasure to have met many people outside of my lab as well, including members of Snail lab, Judith and Miguel (from Yelamos lab) Judith (From Pilar Navarro's lab) and Laura Soria. Budour, your positive attitude is remarkable and I wish you the best in your PhD and

everything else that future hold for you. Thank you all for the laughs, fun and your friendship.

A special thanks to Laura Xicota Vila, you're a dear friend to me. Thank you for your live translations during Spanish lectures that I didn't understand a word of. And for many stimulating conversations and joyful moments we've shared together over the past four years. I'll cherish the many moments I have spent singing with you in the choir as well.

I am thankful to Institut Hospital del Mar d'Investigacions Mèdiques (IMIM) for funding the printing of this thesis. I'd like to especially thank IMIM secretary Silvia for all your help through these four years.

Lastly, I want to thank the inspiring words in the cartoon below that I saw stuck on a cabinet in the lab on my first day at work and it has kept me motivated throughout the past four years.

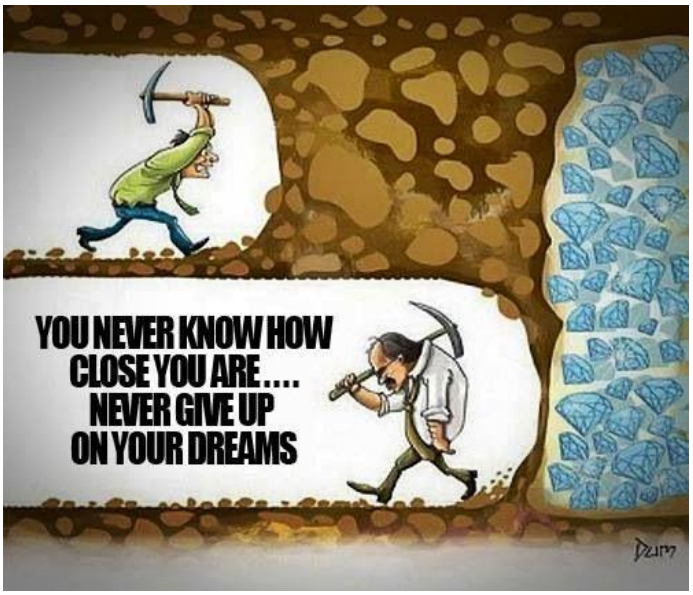

ABSTRACT

ABSTRACT

Rearrangements involving the mixed lineage leukemia gene (MLL) are found in majority of human infant leukemias (>60% of ALLs, 35% of AMLs) and are associated with dismal prognosis of these patients. They are also found in a small percentage of childhood and adult leukemias (10% cases), making MLL-rearranged leukemias ideal for this study. We performed induction of the leukemic MLL-ENL chromosomal translocation in hematopoietic cells at different developmental stages i.e., fetal liver (FL, E12.5) and bone marrow (BM, P60) to develop disease models that can recapitulate human infant and adult leukemias respectively. After evaluating several models to induce MLL-ENL recombination, we have reproducibly obtained leukemia in adult animals with the interferon inducible Mx1-Cre line. The embryonic model of MLL-ENL leukemia was also developed with partial success and it is more aggressive compared to the adult leukemia. In conclusion, we have developed a novel embryonic leukemia model to study infant leukemia ontogeny.

RESUMEN

En la mayoría de las leucemias humanas del lactante (> 60% de los casos de ALL, 35% de los casos de AML), se encuentran reordenamientos relacionados con el gen de la leucemia de linaje mixto (*mixed lineage leukemia*, MLL), que se asocian con un mal pronóstico de estos pacientes. También se encuentran en un pequeño porcentaje de casos de leucemias infantiles y de adultos (10% de casos), por lo que las leucemias con reordenamientos en MLL resultan ideales para este estudio. Hemos realizado la inducción de la translocación cromosómica leucémica MLL-ENL en las células hematopoyéticas en diferentes etapas de desarrollo, en el hígado fetal (*fetal liver*, FL E12.5) y en la médula ósea (*bone marrow*, BM P60), para desarrollar modelos de enfermedades que puedan recapitular las leucemias humanas del lactante y adultas, respectivamente. Después de evaluar varios modelos para inducir la recombinación de MLL-ENL, hemos generado de forma reproducible, leucemia en animales adultos con la línea de Mx1-Cre inducible por interferón. El modelo embrionario de leucemia inducida por MLL-ENL también se desarrolló con éxito parcial y es más agresivo en comparación con la leucemia en adultos. En conclusión, hemos desarrollado un nuevo modelo de leucemia embrionaria para estudiar la ontogenia de la leucemia del lactante.

PREFACE

PREFACE

I have focused my doctoral research on studying leukemias arising in infants that are younger than a year. While it is a rare disease, prognosis of infant leukemia patients is dismal and very little is known about the disease development process. My work is focused on developing mice models of infant and adult leukemias that are driven by a common chromosomal abnormality (MLL-gene rearrangements). These disease models might prove useful in understanding this aggressive disease and in finding targeted therapies to have favorable prognosis of these patients.

I was awarded the FI-AGAUR grant from Generalitat de Catalunya from 2013 to 2016 to pursue my doctoral degree in biomedicine at the University of Pompeu Fabra.

I have conducted my research at the Institut Hospital del Mar d'Investigacions Mèdiques (IMIM) and IMIM has funded the printing of this thesis.

TABLE OF CONTENTS

TABLE OF CONTENTS

Results Part-3

TABLE OF FIGURES

INTRODUCTION

RESULTS PART 1:

Vav1-Cre model of MLL-ENL leukemia

RESULTS PART 2:

β-actin Cre^{ERT} model of MLL-ENL leukemia

STRATEGY I

STRATEGY II

STRATEGY III

RESULTS PART 3:

Mx1-Cre model of MLL-ENL leukemia

Adult model (BM-derived)

Embryonic model (FL-derived)

LIST OF TABLES

INTRODUCTION

MATERIALS & METHODS

RESULTS

ABBREVIATIONS AND ACRONYMS

ABBREVIATIONS AND ACRONYMS

4-OH T	4 hydroxytamoxifen
AF4/AF9	ALL1-fused gene from chromosome 4/9
AGM	Aorta-gonads-mesonephros
ALL	Acute lymphoblastic leukemia
AML	Acute myeloid leukemia
AT-hook	Adenine/Thymine rich region
BM	Bone marrow
BrdU	5-Bromo-2'-deoxyuridine
C	Carboxy terminal
°C	degrees celcius
CAR	CXCL12-abundant reticular cell
CBC	Complete blood count
CD	Cluster of differentiation
CLL	Chronic lymphocytic leukemia
CLP	Common lymphoid progenitor
CML	Chronic myelogenous leukemia
CMP	Common myeloid progenitor
Cre^{ERT}	Tamoxifen-dependent Cre recombinase
CXCL12	Chemokine ligand 12
DAPI	4',6-diamidino-2-phenylindole
DNA	Deoxyribonucleic acid
Dot1l	Disruptor of telomeric silencing 1-like
DotCom	Dot1l-associated complex
dpc	Days post-coitus
E	Embryonic age
e.e	embryo equivalance
EDTA	Ethylenediaminetetraacetic acid
EHT	Endothelial to hematopoietic transition
EMT	Epithelial to mesenchymal transition
ENL	Eleven-nineteen leukemia
ER	Estrogen receptor
ES cells	Embryonic stem cells
FAB	French American British

FACS	Fluorescent-activated cell sorting
FBS	Fetal bovine serum
FITC	Fluorescein isothiocyanate
FL	Fetal liver
GMP	Granulocyte-macrophage progenitor
GVHD	Graft versus host disease
Gy	Gray (unit of radiation)
H3	Histone 3
HC	Hematopoietic cell
HDAC	Histone deacetylase
HOX	Homeobox family of genes
HPC	Hepatic progenitor cell
HSC	Hematopoietic stem cell
IFN	Interferon
IL	Interleukin
IP	Intraperitoneal
Jag1	Jagged1
K4/K79	Lysine 4/79
LIC	Leukemic initiating cell
LMO2	LIM domain only 2
LMPP	Lymphoid-Myeloid primed progenitor
Lox P	Locus of X-over P1 bateriopbhage
LSC	Leukemic stem cell
LT-HSC	Long-term hematopoietic stem cell
MEP	Myeloid-erythroid progenitor
MLL	Mixed lineage leukemia
MSC	Mesenchymal stem cell
Mx1	Myxovirus1
Myc	Avian Myelocytomatosis Viral Oncogene
N	Amino terminal
NK	Natural killer cell
NLL	Normal lower limit
NUL	Normal upper limit
NOD	Non-obsese diabetic
NSG	NOD SCID gamma
OCT	Optimal cutting temperature
P	Postnatal age
PB	Peripheral blood
PBS	Phosphate-buffered saline

PCR	Polymerase chain reaction
PFA	Paraformaldehyde
PolyIC	Polyinosinic-polycytidylic acid
Pre-mNK	Premature natural killer cell
rpm	revolutions per minute
RT	Room temperature
SCID	Severe combined immuno-deficient
SCF	Stem cell factor
SD	Standard deviation
SEC	Super elongation complex
SET	Su(var)3-9 and 'Enhancer of zeste' proteins
ST-HSC	Short-term hematopoietic stem cell
t	Translocation
TP	Transplant recipient
UC	Umbillical cord
VA	Vitelline artery
VV	Vitelline vein
WBC	White blood cell
WHO	World health organization
wt	Wildtype
YFP	Yellow fluorescent protein
YS	Yolk sac

INTRODUCTION

1. HEMATOPOIESIS

1.1. Sites

The knowledge of blood as a vital fluid has existed since ancient times, but the true understanding of its functions as a carrier of oxygen, nutrients and metabolic waste was discovered in the 17th century (Anon 1978).

The pumping of blood from the heart into the body via arteries and its return to the heart from the body via veins with every heartbeat was a concept discovered and described as blood circulation by the physician William Harvey in 1628 (Auffray & Noble 2009). Progress in the understanding of different blood cell components and their functions in the immune system were made thereafter. The discovery of stem cells led to path breaking findings in blood cells development which was poorly understood until then.

Hematopoiesis is the process by which all cellular components of the blood are formed through tightly regulated steps of proliferation and differentiation of hematopoietic stem cells (HSCs). HSCs undergo differentiation to give rise to the lineage-committed progenitors which upon further differentiation can form terminally differentiated blood cells, which are released into blood circulation.

HSCs arise only during gestation in various intra- and extra-embryonic regions (namely, AGM, vitelline arteries, the yolk sac and placenta).

Hematopoiesis occurs in the form of primitive and definitive waves during gestation. The first event in hematopoietic development is termed as the primitive wave of hematopoiesis wherein transient hematopoietic progenitors are found in the extra-embryonic tissue called the yolk sac (YS) at E7[1] in mice (de Jong & Zon 2005).

Blood circulation is initiated in the embryo by E9. Although, in time primitive hematopoietic cells get replaced by definitive cells, defects in primitive hematopoiesis leads to embryonic lethality as early as E10 (Fujiwara et al. 1996). The definitive wave of hematopoiesis marks emergence of definitive HSCs at E10.5-E11, and these HSCs can give rise to all blood cell components throughout adulthood (Lemischka 1991; Spangrude et al. 1991; Cumano & Godin 2007).

The first definitive HSCs emerge in the dorsal aorta within the aorta-gonads-mesonephros (AGM) region at E10.5 (Medvinsky & Dzierzak 1996). Additionally, functional HSCs and hematopoietic progenitors are also found in other sites including the avian allantois (Caprioli et al. 1998), mouse vitelline and umbilical arteries (de Bruijn et al. 2000), and mouse placenta (Alvarez-Silva et al. 2003; Ottersbach & Dzierzak 2005; Gekas et al. 2005). All the hematopoietic stem and progenitor cells from these sites migrate to the fetal liver by E12.5 for HSCs amplification which occurs until E16.5 (North et al. 1999).

[1] Embryologists have described embryonic age (E) in terms of days' post coitus (dpc) (Rugh, 1968; Theiler, 1989; Snell and Stevens, 1966; Kaufman, 1991; 1992)

HSCs then migrate to their ultimate hematopoietic niche, the bone marrow (BM) where they reside and are maintained throughout the adult life (Mikkola & Orkin 2006).

1.1.1. Extra-embryonic sites

The primitive wave of hematopoiesis is detected within the YS at E7, wherein hematopoietic progenitors arise from the vascular endothelial walls of the tissue to form clusters of cells called blood islands (Maximow 1909; Gordon 1972) (Fig. I1). These progenitors give rise to macrophages and large nucleated erythrocytes called 'primitive erythroblasts' by E8.25 (Palis et al. 1999)

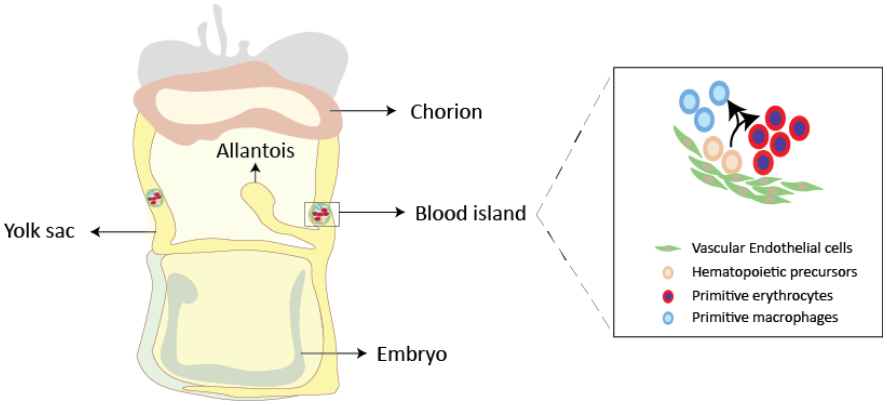

Fig.I 1: Primitive wave of hematopoiesis in the yolk sac blood islands: The primitive wave of hematopoiesis is known to arise in an E7 mouse embryo. The primitive hematopoietic progenitor cells arise within the highly vascularized extra-embryonic YS tissue. The blood islands are found within the YS region adjacent to the allantois. The allantois later gives rise to the umbilical cord. YS blood islands are constituted of vascular endothelial cells and hematopoietic progenitor cells which give rise to primitive erythroblasts and primitive macrophages. YS: yolk sac, E7: embryonic age of 7 (days post-coitus)

The YS is a highly vascularized tissue surrounding the embryo consisting of both endothelial as well as hematopoietic precursors. The hematopoietic precursors produce primitive erythroblasts and macrophages which provide blood circulation to the embryo by E9. These primitive erythrocytes carry the maternal derived oxygen through the embryo body. The multipotent hematopoietic progenitors called EMPs (Erythroid Myeloid Progenitors) found in the YS are a scarce population and have been characterized by the phenotypic markers: $CD45^{low}$ c-kit^{High} $AA4.1^{+}$ by E9 (Jaffredo et al. 2000; Yamasaki et al. 2011). Due to the low number in which these progenitors are found within the YS, studies were conducted to test the multipotency of these cells in-vivo. These cells required a prior clonal expansion in-vitro but they could give rise to all blood cell lineages in-vitro and in-vivo. The endothelial microenvironment in the tissue plays an important role in supporting the emergence of the hematopoietic progenitors (Auerbach et al. 1996).

Apart from the YS, the other extra-embryonic tissue in the developing embryo with hematopoietic activity is the placenta. The placenta (latin for 'flat cake') was first described in the 16^{th} century as a disc that connects the maternal and fetal vasculature. In humans, the fetal blood flow is established by the fourth week of gestation and fully oxygenated blood is transported to the fetus via the placenta through the umbilical arteries (Péault & Tavian 2003).

The placenta has been deemed a site of hematopoietic activity in the developing embryos in mice (and in humans), due to the detection of hematopoietic progenitors at E8.5-9 and that of functional HSCs by E10.5-11(Alvarez-Silva et al. 2003). HSCs and progenitors were found

to reside in the mesodermal-derived allantois region of the placenta, which generates the fetal vasculature (Caprioli et al. 1998; Ottersbach & Dzierzak 2005; Zeigler et al. 2006) (Fig. I2).

It was thought that, as a highly vascularized and growth factor rich extra-embryonic tissue, the placenta would be an able niche for supporting HSCs and their expansion, but it is unknown whether HSCs originate there.

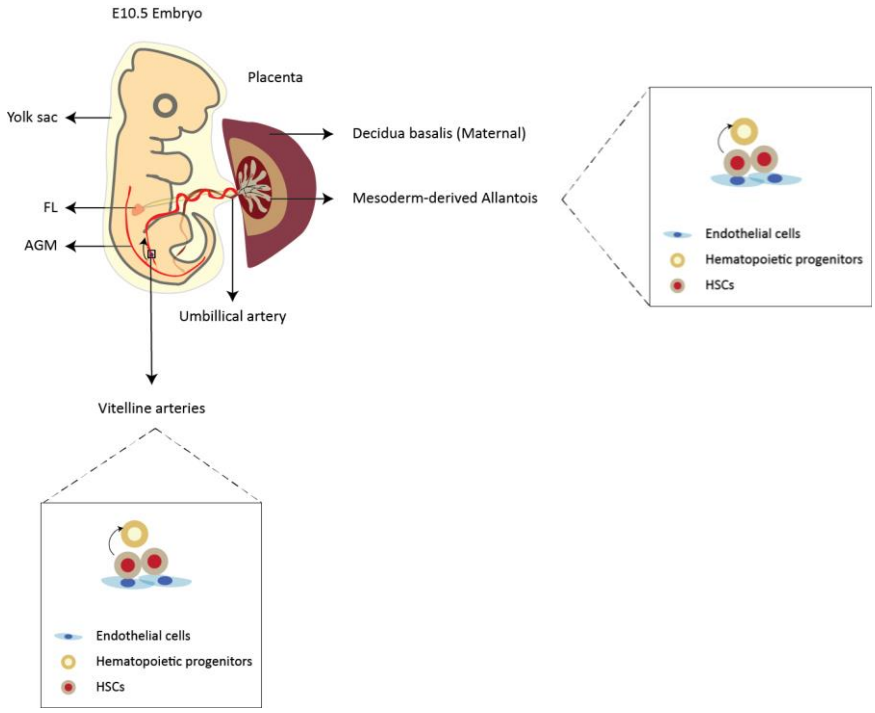

Fig.I 2: Hematopoiesis in placenta and vitelline arteries: HSCs and progenitors are found in the mesoderm derived allantois in the placenta at E10.5 and in VA connected to the AGM. HSCs: Hematopoietic stem cells, E10.5: embryonic age of 10.5 (days post-coitus), VA: vitelline arteries, AGM: aorta-gonads-mesonephros

Studies support the finding that emergence of the first definitive HSCs occurs in the aorta-gonads-mesonephros (AGM) region in the caudal

part of embryo proper at E10.5-11 (Medvinsky & Dzierzak 1996). In humans it is clear that HSCs first arise in the AGM. However, in mice the origin of HSCs is a bit controversial as a recent study described HSC potential in the placenta as well (Pereira et al. 2016).

Next, the HSCs migrate to the fetal liver via the placenta through fetal blood circulation. Although AGM might be the only region for definitive HSCs emergence, hematopoietic progenitors and HSCs found in mouse placenta at E10.5 have been demonstrated to be functionally competent. Moreover, there is an expansion of the HSCs in the placenta by E12.5-E13 which is 15-fold higher than the number of HSCs found in either the AGM or the extra-embryonic yolk sac (YS) at that stage (Gekas et al. 2005). This suggested the competence of placenta microenvironment as an HSC niche in the fetus to amplify and maintain HSC pool.

The HSC-rich population within the placenta is characterized by cells expressing $CD31^{+}CD34^{+}$ c-Kit^{+} $CD150^{-}CD48^{-}$ surface markers. At E12 this population was transplantable and gave rise to all different blood lineages in the recipient mice. This suggested that the placenta consists of a population more immature than the $CD150^{+}CD48^{-}$ HSC population found in the fetal liver (McKinney-Freeman et al. 2009).

This was confirmed in hematopoietic development in human embryos as well, wherein placenta is found to bear $CD34^{+}$ functional HSCs at as early as 9 weeks of gestation, and they are found throughout embryonic development (Robin et al. 2009). Once it was established that HSCs were found in multiple intra- and extra-embryonic regions during stages E10.5-11 i.e., in the AGM and placenta respectively (Kumaravelu et al.

2002), further studies were done to explore the other anatomical regions during these early stages of gestation.

Definitive HSCs were found within the umbilical cord at E11, HSC-containing cluster-like structures were found in the vitelline arteries (VA) that are connected to the AGM by E10.5, and in the pair of vitelline veins (VV) that are connected to the fetal liver (de Bruijn et al. 2000; Gordon-Keylock et al. 2013) (Fig. I2).

Transplantation of HSCs taken selectively from the VA and VV was performed in adult irradiated recipients. Only the HSCs from VA showed long term repopulation capability and not those from the VV region. The origin of these HSCs found in VA is still under debate. The frequency of these definitive HSCs found in the VA, characterized as VE-Cadherine^{+}CD45^{+} cells, are far lower than those found in the AGM region at the same stage E10.5 (Gordon-Keylock et al. 2013).

1.1.2. Aorta-Gonads-Mesonephros

Major source of HSCs and progenitors during embryonic development is the ventral part of the aorta, the largest artery (Medvinsky et al. 1993; Godin et al. 1993; Müller et al. 1994; Dzierzak 2002). The aorta-gonads-mesonephros (AGM) region is formed from the mesodermal germ layer that is in close interaction with the endoderm (Tam & Behringer 1997). The appearance of paired aortas is first observed at E8 (Rugh, 1968). They eventually merge to form the single dorsal aorta by E9 (Kaufman 1994; Garcia-Porrero et al. 1995), at which point connection to the placenta is established via vitelline arteries.

The first definitive HSCs arise from the hemogenic-endothelium that lines the dorsal aorta at E10.5 in the form of budding clusters via a process of endothelial to hematopoietic transition (EHT) (Gama-Norton et al. 2015; Zhen et al. 2013; Zhang et al. 2015) (Fig, I3).

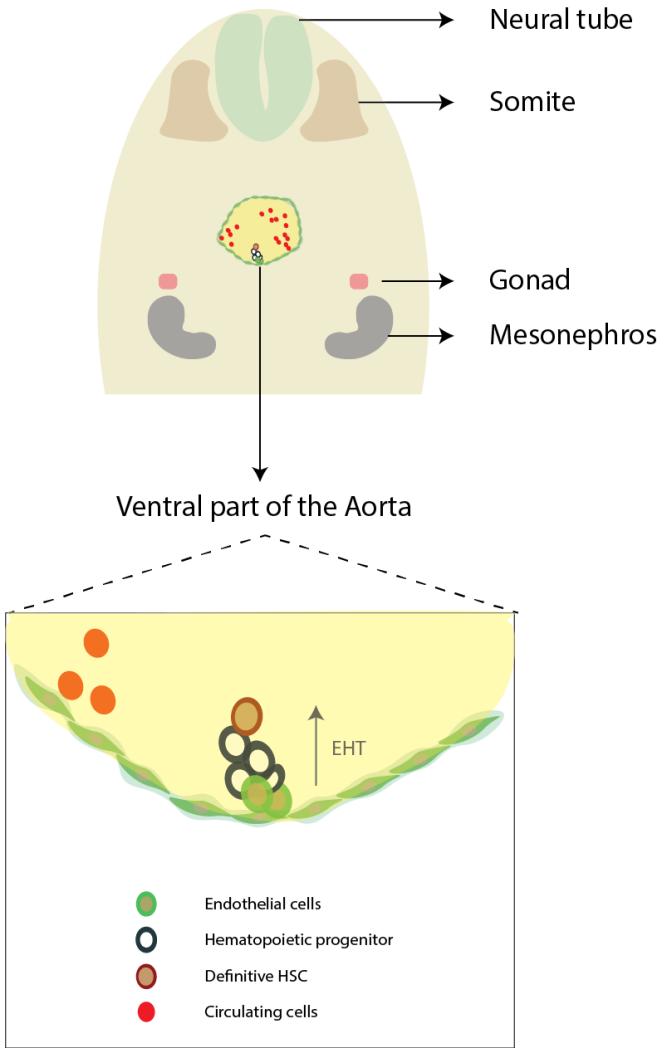

Fig.I 3: Definitive hematopoiesis in AGM: Upper panel: A transversal section of the AGM region is shown. Lower panel: Magnification of the ventral part of dorsal aorta is shown. The first definitive HSCs emerge from the hemogenic endothelium of the dorsal aorta at E10.5 in mice embryos through EHT process. AGM: aorta-gonads-mesonephros, EHT: endothelial to hematopoietic transition, HSCs: hematopoietic stem cells, E10.5: embryonic age of 10.5 (days post-coitus)

This process is regulated by the activation of Notch signaling pathway upon the interaction of the Jag1 ligand with the Notch1 receptor in a cell-cell contact dependent manner (Gama-Norton et al. 2015; Robert-Moreno et al. 2005; Robert-Moreno et al. 2008).

The populations undergoing EHT give rise to HSCs within the 'budding cluster-like' structures. The cells within these clusters have been characterized by the surface markers CD31 and VE-Cadherin (markers of endothelial cells), c-Kit, CD41 and CD201-EPCR (pan-hematopoietic markers) and sca1 and CD45 (markers of definitive hematopoietic cells).

The AGM-derived HSCs were functional and could repopulate a lethally irradiated mouse (Kumaravelu et al. 2002; Medvinsky & Dzierzak 1996). Explant cultures and repopulation studies in mice showed long-term multilineage reconstitution potential of only the intraembryonic para-aortic splanchnopleura (PSp)-AGM tissue and not of hematopoietic precursors found in the YS prior to the onset of circulation (Cumano et al. 2001). The multilineage potential of the early intraembryonic stem cells was also shown by studies done in allogeneic chick yolk-sac-embryo chimeras (Lassila et al. 1982). The early chicken yolk sac produced only transient erythroid stem cells, whereas the intraembryonic stem cells could produce definitive erythrocytes, T- and B-lymphocytes.

1.1.3. Fetal Liver

The pre- and definitive HSCs found in the different regions of a developing embryo including AGM, VA, YS and placenta migrate to the fetal liver (FL) via circulation by E12.5 in mice which remains the main site of HSCs amplification until E16.5. This was demonstrated by Runx1 labelling of cells, since the expression of this gene is found in HSCs (North et al. 1999; North et al. 2002; Jaffredo et al. 2003).

The first hematopoietic progenitor cells to reach the fetal liver by E12.5 arrive from the YS blood islands via vitelline veins through blood circulation (Samokhvalov et al. 2007). This is followed by the hematopoietic cells containing HSC activity from AGM, placenta and vitelline arteries (Cumano & Godin 2007).

There is a 38-fold increase in HSCs with competitive repopulation capacity in FL tissue by E16 when compared to FL cells at E12.5 (Ema & Nakauchi 2000). Although the HSCs were found to be enriched within the $Thy^{low}Sca\text{-}1^{+}lineage^{-}Mac\text{-}1^{+}$ population, the use of SLAM markers helped define a purer population of HSCs in the FL i.e., $CD150^{+}CD48^{-}Sca\text{-}1^{+}lineage^{-}Mac\text{-}1^{+}$ (Kim et al. 2006).

Fetal liver microenvironment is known to not only support the expansion of HSCs but also differentiation of some of the HSCs into progenitors, making FL the primary site of hematopoietic expansion in the embryo (Fig. I4). The lymphoid as well as myelo-erythroid progenitors are known to arise in the liver (Mikkola & Orkin 2006).

The stromal cells of the FL exhibiting epithelial to mesenchymal transition (EMT) are known to enhance interaction of HSCs and provide hematopoietic supportive capacity (Chagraoui et al. 2003). Other types of stromal cells found in the fetal liver include the Nestin^{+} hepatic progenitor cells (HPCs) that have been found to enhance HSC maintenance and expansion in-vitro (Moore et al. 1997; Chou & Lodish 2010).

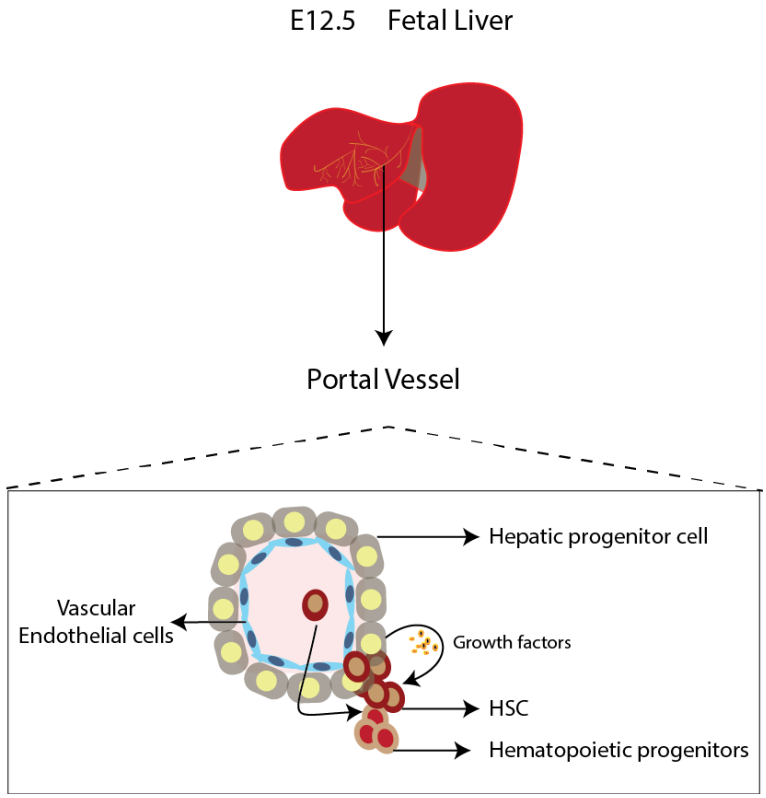

Fig.I 4: Fetal Liver hematopoiesis: HSCs migrate from other hematopoietic sites such as the AGM, placenta, YS and VA to the fetal liver by E12.5 in mice embryos. Here the HSCs undergo expansion and differentiate to form more committed progenitors. The HSCs arrive via the portal vessels in to the liver which provides a conducive niche for HSC expansion and differentiation. Hepatic progenitor cells adjacent to the vascular endothelial cells provide growth factors necessary for HSCs expansion in this tissue from E12.5-16.5. HSCs: Hematopoietic stem cells, FL: fetal liver, AGM: aorta-gonads-mesonephros, YS: yolk sac, VA: vitelline arteries, E12.5: embryonic age of 12.5 (days post-coitus)

It was found in E15 FL that a proportion (about 2%) of hepatic progenitor cells expressing $SCF^{+}DLK1^{+}$ were able to secrete all the cytokines required for HSCs expansion, demonstrating the supportive role of FL microenvironment in hematopoiesis (Chou & Lodish 2010).

Arterial portal vessels are the second HSC supportive niche in the fetal liver. Stromal niche cells are found adjacent to the FL arterial vasculature which provide growth factors that enhance HSCs expansion in this niche (Hahn et al. 2005; Khan et al. 2016) (Fig. I4). Arterial portal vessels are a critical and an integral part of all of the different hematopoietic niches, and they provide an adaptive niche for HSCs.

1.1.4. Fetal and Adult bone marrow

The fetal liver provides a supporting niche for HSCs expansion until E16.5 after which they migrate to the fetal bone marrow (BM) until birth (Göthert et al. 2005) (Fig. I5). The fetal bone marrow development occurs by E15-15.5 with osteogenesis, vascularization of the primordium and mineralization to provide stroma derived factors, which are enablers for proper homing of HSCs (Mackie et al. 2008; Zou et al. 1998; Adams et al. 2007). Postnatally, bone marrow continues to be the niche of HSCs maintenance throughout adult life (Mikkola & Orkin 2006).

It has been noted that HSCs in AGM, YS and placenta arise from or localize near specialized vascular endothelial cells and the HSCs found in the bone marrow are also found to reside in the trabecular region of the femur and tibia (Hirschi 2012) (Fig. I6).

These HSCs reside adjacent to two distinct niches that support their survival and proliferation (Kunisaki et al. 2013). The niches are:

1. Perivascular niche constituted of sinusoidal endothelial cells, perivascular cells; and
2. Endosteal niche constituted of the stromal components including osteoblasts derived from mesenchymal stem cells (MSCs), adipocytes and reticular cells.

The cells of the endosteal niche secrete chemokines and growth factors (such as CXCL2, a chemokine factor required for HSC homing) that support the quiescent state of HSCs (Wright et al. 2002; Zhang et al. 2003; Taichman 2005).

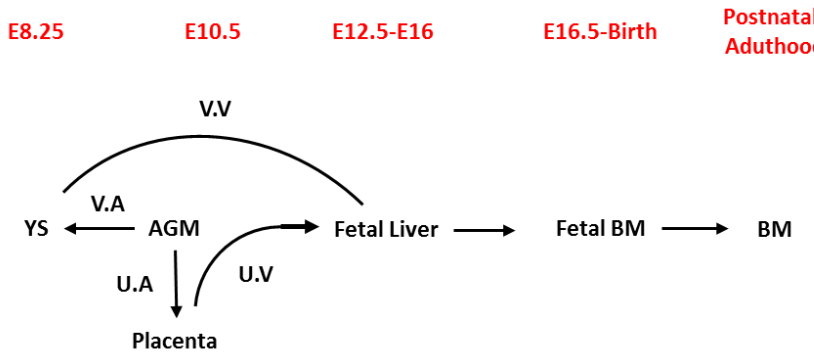

Fig.I 5: Hematopoietic development in multiple sites of a mouse embryo: HSCs and hematopoietic progenitors arising at multiple intra- and extra-embryonic regions during gestation migrate to the FL for HSCs amplification and finally reside in the BM. Primitive hematopoietic cells from E8 YS, definitive HSCs and progenitors from E10.5-E11 AGMs, VA and placenta form the HSC pool which is then amplified from E12.5-E16.5 in the FL. Postnatally, BM maintains this HSC pool and all the distinct blood cell components are formed through regulated proliferation and differentiation steps. YS: yolk sac, VA: vitelline arteries, VV: vitelline veins, UA: umbilical artery, UV: umbilical veins, AGM: aorta-gonads-mesonephros, FL: fetal liver, BM: bone marrow, E: embryonic age (days post-coitus), HSC: hematopoietic stem cell

Loss of function studies highlighted the importance of both niches in the fetal bone marrow (Coşkun et al. 2014). The vasculature is important for production of multi-lineage hematopoietic progenitors, and the osteoblastic niche plays a role in the maintenance of long term repopulation capacity of HSCs in the fetal bone marrow (Coşkun et al. 2014). Transcriptional regulators (such as c-Myc) and repressors (such as Bmi1, Tel/Etv6) that are dispensable for embryonic hematopoiesis become essential in the maintenance of adult HSCs (Wilson et al. 2004; Hock et al. 2004; Park et al. 2003).

HSCs in the fetal bone marrow are found to be cycling until 1 week post birth (Bowie et al. 2006). However, in the adult bone marrow niche, majority of the HSCs stop diving and become quiescent (75% are in G0 phase and only 10% in the S phase of cell cycle) (Cheshier et al. 1999; Wilson et al. 2007).

Within the BM, HSCs are required to proliferate to maintain the HSC poo and differentiate to give rise to all blood cell lineages. These two functions are tightly regulated by cell intrinsic and extrinsic signals provided by the niches.

Specifically, the Notch pathway regulates hematopoiesis in distinct ways during embryonic and adult hematopoiesis. Notch signaling is found to be crucial during mid-gestation for definitive HSC emergence, however it is found to be dispensable by E12.5 stage in mice embryos and its role in maintenance of adult HSCs maintenance in the BM is not clear (Bigas et al. 2012; Maillard et al. 2008).

The definitive HSCs found in the pre-natal or fetal bone marrow by E16.5 have been identified by the same markers as those found in the

adult bone marrow i.e., they express lineage$^-$ sca1$^+$c-Kit$^+$ markers, and are so termed as the LSK population (Morrison et al. 1994). The exact position where LSK HSCs reside in the fetal BM is still debated. The BM HSCs have been further characterized as LSK CD41$^-$CD48$^-$ CD150$^+$ by gaining the SLAM marker CD150 (Kim et al. 2006).

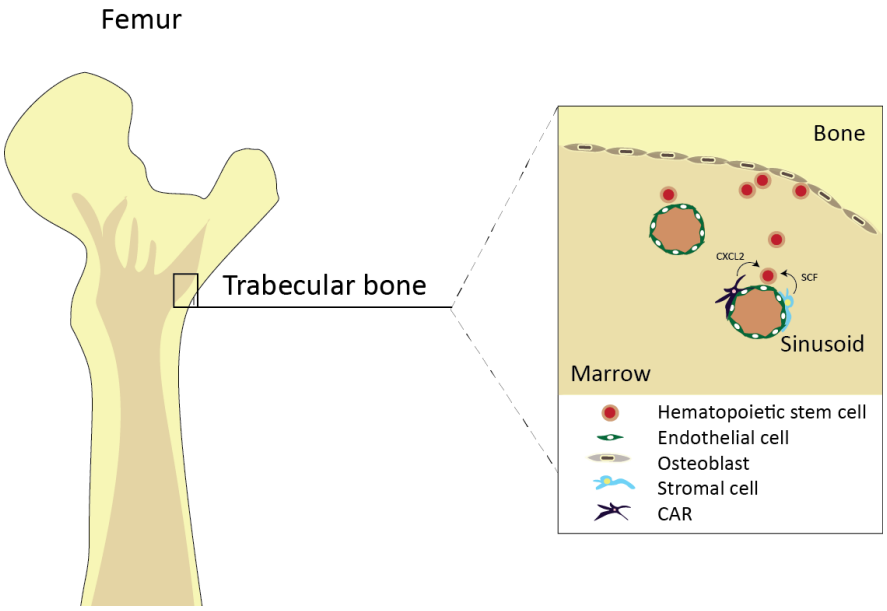

Fig.I 6: Hematopoietic niche in the bone marrow: HSCs reside within the marrow of the trabecular bone. Bone marrow is a highly complex tissue that provides a conducive microenvironment for maintenance of HSCs. The marrow is a highly vascularized tissue and HSCs are largely found adjacent to the sinusoids (blood vessels). MSC-derived cells such as CARs or pericytes and stromal cells provide growth factors (such as SCF, CXCL2) that influence the self-renewal, proliferation and differentiation aspects of HSCs. HSC: hematopoietic stem cell, MSC: mesenchymal stem cell, CAR: CXCL12-adundant reticular cell, SCF: stem cell factor, CXCL2: chemokine ligand 12.

In summary, hematopoiesis is a complex process involving multiple sites that provide conducive microenvironments for emergence, amplification and maintenance of HSCs.

To summarize, HSCs and hematopoietic progenitors arise during embryonic life from E7-E10.5 in the YS, AGM, placenta and VA regions during gestation. HSCs are no longer formed postnatally, so their pool is amplified within the FL until E16.5 after which they relocate to their ultimate niche i.e., the BM. Maintenance of HSCs occurs in the specialized bone marrow niche, throughout adult life.

1.2. Hierarchy of hematopoietic cells development

HSCs have self-renewal ability and multi lineage differentiation potential. Fate determining steps regulate HSCs differentiation to give rise to distinct hematopoietic progenitor cells (Wilson & Trumpp 2006). These committed progenitors can further give rise to the distinct blood cell lineages (Fig. I7). The terminally differentiated cells formed in this manner have reduced self-renewal and proliferation capacities.

HSCs are multipotent cells and are divided into two types, the long-term HSCs (LT-HSCs) and short-term HSCs (ST-HSCs). LT-HSCs have long term proliferation potential and are the most primitive HSCs.

The evidence of long term repopulation and clonogenic capacity of the LT-HSCs was first described in 1961 (Till & Mcculloch 1961). Transplantation of normal whole BM cells was conducted into adult lethally irradiated recipient mice. Engrafted cells formed colonies in spleens of the recipient mice by 11th day post-transplantation. These cells were referred to as "colony forming units". This method was described for studying the long term proliferation and repopulation ability of this very minor LT-HSC population in the bone marrow.

Short term HSCs (ST-HSCs) were later defined as a population that had more 'pluripotent progenitor like' properties when compared to LT-HSCs. This was due to the limited capacity of these cells to regenerate only the lymphoid and myeloid populations upon reconstitution (Kondo et al. 2003; Weissman & Shizuru 2008).

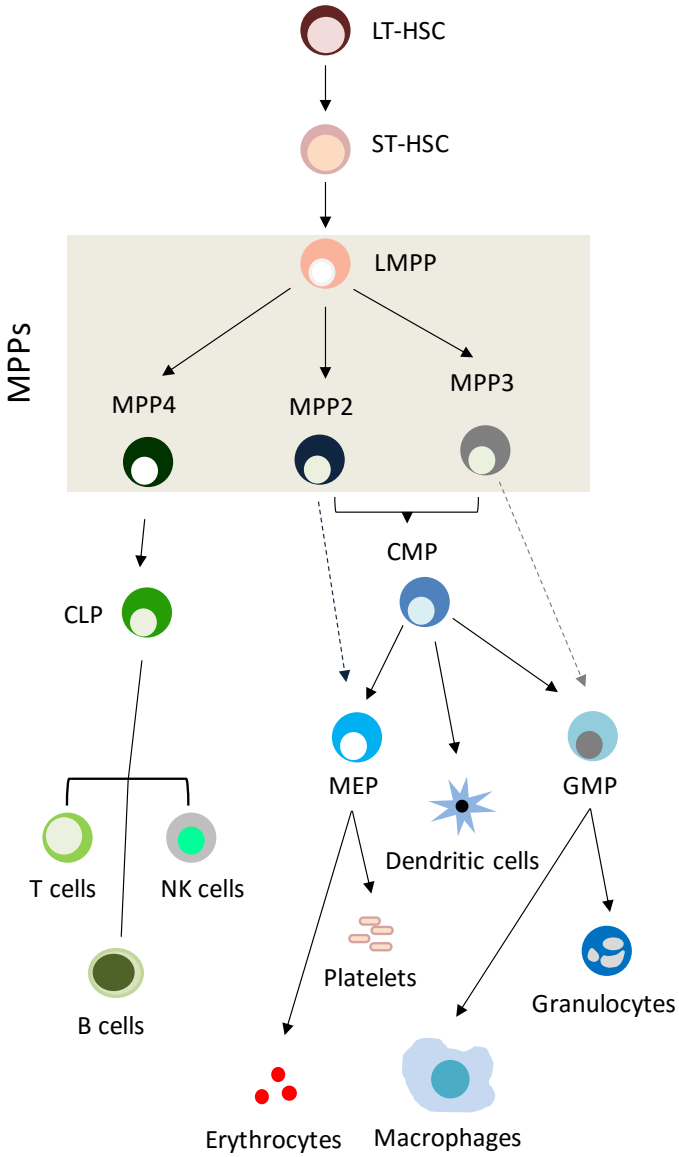

Fig.I 7: The Hierarchy of hematopoietic cells: Hematopoiesis occurs though tightly regulated proliferation and differentiation steps. The multipotent hematopoietic stem cells (LT-HSCs) maintain the HSC pool in bone marrow and give rise to the multipotent progenitors (LMPPs) which divide to give rise to either CMP or CLP cells. Lineage-primed progenitors produce terminally differentiated myeloid cells, lymphocytes and erythrocytes. HSC: hematopoietic stem cell, LT: Long-term, ST: Short-term; LMPP: lymphoid-myeloid primed progenitors; CLP: common lymphoid progenitor, CMP: common myeloid progenitor, GMP: granulocyte-macrophage progenitor, MEP: megakaryocyte-erythroid progenitor. MPP2,3,4: subsets of multipotent progenitors adapted in the scheme based on data from (Pietras et al. 2015)

Table1: Phenotypic characterization of human & murine hematopoietic cells:

	Mouse	Human
LT-HSC	LSK $CD150^{+}CD48^{-}$ $CD34^{+}CD135^{-}CD34$-Flk2-	$Lin^{-}CD34^{+}CD38^{-}$ $CD49f^{+}CD90^{low}$ $CD45RA^{-}$
ST-HSC	LSK Flk2-CD150-CD48-	
MPP2	LSK Flk2-CD150+CD48+	-
MPP3	LSK Flk2-CD150-CD48+	
MPP4	LSK Flk2+CD150-CD48+	
LMPP	LSK $CD150^{-}CD48^{-}$ $CD34^{hi}CD135^{+}CD34^{+}Flk2^{+}$	$Lin^{-}CD34^{+}CD38^{+}CD49f^{-}CD90^{-}$ $CD45RA^{-}$
CLP	LSK $Flk2^{+}IL7R\alpha^{+}$	$Lin^{-}CD34^{+}CD38^{+}$ $CD10^{+}$
CMP	Lin-$Sca^{-}c\text{-}Kit^{+}Thy1^{-}IL7R\alpha^{-}$ $Fc\gamma RI^{lo}CD34^{+}CD16/32^{mid}$	$Lin^{-}CD34^{+}CD38^{+}CD45RA^{-}$ $IL3R\alpha^{lo}$
GMP	Lin-$Sca^{-}c\text{-}Kit^{+}Thy1^{-}IL7R\alpha^{-}$ $Fc\gamma RI^{hi}CD34^{+}$	$CD34^{+}CD38^{+}CD45RA^{+}IL3R\alpha^{+}$
MEP	Lin-$Sca^{-}c\text{-}Kit^{+}Thy1^{-}IL7R\alpha^{-}$ $Fc\gamma RI^{lo}CD34^{-}$	$CD34^{+}CD38^{+}CD45RA^{-}$

The multipotent progenitor cells (MPPs) derived from HSCs are a heterogeneous population and they have recently been described as pre-progenitors that are partially committed to one fate at a much earlier stage (Paul et al. 2015; Osawa et al. 1996; Seita & Weissman 2010). MPPs have been further characterized into three subsets MPP2, MPP3 and MPP4, based on their functions in lineage specification (Pietras et al. 2015). MPPs 2 and 3 enhance production of GMPs with MPP2s being more megakaryocyte-biased and MPP3 are more granulocyte-macrophage-biased. The MPP4s are more lymphoid-primed progenitors. These cells have the potential to give rise to oligo-potent progenitors that are either lymphoid lineage primed (CLPs) or myeloid lineage primed (CMPs) (Kondo et al. 1997; Karsunky et al. 2008; Serwold et al. 2009; Akashi et al. 2000). The CLPs produce T- and B-lymphocytes as well as natural killer cells (Akashi et al. 2000). While CMPs can give rise to all the different forms of myeloid colonies in clonogenic assays, the MEPs and GMPs have restricted ability to give

rise to Erythroid/megakaryocyte and Macrophage/Granulocyte cells (Eosinophils, basophils, neutrophils) respectively (Iwasaki et al. 2005; Arinobu et al. 2005) (Fig. I7). Fate determination of HSCs occurs upon cell division, to give rise to differentiated progenitors through cell intrinsic or extrinsic signals. Wherein, lineage specific genes get activated along with silencing of lineage-unspecific genes.

Distinct transcriptional regulators enable cell fate decisions to produce differentiated cells while also enabling HSC pool maintenance. Transcription factors such as Cebpα, C-myb (CCAAT-enhancer binding protein alpha) are known to be necessary for production of GMPs and for its transition to CMPs but not for MEPs production (Zhang et al. 1997; Zhang et al. 1999; Zhang et al. 2004; Rosenbauer & Tenen 2007; Lieu & Reddy 2012). PU.1 is found to be necessary for both maintenance and differentiation of HSCs (Dakic et al. 2005; Mak et al. 2011). Whereas, Hmbg3 (High mobility group binding protein) is dispensable for HSCs maintenance, but essential for the production of CLPs and CMPs (Nemeth et al. 2006). In contrast, GATA1 is required for MEP production as opposed to CML or CLP production (Morceau et al. 2004; Bresnick et al. 2010). Furthermore, IL7R (Interleukin 7 receptor) is found to be upregulated in CLP cells which is required for the development of lymphocytes (Akashi et al. 2000).

In this manner, it has been demonstrated that tightly regulated network of certain important genes, some of which are mentioned above, decide the fate of HSCs. The expression of such genes, at distinct stages in the hierarchy, and at the optimal levels are required to properly regulate lineage commitment and maintain the HSCs pool (Laslo et al. 2008; Fiedler & Brunner 2012).

2. LEUKEMIA

Leukemia is a disorder of the hematopoietic system, characterized by an increased proliferation of leucocytes or blasts (white blood cells) in the bone marrow. It is known to be a heterogeneous disease.

The disease was described for the first time by the ancient Greeks in as early as the 4th century B.C (Greaves 2000). However, it wasn't until the 19th century that physicians officially described leukemia for the very first time. The physicians Marie Francois Xavier Bichat, Alfred Velpeau, Alfred Donné, John Bennett, and Rudolf Virchow shared their unique understandings of the disease (Fig. I8). The observations they gathered from patient cases helped uncover the imbalance they found between the normally occurring white and red blood cells in the disease. High white blood cells found in these patients led to it being termed as "weisses blut" (German for "white blood").

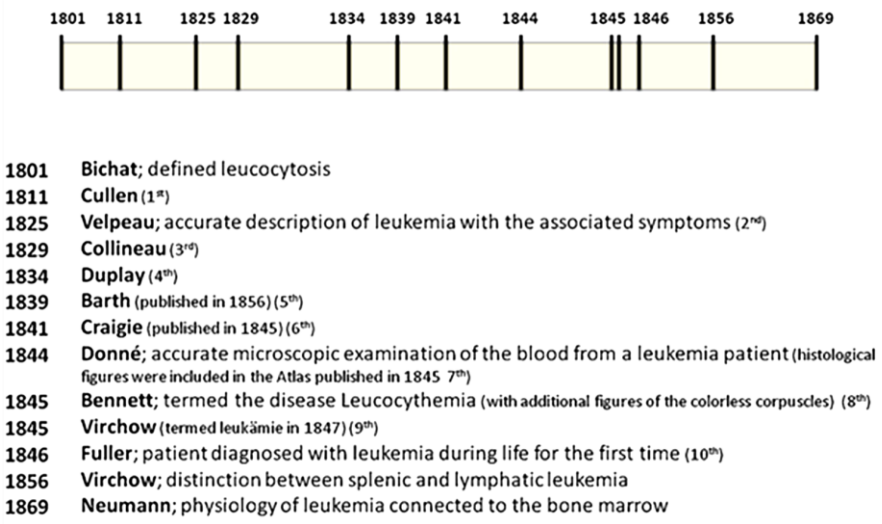

Fig.I 8: Historical overview of the understanding of leukemia (Kampen 2012)

The condition was later termed as 'leukamie' by Virchow in 1847, who described lymphatic leukemia after examining a few patient cases (Kampen 2012).

The understanding of leukemia has continued to evolve ever since. This has been possible through development of cytogenetic and molecular genetic techniques within the past two centuries, since the discovery of the disease. Various genetic abnormalities are known to be implicated in specific subtypes of leukemias. Characterization of leukemia by these means has aided in a better understanding of the disease and in finding suitable therapies.

2.1. Classification of leukemias:

Leukemias have been broadly classified into Chronic and Acute subtypes, by the World Health Organization (WHO) based on clinical and pathological analysis. These two subtypes largely differ in the latency of disease development and leukemic cell maturity.
Based on the clinical and biological characteristics, leukemias are further subdivided into Chronic Myelogenous Leukemia (CML), Chronic Lymphocytic Leukemia (CLL), Acute Myeloid Leukemia (AML), Acute Lymphoblastic Leukemia (ALL). This classification was based on the lineage-bias of leukemic blasts found in the disease.

2.1.1. Chronic Leukemias

The accumulation of leukemic blasts in chronic leukemias occurs over a long period of time, it can take up to many years before the patients start to present symptoms of the disease and need treatment. General symptoms observed include hemorrhages, anemia-related symptoms, easy bruising, purpura, petechiae. The diagnosis is often made during routine checkups as the disease can be quite asymptomatic. The blasts in chronic leukemias consist of lineage-committed/mature but irregular white blood cells. There are two major subtypes:

2.1.1.1. Chronic Lymphocytic Leukemia (CLL)

CLL arises as a result of accumulation of lymphocytes that become functionally incompetent. CLL can exist in one of two forms in a patient. The majority of cases (> 95%) are B-cell CLL having an increased number of irregular B cell blasts (Byrd 2015). Only a very small percentage of the patients have T-cell CLL. In both cases though, the disease is monoclonal.

2.1.1.2. Chronic Myelogenous Leukemia (CML)

This disease is more commonly found in adults > 45 years of age and it is more common in men than women. It accounts for 14% of all leukemias and up to 20% of adult leukemias (Faderl et al. 1999). Though it can affect people of all age groups, it is rarely found in children.

In CML patients, the bone marrow becomes populated with immature hematopoietic stem cells and differentiated granulocytes and there is an overall reduction of other WBCs, erythrocytes and platelets.

2.1.2. Acute Leukemias:

Acute leukemias affect patients of all ages including infants, older children and adults (> 60 years of age). Acute leukemias are heterogeneous hematological malignancies affecting either the lymphoid progenitor cells or the myeloid progenitors giving rise to acute lymphoblastic leukemia (ALL) or acute myeloid leukemia (AML) respectively. Disease development involves clonal expansion of leukemic blasts in the bone marrow, which are released into the circulation and infiltrate the peripheral organs including the spleen, liver, thymus etc.

2.1.2.1. Acute Lymphoblastic Leukemia (ALL)

ALL is the most common type of leukemia found in children. ALL can develop as a result of a combination of genetic, biologic or environmental factors but the majority are driven by gene translocations (>65 %) (Freireich et al. 2014).

The development of ALL is a result of rapid accumulation of leukemic blast cells in the body. There is an increased production of abnormal lymphocytes in the bone marrow (known as lymphoblasts or leukemic blasts) which are functionally incompetent as lymphocytes.

They eventually get released into circulation in peripheral blood and can accumulate in different organs such as the spleen and liver to form leukemic infiltrations in the body (Rytting 2014).

ALL can occur in one of three different forms based on the specific lineage affected i.e, pre-B cell, B-cell or T-cell ALL (Kebriaei et al. 2002; Pui et al. 2008).

The prognosis and treatment of ALL patients rely on various factors including the age of patient at diagnosis, subtype of leukemia. Children have a better prognosis than adults and B-cell ALL patients have a worse outcome when compared to T-ALL patients (Bassan & Hoelzer 2011). Within pediatric leukemia patients, the newborns younger than one year of age have a worse prognosis and have been categorized as infant leukemia patients. In adult ALL patients there are various genetic abnormalities that can drive the pre-B/B-/T-cell ALL (Fig. I10-D). Whereas, majority of infant ALL patients (>60%) carry a rearrangement in the mixed lineage leukemia (MLL) gene (chromosome 11q23) (Fig. I10-C) (Felix & Lange 1999).

The prognosis of infant leukemia patients is worse when compared to older children with ALL. Moreover, infant ALL patients carrying an MLL-gene rearrangement have a worse median survival when compared to patients carrying a non-MLL gene rearrangement (Fig. I9) (Slany et al. 2009; Hilden et al. 1995). There are also clinical distinctions between infant and childhood ALL diseases. Depending on the fusion partner of MLL, either B-cell ALL or T-cell ALL arises in infants. Majority of adult patients have T-cell ALL (Reaman et al. 1985; Pui & Evans 1999). ALL is a rare disease in adults. Response to therapy is

quite poor in infant and adult leukemia patients as opposed to the favourable prognosis observed in older children (>1 yr - 18yrs of age).

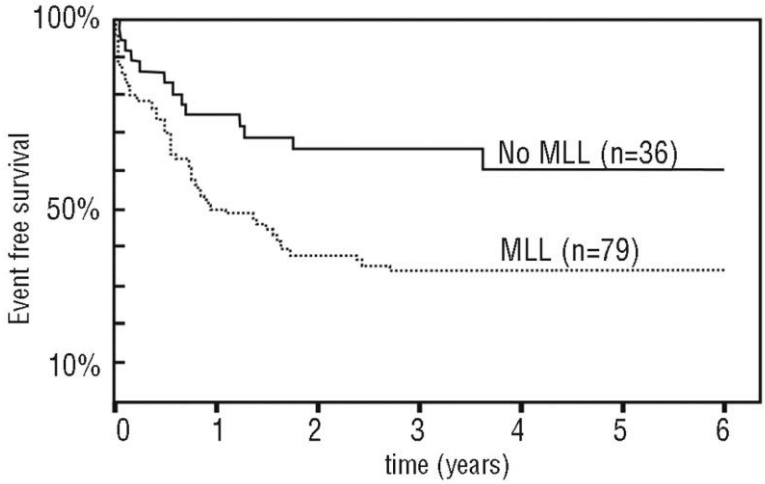

Fig.I 9: 5-year EFS of infant ALL patients based on MLL status: The survival curve is adopted from (Hilden et al. 1995; Slany 2009). <40% of Infant ALL patients that carry rearrangement in the MLL gene survive 5 years post diagnosis. Whereas, infant ALL patients that carry a gene rearrangenemt other than MLL have a significantly higher survival rate. EFS: event free survival, MLL: Mixed lineage leukemia, ALL: Acute lymphoblastic leukemia

2.1.2.2. Acute Myeloid Leukemia (AML)

AML disease affects the myeloid lineage of blood cells and is characterized by a rapid accumulation of abnormal white blood cells in the bone marrow. The early symptoms of AML are quite general including fever, weight loss, shortness of breath, anemia (Hoffman 2013). But, it progresses rapidly and requires immediate treatment in the absence of which it is fatal.

There are two main systems of classifications used for further characterization of AML into its subtypes (Bennett et al. 1976). The first and older system of classification (1970-1980s) was provided by the French American British (FAB) experts who divided AML into eight subtypes based on the type of leukemic blasts cells found at diagnosis as well as the stage of maturity of these cells.

The more recent WHO classification (Updated recently - 2008), on the other hand, uses patient's prognostic factors. It takes into account the combined morphologic, immunologic, cytogenetic as well as molecular genetic features of the disease to classify AML into its many subtypes (Estey et al. 2006; Vardiman et al. 2002).

AML in adults can arise due to DNA damage by exposure to carcinogens, chemicals (drugs), ionizing radiations, among others. Therapy-related AML in often found in adult patients. It occurs as a result of mutations conferred by chemo/radiation therapy used in treating a primary malignancy (Sandler & Ross 1997). The use of certain chemotherapeutic drugs (such as those targeting topoisomerase II) leads to formation of DNA breaks to induce apoptosis in cancer cells. However, they also cause DNA breaks in normal/healthy cells which can result in cytogenetic abnormalities. Such gene rearrangements (such as that of the MLL gene which can form fusions with one of its many partners) then drive different myeloproliferative disorders in these patients (Fig. I10).

2.1.2.3. Infant Leukemias

Leukemia is the most common type of cancer found in children. Pediatric leukemias subgroup affecting newborns have been characterized as infant leukemias based on certain unique characteristics of the disease. Infant leukemias have a short latency as they arise within a year of birth and are aggressive in nature with extremely poor prognosis (only 40% of infant leukemia patients have a 5-year event-free survival).

Prenatal origin of infant leukemias has been one of the landmark discoveries made in the field of infant leukemia research (Greaves et al. 2003; Gale et al. 1997). Mel Greaves identified chromosomal translocations in archived neonatal blood spots of patients that subsequently developed the leukemia (carrying the same fusion gene at diagnosis).

Moreover, studies of monozygotic twins have shown a 100% concordance rate of leukemia development in both siblings, suggesting that a leukemic clone originating in one twin migrated to the co-twin via the fetal anastomoses (Greaves et al. 2003; Hong et al. 2008). This study shed light on the distinction in nature of leukemias arising from an immature hematopoietic environment which has been crucial in understanding disease development.

This characteristic could be responsible for distinct features of infant leukemias when compared to childhood (>1 year – 18 years) and/or adult leukemias (>18 years). These findings give us good reason to question the possibility that transformation capacities of hematopoietic cells found in a developing embryo might be distinct from that in adults.

Moreover, infant leukemia patients do not respond well to conventional therapies and often die due to the high toxicity incurred by chemo or radiation therapy. Trouble with the use of conventional therapies for treating neonates when compared to older children is that neonates have a rapidly changing physiologic process that governs the disposition of drugs negatively. Some of these major factors that are now taken into consideration while planning the therapy are listed (Table. 2) (Biondi et al. 2000).

Table 2: Infants versus children and adults

Adapted from review (Biondi et al. 2000)

	Infants (<1 yr)	**Children (>1-18 yrs)**	**Adults (> 18 yrs)**
Total body water content (% body wt)	75	60	55
Extracellular water (% Total body water)	45	30	20
Drugs binding to serum proteins	Less avid	Higher affinity	Higher affinity
P450 enzyme activity	Low metabolic activity	High	High
Antineoplastic drugs cytotoxicity	Low	Effective	Effective
Renal tubular function and glomerular filtration rate	Developing up to 7 months	Higher	Optimal
Anatomical differences (Body wt/Body surface area)	18	25	40

MLL gene rearrangements are present in a significant percentage of infant AML and ALL patients (35% and 60% respectively) (Martinez-Climent et al. 1995; Pui 1995) (Fig. I10). There is a rapid accumulation of monoblasts/lymphoblasts that leads to hyperleukocytosis and affects the central nervous system (Sorensen et al. 1994). Although prognostic factors for infant leukemia patients are not well defined, some studies have identified factors associated with poor prognosis of these patients.

Involvement of MLL gene rearrangement, subtype of acute leukemia, high leukocyte count as well as the male gender of the patients are known to be associated with poor prognosis (Pui et al. 1994; Lie et al. 1996). Chemotherapy and/or allogenic hematopoietic stem cell transplantation is the treatment of choice for infants with AML, nevertheless some patients still relapse and die.

The need to find more efficient treatment options for infant leukemias is therefore a priority. The mechanism of leukemogenesis in infants is poorly understood although secondary mutations are rarely required especially when MLL-gene rearrangements occur (Chen et al. 2011; Jansen et al. 2007; Stam et al. 2014).

There is great debate in the field regarding the cell of origin of these aggressive infant leukemias. Studies have referred to these cells as 'Leukemia initiating cells' (LICs) and sometimes even 'Leukemic stem cells' (LSCs) (Fig. I14). The debate persists due to lack of an appropriate disease model that can efficiently recapitulate human infant leukemias to answer some of those crucial questions.

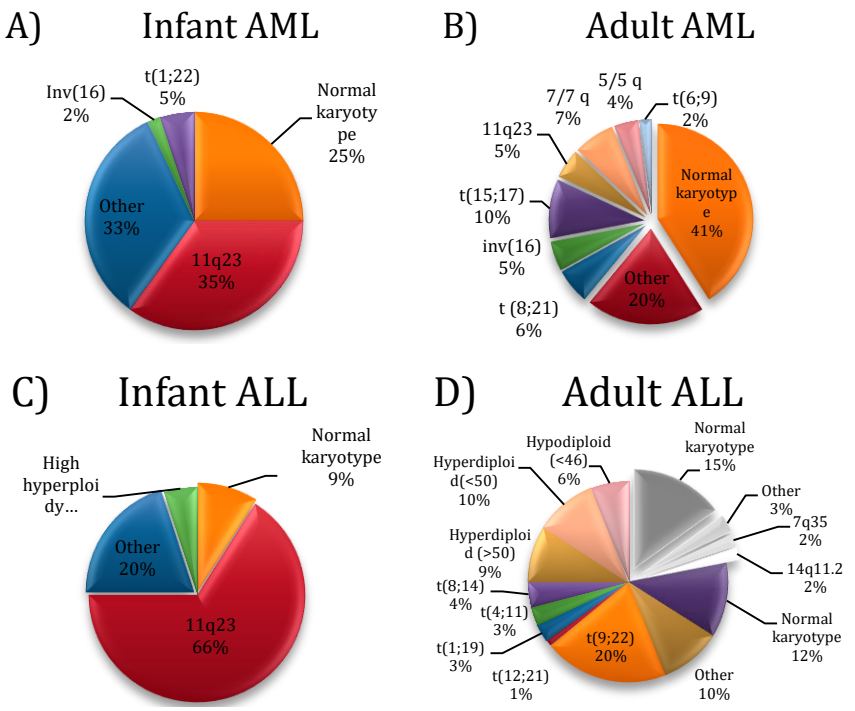

Fig.I 10: Cytogenetic abnormalities observed in human AML and ALL patients: Major genetic abnormalities (mutations/translocations) found in A) human Infant AML leukemia patients; B) human Adult AML patients; C) human Infant ALL leukemia patients and D) human Adult ALL patients are represented above. Majority of human Infant AML and ALL patients **(A and C)** carry an MLL-gene rearrangement whereas human Adult AMLs and ALLs **(B and D)** are driven by one of many different gene abnormalities. MLL-gene rearrangements are implicated in both age groups and in both subtypes of acute leukemias. They are present in a higher proportion of infant leukemia patients when compared to the significantly smaller proportion (5%) of adult patients. In **(D)** Black and grey panels represent T-ALL cases and colored panels represent B-ALL cases. B-/T-ALL: B-cell/T-cell acute lymphoblastic leukemia, MLL: mixed lineage leukemia, AML: acute myeloid leukemia

3. MLL GENE:

3.1. Normal functions

The MLL gene is known as mixed lineage leukemia or myeloid lymphoid leukemia gene, it is present on the q arm of chromosome 11 (11 q23) and it is a human homolog of the Trithorax gene in drosophila (Tkachuk et al. 1992). MLL gene is primarily known to regulate the embryo body development along the anterior-posterior axis (head-tail axis) similar to the role of trithorax gene in drosophila (Breen & Harte 1993).

MLL also has a major role in the embryonic hematopoietic development by regulating the expression of its downstream target genes (such as homeobox genes, Meis1, Pbx) (Hess et al. 1997; Kawagoe et al. 1999).

MLL is a methyltransferase known to mono-,di- or tri methylate lysine 4 of histone H3 (H3K4) which is a transcriptional activation mark (Shilatifard 2006; Krivtsov & Armstrong 2007) (Fig. I11). Downstream target genes of MLL are then actively transcribed. The Hoxa cluster of genes which are a target of MLL, are expressed in hematopoietic cells, specifically in the primitive hematopoietic stem and progenitor cells (Krivtsov et al. 2008). Complete knockdown of the Hoxa cluster genes significantly altered the functional activity of LT-HSCs (Lebert -Ghali et al. 2010). And, overexpression of only Hoxa9 gene rescued this phenotype. Further studies will help identify specific Hoxa cluster genes necessary for maintaining normal hematopoietic stem and progenitor cells.

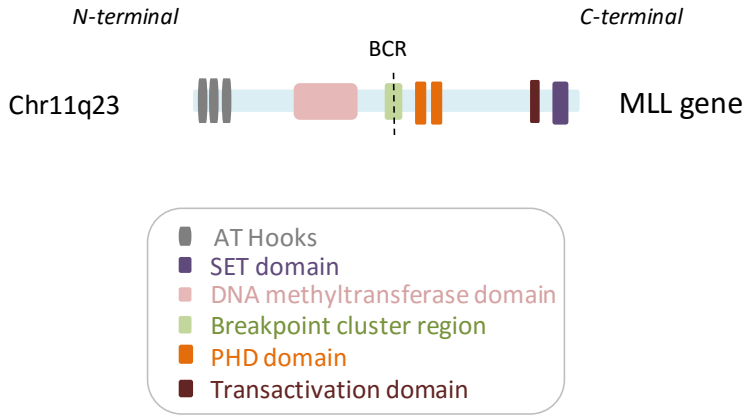

Fig.I 11: The different domains of MLL gene: The mixed lineage leukemia gene has DNA methyltransferase activity for which it binds the minor groove of DNA by the AT-hook domain (grey) and methylates lysines on histones by DNA methyltransferase domain (pink). MLL gene is able to form fusion oncogenes by binding to one of its many partner genes, in which the gene is cleaved at the breakpoint cluster region (green). Only the N-terminal domain of MLL gene is retained in the fusion. MLL: mixed lineage leukemia

Early studies, of knocking out MLL gene in mice, have shown that it is indispensable for embryonic hematopoiesis. Homozygous deletion of MLL led to embryonic lethality wherein embryos could not develop past E10.5 stage. MLL-null embryos had defects in yolk sac as well as fetal liver (Hess et al. 1997). Hematopoietic progenitor cells within the YS of MLL-null-embryos had a significantly reduced clonogenic potential in-vitro (Hess et al. 1997).

MLL gene is expressed in the majority of adult bone marrow cells including the lymphocytes (B and T) as well as myeloid cells (granulocytes and macrophages) but not in erythrocytes. The role of MLL-gene in maintenance of hematopoietic stem and progenitor cells in adults was therefore investigated.

Different mice models have been used to knock-out MLL gene in hematopoietic cells during embryonic and adult hematopoiesis. The constitutively active Vav1-Cre and conditional Mx1-Cre models, amongst others, were used to excise the MLL gene in hematopoietic cells of the fetal liver and bone marrow tissues (Gan et al. 2010a; Kühn et al. 1995). Although no phenotypic defects were found in fetal liver hematopoiesis of MLL-null embryos, functional assays showed presence of a significantly reduced number of competent/functional hematopoietic stem and progenitor cells.

Similar defects were observed in the hematopoietic cells of bone marrow tissue upon deletion of MLL gene in the adult mice (McMahon et al. 2007; Yu et al. 1995). These studies have highlighted the crucial role of MLL gene in not only establishing embryonic hematopoiesis but also in maintenance of postnatal hematopoiesis.

3.2. Role in disease

The MLL gene is capable of undergoing rearrangements with one of its many partner genes (>60 partners have been identified so far) (Table. 3). MLL-gene rearrangements are implicated in acute leukemias affecting patients of all age groups (Muntean & Hess 2012) (Fig. I12). It was first identified as part of a chromosomal translocation in hematologic cancers (Heim et al. 1988; Thirman et al. 1993). MLL gene plays an important role in B lymphopoiesis, so it is not surprising that human acute lymphoblastic leukemias involving MLL-rearrangements are largely B-ALLs while a smaller percentage constitute T-ALL cases (Gan et al. 2010b).

Rearrangements involving the MLL gene are present in up to 85% of infant leukemia cases (Biondi et al. 2000). These rearrangements are known to occur prenatally in these patients as shown by path breaking studies conducted by Mel Greaves (Greaves et al. 2003; Gale et al. 1997).

The involvement of MLL gene rearrangement is a major factor that dictates prognosis of infant leukemia patients. MLL-rearrangements contribute to majority of infant leukemia cases when compared to the significantly smaller proportion of other childhood (>1-18 years of age) and adults (>18 years) leukemia cases (approximately 10% in total). The adult leukemia patients carrying an MLL-rearrangement have a better prognosis when compared to infant-pediatric leukemia patients (Behm et al. 1996).

In MLL-rearranged leukemias, the conventional downstream target genes are found to be ectopically expressed. MLL fusion genes drive overexpression of downstream target genes Hoxa9, Hoxa10, Meis1 and PbX that drive leukemogenesis by maintaining a constant proliferative state of leukemic cells and arrest differentiation (Zeisig et al. 2004; Rozovskaia et al. 2001; Lawrence et al. 1999; Schnabel et al. 2000; Shen et al. 1999). Hox genes play a crucial role in the axial patterning during embryogenesis, as well as in hematopoietic development (Krumlauf et al. 1994). Hoxa and Hoxb genes are expressed in distinct hematopoietic stem and progenitor cells and disruption of Hoxa9 gene leads to reduction in granulocytes and lymphocytes (Schnabel et al. 2000).

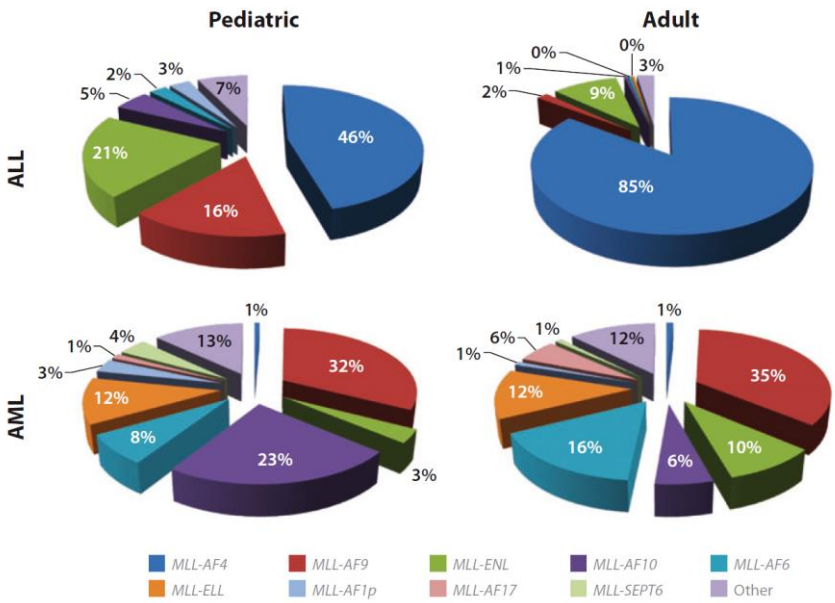

Fig.I 12: Proportions of MLL gene translocations involved in acute leukemias in children and adults (Muntean & Hess 2012)**:** The most common MLL fusion partners that together contribute to 90% of MLL-rearranged leukemias are represented above. ENL is one of the most common fusion partners of MLL gene, after AF4 and AF9. MLL-ENL translocations drive AML, ALL as well as mixed leukemia subtypes in pediatric and adult patients making it a good model to study and compare the disease arising in patients of all age groups.

Moreover, overexpression of Hoxa9 gene has been correlated with treatment failure in AML cases (Rozovskaia et al. 2001). Although the function of Meis1 in regulating hematopoiesis is not fully understood, it is known that Mesi1 gene, like Hox genes, is expressed in the hematopoietic stem and progenitor cells and its expression is reduced in more differentiated cells. Also, the overexpression of Meis1 and Hoxa9 genes has been demonstrated to be sufficient to immortalize hematopoietic progenitor cells and drive acute leukemias (especially AML) (Argiropoulos et al. 2007; Kumar et al. 2009; Lawrence et al. 1999).

3.3. Fusion partners

MLL-gene is capable of forming fusions with one of its many partner genes (>60) (Table. 3) (Meyer et al. 2009; De Braekeleer et al. 2005). This process involves cleavage of the MLL gene within the breakpoint cluster region (8.3 kbp region within intron 11 of the MLL gene) (Stanulla et al. 1997; Canaani et al. 2004; Broeker et al. 1996) (Fig. I11). The N-terminal domain of the MLL gene is conserved while the C-terminal domain of its partner gene is conserved.

The AT-hook domain of the MLL gene is retained which enables binding of MLL-fusion gene to the minor groove of DNA. However, the original methyltransferase activity of MLL gene (methylation of lysine 4 on histone H3), which occurs by the SET domain in C terminal region of the gene, is lost (Fig. I11) and it is replaced by the new methyltransferase activity recruited by its partner gene. The binding of MLL-fusion proteins to the downstream targets are known to enhance modification of lysine 79 on histone H3 (H3K79) which is also a transcriptional activation mark (Milne et al. 2005; Slany 2009). The partner that MLL becomes associated with plays a role in various aspects of the disease including disease phenotype.

The MLL-fusion proteins are known to recruit macromolecular transcriptional complexes such as super elongation complex (SEC), Dot1l associated-complex (Dotcom) (MLL partners such as ENL, AF9 can recruit Dotcom or SEC complexes) (Kuntimaddi et al. 2014; Mohan et al. 2010). In some cases, they are also known to interact with Histone deacetylase family of proteins (HDACs) as a part of the polycomb

repressor group of complexes (Muntean & Hess 2012) wherein, they are able to interact with many of its regulatory enzymes.

AF4, AF9 and ENL are the most common MLL partner genes implicated in human B-cell ALL, AML and AML/ALL/mixed leukemias respectively (Fig. I12). All three of these genes are known to be transcriptional trans-activators. The mechanisms underlying normal functions of these genes are not clearly understood. The AF4 gene plays an essential role during lymphopoiesis, it is expressed in developing thymocytes and mature lymphoid organs. AF4 gene consists of proline and serine rich trans-activating domains in the C-terminal. This region is conserved in the MLL-AF4 fusion in t(4;11) which is the most common translocation in infant leukemias and drives majority of infant B-cell ALLs (Morrissey et al. 1993). The AF9 gene, which was first described in t(9;11) driven AML, is found to be highly expressed in normal HSCs and it is also known to play a role specific cell fate decisions for lineage commitment during normal hematopoiesis (Leach et al. 2013; Collins et al. 2000; Krivtsov et al. 2006).

Table 3: Fusion partners of MLL implicated in different leukemias:

Adapted from (Meyer et al. 2009; De Braekeleer et al. 2005)

Name	**Functions**	**Cytogenetic abnormality**	**Disease**
AF1p/ EPS15/ MLLT5	Tyrosine kinase substrate, Putative signal transduction, Probable EGFR	t(1;11) (p32;q23)	Therapy related ALL, M5 AML, CML
AF1q	Growth factor	t(1;11) (q21;q23)	FAB M4 AML

AFF3/ LAF4/ MLLT2	Putative transcription activator	t(2;11)(q11.2-q12;q23)	ALL
SEPT2	Filament-forming cytoskeletal GTPase	t(2;11) (q37;q23)	AML, MDS,
NCKIPSD/ AF3P21	SH3-containing protein	t(3;11) (p21;q23)	AML
DCP1A/ EEFSEC/ SELB	mRNA-decapping complex, Transactivator of SMAD4	t(3;11) (p21.3;q23)	ALL
GMPS	Cell division, Guanosine mono-P synthetase	t(3;11) (q24;q23)	AML
LPP	Putative signal transduction	t(3;11)(q27Bq28;q23)	AML
FRYL	Regulates actin in cytoskeleton	t(4;11) (p12;q23)	ALL, AML
SEPT11	-	t(4;11) (q21.1;q23)	CML
AF4/AFF1/ MLLT2/FEL	Transcription activator	t(4;11) (q21;q23)	T-ALL, AML
SORBS2/ ARGBP2	Adaptor protein	t(4;11) (q35.1;q23)	AML
CENPK/ FKSG14	-	complex abnormalities	AML
AFF4/ AF5Q31	Transcription activator	ins(5;11) (q31;q13q23)	ALL
ARHGAP26/ GRAF	Negative regulator of RhoA and its GTPase activating protein	t(5;11) (q31;q23)	JMML
SMAP1	-	t(6;11) (q12B13;q23)	AML
AF6q21/ FKHRL1/ FOXO3A	Transcription factor forkhead, DNA binding	t(6;11)(q21;q23)	AML
AF6/ MLLT4	Signal transduction α-helical coils	t(6;11)(q27;q23)	AML, ALL
TNRC18/ KIAA1856	-	t(7;11)(p22.1;q23)	ALL
AF9/ MLLT3/ LTG9	Transcription activator	t(9;11)(p22;q23)	AML, ALL
DAB2IP/ AF9Q34/ DIP1/2/ KIAA1743	Negative regulator of RAS proteins activity	t(9;11) (q33.1Bq33.3;q23)	AML
FNBP1/ FBP17/ KIAA0554	Telomere maintenance	ins(11;9)(q23;q34) inv(11)(q13q23)	AML
LAMC3	Expressed in developing human fetal brain	t(9;11)(q31Bq34;q23)	AML

ABI1/ SSH3BP1/ E3B1	Cell growth inhibitor Signal transduction	t(10;11)(p11.2;q23)	AML
AF10/ MLLT10	Transcription activator Leucine zipper	ins(10;11) (p12;q23q13)	AML, ALL
NEBL		ins(10;11)(p12;q23)	AML
TET1/ LCX/ KIAA1676	Zinc-binding CXXC domain TET1 Methyltransferase domain	t(10;11)(q21;q23)	AML
NRIP3	Implicated in sarcoma	inv(11)(p15.3q23)	AML
ARHGEF17	Related pathways: Signaling by FGFR and by GPCR	t(11;11)(q13.4;q23)	AML
C2CD3/ DKFZP586P 012	Regulator of centriole elongation	inv(11)(q13.4q23)	AML
PICALM/ CALM	Role in integration of signals from different pathways	32 inv(11)(q14q23)	AML
MAML2	transcriptional coactivator for NOTCH proteins	inv(11)(q21q23)	T-ALL, AML
CBL/ CBL2	Negative regulator of tyrosine kinase-mediated signaling	del(11)(q23q23.3)	AML
ARHGEF12/ LARG/ KIAA0382	Rho guanine nucleotide exchange factor	del(11)(q23q23.3)	AML
BCL9L	Transcriptional activator	del(11)(q23q23.3)	ALL
TIRAP	Adapter involved in TLR2 and TLR4 signaling	del(11)(q23q24.2)	AML
DCPS	Scavenger enzyme Inhibits activation-induced cell death	del(11)(q23q24.2)	AML
CIP29	DNA transcription	t(11;12)(q23;q13.2)	AML
GPHN/ KIAA1385/ GPHRYN	Gly-receptor associated protein	t(11;14)(q23.3;q23. 3)	AML, T-ALL
KIAA0284/ CEP170B	Role in Microtubule organization	t(11;14) (q32.33;q32.33)	AML
CASC5/ AF15Q14	Growth repressor	t(11;15)(q23;q14)	AML, ALL
MPFYVE/ ZFYVE19	Signal transduction	t(11;15)(q23;q14)	AML
CBP/ CREBBP	Transcription coactivator,Histone acetyltransferase	t(11;16)(q23;p13.3)	MDS,AML,T -ALL

GAS7/ KIAA0394	Growth-arrest specific protein	t(11;17)(q23;p13.1)	AML
AF17/ MLLT6	Transcription factor	t(11;17)(q23;q21)	AML
ACACA	biotin carboxyl carrier protein, biotin carboxylase and carboxyltransferase	ins(11;17)(q23;q21)	AML
MLLT6/ AF17	Transccription factor	t(11;17)(q23;q21)	AML
LASP1/MLN 50/LIM/ SH3protein1	-	t(11;17)(q23;q11Bq 21.3)	AML
SEPT9/ MSF/ KIAA0991	Cell cycle regulation Signal transduction Cytoskeleton organization Putative GTP binding domain	t(11;17)(q23;q25)	AML
ELL/ MEN	Transcription elongation factor Regulation of cell growth and survival	t(11;19)(q23;p13.1)	AML
SH3GL1/ EEN	α-helical coils Signal transduction	t(11;19)(q23;p13)	AML
ENL/ MLLT1/ LTG19	Transcription activator	t(11;19)(q23;p13.3)	AML, B-ALL, T-ALL
ASAH3/ ACER1	Regulates keratinocyte proliferation and apoptosis	t(11;19)(q23;p13.3)	ALL

Table3: Fusion partners of MLL implicated in different leukemias: The most common partners of MLL-gene have been highlighted in the table (pista). MLL: mixed lineage leukemia, AML: acute myeloid leukemia; B-/T-ALL: B-cell/T-cell acute lymphoblastic leukemia; MDS: myelodysplastic syndrome; CML: chronic myelogenous leukemia; JMML: juvenile myelomonocytic leukemia

4. ENL GENE

The eleven-nineteen leukemia gene (ENL) is present on the p arm of chromosome 19 (19p13). ENL gene is also known as MLLT1, BAM11 or LTG19. It was one of the first fusion partners to be identified. It has high serine and proline content which is a hallmark for transcriptional control (Yamamoto et al. 1993).

It was first identified as a fusion partner of MLL in a human acute leukemia case t(11;19) and was then termed ENL (eleven-nineteen leukemia) (Tkachuk et al. 1992) (Fig. I13). The AF9 and ENL genes share high sequence conservation (Prasad et al. 1995; Erfurth et al. 2004; Rubnitz et al. 1994).

The C-terminal region constituting the 90kDa trans-activating domain is conserved in the MLL-ENL fusion, similar to the MLL-AF9 fusion. The sequences for nuclear targeting are also retained in these fusions.

The exact function of the ENL gene remains unknown still. Homozygous deletions of ENL/MLLT1 gene in mice led to embryonic lethality, wherein embryos did not develop beyond E8.5 stage suggesting it plays an important role in embryonic developmental process (Doty et al. 2002). ENL expression detection was conducted in different cell lines. It was found to be highly expressed in embryonic cell lines GS and P19 as well as in lymphoid cell lines p5424, sp04, 70Z/3, WEHI231, and A20 suggesting it may play a role in early embryonic development. But it could not be detected in the two myeloid cell lines p388D1 and WEHI3 (Doty et al. 2002).

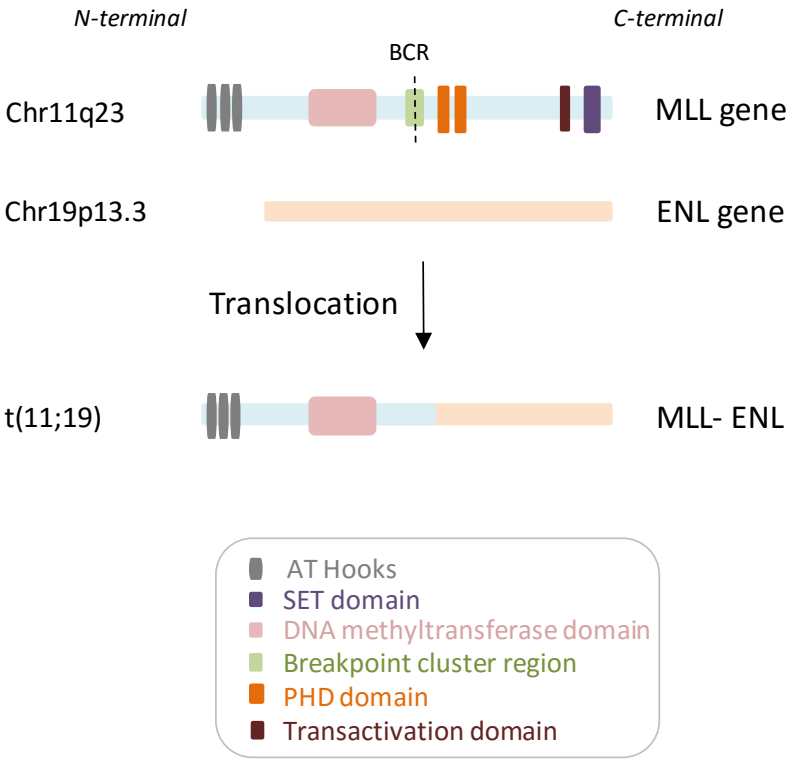

Fig.I 13: t(11;19) resulting in formation of MLL-ENL and reverse genes: Translocation t(11;19) comprises formation of MLL and ENL fusion genes. The N-terminal domain of MLL gene is conserved in the fusion that fuses to the C-terminal region of ENL gene. The AT-hook domain of the MLL gene and the trans-activation domain of ENL genes are retained. In the human disease the reverse fusion gene EML-MLL is formed as well. The original methyltransferase activity of MLL (H3K4 mono/di/tri methylation) is lost upon cleavage within the BCR in intron 11 of MLL gene. MLL: mixed lineage leukemia, ENL: eleven-nineteen leukemia, AT: adenine/thymine, BCR: breakpoint cluster region

The MLL-ENL and its reverse fusion gene ENL-MLL are known to be equally important in contributing to leukemogenesis (Fig. I13). They are sufficient to drive the leukemia which is why secondary mutations are rare in the leukemia patients carrying t(11;19).

Additionally, leukemias arising from an MLL rearrangement are constituted of homogenous blast populations, thus identifying the cell of origin will aid in the therapeutic targeting. It has been suggested that there may be co-recruitment of the SEC and Dotcom complexes in case of t(11;19). This would drive transcription since the ENL protein is a composite part of both the complexes.

5. LEUKEMIA MICE MODELS TO REPRODUCE HUMAN INFANT DISEASE

The understanding of biological features of distinct forms of leukemias has been possible to a large extent by the use of animal models. We have gained important insights into the disease including discovery of leukemia initiating cells using animal models (Cook & Pardee 2013).

The poor survival of infant leukemia patients has led to intensive studies in this field. The conventional therapies are often unable to treat these patients or improve the survival to >40%. To improve therapeutic strategies to treat these patients, we need to have a better understanding of the disease.

Inbred mice make for suitable models to study the human disease as their genome is closely related to humans, they are easy to house and maintain and they reproduce fast (within 20 days). It is also possible to have access to tissues from different developmental stages to perform in-vitro as well as in-vivo assays and to genetically modify them (Weissman & Shizuru 2008; Doulatov et al. 2013). Testing therapeutic agents to treat human diseases were one of the first reasons for which animal models were used. Developing leukemia mice models will aid in characterizing diseases (such as infant leukemias) that remain immune to conventional therapies and to test novel therapies to treat them.

Various strategies have been implemented to achieve this by developing animal models of acute leukemias. This has been made possible using the knowledge we have from genetics of acute leukemias in pediatric and adult patients.

Several leukemia mice models have been generated involving MLL gene rearrangements using some of the strategies mentioned below (Corral

et al. 1996; Forster, Pannell, Lesley F. Drynan, et al. 2003; Metzler et al. 2006). However, a faithful reproduction of human infant leukemias has not been successful in terms of aggressiveness, latency and subtype. These are some of the strategies that have been used:

1. Carcinogen-induced models:

   This was an initial approach to developing animal models of acute leukemias. It involved the exposure of rats and mice to X-ray radiations which have carcinogenic potential and leukemia mice models were first described in 1991 by this means (Upton 1975; Little 2000). In years that followed murine or human hematopoietic cells were treated with carcinogens (anti-metabolite agents such as 3-methylcholantrene) in-vitro which were later transplanted into mice to develop AML disease models (McCormack et al. 2005; Skipper & Perry 1970). However, these diseases had features quite distinct from the human disease making them clinically irrelevant disease models.

2. Viral models:

   This approach was first implemented to develop an AML mouse model (Friend 1957). It involves, insertion of a chromosomal aberration (such as a MLL-fusion resulting from a chromosomal translocation) into a viral vector to transduce cells. Different studies have transduced fusion oncogenes into embryonic stem cells or human cord blood $CD34^+$ cells or murine hematopoietic stem cells (Lin- $Sca1^+$ Kit^+) in in-vitro cultures. Transduced cells are injected into mice by performing transplantations to develop and study the leukemia development.

Several acute leukemia mice models have been developed using this strategy by targeting different genes that have been implicated in human infant leukemias. An AML model driven by t(11;19) was developed using the current strategy. To recapitulate human infant disease, MLL-ENL fusion was introduced to human cord blood cells and murine stem cells in-vitro via retroviral transduction of the fusion oncogene (Barabé et al. 2007; Zuber et al. 2009a). Transduced cells were then transplanted into mice to develop AML disease. Similar studies were performed by transducing MLL-AF9 and MLL-AF4 fusion genes and murine models were generated of human infant AML and B-ALL diseases respectively (Cook & Pardee 2013; Beer et al. 2015; Wei et al. 2008; Schmitt et al. 2000). While such models are beneficial for testing preclinical efficacy of different drugs, they are not suitable models to study disease development. By relying solely on cell-autonomous modifications they failed to describe and recapitulate complex diseases that rely on cancer microenvironment which plays a crucial role in disease development and in response to therapy.

3. Transgenic models:

Animal transgenesis has been used to study normal function of genes and to develop human disease models by knocking out or introducing gene aberrations into mice or in murine embryonic stem (ES) cells (Gama Sosa et al. 2010). This strategy has been widely used to develop mice models of human leukemias. Expression of oncogenes (such as MLL-fusions) or silencing of tumor suppressor genes (such as retinoblastoma) can be done using this strategy. Further advances in the field allow conditional

expression of gene aberrations using drug inducible Cre/LoxP systems or doxycycline/Tet on-off systems (Heyer et al. 2010; Belizário et al. 2012). Cre recombinase is an enzyme that specifically recognizes and cleaves 11bp palindromic sequences called LoxP sites.

To develop murine models of childhood leukemias, transgenic mouse models were also used. Lmo2-Cre mice (constitutive, hematopoietic specific Cre) were crossed with MLL-LoxP,ENL-LoxP transgenic mice (Collins et al. 2000). The aggressive AML disease developed in mice with the Lmo2-Cre closely resembled the human pediatric disease carrying the MLL-ENL translocation. The disease was characterized by $Mac1^{+}Gr1^{+}$ leukemic blasts and drove an aggressive disease as is found in humans (Forster, Pannell, Lesley F. Drynan, et al. 2003; Collins et al. 2000; Daser & Rabbitts 2004). Though the use of constitutive Cre mice to develop MLL-rearranged leukemias has been informative in disease characterization, it does leave many questions unanswered.

Finding the cells that are capable of giving rise to leukemia upon undergoing translocation in-vivo, and identifying their developmental stage are important questions to be answered. Murine models carrying an inducible Cre transgene might prove beneficial in gaining insights into disease development, identification of leukemic cell of origin and ultimately finding novel targeted therapies to attain complete remission in leukemia patients.

4. Knock-in/Knock-out Models:

For leukemias to develop, there is a need for a secondary mutation to occur. The first hit such as a chromosomal abnormality is often

insufficient by itself to give rise to the disease. Many studies have been focused on identifying candidate genes that are found to be either up or downregulated in the human leukemias.

Knock-in mouse models have been generated with such genes including Hoxa9, Meis1, Flt3, K-ras to develop leukemia mouse models by crossing them with transgenic mice carrying other oncogenes or fusion genes to mimic the second recombination event that might be occurring in the human disease (Nakamura et al. 1997; Rozovskaia et al. 2001; Argiropoulos et al. 2007; Greenblatt et al. 2012; Chan et al. 2004). Similarly, in knock-out models certain tumor suppressors were knocked out in mice to enable leukemia formation (Yu et al. 2010; Cutts et al. 2009).

There are two drawbacks to using these models:

(i) they drift from the human phenotype, which reduces the clinical relevance of using such models

(ii) they lack heterogeneity that often characterize human disease

5. Xenograft model:

Xenografts are the transplantation of human cancer cells into immunocompromised mice to study the primary cancer cells in mice. These models are an alternative strategy to study the human disease more closely in mice to test drugs and assess their preclinical activity. This technique has been improved to reach efficient engraftment of human cells into mice.

Immunocompromised mice were developed from Non-obese diabetic (NOD)/Severe Combined Immuno-Deficient (SCID)

(NSG) mice that have no B-, T- lymphocytes, natural killer cells and monocytes with the additional deletion of IL2Rγ gene (Interleukin 2r gamma receptor).

Xenograft models have the advantage of using human cancer samples (primary samples or cell lines) to develop a reproducible disease model in mice, for which the hosts are readily available to have a statistically viable and clinically relevant disease model (Teicher 2006).

Primary human adult leukemia cells carrying MLL-ENL and MLL-AF9 fusions have been xenotransplanted into immunocompromised mice and the human disease could be recapitulated successfully (Barabé et al. 2007). However, performing the same for an infant leukemia model would be difficult due to the pre-natal origin of the human disease.

While xenograft models are an appealing tool to test drugs, it has several limitations in studying disease development. Some of these drawbacks include the non-physiological approach of translocation induction in-vivo, that is achievable using transgenic mice. And, there is an increasing risk of graft versus host disease (GVHD).

With advances that have been made in developing transgenic mice, it seems to be the more feasible approach of developing an MLL-rearranged mouse model that will aid in understanding infant leukemia disease ontogeny.

6. LEUKEMIA INITIATING CELLS:

'Leukemia initiating cells' (LICs) or 'Leukemic stem cells' (LSCs) possess the ability to generate leukemias. They possess self-renewal ability and a proliferative advantage by which they produce leukemic blast load in the body (Fig. I14). Earlier studies dating back to two decades ago, suggested that LSCs or LICs originated from HSCs. It is thought that HSCs upon undergoing driving mutations (such as MLL-gene rearrangements) gave rise to the disease by exploiting their characteristics of self-renewal to maintain the LIC/LSC pool (Passegué et al. 2003; Wang & Dick 2005; Bhatia et al. 1997; Jordan 2007).

Consequently, the presence of these mutant HSCs and often their quiescent nature would make treatment by conventional therapies difficult and the newly generated blast load will lead to relapse (Fig. I14). These studies also suggested that such a reservoir could only exist in the form of mutant HSCs and not progenitors.

It is known that MLL gene rearrangements are potent oncogenes on their own without the need of a secondary mutation. More recently, many studies have shown the ability of MLL-fusions alone to transform progenitor cells such as LMPPs or GMPs into becoming LICs (McKenzie 2005; Goardon et al. 2011). It was also shown that HSCs upon transduction with the MLL-fusion genes are unable to give rise to leukemias whilst LMPPs or GMPs have leukemogenic potential, contradicting the early studies (Ugale, Gudmundur L. Norddahl, et al. 2014; Taussig et al. 2008). Irrespective of the developmental state of the cell of origin of these

leukemias, it is clear that a single cell upon undergoing an MLL-rearrangement can give rise to these clonal diseases.

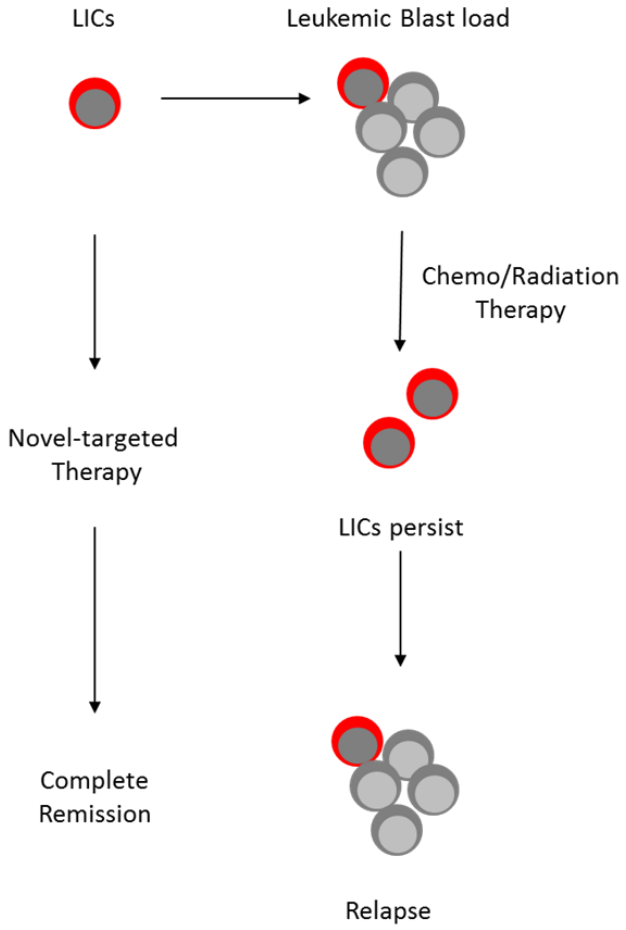

Fig.I 14: Leukemia initiating cells (LICs): Represented above is a scheme describing the likely manner in which an MLL-rearrangement-derived LICs function in the human disease. Irrespective of cell of origin, the LICs have stem cell like properties. They have self-renewal capacity, are highly proliferative and have decreased apoptosis. They are able to give rise to the leukemic blast load leading to clinical symptoms of the disease such as leukocytosis. While conventional therapies, such as chemo- or radiation-therapies, are able to decrease leukemic blast load, the LICs are often resistant to these conventional therapies and can repopulate leukemic blasts causing a relapse in patients. One of the hypothesis supporting this resistance is the quiescent or semi-quiescent state of LICs that enable them in escaping conventional therapies that are targeted at killing highly proliferative populations such as the LIC-derived progenitors or leukemic blast cells. There is a need for novel targeted therapy to selectively kill LICs to obtain complete remission in patients.

OBJECTIVES

OBJECTIVES

Pediatric leukemias, especially infants carrying alterations in the MLL gene, clearly have distinct characteristic features when compared to adult acute leukemias. The in-utero chromosomal transformation, the developing environment and immature hematopoietic cells within an embryo might be some of the critical contributing factors to the aggressive nature of this disease.

The aim of this thesis is to develop a mouse model of acute leukemias carrying an MLL gene rearrangement, in order to recapitulate the human infant and adult leukemias. We have worked specifically with the MLL/ENL t(11;19) as it is implicated in leukemias occurring in all age groups and gives rise to either an AML, ALL or mixed leukemia in humans (Pui et al. 1994; Rubnitz et al. 1999).

Several studies have developed MLL-ENL fusion driven leukemia mice models using different strategies as mentioned earlier. Some were successful at developing AML model of disease to an extent while others showed a chronic phenotype with lower penetrance. To this goal, we have compared infant and adult MLL-ENL leukemia mouse models to further understand infant leukemia development and to compare it to adult leukemias. We have compared transformation capacities of distinct hematopoietic tissues at different stages of hematopoietic development upon t(11;19) induction as illustrated below.

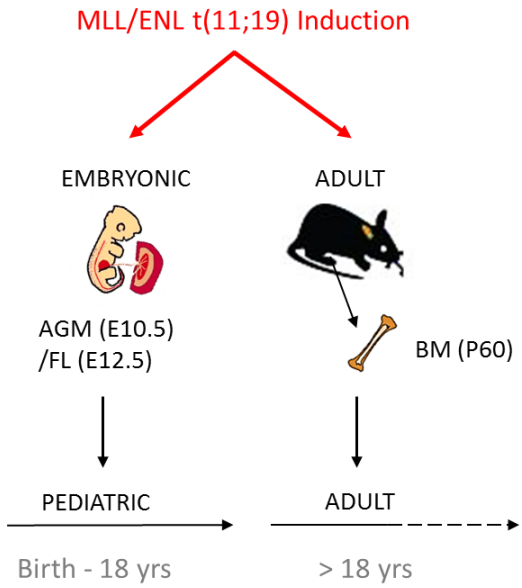

Schematic representation

MATERIALS AND METHODS

MATERIALS AND METHODS

I. ANIMAL EXPERIMENTS (IN-VIVO ASSAYS)

Animal models are widely used to study human diseases. It is also possible to have access to tissues from different developmental stages to perform in-vitro as well as in-vivo assays as well to genetically modify them (Weissman and Shizuru, 2008; Doulatov et al. 2012).

The animals used for this project were housed in the Animal facility at Parque de Recerca y Investigación Biomédica de Barcelona (PRBB). All of the mice we have used during the project are of C57BL6 strain (of CD45.1/CD45.2/CD45.1-CD45.2 background).

All protocols performed with mice were approved by the Committee for Animal Experimentation at the Institut Hospital del Mar d'Investigacions Mediques (IMIM, in Barcelona, Spain) and handling of mice were under the guidelines provided by Animal Care Committee at the Generalitat de Catalunya.

i. Mice colonies used:

a. MLL-LoxP, ENL-LoxP:

These transgenic mice were gifted to us by Dr. Terrence H. Rabbitts, they were generated in his lab (Collins et al. 2000). To generate these mice, LoxP sites were inserted into the MLL and ENL genes. The LoxP sites were inserted in mouse MLL and ENL genes at positions

homologous to the breakpoints regions found in human disease. ES cells carrying these MLL-LoxP and ENL-LoxP genes were able to give rise to mice upon insertion in a blastocyst.
These MLL-LoxP,ENL-LoxP mice were crossed with Cre mice to initiate Cre-mediated translocation t(11;19) formation in a constitutive or inducible manner.

b. Vav1-Cre:

The Vav1-Cre mice were generated by Thomas Graf (Stadtfeld & Graf 2005) and were gifted to us by Dr. Graf. Vav1-Cre is constitutively active that targets definitive hematopoietic cells from E11 onwards in the mouse embryo (Bustelo et al. 1993). The Cre is expressed through adulthood.

c. β-actin Cre^{ERT}:R26-YFP:

The β-actin Cre^{ERT} mice were a gift from Andrew P McMahon in whose lab these mice were generated (Hayashi & McMahon 2002). It is an inducible Cre model. The expression of Cre is under the control of the β-actin promoter. The β-actin Cre^{ERT} mice were crossed with R26 Lox-Stop-Lox YFP mice to have a reporter to detect recombined cells.

It is a tamoxifen inducible Cre in the absence of which the Cre^{ERT} complex remains inactive in the cytoplasm. Upon tamoxifen induction the Cre-^{ERT} is activated and can translocate to the nucleus allowing initiation of Cre-mediated recombination of LoxP sites to occur. Upon Cre-induction, YFP would be expressed from Rosa26 locus in all

induced cells. We could trace the recombined cells by YFP-expression. The formation of MLL-ENL and reverse ENL-MLL fusion genes should then occur in parallel with YFP-expression in the same cells.

d. Mx1-Cre:

The Mx1-Cre mice were a gift to us from the lab of Dr. Cristina Lopez, UPF, Barcelona, Spain (Kühn et al. 1995). It is also an inducible Cre mouse model. The expression of Cre is under the control of Myxovirus resistance 1 promoter. It encodes for an IFN inducible nuclear protein conferring resistance to influenza virus. Mx1 allele is silent in healthy mice, but can be induced to high levels of transcription with Interferon or Polyinosinic-polycytidylic acid (poly IC is a synthetic analog of dsRNA). Poly IC induces IFN-1 production, allowing initiation of Cre-mediated MLL-ENL translocation.

e. CD45.1 and CD45.1-CD45.2:

These mice were used in competitive transplantation experiments. CD45.1 mice were used as transplant recipient mice in all of the experiments and were lethally irradiated prior to transplantation. Irradiation was performed with 2 doses of 4Gy each given 3 hours apart. From the CD45.1-CD45.2 chimera mice we obtained competitor cells for the in-vivo transplantation assays. 200,000 whole bone marrow cells were transplanted along with donor samples per transplant recipient.

ii. Cre-inductions in-vivo

a. Induction of β-actin Cre^{ERT}:R26-YFP:

The MLL-LoxP,ENL-LoxP mice were crossed with β-actin Cre^{ERT}:R26-YFP mice. Initiation of Cre-mediated recombination was performed in-vivo using tamoxifen. Inductions were performed at different stages of embryonic and adult hematopoietic development. The stages were at E8.5, E12.5 during gestation to induce hematopoietic cells in the aorta-gonads-mesonephros (AGM) and fetal liver (FL) tissues respectively. Adult hematopoietic cells were obtained from the bone marrow of P60 (2 months old) mice coming from the crossing.

Tamoxifen (T5648 – Sigma Aldrich©) was dissolved in ethanol and diluted in corn oil in 1:5 proportion to prepare stock solutions of 20 mg/ml concentration. The stock solutions were stored at -20°C for long-term use. Tamoxifen was administered via intraperitoneal injections in-vivo during gestation and in adult mice at the stages mentioned above. Tamoxifen was titrated in-vivo in β-actin Cre^{ERT}:R26-YFP mice (Results Table-2). Optimized concentration used was 75 mg/kg body weight. The optimal tamoxifen doses at 75 mg/kg wt concentration were (Fig. R2.II – B,C):

- 1 dose in pregnant mice (at E8.5 or at E12.5),
- 5 doses in adult mice (at P60) administered over 5 consecutive days

b. PolyIC induction of Mx1-Cre:

The MLL-LoxP,ENL-LoxP mice were crossed with Mx1-Cre^{+} mice. The initiation of Cre-mediated recombination was carried out using polyIC (tlrl-pic, Invivogen©). Inductions were performed via intraperitoneal injections of PolyIC in pregnant mice at E12.5 and in adult mice at P60.

PolyIC to be administered in-vivo was dissolved in sterile distilled saline to prepare stock concentrations of 1mg/ml and stored at -20°C for long-term use. Protocols implemented for optimal Cre-inductions were:

- injecting 15 μg/g of polyIC in adult mice (P60 stage) for 5 days given every other day (Klinakis et al. 2011)
- injecting of 20 μg/g of polyIC in pregnant mice at E12.5 (Arrode-Brusés & Brusés 2012)

iii. Tissue dissection

Mice were euthanized by cervical dislocation/carbon-dioxide asphyxiation followed by cervical dislocation. The skin was sterilized with ethanol and dissection was performed using forceps and scissors.

a. Embryonic tissues:

The peritoneum was opened and embryos were separated from uterine horns. Embryos were placed in PBS (Biological Industries Ref. 02-023-1A) solution on ice (Nagy et al. 2014; Morgan et al. 2008; Baron & Mohn 2005).

The embryos were placed in a 10 cm petri-dish (Sigma-Aldrich BR452010) with PBS under a bright field microscope. Using forceps the endometrial tissues were separated from the embryos to visualize the embryo proper and placenta. The placenta was then separated from the embryo followed by separation of yolk sac layer around the embryo body.

AGM

Dissection of the aorta-gonads-mesonephros (AGM) tissue was done from E10.5 embryos (35-39 somite pairs) using 28-30 gauge needles (BD- 328203). The AGM region is visible by the bloodline running through it. The limbs were dissected out along with portion of embryo body above the forelimbs. Thereafter, dorsal portion containing somites were dissected out without touching the AGM region. The side tissues were excised away from the AGM tube to get rid of as much excess tissues as possible. The AGM was suspended in sterile PBS fetal (PBS with 10% fetal bovine serum [Biological Industries 04-007-1A]) on ice.

FL

Dissection of the fetal liver (FL) tissue was done from E12.5/E14.5 embryos as previously described (Baron & Mohn 2005). Fetal liver was visible as the lobes of the liver are visible by these stages. 30 gauge needles were placed along anterior and posterior regions of liver, parallel to one another. The liver was dissected out by making a final excision in its ventral portion to separate the lobes from the embryo body. The excess tissues were separated from the liver lobes and the liver was suspended in sterile PBS fetal on ice.

b. Adult tissues: BM

The hindlimb of the euthanized mouse was held in place using a forcep. Dissection was performed along the femur and tibia using scissors. At the hip-joint the bone was excised. Femur and tibia were separated from the dissected limb and it stored in PBS on ice until BM cells were obtained from the bone.

iv. Tissue disaggregation

AGM

The dissected AGMs were disaggregated using collagenase (Sigma Ref. C0130). For disaggregating 1 AGM, 50 µl of collagenase (1.25 mg/ml) was diluted in 250 µl of sterile PBS fetal was used.

- Tissue was disaggregated in this solution by pipetting once every 10 minutes during 20-25 minutes of incubation in a 37°C water bath.
- The cells were washed twice with 1 ml of PBS fetal and centrifuged at 1200 rpm for 5 minutes.
- The pellet was re-suspended in PBS fetal and filtered through cell strainer 40µm (Fisher scientific 08-771-1) have a single cell suspension.

FL

The dissected tissue was suspended in 500 µl of sterile PBS fetal solution

- Disaggregation of the fetal liver tissue was done mechanically by pipetting.

- This was done until there were no clumps/aggregates visible.
- The cell suspension was then passed through a 40µm cell strainer to obtain single-cell suspension.

BM

Femurs dissected from euthanized mice were cleaned using a blade until only the bone remained rid of any flesh. The very edges of the femur were cut using the blade to have open ends on the bone to allow flushing of the marrow.

- Bone marrow cells were flushed out using an insulin syringe filled with 1 ml of sterile PBS fetal and collected in 1ml eppendorf.
- BM cells were disaggregated in a similar manner to fetal liver cells.
- Pipetting was done till no clumps of cells were visible any longer followed by passing cells through a 40µm cell strainer to obtain single-cell suspension.

v. Competitive Transplantation Assay:

In-vivo transformation capacity was assessed by performing competitive transplantation of induced cells. Competitive transplantations were performed of transformed donor cells (AGM/FL/BM) along with competitor cells (whole BM) in lethally irradiated recipients using the allelic variants of CD45. Inductions (in-vivo/in-vitro) were done as described in Methods I-ii and II-ii. 48 hours post-inductions the tissues were transplanted competitively as follows:

- Recipients (CD45.1): Lethally irradiated with two doses of 4 Gy each given 3 hours apart each.
- Donor cells (CD45.2): induced 1e.e. AGM/1 e.e. FL or 10 million whole BM cells
- Competitor cells (CD45.1-CD45.2): 200,000 whole BM cells

Cells to be transplanted were filtered to have a single cell suspension in 150 µl of sterile PBS. Transplantations were performed retro-orbitally in mice. Post-transplantation, antibiotics were given to mice in drinking water for four weeks.

II. IN-VITRO ASSAYS:

i. Cell culture:

Single cell suspensions of AGM/FL/BM cells from MLL-LoxP,ENL-LoxP:β-actin Cre^{ERT}:R26-YFP mice were cultured in-vitro. The optimized culture medium used for plating these cells was Isscove's modified Dulbecco's medium (IMDM) (Thermo fisher scientific: 12440053), with growth factors, as mentioned in Table-1.

Table-1: Hematopoietic cells culture media constituents:

Isscove's medium (IMDM)	**Company/Reference**	**Volume (in µl)**
FBS (Fetal bovine serum)	Biological Industries 04-007-1A	100
Stem cell factor	Sigma-Aldrich SRP3234	100
IL3	Sigma-Aldrich SAB1409242	100
Penicillin/Streptomycin	Biological Industries Ref. 03-031-1B	10
IL6	I9646 Sigma-Aldrich	1
Total	-	1000

500 µl of this culture medium was used for plating 100,000 cells from AGM/FL/BM tissues in 12 well petri-plates (Sigma-Aldrich CLS3513). Cultures were maintained for 48 hours, during which in-vitro induction was performed (Methods II-ii). This was followed by performing in-vivo transplantation assay.

ii. Cre induction in-vitro (4-hydroxytamoxifen):

The induction of β-actin Cre^{ERT}:R26-YFP cells could also be done in-vitro. Single cells were obtained from E10.5 AGM/E12.5 FL/P60 BM tissues coming from the crossing of MLL-LoxP,ENL-LoxP mice with R26-YFP:β-actin Cre^{+} mice.

Liquid culture of these cells were maintained in-vitro for two days (Methods II-i). To perform in-vitro induction of these cells we used the compound 4-Hydroxytamoxifen (4-OHT) (Sigma-Aldrich H7904/H6278). It is the active metabolite of tamoxifen. 4-OHT stock was prepared at 20 mg/ml concentration by dissolving it in sterile 100% Ethanol (Merck Ref. 1.00983.2500), until the solution turned clear and no precipitates were present. It was stored at – 20°C for long-term use and protected from light. Titrations of 4-OHT were performed in-vitro (Results R2.I section) to achieve the optimal dose to use. It was found to be 5 µm of 4OHT to be added to cell culture per day for two consecutive days.

III.DNA EXTRACTION

DNA was extracted from different tissues including peripheral blood (PB), bone marrow (BM) cells, AGM and FL tissues. The same protocol was used for all tissues. Prior to extracting DNA from PB and BM, lysis of erythrocytes was conducted using ACK Lysing buffer (Thermo fisher scientific: A1049201). 500 µl of buffer was added to re-suspend the pellet of cells and vortexed briefly. Incubation was done at room temperature for 10 minutes. The sample was then washed with 1 ml of PBS fetal and centrifuged at 1200 rpm for 5 minutes twice. The pellet was re-suspended in 50 µl of NaOH-EDTA (25mM) solution and incubated at 94°C for 1 hour. Thereafter, equal volume i.e. 50 µl of TRIS buffer (10Mm, pH 7.6) was then added to the sample. The tube was centrifuged at 1200 rpm for 5 minutes. The supernatant containing DNA was stored at -20 °C.

IV.PCRs

It is a molecular biology technique performed to generate millions of copies of a specific DNA sequence by amplifying it. It relies on repeated cycles of heating and cooling for denaturation and enzymatic replication of DNA. Short DNA fragments containing sequences that are complementary to the target region are used along with DNA polymerase to achieve repeated amplification of selective region of DNA. This technique has varied applications including early detection of malignant diseases such as leukemias.

i. Genotyping

PCRs were performed to genotype the mice to detect the Cre gene to note differences between Cre^+ versus Cre^- (control) mice, as well as to detect the MLL-ENL fusion gene. DNA used to perform the PCRs were extracted from different tissues as described above (Methods III). The PCR conditions are summarized below:

Vav1-Cre

Vav1-Cre genotyping PCR was performed from DNA extracted as described in the section above (Methods III). The reaction mix was prepared as per the manual protocol of Taq polymerase (Roche diagnostics – Catalog No. 11418432001). 2 µl of template DNA was taken in a total reaction mix of 25 µl volume. 0.25 µl of each primer (10mM) were used per reaction for detecting Vav1-Cre gene of 232 bp. The sequences of primers are mentioned in the Table-2 and PCR conditions in Table-3.

β-actin Cre

β-actin Cre genotyping PCR was performed from DNA extracted as described in the section above (Methods III). The reaction mix was prepared with Taq polymerase from Biorad (Catalog No. 170-8870). 2 µl of template DNA was taken in a total reaction mix of 25 µl volume. 0.5 µl of each of the primers (10mM) were used per reaction for detecting β-actin Cre gene at 270 bp. The sequences of primers are mentioned in the Table-2 and PCR conditions in Table-3.

Mx-1 Cre

The Mx1-Cre genotyping PCR was performed from DNA extracted as described in the section above (Methods III). The reaction mix was prepared with Taq polymerase from Biorad (Catalog No. 170-8870). 2 µl of template DNA was taken in a total reaction mix of 25 µl volume. 0.5 µl of each of the primers (10mM) were used per reaction for detecting Mx1-Cre of 240 bp. The sequences of the primers are mentioned in the Table-2 and PCR conditions in Table-3.

ii. MLL-ENL Translocation

The detection of MLL-ENL fusion gene was done by PCR using primers previously described in (Cano et al. 2008b). The PCR conditions were performed as described in the paper using Taq polymerase from Biorad (Catalog No. 170-8870). 0.5 µl of Primers (at 10mM stocks) were used in the 25 µl total PCR mix consisting of 2 µl of template DNA. The sequences of primers used are mentioned in the Table-2 and PCR conditions in Table-3.

Table-2: Primer sequences:

	Forward primer (5' → 3')	**Reverse primer (5' → 3')**
Vav1-Cre	GCGGCATGGTGCAAGTTGAAT	CGTTCACCGGCATCAACGTTT
β-actin Cre	CCTGGCGATCCCTGAACATGTCC	CTCTAGAGCCTCTGCTAACC
Mx1-Cre	ACGACCAAGTGACAGCAATG	CTCGACCAGTTTAGT TACCC
MLL Wt	ACCAACAGCAACCCTTTTTG	ATGATGCCACTGTGCTGTGT
MLL-ENL	GTCCCCATAACACCCAGAGTAGTG	CTGGCCTAGGATACAGTCAGTG

Table-3: PCR conditions

Steps	Conditions	Vav1-Cre	β-actin-Cre^{ERT}	Mx1-Cre	MLL-ENL fusion
1	Pre-denaturation	94^{o}C - 2 mins	94^{o}C - 3 mins	94^{o}C - 3 mins	94^{o}C - 3 mins
2	Denaturation	94^{o}C - 20 sec	94^{o}C - 30 sec	94^{o}C - 2 mins	94^{o}C - 30 sec
3	Annealing	58.1^{o}C - 10 sec	51^{o}C - 1 min	63^{o}C - 30 sec	61^{o}C - 30 sec
4	Extension	72^{o}C – 30 sec	72^{o}C - 1 min	72^{o}C – 30 sec	72^{o}C - 30 sec
2 to 4	Number of Cycles	40	30	30	40

iii. Agarose Gel Electrophoresis

7 µl of DNA loading buffer was added to each PCR product (of 25 µl volume). 15 µl of each PCR products with loading buffer were loaded on 2% agarose gel (50004 Lonza, Cultek S.L.) prepared with sybersafe (S33102, Life technologies). PCR products were loaded alongside 5 µl of 100 bp DNA ladder (SM0241, Fermentas) within the electrophoretic tank filled with 1X TAE buffer and run at 90 volts for 20 minutes. The gels were then placed inside a UV-transilluminator and the size of PCR products could be noted by comparing the position of the band with respect to that of the ladder.

V. COMPLETE BLOOD COUNTS ANALYSIS

Complete blood count analysis is a blood test that measures several components and features of blood including the total number of white (leucocytes) and red blood cells (hematocrit) the body. It also evaluates the overall health by detecting infections or leukemia. Peripheral blood was collected from mice by bleeding them from their tail vein one-month post-transplantation or post induction in-vivo and monthly thereafter. Blood samples were analyzed on Advia120 (Siemens) instruments to note complete and differential blood counts.

VI. FLOW CYTOMETRY ANALYSIS

Flow cytometry is an analytical laser- or impedance-based technology used for cell-sorting, cell-counting and biomarker detection by passing cells suspension through electronic detection apparatus. It is a very potent technique that offers a "high-throughput" automated quantification of fluorescent signals from individual cells.

LSRII (BD Biosciences) was used for flow cytometry analysis of bone marrow and peripheral blood cells. The lysis of erythrocytes from peripheral blood samples was performed using ACK lysis buffer as described earlier (Methods III). Post-lysis the samples were washed twice with 1 ml of PBS fetal by centrifugation at 1200 rpm 5 minutes each.

Prior to antibody staining, cells were blocked in 20% rat serum (in fetal PBS) at RT for 15 minutes. Samples were washed once in 1 ml of PBS fetal at 1200 rpm for 5 minutes.

i. Recombination detection

Transformed MLL-ENL:R26-YFP:β-actin Cre^+ cells would express YFP upon Cre-induction. To detect these recombined cells, we performed flow cytometry analysis where YFP^+ cells were detected in the FITC channel. To exclude dead cells 4,6-Diamidino-2-phenylindole (Sigma-Aldrich D9542) was used at 5 μg/ml concentration.

ii. Lineage analysis

Flow cytometry analysis was used to detect contribution of PB/BM cells to different hematopoietic lineages and for identifying leukemic blast populations. Donor, competitor and recipient cells in transplant recipients were detected using antibodies against CD45.1 and CD45.2 surface markers respectively. Donor cells were $CD45.2^+CD45.1^-$, competitor were $CD45.2^+CD45.1^+$ and endogenous recipient cells were $CD45.2^-CD45.1^+$. Myeloid, T- and B-lymphocytes were also detected using lineage specific antibodies.

The antibodies used for all the experiments were against the surface markers sca-1, c-Kit, CD45.1, CD45.2, B220, CD11b, Gr1, CD3, CD4, CD8, and streptavidin. Antibodies were obtained from BD Biosciences Pharmingen or eBioscience.

For staining approximately 1,00,000 PB/BM cells 0.25 μl of antibody was used in 50 μl of PBS fetal. Incubation was done at 4°C for 35-40 minutes in dark. Post-staining, samples were washed once with 1 ml of PBS fetal and centrifuged at 1200 rpm for 5 minutes.

Dead cells were excluded using 5 μg/ml of DAPI (4,6-Diamidino-2-phenylindole (Sigma-Aldrich D9542) staining. Each sample was suspended in about 350 μl of PBS fetal with DAPI and filtered onto cytometry tubes. PBS fetal was used as standard buffer for preparing antibody staining solutions.

VII. PERIPHERAL BLOOD SMEARS

Peripheral blood smears were prepared to observe leukocytosis in parallel with the complete blood counts and flow cytometry analysis. Wright-Giemsa stained peripheral blood smears were prepared to observe the morphology of highly proliferative leukemic blast cells found in circulation upon disease initiation. Smears of peripheral blood were prepared from blood extracted from the tail vein of mice. 5 μl of peripheral blood diluted in fetal PBS at 1:1 ratio was pipetted onto an edge of the adherent side of frost end slides (Sigma-Aldrich S8400). A second, unused slide was placed at a 45-degree angle to the slide to spread the drop of blood across the length of the slide to form an even smear.

Once the smear had air dried Wright-Giemsa staining was carried out to visualize the WBCs morphologically (Methods IX). Giemsa stained PB smears were observed under a light microscope.

VIII. BONE MARROW CYTOSPIN

Bone marrow samples taken from euthanized mice were disaggregated to get single-cell suspension as previously described (Methods I.iv-c). BM cells suspension was prepared at 100 cells/µl volume after counting total cells and preparing the required dilutions.

A clean frost end glass slide was placed onto the metal Cytoclip (Fisher scientific 10-357) with the adherent side facing up. A blot paper of same size as the slide was placed over it with a hole punched in to allow the cells to adhere to the slide only within that periphery. Finally, the Cytofunnel (Thermo fisher scientific 1102548) was aligned on top of it and the Cytoclip was locked to hold the slide, funnel and paper in place. Then 120 µl volume of BM cell suspension was pipetted into the Cytofunnel and the Cytoclip was centrifuged in the Cytocentrifuge (Thermo fisher scientific A78300003) at 1200 rpm for 3 minutes.

At the end of centrifugation, the slides were dismounted carefully and allowed to air dry. Thereafter, Wright-Giemsa staining was performed to observe morphology of the BM cells (Methods IX).

IX. WRIGHT-GIEMSA STAINING

Wright-Giemsa stain is a histologic stain that facilitates the differentiation of blood cell types. It is classically a mixture of eosin (red) and methylene blue dyes used primarily to stain peripheral blood smears and bone marrow cells which are examined under a light microscope. In cytogenetics, it is used to stain chromosomes to facilitate diagnosis of syndromes and diseases.

Wright-Giemsa staining was performed to observe morphology of the BM hematopoietic cells by distinctly staining the nucleus and cytoplasm of cells. The staining was performed on PB smear or BM cytospin that were prepared as described in the sections above (Methods VII and VIII). The slides were placed on a metallic rack and submerged in coplin jars with staining panoptic solutions 1, 2 and 3 sequentially for 30 seconds each (WG16-500ML; WG32-1L; WG80-2.5L; WG128-4L) to fix and perform cytoplasm followed by nuclear staining respectively. The stained slides were then washed in distilled water twice and then allowed to air dry.

X. HISTOLOGICAL ANALYSIS OF ORGANS:

The organs were collected from diseased/euthanized mice to perform histological analyses. The aspects of organs were noted. Splenic aspects (size and weight of the spleens) were measured. If splenomegaly was observed, histological analysis was performed to check for leukemic infiltrates in the peripheral organs.

i. Embedding in paraffin

To observe histology of organs retrieved from mice (Cre^+/control), organ fixation was performed in paraffin or OCT to prepare blocks.

- Organs were fixed overnight in 4%Paraformaldehyde (PFA, P6148 Sigma-Aldrich) away from light.
- Next morning PFA was disposed off carefully and organs were washed with commercially available PBS (02-023-1A, Biological

Industries). Washing was done at RT on the shaker for 30 minutes by changing PBS once every 15 minutes.

- The organs were dehydrated by passing them through a battery of different grades of ethanol (25%, 50%, 75%, 90% and 100% each for 15 minutes at RT on the shaker) and ultimately in Xylene for 30 minutes at RT.
- The organs were then placed in plastic cassettes or embedding mold (Tissue-Tek Ref.4583) to embed them in paraffin.
- Liquid paraffin was poured onto the cassettes/molds containing the organs and incubated at 65°C for at least an hour. The paraffin was changed and incubation was done overnight at 65°C.
- Next morning the paraffin as changed again and incubated for an hour at 65°C. Thereafter blocks were prepared by allowing the paraffin to solidify at RT and blocks were stored at 4°C for short-term use and at -80°C for long-term use.

ii. Embedding in OCT (Optimal Cutting Temperature compound):

For embedding organs in OCT compound (Fisher scientific 23-730-571), the initial fixation was similar to paraffin embedding protocol as described above (Methods X-i). An overnight fixation of organs was performed in 4%PFA at 4°C. The excess PFA was washed off with sterile commercially available PBS for 30 minutes at RT while changing the buffer once.

- Organs were then places in 30% sucrose solution (Sigma Ref. 84097-1KG) at RT on the shaker until the organs sink to the bottom.
- The excess solution was wiped off using a blotting paper before placing the organs in the embedding mold (Tissue-Tek Ref.4583).
- OCT was poured over the organ in mold until the organ was submerged in it, this was done carefully ensuring no bubbles were formed.
- Snap freezing was done of the molds using isopentane mixed with dry ice. The OCT blocks were then stored at -80 ^{o}C

XI. HEMATOXYLIN - EOSIN STAINING

The histological analysis of organs was done by performing Hematoxylin-Eosin staining of organs sections. 8-10 μm thick sections were cut on the microtome from paraffin blocks of organs.

Hematoxylin and Eosin staining is the most widely used staining in histology to confirm the integrity of the tissue and its cellular composition and organization. Hematoxylin is a dark blue/violet stain that is basic (positive) and binds to basophilic substances, such as the DNA and RNA (which are acidic and negatively charged). Eosin is a red/pink stain that is acidic (negative). It binds to acidophilic (also known as eosinophilic) substances, such as positively charged amino acid side chains. Most proteins in the cytoplasm and in the extracellular matrix are basic (positively charged due to arginine or lysine amino acidic residues), so they stain in varying degrees of pink.

Prior to performing the staining, slides were dewaxed.

Dewaxing and Rehydration

- Slides were heated at 65°C for 1-2 hours (or overnight if they were re-paraffinated for long-term storage).
- Slides were passed through xylene and 100% ethanol for 20 minutes each followed by passage through grades of 96%, 70% and 50% of ethanol for 10 minutes each.

Staining

- The slides were washed with distilled water for 10 minutes at RT and stained with Hematoxylin staining solution for 30 seconds.
- This was followed by washing off the excess stain by passing slides in a coplin jar of tap water for apt toning of the Hematoxylin stain.
- The slides were then passed through 80% ethanol with 0.15% HCl for 30 seconds followed by treatment with ammonia water (0.3%) for 30 seconds; with intermediate washes in distilled water.
- Slides were then placed in 96% ethanol solution for 5 minutes
- Thereafter, Eosin staining was performed by placing slides in Eosin staining solution for 5 seconds.
- The slides were then passed through the dehydration battery of 100% ethanol followed by xylene treatments for 10 minutes each. Slides were then mounted with DPX (Merck Ref. 1.01979.0500) and allowed to air dry overnight and stored at RT.

RESULTS

RESULTS PART-1

CHARACTERIZATION OF MLL-ENL TRANSLOCATION T(11;19) INDUCED LEUKEMIA

CONSTITUTIVELY ACTIVE VAV1-CRE:MLL^{LoxP}ENL^{LoxP} MOUSE MODEL

Studying MLL-ENL leukemia using the constitutively active, hematopoietic specific Vav1-Cre mouse model:

The MLL-ENL translocation t(11;19) can give rise to either an acute myeloid leukemia (AML), acute lymphoblastic leukemia (ALL) or mixed leukemia in humans (Pui et al. 1994; Rubnitz et al. 1999; Forster, Pannell, Lesley F Drynan, et al. 2003). We wanted to first study and characterize the disease driven by this translocation in mice. In order to do so, we made use of the Vav1-Cre mice (Stadtfeld & Graf 2005).

The Vav1 gene is expressed selectively in the hematopoietic compartment and Vav1-Cre is constitutively active from E11 onwards in the mouse embryo and it is active throughout adulthood (Bustelo et al. 1993).

To develop the leukemia model MLL-LoxP,ENL-LoxP mice were crossed with Vav1-Cre mice to allow translocation to occur in-vivo and to follow MLL-ENL fusion driven disease in the Cre^+ progeny (Fig. R1-A).

Cre activation during embryonic development was confirmed by detecting the MLL-ENL fusion gene by PCR in the embryonic tissues at E11 (Fig. R1-B). DNA was extracted from AGM and FL tissues of E11 MLL-ENL:Vav1-Cre^+/control embryos and the MLL-ENL fusion gene could be detected in both the tissues confirming Cre activation and efficient Cre-mediated recombination (Fig. R1-B).

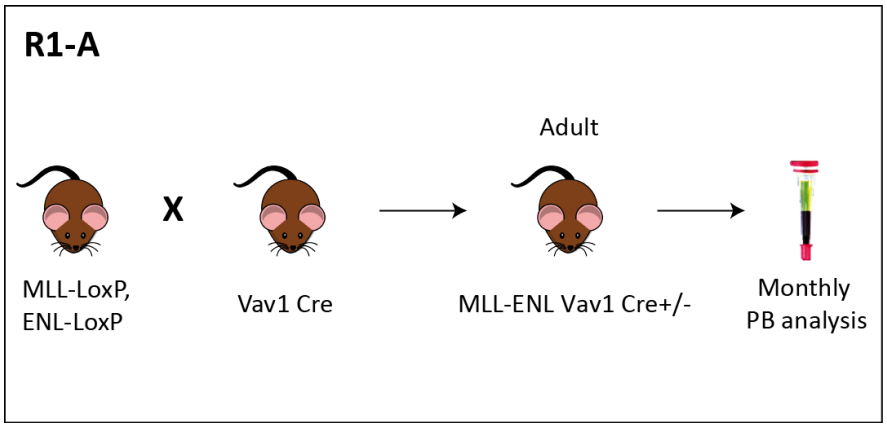

R1 A: Experimental strategy used to develop an in-vivo MLL-ENL leukemia model using the constitutively active Vav1-Cre: The MLL-LoxP, ENL-LoxP mice were crossed with Vav1-Cre mice. One-month old adults (P30) MLL-ENL:Vav1-Cre^{+} and control littermates from the crossing, were bled from the tail vein and blood analyses was conducted monthly thereafter. MLL: mixed lineage leukemia, ENL: eleven-nineteen leukemia, PB: peripheral blood, P30: 1 month old mice (postnatal age of mice)

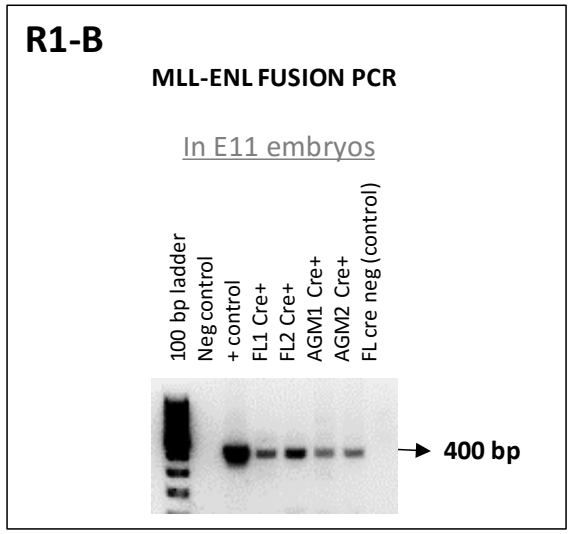

R1 B: Detecting MLL-ENL fusion gene in embryonic tissues: PCR was performed to detect the MLL-ENL fusion gene (400bp) as previously described (Cano et al. 2008b) using DNA extracted from the AGM and FL tissues of MLL-ENL,Vav1-Cre^{+}/control embryos. The PCR products were run on 2% agarose gel alongside 100bp DNA ladder. MLL: mixed lineage leukemia, ENL: eleven-nineteen leukemia, PCR: polymerase chain reaction, bp: base pairs, DNA: Deoxyribonucleic acid, AGM: aorta-gonads-mesonephros, FL: fetal liver, E11: embryonic age of 11 (days post-coitus)

All MLL-ENL:Vav1-Cre^{+} mice developed a lethal disease in less than 90 days of age while control mice remained healthy (Fig. R1-C).

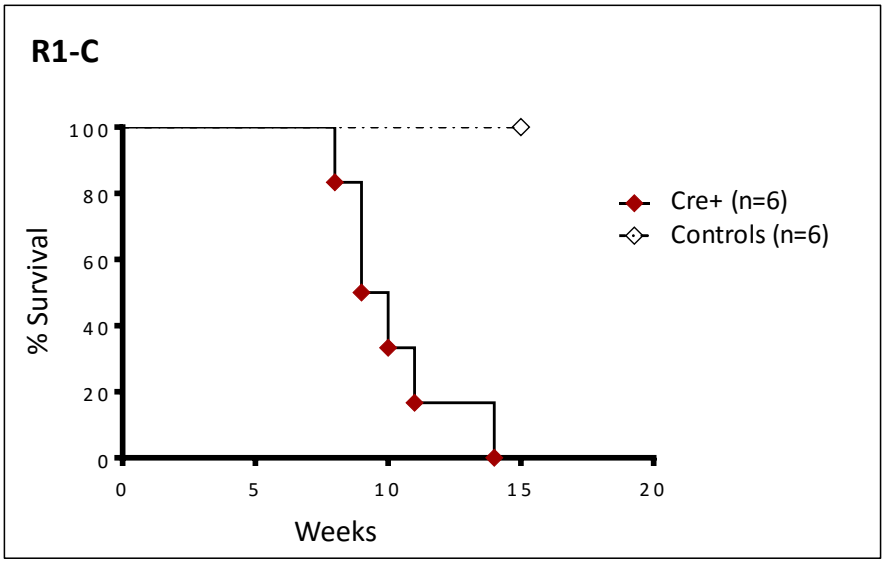

R1 C: Kaplan-Meier survival curve represents the median survival of MLL-ENL:Vav1-Cre^{+} and control mice. Data is shown for n=6 mice each. MLL: mixed lineage leukemia, ENL: eleven-nineteen leukemia.

At the point of terminal illness, mice were euthanized and organs (such as spleen, femurs, liver, lungs) were collected for further analysis. The presence of the MLL-ENL fusion gene was confirmed within BM cells of the leukemic mice by performing PCR (Fig. R1-D).

Prior to that, the disease in Cre^{+} mice was characterized during the monthly blood analyses. The first time-point of this analysis was post-weening at 1 month of age (P30) of Cre^{+} and control (cre negative) mice. The mice were bled from the tail vein and PB analyses were performed to detect disease onset and to follow its progression.

Complete blood count (CBC) analysis was performed to detect total number of leucocytes present in the mice. We could detect disease onset by the second month of blood analysis (P60) (Fig.R1-E).

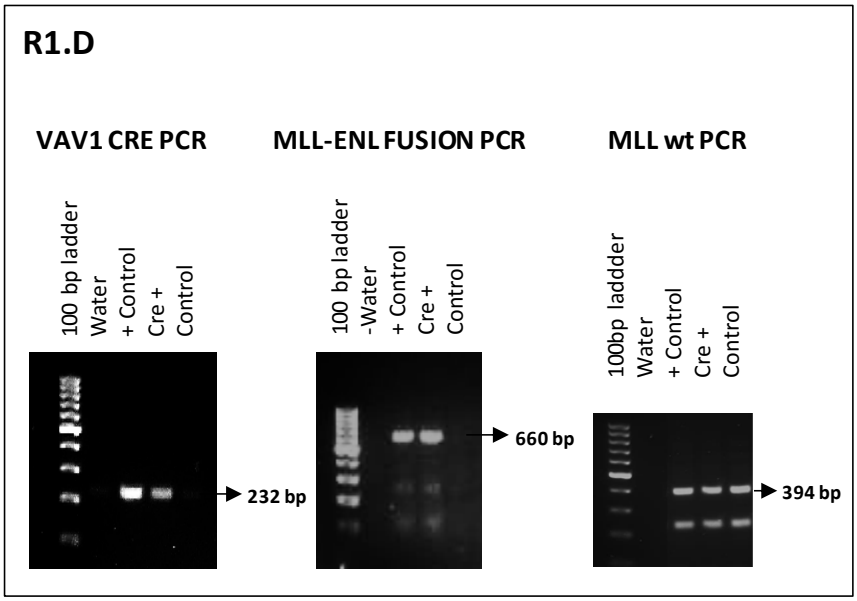

R1 D: Detecting MLL-ENL fusion gene by PCR in diseased mice: DNA was extracted from BM of Cre^+/control mice to perform these PCRs. Left panel - Genotyping PCR was performed to detect presence of Cre gene (232bp) to note the lack of Cre expression in controls. Middle panel – MLL-ENL fusion gene (660bp) was detected by PCR. Right panel – A control PCR was performed to detect the wildtype MLL gene (394bp) which would be present in both Cre^+ and control mice. The PCR products were run on 2% agarose gel alongside the 100bp DNA ladder. Representative gel pictures are shown here. MLL: mixed lineage leukemia, ENL: eleven-nineteen leukemia, PCR: polymerase chain reaction, wt: wildtype, bp: base pairs, DNA: Deoxyribonucleic acid

The differential blood counts at 2 months of age (P60) showed a significant increase in the total white blood cells (WBCs) of Cre^+ mice (>10 fold higher) when compared to the controls (Fig.R1-E). Control mice had WBCs within the normal range (2.6×10^9 – 13.2×10^9/l). Leucocytosis was found in Cre^+ mice resulting from the MLL-ENL translocation.

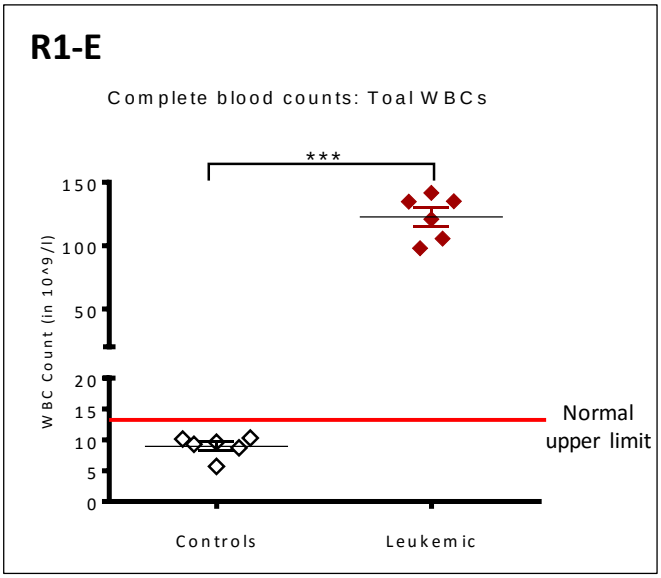

R1 E: Complete blood count (CBC) analysis: Total WBCs counts (x 10^9/liter) in PB of Cre^+/control mice were analyzed using a hemocytometer on a monthly basis. Cre^+ mice at 2 months of age (P60) showed a significantly higher number of WBCs (up to 150 x10^9/l) when compared to controls that had WBCs (<13 x 10^9/liter) within the normal range. Statistical analysis was performed using the Student's t-test (*** : $p<0.001$). PB: peripheral blood, NUL: normal upper limit, WBC: white blood cells

These results concurred with the findings of Wright-Giemsa stained peripheral blood smears (Fig. R1-F) wherein, significantly higher number of WBCs were found in circulation in Cre^+ mice, when compared to controls.

Morphological observations of WBCs from Cre^+ mice under the microscope showed presence of largely granulocytes (eosinophils, basophils, neutrophils) (Fig. R1-F). The disease in these mice progressed rapidly after the second month (P60 onwards) and it was fatal by the 3rd month (P90) (Fig. R1-C). Whereas the control mice remained healthy.

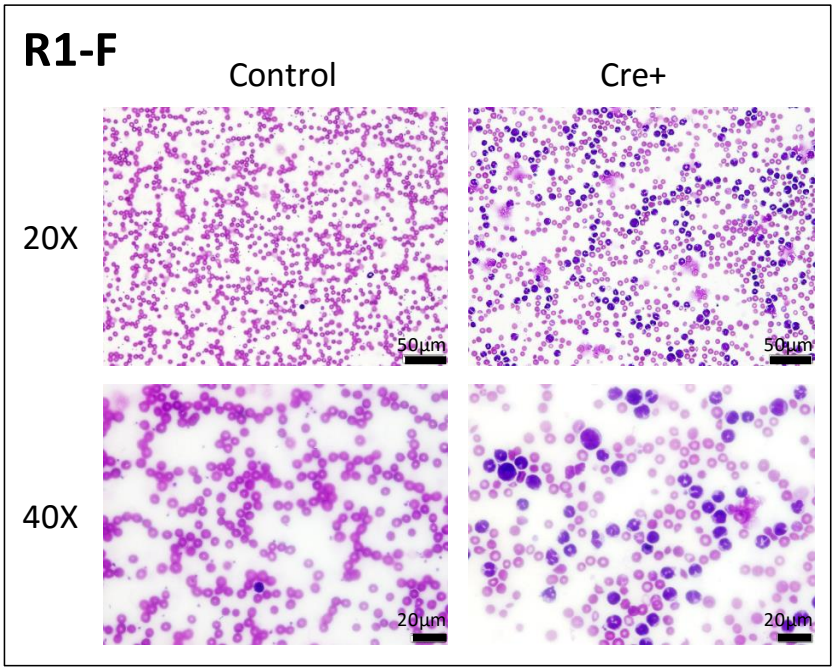

R1 F: Peripheral blood smears: Representative Wright-Giemsa staining was performed on PB smears of control and Cre$^+$ mice at second month of analysis (P60 stage). Two different magnifications, 20X and 40X are shown. PB: peripheral blood, P60: 2 months old mice (postnatal age of mice)

We further characterized the leukemia by flow cytometry analysis of PB samples to identify the blast load population. PB cells were stained with antibodies against specific blood cell lineages.

Similar to our findings of disease onset by CBCs and PB smear analyses, we observed a drastic change in lineage distribution of PB cells in Cre$^+$ mice from P30 to P60 stage (Fig.R1-G,H).

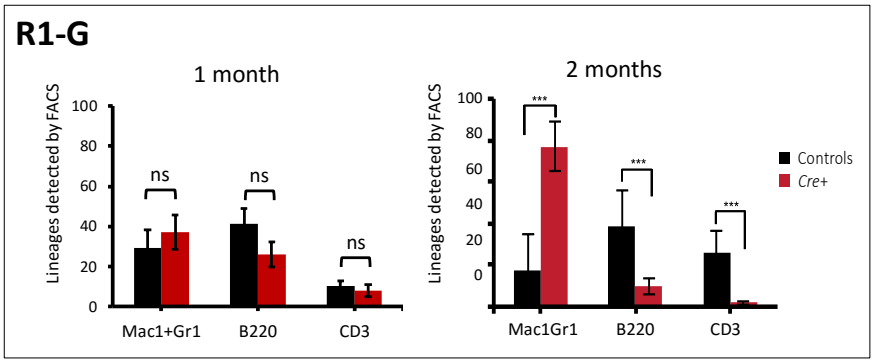

R1 G: Leukemic blast load detection: Flow cytometry analysis of blood cell lineages from MLL-ENL:Vav1-Cre^{+}/control mice was performed monthly. PB cells were stained with antibodies against the surface markers Mac1, Gr1, B220 and CD3e to detect myeloid, B- and T-lymphocyte populations respectively. The blood analysis of control versus Cre^{+} mice at P30 and P60 stages are shown above. Values are represented as Mean±SD (n=6 each). Student's t-test was performed for statistical analysis (*** : $p<0.001$, ns [not significant]: $p>0.05$). MLL: mixed lineage leukemia, ENL: eleven-nineteen leukemia, PB: peripheral blood.

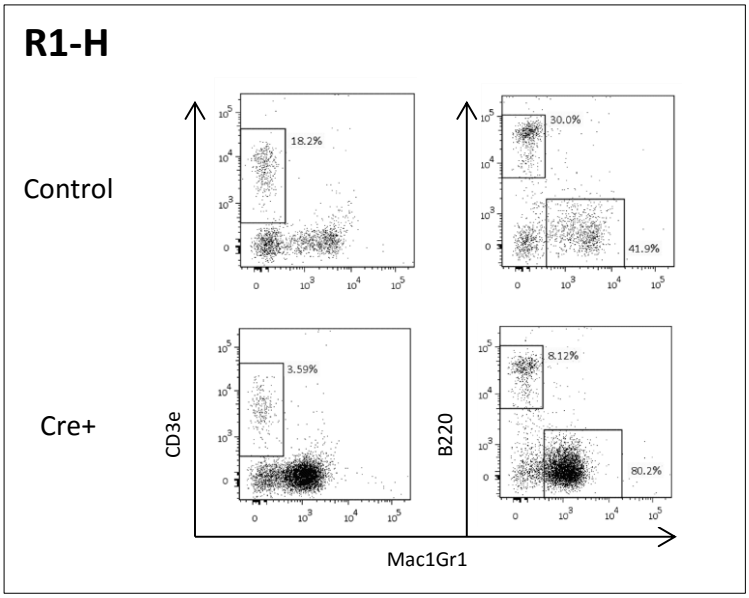

R1 H: Identifying leukemic blast load by flow cytometry: Representative flow cytometry plots of Cre^{+} (lower row) and control (upper row) PB analysis at 2 months of age (P60) are shown here. Antibodies against CD3e, B220, Mac1 and Gr1 were used to stain PB cells for detecting the distinct blood cell lineages. PB: peripheral blood, P60: postnatal age of mice of 60 days

There was a significant increase in contribution of PB cells to the myeloid compartment in Cre$^+$ mice as opposed to the normal distribution to myeloid and lymphocyte lineages found in control mice (Fig.R1-G). The majority of blood cells in Cre$^+$ mice by P60 stage were Mac1$^+$Gr1$^+$ (Fig.R1-H).

The final analysis of diseased Cre$^+$ mice were performed in a similar manner with leukemic blasts detection within the bone marrow of these mice by flow cytometry analysis (Fig.R1-I). The majority of BM cells (>90%) were myeloid (Mac1$^+$Gr1$^+$ cells) in Cre$^+$ mice similar to what was found in PB analysis at P60 stage (Fig.R1-I).

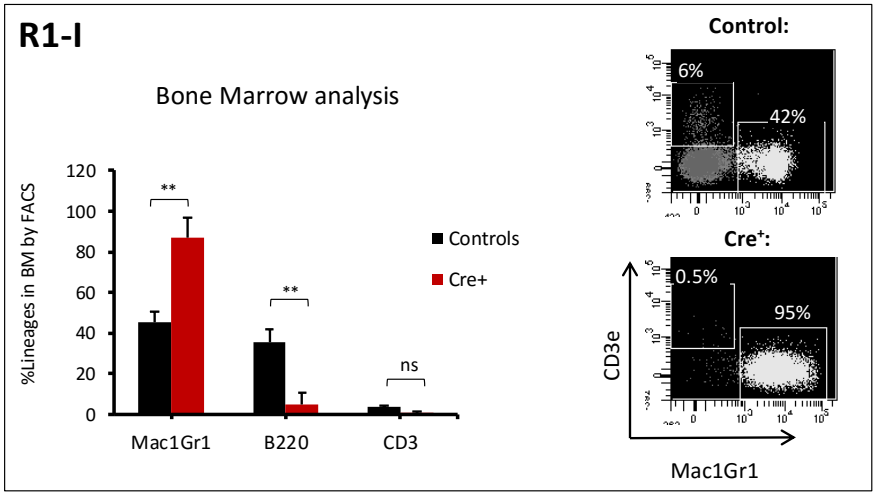

R1 I: Lineage distribution analysis of BM cells from MLL-ENL,Vav1-Cre$^+$/control mice was performed by FACS. BM cells were stained with antibodies against Mac1, Gr1, B220 and CD3e to detect myeloid, B- and T-lymphocyte populations respectively. Values are represented as Mean±SD with n=6 mice per group. Student's t-test was performed for statisical analysis (** : $p<0.01$, ns [not significant]: $p>0.05$). Representative FACS plots are represented in the right panel. MLL: mixed lineage leukemia, ENL: eleven-nineteen leukemia, BM: bone marrow, FACS: fluorescent-activated cell sorting

In humans, MLL-rearranged leukemias result in leukemic infiltration in multiple organs. Therefore, we checked for infiltration in the current mouse model as well. Different peripheral organs were collected from diseased Cre^+ mice.

Splenomegaly was clearly visible in Cre^+ leukemic mice when compared to normal spleens of control mice (Fig. R1-J).

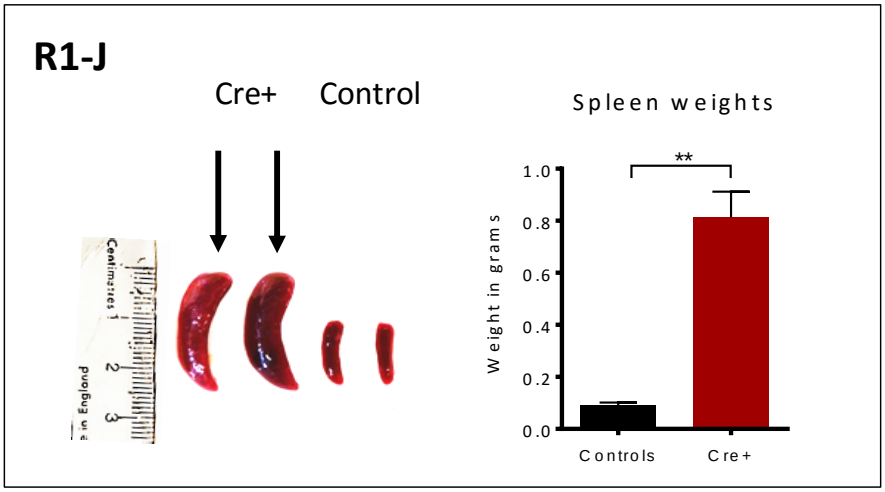

R1 J: Splenomegaly was observed in Cre^+ leukemic mice (arrows) when compared to controls. Representative pictures of spleens from Cre^+ and control mice are shown. Quantifications of weights of Cre^+ versus control spleens are shown. Values are represented as Mean±SD with n=6 mice per group. Student's t-test was performed for statistical significance (** : $p<0.01$)

We performed Hematoxylin-Eosin staining of paraffin embedded peripheral organs sections (including the spleen, liver and lungs) from Cre^+ and control mice and we could detect leukemic infiltrates within various sites of these organs (Fig.R1-K).

The red and white pulp regions of the spleens from Cre^+ mice were completely disrupted as a result of the disease (Fig.R1-K Right panel). Leukemic infiltrates could also be detected in the lungs and in the liver

invading through the vasculature and colonizing distinct lobes (Fig.R1-K Middle and Left panel).

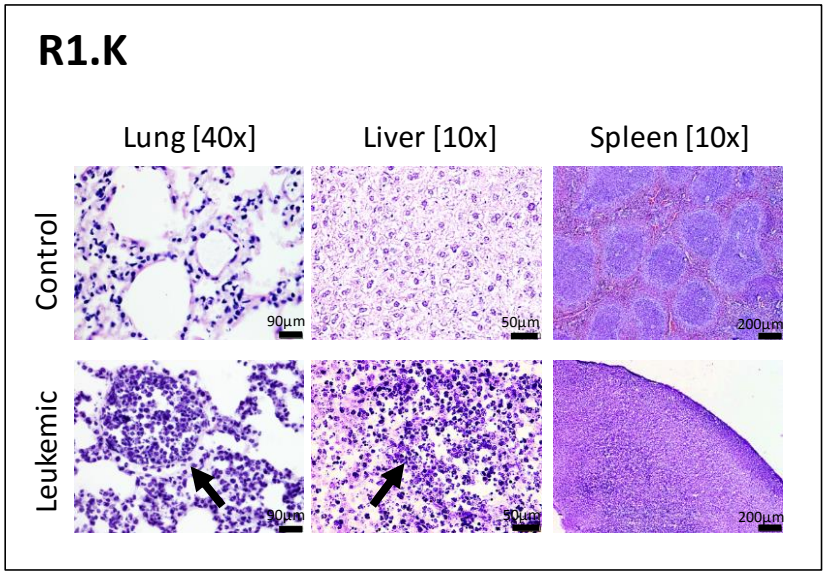

R1 K: Leukemic infiltration detection: Hematoxylin-Eosin staining was performed on paraffin embedded sections (10 µm thick) of organs (livers, lungs and spleens) collected from euthanized MLL-ENL:Vav1-Cre$^+$/control mice. Leukemic infiltrates (arrows) were detected in all three organs of diseased Cre$^+$ mice while the organs of control mice had normal histology. Representative pictures are shown here at the designated magnifications. MLL: mixed lineage leukemia, ENL: eleven-nineteen leukemia

With this model we could conclude that Vav1-Cre-mediated MLL-ENL translocation led to development of an acute myeloid leukemia in mice.

RESULTS PART-2

DEVELOPING T(11;19) INDUCED LEUKEMIA MOUSE MODEL:

Recapitulating human pediatric and adult leukemias

INDUCIBLE B-ACTIN CRE^{ERT}:MLL^{LoxP} ENL^{LoxP} MOUSE MODEL

Developing embryonic and adult MLL-ENL leukemia mice models using the inducible β-actin Cre^{ERT}:

The constitutively active Vav1-Cre aided in establishing and characterising MLL-ENL driven AML disease in mice. However, the constitutive nature of Vav1-Cre was a drawback as the timing of Cre-mediated translocation initiation could not be controlled. Therefore, we used an inducible Cre model to induce MLL-ENL translocation at the desired stages of hematopoietic development. The tamoxifen inducible β-actin Cre^{ERT} mice, generated in the lab of Dr. Andrew McMahon (Hayashi & McMahon 2002), were crossed with the R26-YFP LoxP-STOP-LoxP mice in order to follow the recombined cells by YFP-expression. The β-actin Cre^{ERT}:R26-YFP mice were then crossed with the MLL-LoxP, ENL-LoxP mice (Collins et al. 2000).

Since one feature of infant leukemias is that they develop in-utero, we aimed to model this disease by performing Cre-induction at different stages of embryonic hematopoietic development (Fig. R2):

(i) in the aorta-gonads-mesonephros (AGM) region around E10.5 stage (Medvinsky et al. 1993; Müller et al. 1994; Dzierzak 2002);

(ii) in the fetal liver (FL) at E12.5, where they undergo expansion until E16 (North et al. 1999; Jaffredo et al. 2003; North et al. 2002).

To be able to compare the leukemias derived from embryonic cells with adult hematopoietic cells, we performed Cre-induction in two months old (P60) mice to target hematopoietic cells within the bone marrow (BM) tissue.

The different strategies we used to develop the embryonic and adult MLL-ENL leukemia models using the inducible β-actin Cre^{ERT} mice were (Fig. R2):

Strategy I: Competitive transplantation of in-vitro induced embryonic and adult hematopoietic tissues into lethally irradiated adult recipients

Strategy II: In-vivo induction of recombination at embryonic and adult stages

Strategy III: Competitive transplantation of in-vivo induced embryonic and adult hematopoietic tissues into lethally irradiated adult recipients

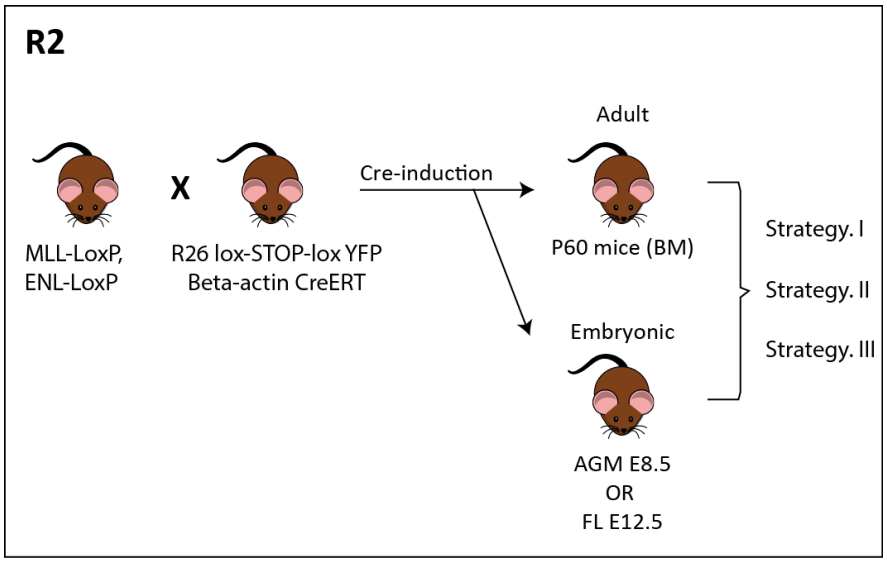

R2: Experimental strategies implemented for developing embryonic and adult MLL-ENL leukemia models using the inducible β-actin Cre^{ERT}:R26-YFP mice: MLL-LoxP,ENL-LoxP mice were crossed with β-actin Cre^{ERT}:R26-YFP mice. Three distinct strategies were implemented for performing Cre-inductions in embryonic (E8.5 AGMs/E12.5 FLs) and adult (P60 mice BM) hematopoietic tissues to develop MLL-ENL driven leukemia models. MLL: mixed lineage leukemia, ENL: eleven-nineteen leukemia, AGM: aorta-gonads-mesonephros, E8.5/12.5: embryonic age of 8.5/12.5 (days post-coitus), BM: bone marrow, P60: 60 days post-birth

Strategy - I

Competitive transplantation of in-vitro induced embryonic and adult hematopoietic tissues into lethally irradiated adult recipients

The first strategy we implemented to initiate Cre-mediated recombination was in-vitro induction using 4-hydroxytamoxifen (4-OHT) (R2.I-A).

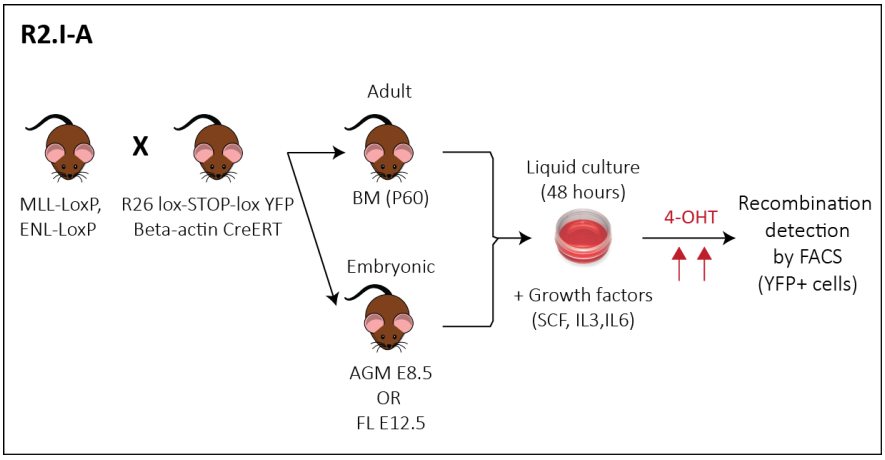

R2.I - A: Strategy I – The Experimental set up for in-vitro induction of β-actin Cre^{ERT} mice: MLL-LoxP, ENL-LoxP mice were crossed with β-actin Cre^{ERT}:R26-YFP mice. Single cells from E10.5 AGM, E12.5 FL, P60 BM tissues were cultured in-vitro in Isscove's culture medium along with growth factors (such as SCF, IL3, IL6) and maintained for 48 hours. To initiate Cre-mediated recombination, 4 hydroxy-tamoxifen (4-OHT) was added to the cultures. Titrations were performed to optimize the dose of 4-OHT. We tested different concentrations of the compound (within the range of 100nM - 10μM as listed in Table-1), by adding it to the cell cultures for two consecutive days. Recombination efficiency was assessed by detecting YFP^{+} cells at the end of the two-day culture by flow cytometry analysis. MLL: mixed lineage leukemia, ENL: eleven-nineteen leukemia, AGM: aorta-gonads-mesonephros, E8.5/12.5: embryonic stage of 8.5/12.5 (days post-coitus), BM: bone marrow, P60: 60 days post-birth, SCF: stem cell factor, IL: Interleukin

We collected embryonic and adult hematopoietic tissues at different stages of hematopoietic development (E10.5 AGMs/E12.5 FLs/P60 BM). The single-cell suspensions were maintained in culture for two days.

To optimize the dose for embryonic and adult tissues, titrations of 4-OHT were performed in-vitro by adding 4-OHT to liquid cultures at increasing concentrations (as listed in Table-1).

YFP-expression was detected by flow cytometry to assess Cre-mediated recombination efficiency (Fig. R2.I-B). Although results obtained by the use of 5 μM or 10 μM concentrations of 4-OHT resulted in similar recombination efficiencies, we opted to use 5 μM/day dose as it was less toxic to cells in culture.

The optimal dose of 4-OHT used in-vitro for all three tissues (AGM, FL and BM) was 5 μM/day for two consecutive days.

With the optimized in-vitro induction strategy, we were able to obtain average induction efficiencies of 75%, 40% and 20% in the AGM, FL and BM tissues respectively (by measuring YFP^+ cells by FACS) (Fig. R2.I-B). Significantly lower YFP-expression was obtained in the adult tissue when compared to the embryonic tissues.

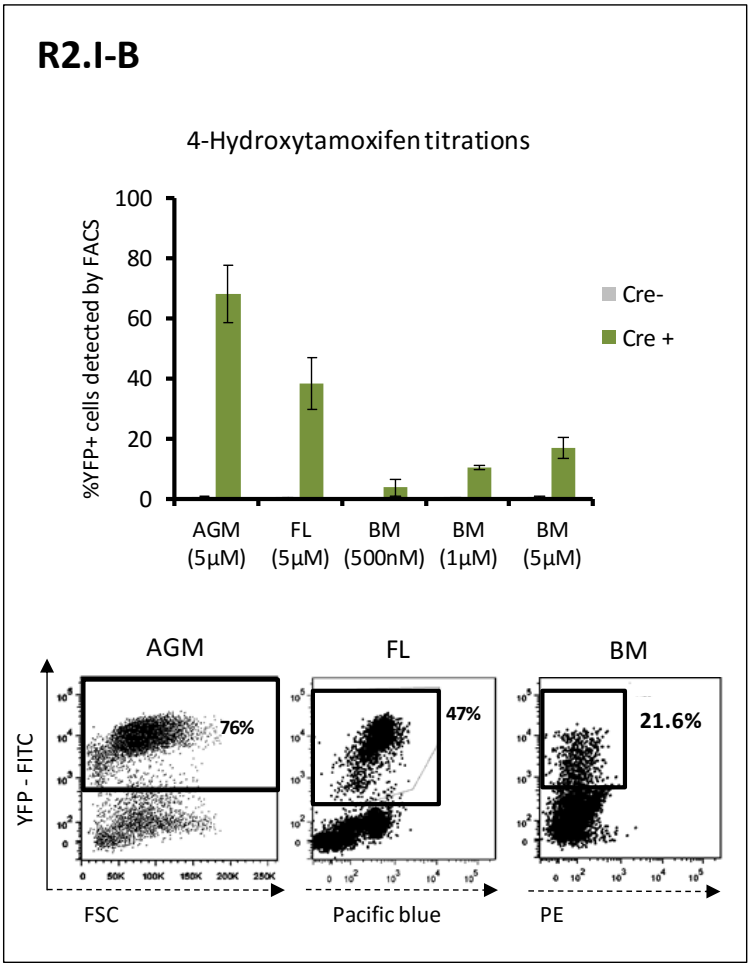

R2.I - B: Recombination efficiency post-4-OHT titrations in-vitro – Titrations of 4-hydroxytamoxifen were performed in-vitro and the optimal dose of use was 5µM/day for two consecutive days in liquid cultures of AGM, FL and BM cells. YFP$^+$ cells were detected in the FITC channel by flow cytometry analysis. Upper panel - Quantifications of recombination efficiency achieved in the three tissues at distinct concentrations of 4-OHT are represented. Pooled data of three independent experiments are shown above. Lower panel - Representative flow cytometry plots of YFP$^+$ cells obtained in AGM, FL and BM tissues post in-vitro inductions are shown. For the inductions in embryonic tissues, one experiment constitutes pool of Cre$^+$/ Cre$^-$ (control) littermates from one pregnant mouse. For adult (BM) induction, one experiment constitutes BM cells from one adult MLL-ENL:R26-YFP:β-actin Cre$^+$/control mouse each. Values are represented as Mean±SD. AGM: aorta-gonads-mesonephros, E8.5/12.5: embryonic stage of 8.5/12.5 (days post-coitus), BM: bone marrow, P60: postnatal age of mice of 60 days

Table-1: 4-hydroxytamoxifen titrations in-vitro

Tissue		Concentration	% YFP$^+$ cells
Whole BM		100 nM	1.21
		500 nM	2.96
		1 μM	5.15
		5 μM	10.68
		10 μM	9.867
Ficoll fractionated:	**50,000 cells**	500 nm	11.7
		1 μm	10.6
		5 μm	13.1
	100,000 cells	500 nm	10.1
		1 μm	11
		5 μm	21.6
AGM	**Liquid culture**	5 μm	62%
	Explant	5 μm	35%
Fetal Liver		5 μm	54%

Highlighted boxes (in pista) represent the maximum recombination obtained in the respective tissues. Values are represented as Mean±SD from three independent experiments each.

The in-vitro induced E10.5 AGM/E12.5 FL/P60 BM cells from recombined versus control mice were then transplanted competitively into lethally irradiated adult mice to develop the embryonic- and adult-derived leukemia models (Fig. R2.I-C).

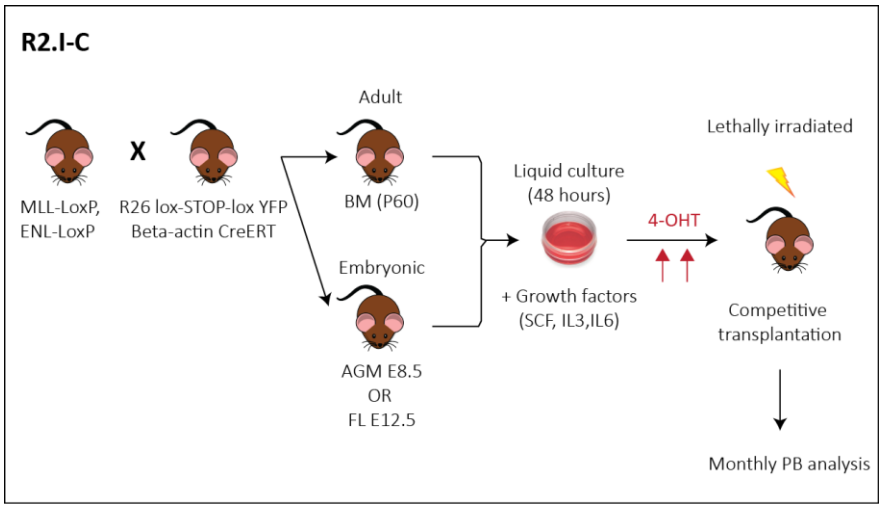

R2.I - C: Comparing transformation capacities of AGM/FL/BM tissues: The in-vitro induction of E10.5 AGM/E12.5 FL/P60 BM cells was done using 5μM of 4-OHT/day for two consecutive days. The induced recombined and control donor cells (CD45.2) were transplanted competitively into lethally irradiated (4Gy, 2 doses) CD45.1 recipient mice. 1 e.e. AGM/1 e.e. FL/10 million P60 BM donor cells with 200,000 whole BM competitor cells from CD45.1-CD45.2 mice were transplanted retro-orbitally into lethally irradiated recipients. One-month post-transplantations, the recipients were bled from tail vein and PB analysis was performed by FACS. MLL: mixed lineage leukemia, ENL: eleven-nineteen leukemia, AGM: aorta-gonads-mesonephros, E8.5/12.5: embryonic age of 8.5/12.5 (days' post-coitus), BM: bone marrow, P60: 60 days post-birth, SCF: stem cell factor, IL: Interleukin, PB: peripheral blood, e.e.: embryo equivalence, FACS: fluorescence-activated cell sorting

The in-vitro induced Cre^{+} or control donor (1 e.e AGM/1 e.e FL/10 million whole BM) cells of CD45.2 strain were transplanted per recipient mouse (CD45.1) alongwith 200,000 normal whole BM competitor cells (CD45.1-CD45.2 strain). Using mice with allelic variants of CD45 allowed distinguishing between the donor, competitor and host cells in the follow-up analyses by FACS. Four weeks post-transplantations, the transplant recipients were bled and PB was analyzed by FACS to detect donor engraftment and lineage contribution of donor-derived cells within the recipient mice (Fig. R2.1-E,F).

The MLL-ENL fusion gene was detected by PCR (Fig. R2.1-D). However, we did not find the MLL-ENL fusion gene in any of the recipients (Cre^+ AGM/FL/BM tissues) at any point of the monthly analyses.

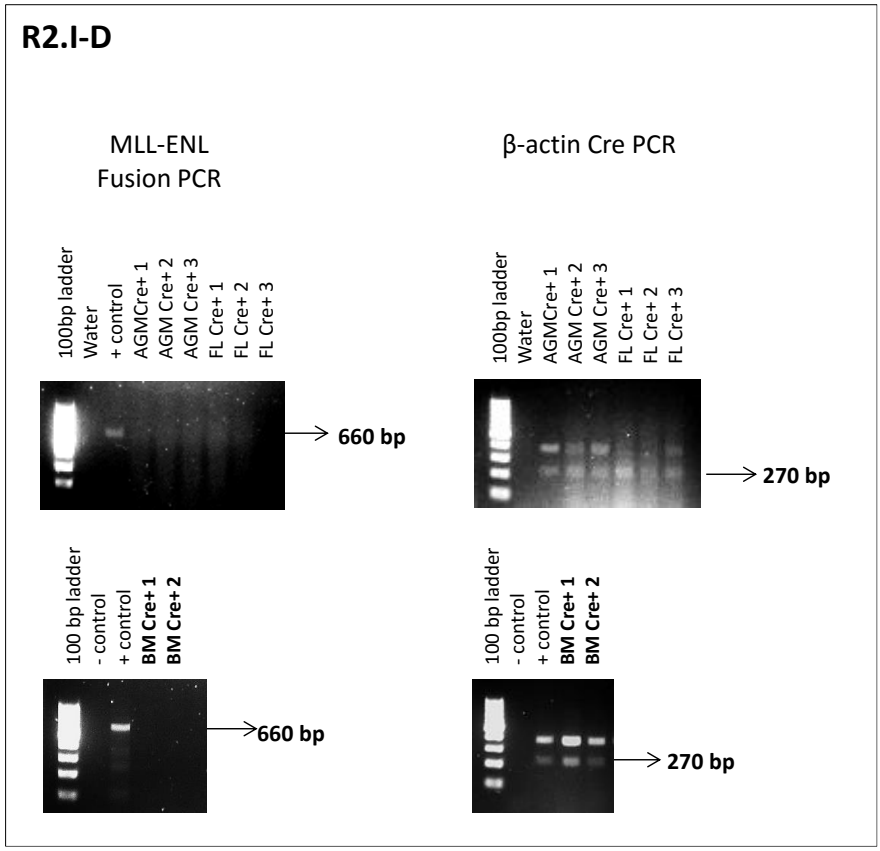

R2.I - D: Translocation detection by PCR: DNA was extracted from BM of all transplant recipients. Left panel- MLL-ENL fusion gene (400bp) was detected by PCR as previously described (Cano et al. 2008b). Right panel: Genotyping PCR was performed to detect the Cre gene (270bp). PCR products were run on 2% agarose gel alongside 100bp DNA ladder. MLL: mixed lineage leukemia, ENL: eleven-nineteen leukemia, AGM: aorta-gonads-mesonephros, E8.5/12.5: embryonic age of 8.5/12.5 (days post-coitus), DNA: deoxyribonucleic acid, bp: base pairs, BM: bone marrow, P60: postnatal age of mice of 60 days, PCR: polymerase chain reaction

Consistent with lack of recombination, no disease development was observed in these mice.

The blood analyses of recipient mice transplanted with Cre^+ and control tissues (AGM/FL/BM) showed similar levels of donor engraftment, and donor-derived cells in these recipients had similar contributions to myeloid and lymphocyte (B and T) lineages (Fig. R2.I-G).

At the end-point (270 days post-transplantations), BM cells were analyzed by FACS and detection of fusion gene was performed by PCR (Fig. R2.I-G).

We detected donor contribution ($CD45.2^+$ cells) as well as YFP-expression in the BM of transplant recipients by FACS (Fig. R2.1-E,F). In average, donor engraftment was 24%, 68% and 90% of Cre^+ AGM, FL and BM cells respectively (Fig.R2.I-E).

Although the donor engraftment of AGM cells was significantly lower than that of FL or BM cells, similar YFP-recombination efficiencies were obtained in all Cre^+ recipients. The average YFP-recombination achieved in all Cre^+ transplant recipients ($CD45.2^+YFP^+$) was 42% (Fig. R2.I-F).

Further, lineage contribution of donor-derived cells in the BM of euthanized transplant recipients was detected by flow cytometry analysis (Fig. R2.I-G).

There was a lack of disease development in all Cre^+ transplant recipients (AGM, FL and BM) likely resulting from inefficient MLL-ENL translocation (Fig. R2.1-D).

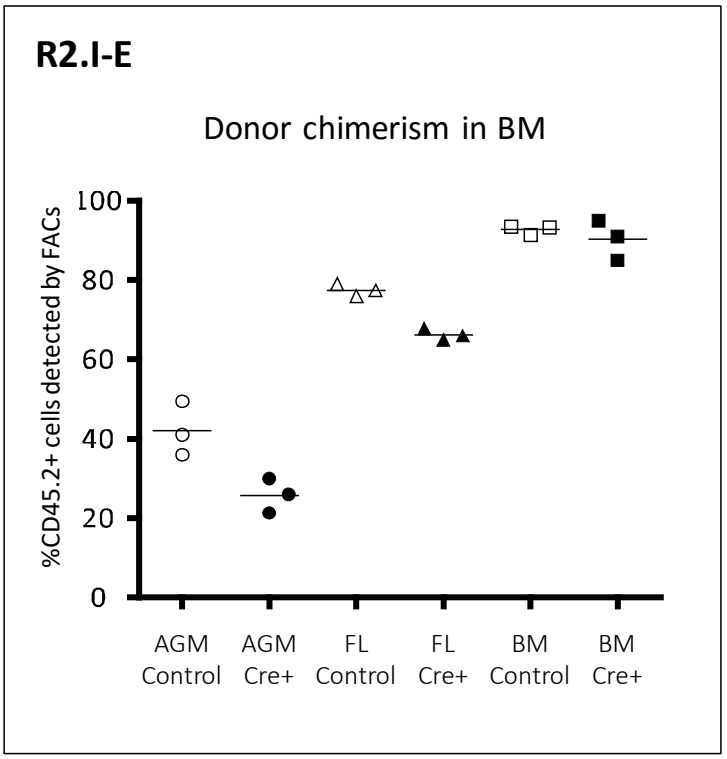

R2.I - E: Donor chimerism in BM of transplant recipients: BM cells collected from euthanized (AGM, FL and BM) Cre^+ and control transplant recipients were analyzed by FACS. BM cells were stained with antibodies against surface markers CD45.1 and CD45.2, to detect the distinct donor, competitor and host populations. Donor engraftment was detected as $CD45.2^+$ $CD45.1^-$ population which is plotted for each of the recipients in this graph. Three recipients each were transplanted with Cre^+ or control donor cells from each of the AGM/FL/BM tissues. AGM: aorta-gonads-mesonephros, E8.5/12.5: embryonic stage of 8.5/12.5 days post-coitus, BM: bone marrow, P60: 60 days post-birth, FACS: fluorescence-activated cell sorting

Concurring with this, we detected no differences in donor contribution to myeloid and lymphocyte (B and T) cells in the BM of all Cre^+ and control transplant recipients (Fig. R2.I-G).

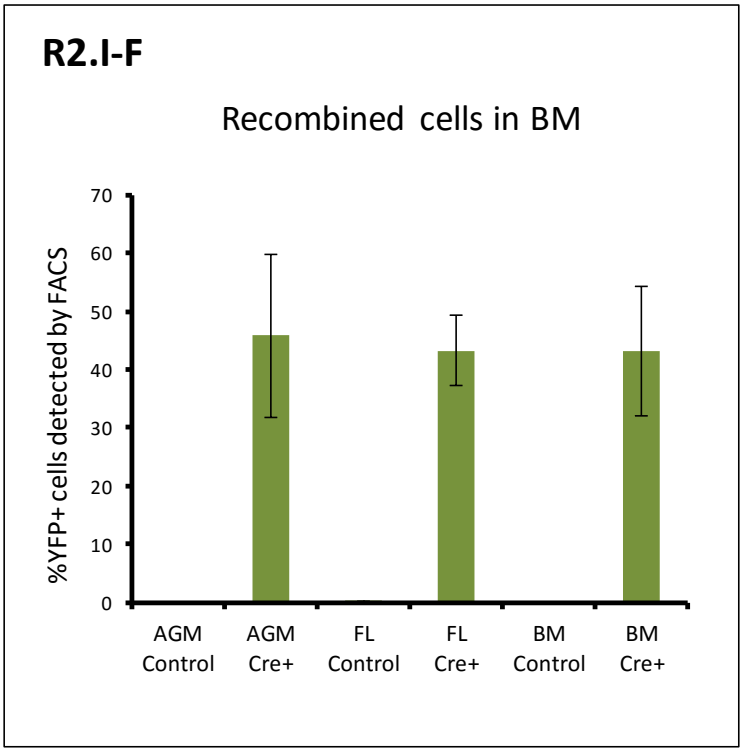

R2.I - F: YFP-recombination in BM of transplant recipients - BM cells of Cre^+ and control AGM/FL/BM transplant recipients were analyzed by flow cytometry for detecting recombination efficiency. YFP^+ cells were detected in the FITC channel by FACS. All Cre^+ transplant recipients (AGM/FL/BM) showed an average YFP recombination efficiency of 42%. No YFP^+ cells were found in controls as expected. Values are represented as Mean±SD. MLL: mixed lineage leukemia, ENL: eleven-nineteen leukemia, AGM: aorta-gonads-mesonephros, E8.5/12.5: embryonic age of 8.5/12.5 (days post-coitus), BM: bone marrow, P60: postnatal age of mice of 60 days

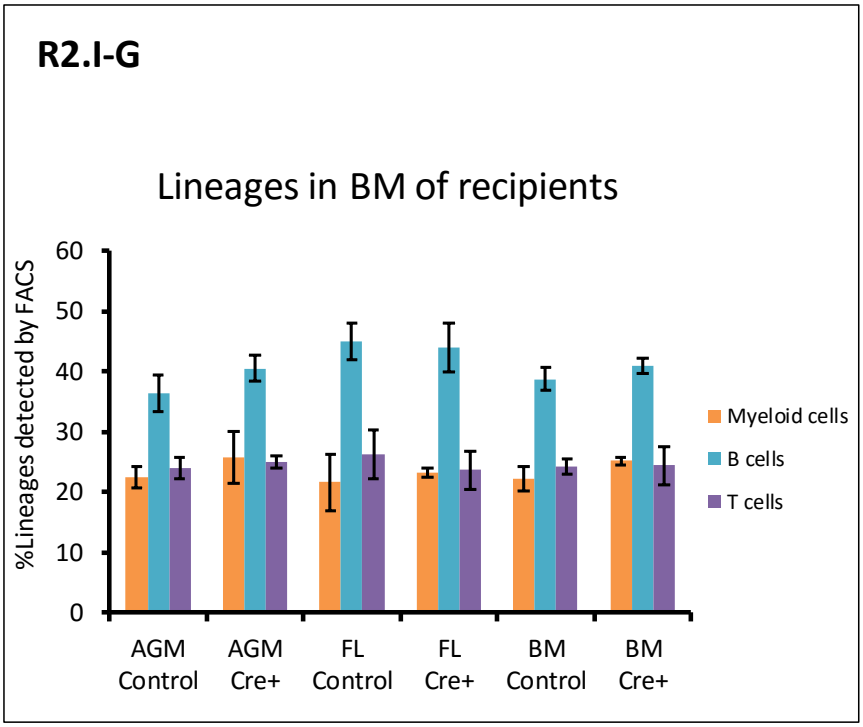

R2.I - G: Contribution of donor cells to distinct hematopoietic lineages in transplant recipients: Lineage distribution analysis was conducted by staining BM cells with antibodies against Myeloid(Mac1), Granulocyte(Gr1), B-lymphocytes (B220) and T-lymphocytes(CD3e) by flow cytometry. Values are represented as Mean±SD. Student's t-test was conducted for statistical analysis and no significant differences were found ($p>0.05$). AGM: aorta-gonads-mesonephros, E8.5/12.5: embryonic age 8.5/12.5 (days post-coitus), BM: bone marrow, P60: postnatal age of mice of 60 days

With these findings we concluded that the in-vitro 4-OHT induction strategy was an ineffcicent means of achieving MLL-ENL translocation in all tissues (AGM, FL and BM). To overcome this problem, we implemented an alternative in-vivo Cre-induction strategy.

STRATEGY - II

In-vivo induction of recombination at embryonic and adult stages

In parallel to the in-vitro system, we developed an alternative strategy for in-vivo Cre-induction by tamoxifen administration at embryonic and adult stages (Fig. R2.II-A). Tamoxifen was administered intraperitoneally in:

(i) pregnant mice at E8.5 or E12.5 to target embryonic hematopoietic cells emerging in the AGM or found in the FL tissues

(ii) adult mice (two months old, P60) to target hematopoietic cells in the BM

To assess tamoxifen dosage for achieving optimal recombination efficiency in embryonic and adult tissues, increasing concentrations was administered as described in previous studies (Table 2) (Hayashi & McMahon 2002).

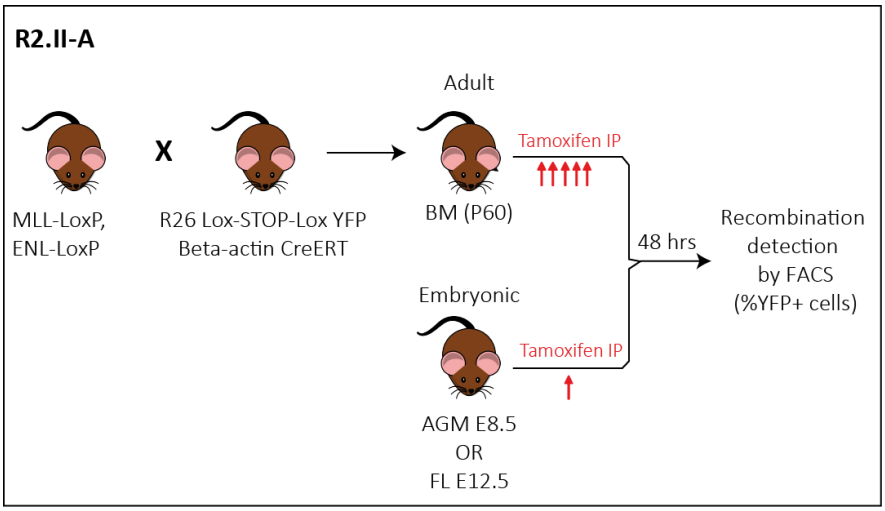

R2.II - A: Experimental strategy for in-vivo Cre-induction: In strategy II, in-vivo Cre-induction was performed by tamoxifen administration at different stages of hematopoietic development. Induction of adult and embryonic tissues required use of different doses of tamoxifen. The detection of recombination efficiency was assessed 48 hours post-induction by detecting YFP-expression in embryonic and adult tissues by FACS. MLL: mixed lineage leukemia, ENL: eleven-nineteen leukemia, AGM: aorta-gonads-mesonephros, E8.5/12.5: embryonic age of 8.5/12.5 (days post-coitus), BM: bone marrow, P60: 60 days post-birth, YFP: yellow fluorescent protein, FACS: fluorescence-activated cell sorting

The YFP^+ cells in AGM and FL tissues were detected 48 hours post-induction by flow cytometry analysis. Efficient YFP-expression was obtained in AGM (83% of YFP^+) and FL (65% of YFP^+) tissues by administering 75 mg/kg of tamoxifen (Fig. R2.II-B, C). Administration of tamoxifen at a higher dose led to abortions (in n>3).

Administering the same dose of tamoxifen (75mg/kg) to adult mice resulted in low recombination efficiency in the BM tissue (12% of YFP^+ cells) (Table 2).

Table-2: Tamoxifen titrations in-vivo

Tissue	Stage	Concentration	% YFP$^+$ cells
BM (Adult mice)	2 months	25 mg/kg (1 dose)	2.39 %
BM (Adult mice)	2 months	50 mg/kg (1 dose)	3.31 %
BM (Adult mice)	2 months	75 mg/kg (1 dose)	11.73 %
BM (Adult mice)	2 months	75 mg/kg (2 doses)	14.21%
BM (Adult mice)	2 months	75 mg/kg (5 doses)	18.21%
BM (Adult mice)	2 months	150 mg/kg (1 dose)	6.4 %
AGM/FL	E 9.5 / E 12.5	75 mg/kg (2 doses)	Abortions
AGM	E 9.5	75 mg/kg (1 dose)	83%
Fetal Liver	E 12.5	75 mg/kg (1 dose)	65%

Highlighted boxes (in pista) represent the maximum recombination obtained in the respective tissues. Values are represented as Mean±SD from three independent experiments each.

To improve recombination efficiency in adults, maximal induction startegy was implemented by administering five doses of tamoxifen over five consecutive days (Hayashi & McMahon 2002). The recombination efficiency improved, though marginally, with upto 20% of YFP$^+$ BM cells detected (Fig R2.II-A,B).

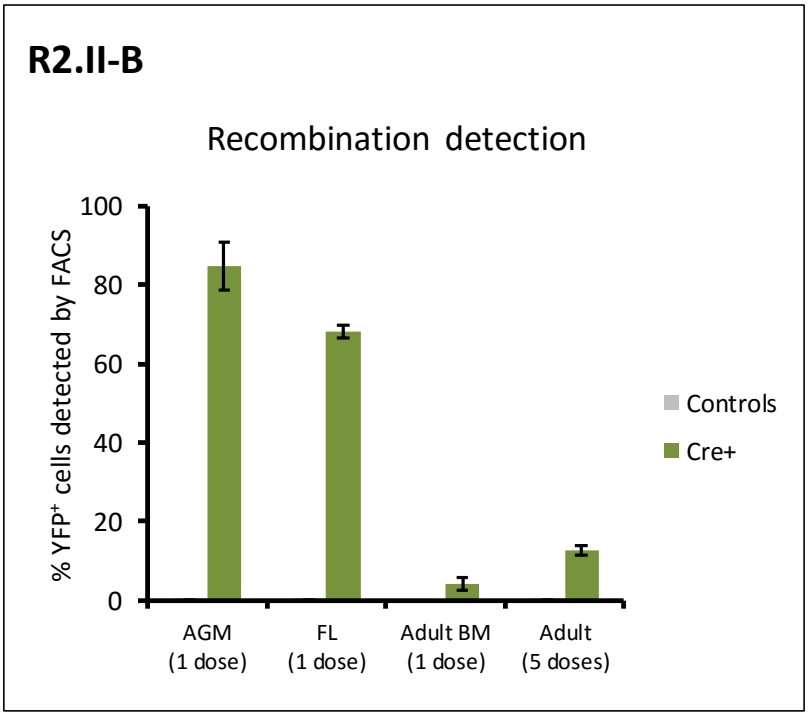

R2.II - B: Optimized tamoxifen dose to be administered in-vivo for Cre-induction: The optimal concentration of tamoxifen administered in-vivo was 75 mg/kg, to induce E8.5 AGMs/E12.5 FLs/P60 BMs from MLL-ENL:R26-YFP:β-actin Cre^+ mice. Recombination efficiencies were measured 48 hours later by detecting YFP^+ cells in embryonic and adult tissues by FACS. Three independent experiments were conducted for each tissue. Values are represented as Mean±SD. MLL: mixed lineage leukemia, ENL: eleven-nineteen leukemia, AGM: aorta-gonads-mesonephros, FL: fetal liver, BM: bone marrow, E: embryonic stage (days post-coitus), P: postnatal age of mice (in number of days), FACS: fluorescence-activated cell sorting

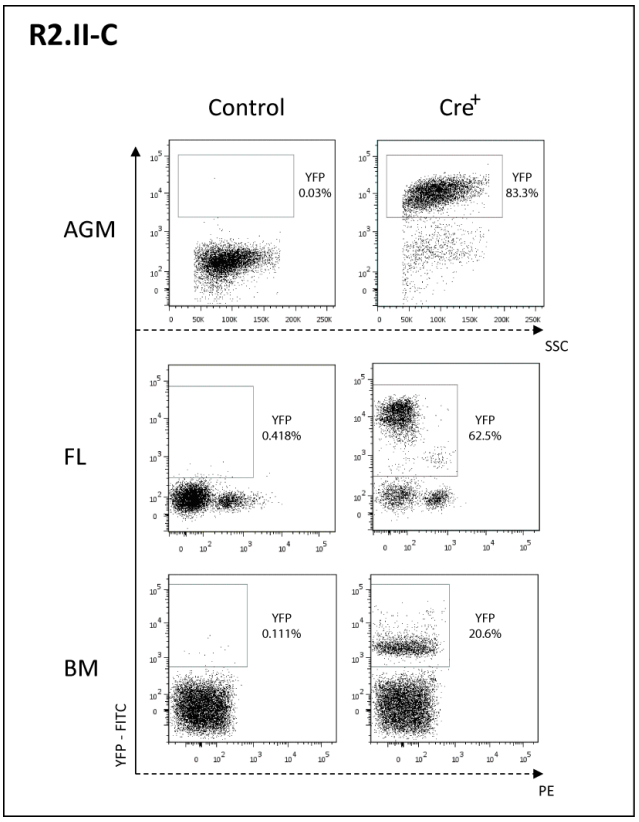

R2.II - C: Representative FACS plots of YFP-expression in embryonic and adult tissues: Two days post Cre-induction(s) the AGM/FL/BM tissues from Cre$^+$ and control mice were analyzed by FACS to detect YFP-expression. The representative flow cytometry plots are shown. YFP$^+$ cells were detected in the FITC channel. MLL: mixed lineage leukemia, ENL: eleven-nineteen leukemia, AGM: aorta-gonads-mesonephros, FL: fetal liver, BM: bone marrow, YFP: yellow fluorescent protein, FACS: fluorescence-associated cell sorting

The optimized in-vivo induction strategy was used to initiate MLL-ENL-translocation in embryonic and adult tissues (Fig. R2.II - D).

Embryo – derived model

To develop an embryonic model of MLL-ENL leukemia, tamoxifen was administered to pregnant mice at E9.5 or E12.5. The progeny would be bled post-weening to perform blood analyses (Fig. R2.II - D).

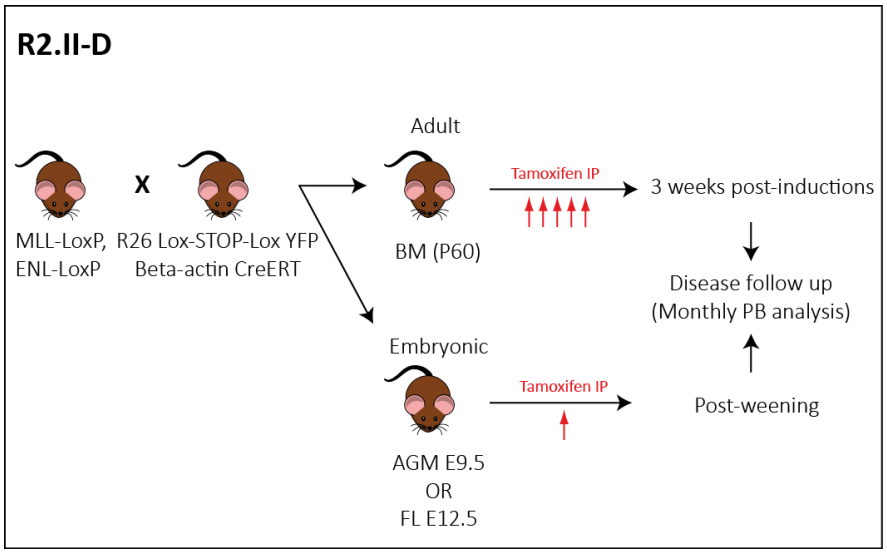

R2.II - D: Strategy II - Experimental set up for developing embryonic and adult leukemias driven by MLL-ENL translocation. In this strategy, in-vivo Cre-induction(s) were performed at embryonic and adult stages (E9.5 AGM/E12.5 FL/P60 BM) of hematopoietic development by tamoxifen administration. To develop the embryonic model, one dose of tamoxifen (75mg/kg) was administered in pregnant mice at either E9.5 or E12.5 stage. For the adult model, mice were treated with five doses of tamoxifen (75mg/kg /dose) over five consecutive days. The follow-up analyses were performed three weeks later and monthly thereafter. MLL: mixed lineage leukemia, ENL: eleven-nineteen leukemia, AGM: aorta-gonads-mesonephros, FL: fetal liver, BM: bone marrow, E: embryonic age (days post-coitus), P: postnatal age of mice (days post-birth), IP: intraperitoneal injections, PB: peripheral blood

Several attempts were made to develop the embryonic MLL-ENL leukemia model using this approach.

However, administration of 75mg/kg tamoxifen at mid-gestation caused dystocia in the pregnant mice. This condition has been previously reported as a result of tamoxifen treatment in pregnant mice (Danielian et al. 1998; Nakamura et al. 2006).

To overcome this side effect and enable normal delivery, we co-administered tamoxifen injections with progesterone hormone which maintains thick uterine lining and proper placenta functioning throughout pregnancy allowing the conceptus to fully develop (Nakamura et al. 2006).

Several tests were performed to optimize the dose of progesterone to be co-administered with tamoxifen in-vivo at E9.5 and E12.5 stages (Table-3).

Table-3: Co-administration of tamoxifen with progesterone to induce embryonic tissues in-vivo

Tissue	Tamoxifen admin.		Progesterone admin.		Observations
	Stage	Dose	Stage	Dose	
AGM	E 9.5	2 mg	E 9.5	50 µg	Dystocia (Analyzed E19) **Fig. R2.II- E,F**
	E 9.5	0.5 mg	E 9.5	2 mg	Delivered (Died at P2)
FL	E 12.5	2 mg	E 12.5	2 mg	Dystocia (Analyzed E19) **Fig. R2.II- G,H**
	E 12.5	2 mg	E12.5 and E16.5	2 mg *(1mg/ dose)*	Stillborn (Analyzed P1) **Fig. R2.II- I-L**
	E 16.5	1.5 mg	E 16.5	2 mg	Died at E19
	E 12.5	1 mg	E 12.5	2 mg	Stillborn

Highlighted box (in pista) represents the maximum recombination obtained with minimum toxicity

In an initial experiment, tamoxifen was co-administered with progesterone (50 µg) at E9.5 stage and dystocia was observed. We then

analyzed the E19 embryos from the euthanized mouse. We obtained a single Cre$^+$ embryo that showed signs of hemorrhages along with two control littermates and two more that were aborted likely due to tamoxifen-related toxicity (Fig. R2.II-E). Progesterone co-administration in this case could not counter the toxicity of tamoxifen to the embryos, probably due to low concentration used.

We detected efficient recombination in the Cre$^+$ embryo with 60% of YFP$^+$ cells in the fetal liver (Fig. R2.II-E).

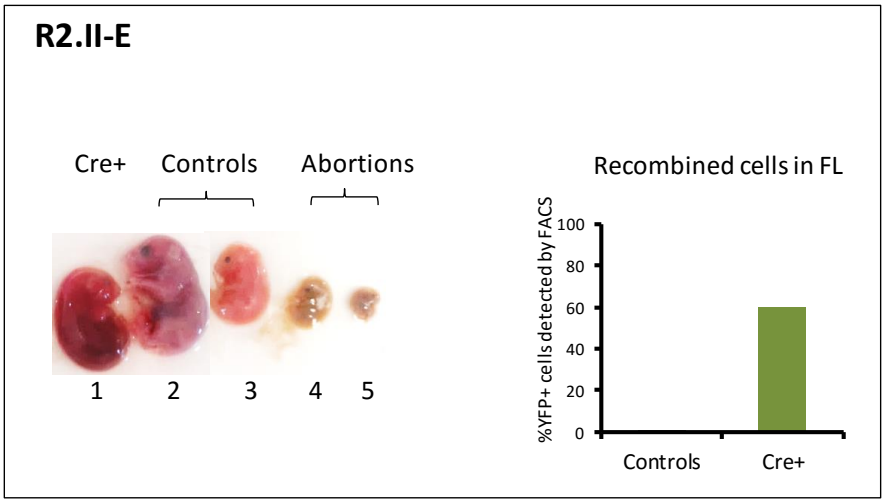

R2.II - E: Induction in embryonic tissue AGM: Tamoxifen (75mg/kg) was co-administered with progesterone (1.5 mg/kg) intraperitoneally in pregnant mice at E9.5 stage. Dystocia was observed at the end of pregnancy. The embryos were collected from the euthanized mouse and analyzed by FACS to detect recombination efficiency in FL of Cre$^+$ embryos. Left panel – The Cre$^+$, control and aborted embryos from the euthanized mouse are shown. Toxicity of tamoxifen in embryos were visible in the form of abortions and hemorrhages in the Cre$^+$ embryo. Right panel - Quantifications of YFP$^+$ cells in the fetal liver of Cre$^+$ versus control embryos are shown. 60% of YFP$^+$ cells were detected within the FL of the Cre$^+$ embryo. AGM: aorta-gonads-mesonephros, FL: fetal liver, YFP: yellow fluorescent protein, E9.5: embryonic age of 9.5 (days post-coitus), MLL: mixed lineage leukemia, ENL: eleven-nineteen leukemia

However, we could not detect the MLL-ENL fusion gene by PCR from FL-derived DNA in the Cre$^+$ embryo (Fig. R2.II-F).

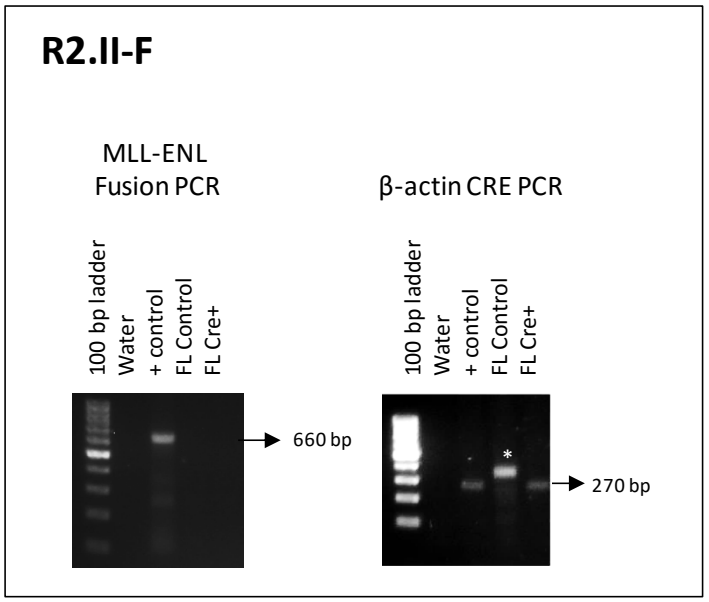

R2.II - F: Translocation detection in embryos induced at E9.5 (AGM): Left panel - MLL-ENL fusion gene (660bp) was detected by PCR in DNA extracted from FL cells of Cre^+ and control littermates. Right panel - Genotyping PCR was performed to detect the Cre gene (270 bp). PCR products were run on 2% agarose gel alongside 100 bp ladder. * represents unspecific band. FL: fetal liver, PCR: polymerase chain reaction, DNA: deoxyribonucleic acid, bp: base pairs, MLL: mixed lineage leukemia, ENL: eleven-nineteen leukemia

In the following experiments, tamoxifen-induced toxicity to embryos and dystocia condition in pregnant mice were countered more effectively by increasing the concentration of progesterone.

However, we could not detect the MLL-ENL fusion gene in any of the experiments where induction was performed at E9.5 stage.

The Cre-induction was then performed at a later stage of embryonic development (at E12.5 to target fetal liver cells) by co-administering optimized doses of tamoxifen and progesterone (Table-3) obtaining similar results of inefficient MLL-ENL translocation.

By targeting hematopoietic cells in AGM or FL tissues, we achieved ≥40% of YFP$^+$ cells (Fig. R2.II-E,G) but the MLL-ENL fusion gene could not be detected by PCR (Fig. R2.II-H).

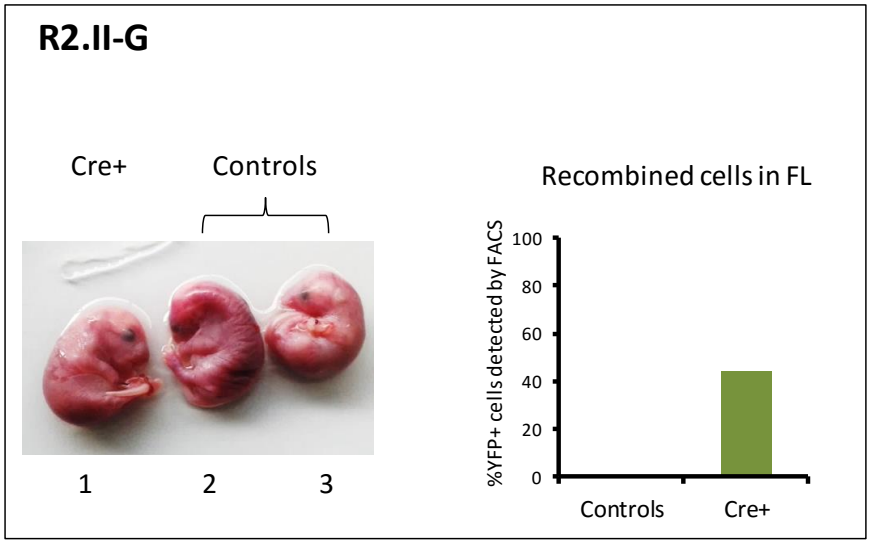

R2.II - G: Induction in embryonic tissue (E12.5 fetal liver): Tamoxifen and progesterone were co-administered (in 1:1 ratio) intraperitoneally in pregnant mice at E12.5. Dystocia was observed towards end-of-gestation, embryos were collected from euthanized mouse and recombination was analyzed (YFP$^+$ cells) by flow cytometry. Left panel – The Cre$^+$ and control littermates obtained in this experiment from the euthanized mouse are shown. Right panel - Quantification of YFP$^+$ cells in the fetal liver of Cre$^+$ versus control (Cre negative) embryos are represented. FL: fetal liver, YFP: yellow fluorescent protein, E12.5: embryonic age of 12.5 (days post-coitus)

Dystocia or obstructed labour, was overcome by administering progesterone at two points during pregnancy, once by co-administering it with tamoxifen at E12.5 and the second administered towards the end-of-gestation (at E16.5 or later) to aid in the delivery process. With this strategy, the parturition occurred with less complications, however, the newborns were either stillborn or they died within two days of birth.

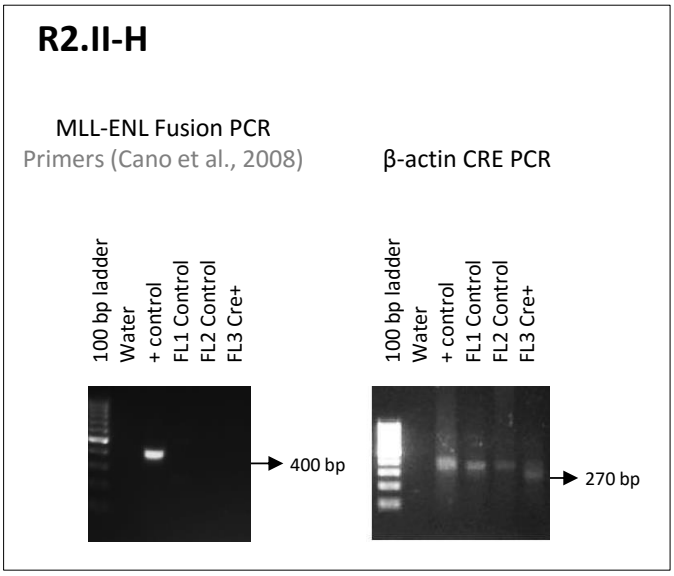

R2.II - H: Translocation detection in embryos induced at E12.5 (FL): Left panel - PCR was performed to detect the MLL-ENL fusion gene (400bp) as previously described (Cano et al. 2008b). DNA was extracted from FL cells of Cre^+ and control littermates. Right panel – PCR was performed to detect the Cre gene (270 bp). PCR products were run on 2% agarose gel alongside 100bp DNA ladder. (The positive control did not work in this case). MLL: mixed lineage leukemia, ENL: eleven-nineteen leukemia, FL: fetal liver, PCR: polymerase chain reaction, DNA: deoxyribonucleic acid, bp: base pairs, E12.5: embryonic age of 12.5 (days post-coitus)

We were able to analyze only one newborn pup (P1) induced at E12.5, that died within a day of being born. We collected the organs to perform different analyses. It was a Cre^+ pup as the Cre gene was detected by PCR (Fig.R2.II-L).

The majority of organs of this Cre^+ P1 pup were YFP^+ when observed under the fluorescent microscope (Fig. R2.II-I). We could also detect YFP^+ cells in organs sections (of liver, lungs, stomach and intestine) under the fluorescent microscope (Fig. R2.II-J).

YFP-expression was also quantified by FACS in fetal liver, bone marrow and thymus of this Cre^+ pup (Fig. R2.II-K). All peripheral

organs showed efficient YFP recombination by immunofluorescence as well as flow cytometry (Fig. R2-II-I,K).

In parallel, we performed histological analysis of the organs of P1 Cre^{+} pup (by Hematoxylin-Eosin staining of organ sections) to observe possible defects in development (Fig. R2.II-J). The histology of all the organs appeared to be normal (Fig. R2.II-J left panel).

DNA was extracted from fetal liver cells of this pup to detect MLL-ENL fusion gene by PCR (Fig.R2.II-I). We did not detect the MLL-ENL fusion gene was likely caused by inefficient Cre-mediated translocation.

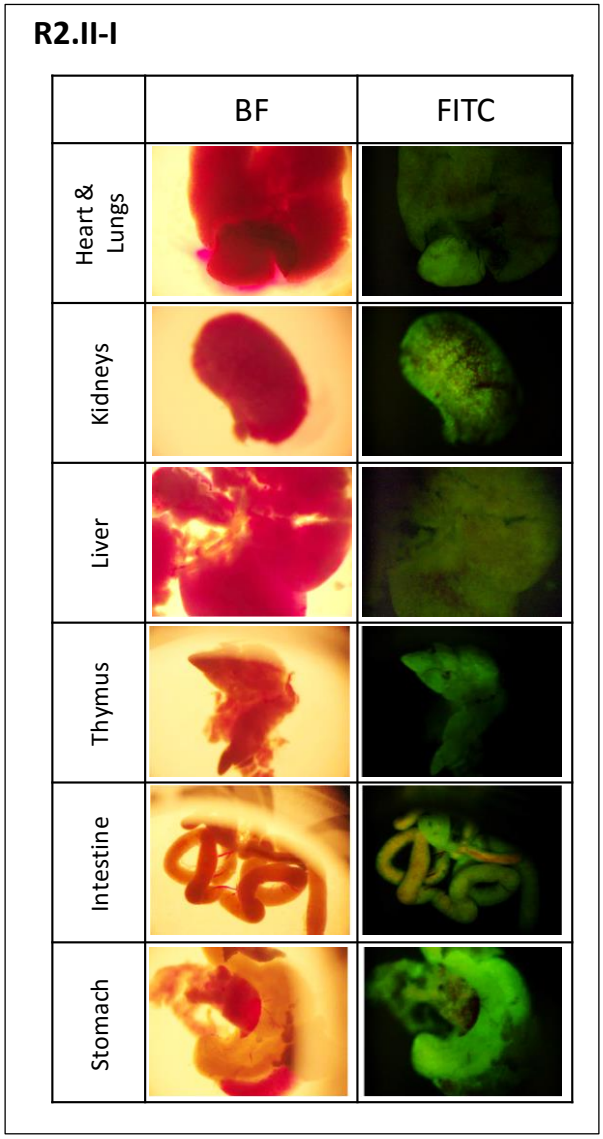

R2.II - I: Recombination detection in organs of Cre$^+$ P1 mouse, induced in-vivo at E12.5 by detecting YFP-expression under fluorescent microscope: Tamoxifen was co-administered with progesterone (in 1:1 ratio) intraperitoneally in pregnant mice at E12.5. We collected the organs from the single Cre$^+$ P1 pup that was successfully delivered but died postnataly by P1. Under the fluorescent microscope in FITC channel, we could detect YFP$^+$ cells in all of the organs including the heart, lungs, kidneys, liver, thymus, intestine as well as the stomach. Images of the organs were taken in the bright field (BF) on the left panel and in FITC channel of the fluroscent microscope on the right panel. MLL: mixed lineage leukemia, ENL: eleven-nineteen leukemia, YFP: yellow fluorescent protein, P1: 1 day old pup (post-natal age of mice), E12.5: embryonic age of 12.5 (days post-coitus)

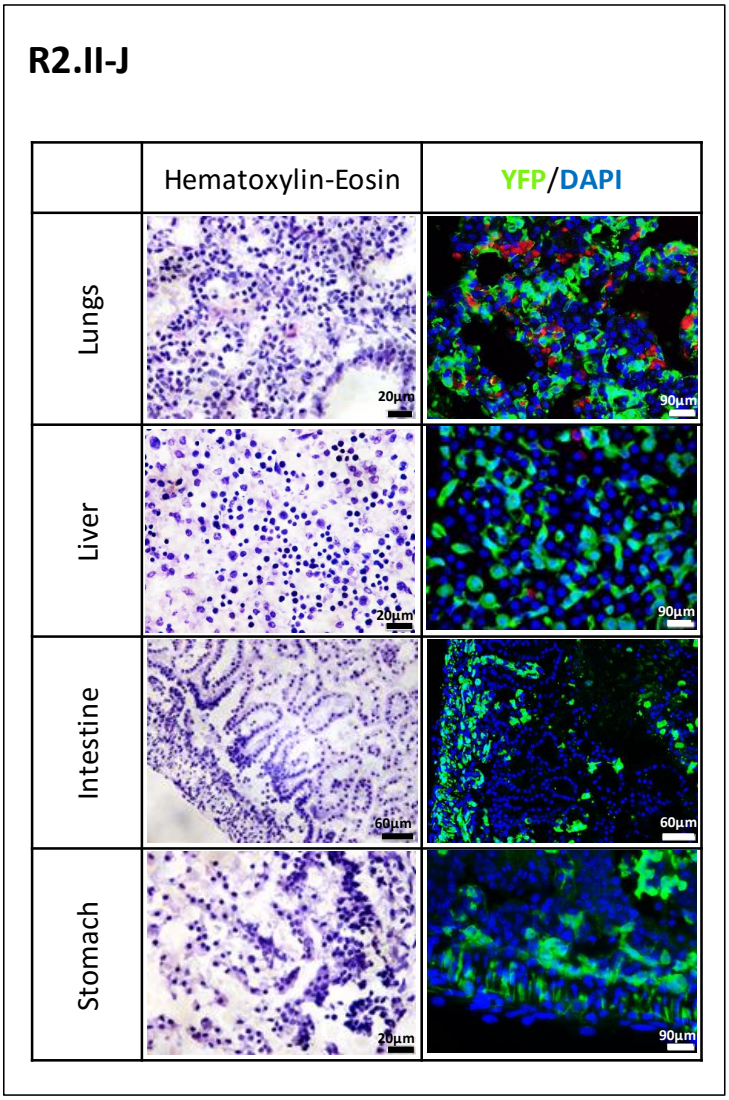

R2.II - J: YFP-expression detection in organ sections of Cre⁺ P1 pup induced in-vivo at E12.5: The organs obtained from the MLL-ENL:R26-YFP:β-actin Cre⁺ P1 pup induced in-vivo at E12.5, were embedded in paraffin (Methods X-i). Hematoxylin and Eosin staining was performed on organ sections (10µm thick) to observe the morphology of the tissues. Left panel – Images of Hematoxylin-Eosin stained organ sections were taken at 20X or 40X magnifications under the bright field microscope. Right panel - YFP⁺ cells were detected in FITC channel in organ sections. Nuclear staining was done with 4',6-diamidino-2-phenylindole (DAPI). No antibody was used to detect YFP⁺ cells. MLL: mixed lineage leukemia, ENL: eleven-nineteen leukemia, YFP: yellow fluorescent protein, DAPI: 4',6-diamidino-2-phenylindole, P1: 1 day old pup (postnatal age of mice), E12.5: embryonic age of 12.5 (days post-coitus)

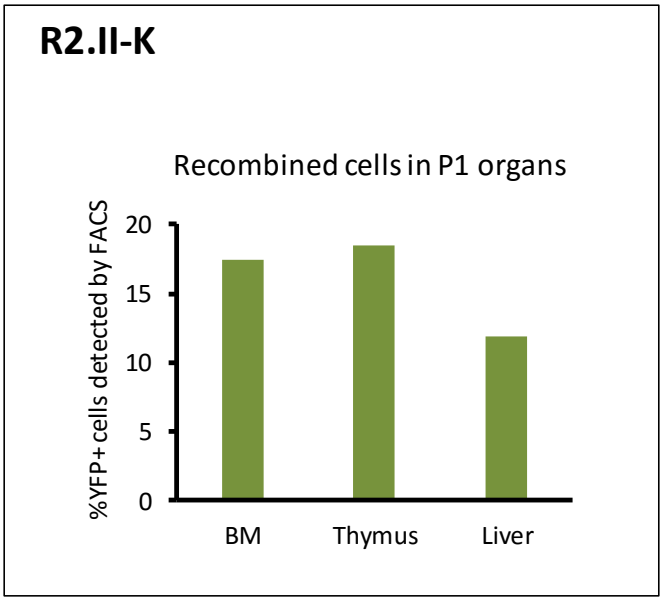

R2.II - K: Detecting YFP$^+$ cells by FACS in distinct organs of Cre$^+$ P1 pup induced in-vivo at E12.5: Quantification of YFP-expression in bone marrow, thymus and liver of the Cre$^+$ P1 pup was done by flow cytometry analysis. YFP was detected in the FITC channel. BM: bone marrow, P1: 1 day old pup (post-natal age of mice), YFP: yellow fluorescent protein

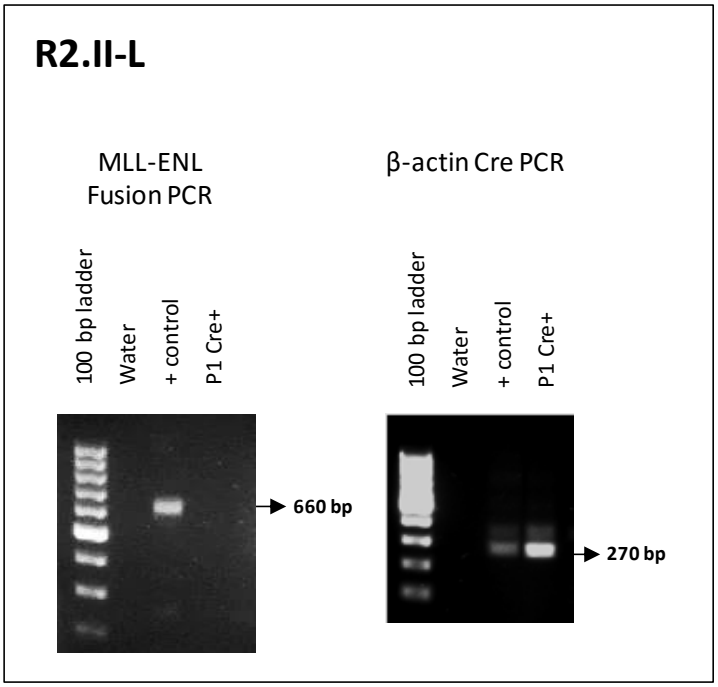

R2.II - L: Translocation detection: Left panel - PCR was performed to detect MLL-ENL fusion gene (660 bp) in fetal liver-derived DNA of P1 Cre^{+} embryos. Right panel – Genotyping PCR was performed to detect the Cre gene (270 bp). PCR products were run on 2% agarose gel alongside 100 bp DNA ladder. MLL: mixed lineage leukemia, ENL: eleven-nineteen leukemia, FL: fetal liver, DNA: deoxyribonucleic acid, bp: base pairs, PCR: polymerase chain reaction

In the current approach, we encountered several complications in developing an embryonic model of MLL-ENL-driven leukemia. While we were able to overcome tamoxifen-induced toxicity to an extent and obtain >40% of YFP-expression in embryonic tissues, we continued to encounter inefficient MLL-ENL translocation. We were unable to develop an embryo-derived leukemia model using this current strategy.

Adult (BM-derived) model

The adult model of MLL-ENL leukemia was developed in parallel with the embryonic model (Fig. R2.II-D). We performed optimized in-vivo inductions in two months old adult (P60) mice to target hematopoietic cells in the BM. Blood analyses were performed to detect disease onset and follow its progression. As observed during tamoxifen titrations, we obtained significantly lower recombination efficiency in adult tissues when compared to embryonic tissues. The maximum YFP-expression detected in the current model was 25% in one of the Cre^+ mice (Fig. R2.II-M).

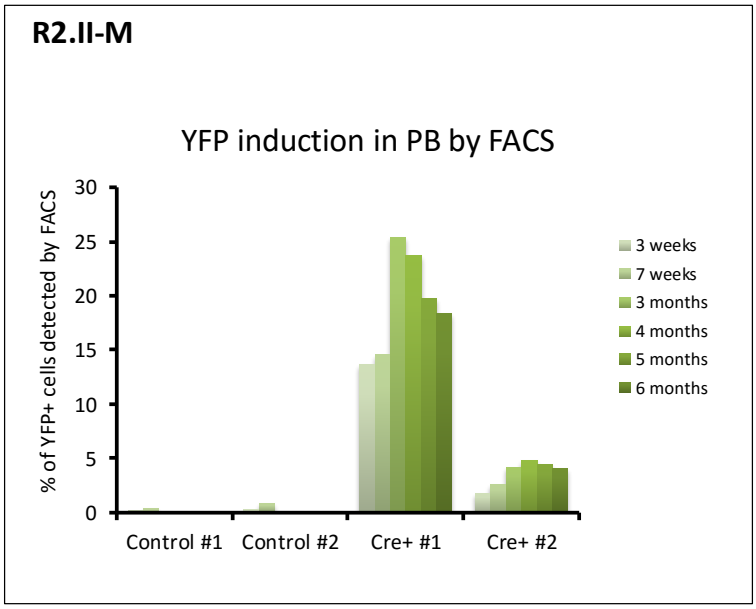

R2.II - M: Recombination efficiency detected by YFP-expression in adult mice induced in-vivo: Monthly PB analysis of MLL-ENL:R26-YFP:β-actin Cre^+ versus control mice was performed by FACS to detect YFP-expression. YFP^+ cells were detected in the FITC channel. Blood analyses performed upto six months is shown. #1 and #2 represent individual Cre^+ or control mice. MLL: mixed lineage leukemia, ENL: eleven-nineteen leukemia, YFP: yellow fluorescent protein, PB: peripheral blood, P60: 2 months old adult mice (post-natal age of mice)

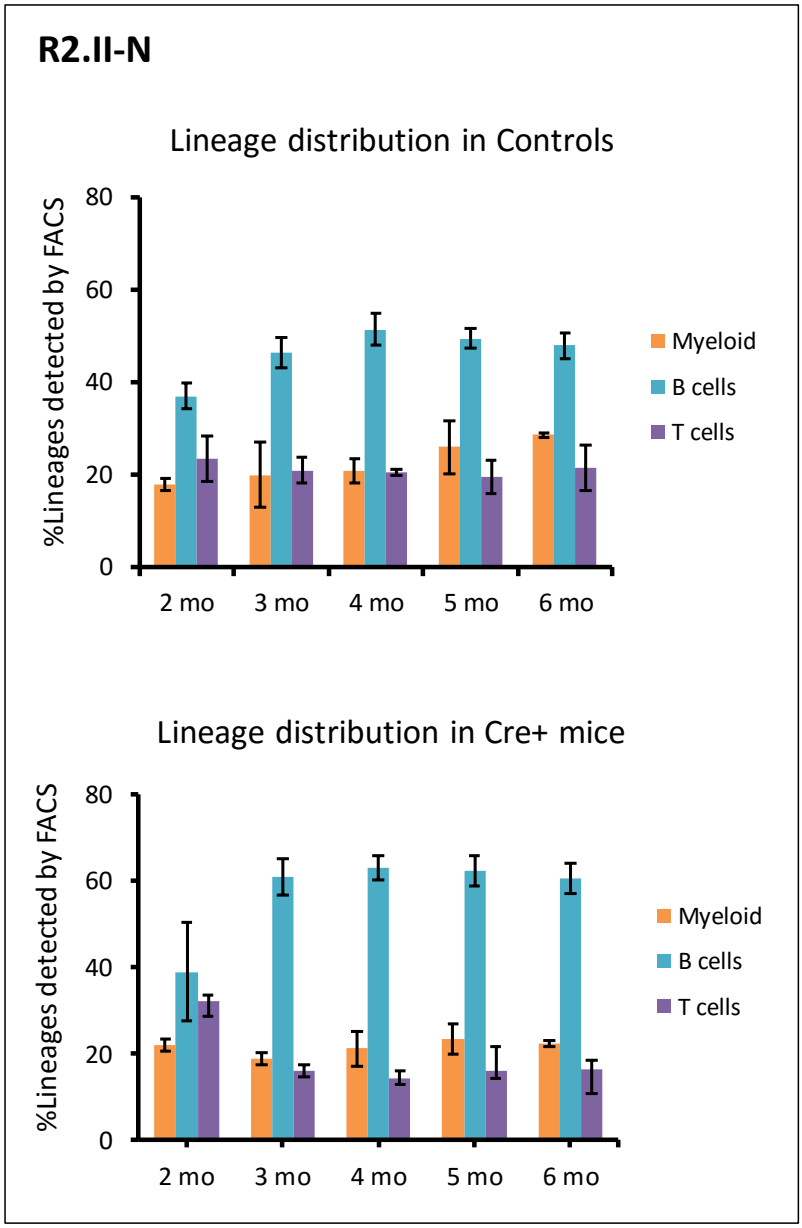

R2.II - N: Lineage distribution analysis in adult mice induced in-vivo: Blood analyses of in-vivo induced adult MLL-ENL:R26-YFP:β-actin Cre^{+} (lower panel) and control mice (upper panel) was performed up to 180 days. PB cells were stained with antibodies against surface markers for Myeloid (Mac1), Granulocytes(Gr1), B-lymphocytes(B220) and T-lymphocytes(CD3e). Values are represented as Mean±SD of n=2 mice each. Student's t-test was performed for statistical analysis (no significant differences were found $p>0.05$). MLL: mixed lineage leukemia, ENL: eleven-nineteen leukemia, PB: peripheral blood

Inefficient MLL-ENL-recombination was observed in the adult model similar to what was observed with the embryonic model. MLL-ENL fusion gene could not be detected by PCR during the monthly analyses up to 180 days post-inductions (Fig. R2.II-O). Concurring with this, no sign of disease was detected in the Cre^+ mice.

Blood analyses by FACS up to 180 days showed no significant differences in contribution to the myeloid and lymphocyte lineages in the Cre^+ versus control mice (Fig. R2.II-N).

The health of these mice was monitored thereafter (post 180 days), and it was only at 540 days post-inductions that one of the two Cre^+ mice showed signs of disease and was euthanized.

The organs were collected from the euthanized mouse to perform end-point analyses. Flow cytometry analysis of BM cells showed increase in percentage of myeloid cells ($Mac1^+Gr1^+$ cells). Considering the slow development of this leukemia and the lineage of leukemic cells, it resembled a chronic myelogenous leukemia (CML-like) (Fig. R2.II-P).

This was further confirmed by the presence of MLL-ENL fusion gene in the BM cells of this diseased mouse by PCR (Fig. R2.II-O-S).

The BM cells of the control mice showed normal contribution to myeloid, B and T-lymphocytes and erythrocytes by FACS (Fig. R2.II-P,Q).

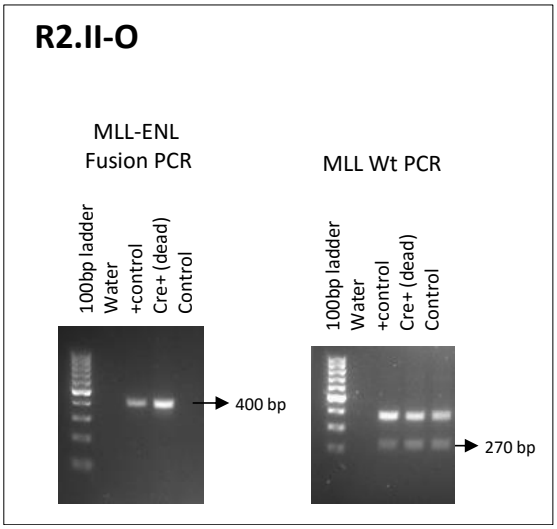

R2.II - O: Translocation detection in Cre⁺ mouse with CML-like phenotype: DNA was extracted from BM of leukemic and control mice. MLL-ENL fusion gene (400bp) was detected by PCR as previously described (Cano et al. 2008b). It was detected in the BM of Cre⁺ leukemic mouse and not in controls. The wildtype allele of the MLL gene (270 bp) was detected by PCR as a control. PCR products were run on 2% agarose gel alongside 100 bp DNA ladder. MLL: mixed lineage leukemia, ENL: eleven-nineteen leukemia, PCR: polymerase chain reaction, DNA: deoxyribonucleic acid, bp: base pairs, CML: chronic myelogenous leukemia

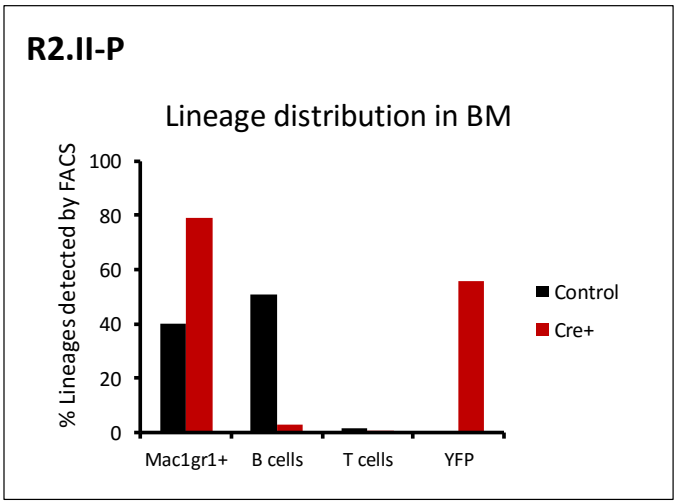

R2.II - P: Detecting leukemic population in the BM of diseased Cre⁺ mouse: 540 days post-inductions one of the Cre⁺ mice died. BM cells were analyzed by FACS. Myeloid, B and T Lineages were detected in BM of Cre⁺ versus control mice. Mac1⁺Gr1⁺ cells were identified as the leukemic population in the Cre⁺ mouse. MLL: mixed lineage leukemia, ENL: eleven-nineteen leukemia, BM: bone marrow, YFP: yellow fluorescent protein, FACS: fluorescence-activated cell sorting

The leukemic blasts could also be identified morphologically as 'myeloid-blast-like cells' by performing Wright-Giemsa staining of BM cells (Fig. R2.II-Q).

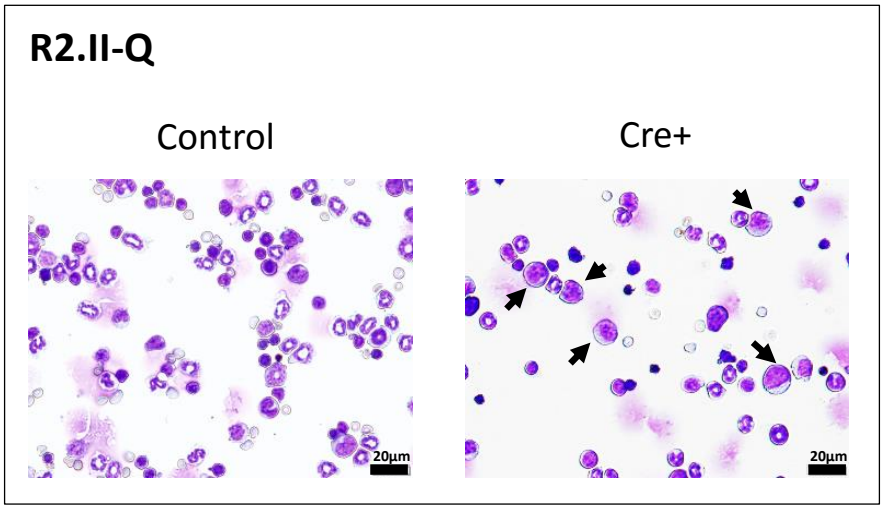

R2.II - Q: Wright-Giemsa staining was performed on cytospin of BM cells taken from euthanized MLL-ENL:R26-YFP:β-actin Cre$^+$ and control mice, 540 days post-in-vivo inductions. Black arrows point to the myeloid blast like cells detected in Cre$^+$ leukemic BM (right panel). Controls showed normal distribution of hematopoietic cells in the BM. Representative images are shown at 40X magnification. MLL: mixed lineage leukemia, ENL: eleven-nineteen leukemia, BM: bone marrow.

Splenomegaly was observed in the leukemic mouse when compared to the control mouse (Fig. R2.II-R). In addition, two tumors were found in the diseased mouse, one adjacent to the neck and the second on one of the kidneys. Leukemic infiltrates were detected in distinct peripheral organs (including the liver, lungs and spleen) by Hematoxylin-Eosin staining of organ sections (Fig. R2.II-S).

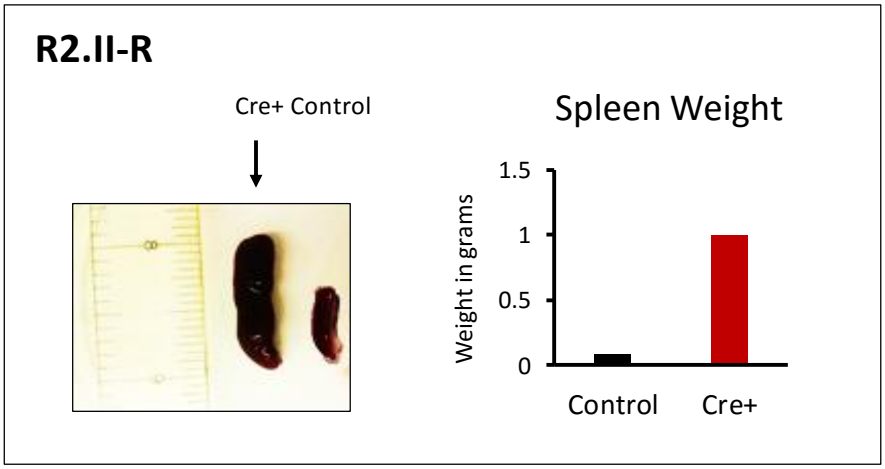

R2.II - R: Splenomegaly observed in Cre$^+$ mouse with CML-like phenotype: Left panel - The MLL-ENL:R26-YFP:β-actin Cre$^+$ mouse that developed leukemia had an enlarged spleen when compared to control. Right panel - Quantifications of splenic aspects (weight of spleens in grams) are represented. MLL: mixed lineage leukemia, ENL: eleven-nineteen leukemia, CML: chronic myelogenous leukemia

This strategy failed to develop embryonic and adult leukemias in the expected timeframe due to inefficient Cre-mediated MLL-ENL-recombination.

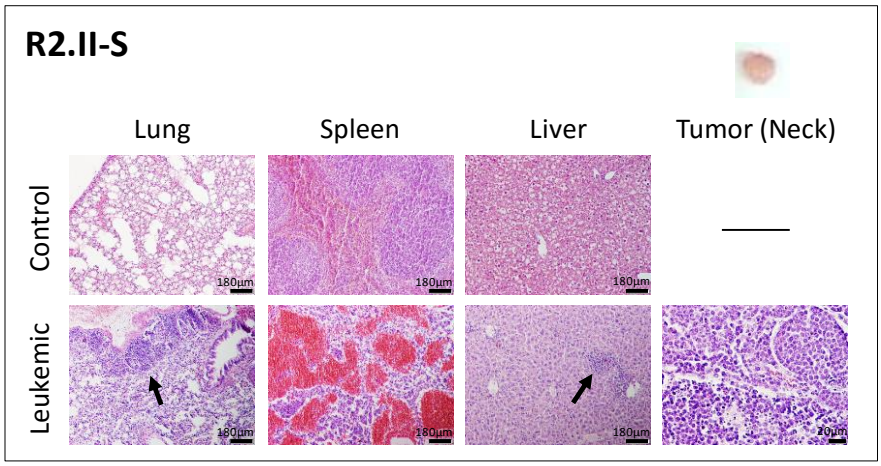

R2.II - S: Infiltration detection: Leukemic infiltrates resulting from the CML-like disease in the Cre^{+} mouse were analyzed by performing Hematoxylin-Eosin staining on paraffin-embedded organ sections (10µm thick). Representative images are shown at 20X magnification. Multiple organ infiltration was observed in the leukemic mouse while organs of control mice had normal histology. Black arrows point to leukemic infiltrates. CML: chronic myelogenous leukemia

STRATEGY - III

Competitive transplantation of in-vivo induced embryonic and adult hematopoietic tissues into lethally irradiated adult recipients

To overcome the complications due to non-hematopoietic recombination from the ubiquitous β-actin expression encountered in developing embryonic and adult leukemia models using strategy II, we further explored in-vivo induction strategy with the aim of directly comparing transformation capacities of embryonic versus adult hematopoietic tissues by transplanting in-vivo induced cells into adult irradiated recipients.

Cre-inductions at embryonic and adult stages were performed as described in the previous section (Fig. R2.III-A). 48 hours post-induction(s), the tissues (E10.5 AGM/E14.5 FL/P67 BM) were transplanted competitively into adult irradiated recipients as previously described in strategy I (See methods I-v) (Fig. R2.III-A). Reconstitution and follow-up analyses of recipients was conducted a month post-transplantations by performing blood analyses (Fig. R2.III-A). Donor engraftment, YFP-expression, lineage distribution and complete blood counts were measured to detect disease onset and follow its progression (R2.III-B,C,D).

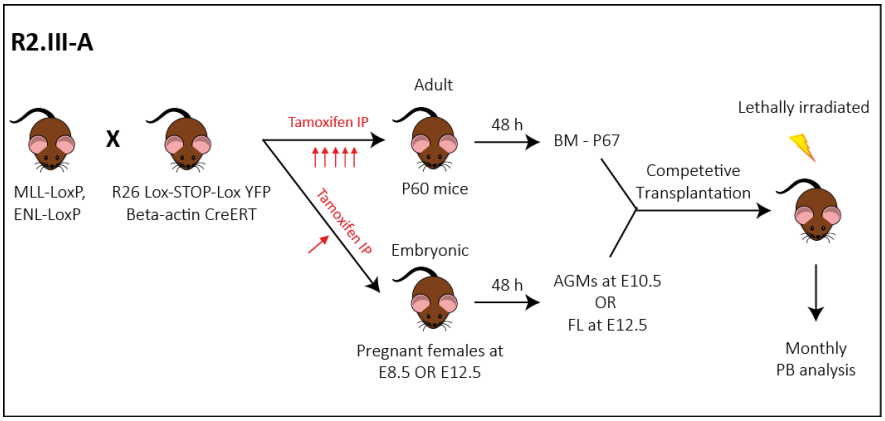

R2. III - A: Strategy III - Experimental scheme to develop and compare embryonic versus adult leukemias driven by MLL-ENL translocations: In this strategy, in-vivo Cre-induction(s) were performed by administering tamoxifen at embryonic (E8.5/E12.5) and adult stages (P60). 48 hours post in-vivo induction(s), we performed competitive transplantations of induced donor cells into lethally irradiated adult recipient mice (See methods I-v). Transplant recipients were bled from their tail vein a month post-transplantation. Blood analyses were done by FACS to detect disease reconstitution and lineage distribution. MLL: mixed lineage leukemia, ENL: eleven-nineteen leukemia, AGM: aorta-gonads-mesonephros, FL: fetal liver, BM: bone marrow, E: embryonic age (days post-coitus), e.e.: embryo equivalence, P: postnatal age of mice (in number of days), IP: intraperitoneal injections, PB: peripheral blood

Donor engraftment was measured ($CD45.2^+$ cells) in blood samples of all transplant recipients by FACS. The average donor reconstitutions of Cre^+ AGM, FL and BM tissues were 42%, 60% and 80% respectively. And, similar engraftments were achieved in control recipients (Fig.R2-III-B). Similarly, engraftment of YFP^+ cells in all Cre^+ recipients (AGM, FL and BM) was around 50% as detected within the donor-derived populations by FACS (Fig.R2-III-C).

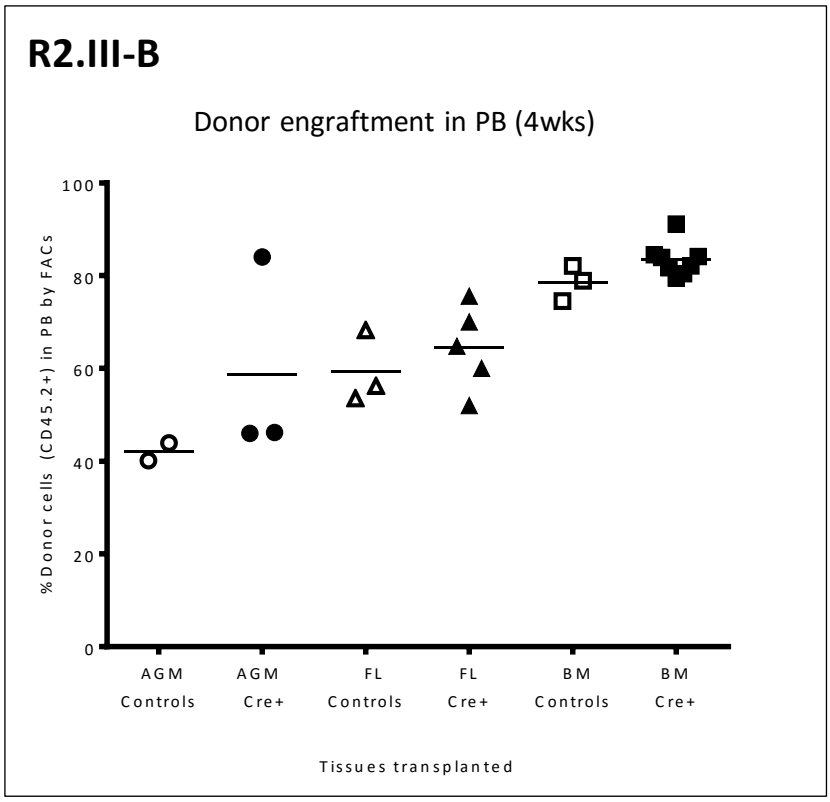

R2. III - B: Donor engraftment in peripheral blood of transplant recipients: Transplant recipients of recombined versus control AGM, FL and BM cells were bled from the tail vein one-month post-transplantation. Donor reconstitution was analyzed by FACS. PB cells were stained with antibodies against surface markers CD45.1 and CD45.2 to measure $CD45.2^{+}CD45.1^{-}$ donor-derived cells in the recipient mice. MLL: mixed lineage leukemia, ENL: eleven-nineteen leukemia, YFP: yellow fluorescent protein, AGM: aorta-gonads-mesonephros, FL: fetal liver, BM: bone marrow, CD: cluster of differentiation, PB: peripheral blood, FACS: fluorescence-activated cell sorting

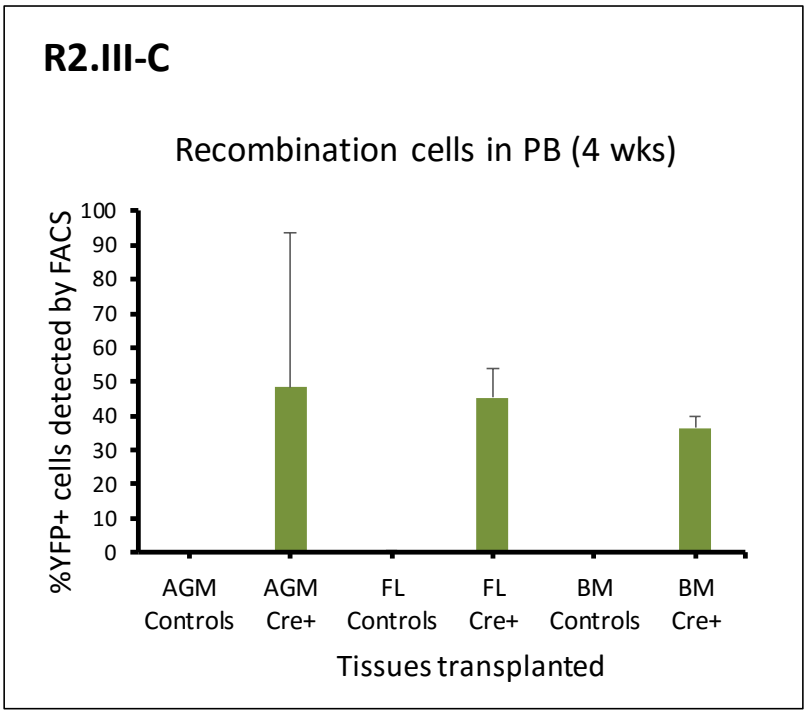

R2. III - C: Detection of the recombined cells within the donor compartment: The transplant recipients of recombined and control AGM/FL/BM tissues were bled one-month post-transplantations from the tail vein. PB was analyzed by FACS to detect YFP^+ cells in donor derived $CD45.2^+$ population in the transplant recipients. YFP^+ cells were detected in the FITC channel. Values are represented as Mean±SD. MLL: mixed lineage leukemia, ENL: eleven-nineteen leukemia, YFP: yellow fluorescent protein, AGM: aorta-gonads-mesonephros, FL: fetal liver, BM: bone marrow, CD: cluster of differentiation, PB: peripheral blood, FACS: fluorescence-activated cell sorting

Blood analyses of all transplant recipients were conducted up to 360 days post-transplantation. The contribution of donor-derived cells to myeloid and lymphoid lineages were comparable in recipients of recombined versus control cells (of AGM, FL and BM tissues) (Fig. R2.III-D). This was likely due to inefficient MLL-ENL-recombination as the fusion gene could not be detected in PB of any of the Cre^+ transplant recipients by PCR.

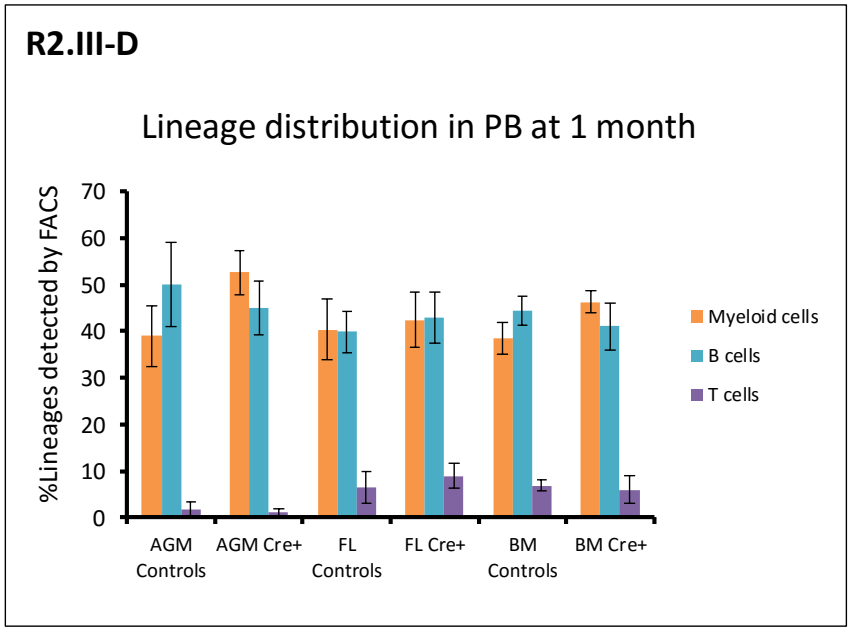

R2. III - D: Lineage distribution analysis of PB from transplant recipients one-month post-transplantation: The transplant recipients of recombined versus control AGM/FL/BM tissues were bled one-month post-transplantations from the tail vein. PB samples were stained with antibodies against surface markers CD45.1, CD45.2, Mac1, Gr1, B220, CD3e to measure myeloid, B- and T-lymphocyte lineages within the $CD45.2^+$ donor-derived cells of recipient mice. Values are represented as Mean±SD. Student's t-test was performed for statistical significance and no significant differences were found ($p>0.05$). MLL: mixed lineage leukemia, ENL: eleven-nineteen leukemia, YFP: yellow fluorescent protein, AGM: aorta-gonads-mesonephros, FL: fetal liver, BM: bone marrow, CD: cluster of differentiation, PB: peripheral blood

The mice were then monitored up to 480 days post-transplantation at which point the final analyses were performed by collecting organs from euthanized mice. Within this period, a portion of Cre^+ transplant recipients (of AGM, FL and BM tissues) died at different time-points. Their end-point analyses were conducted at the corresponding stages and survival of transplant recipients is illustrated (Fig. R2.III-E).

This end-point analyses included detection of:

i. MLL-ENL fusion gene by PCR using BM-derived DNA from all transplant recipients (Fig. R2.III-F),
ii. lineage distribution of donor-derived cells in BM of transplant recipients by FACS (Fig. R2.III-I)
iii. histological analysis of peripheral organs by Hematoxylin-Eosin staining of organ sections (Fig. R2.III-L)

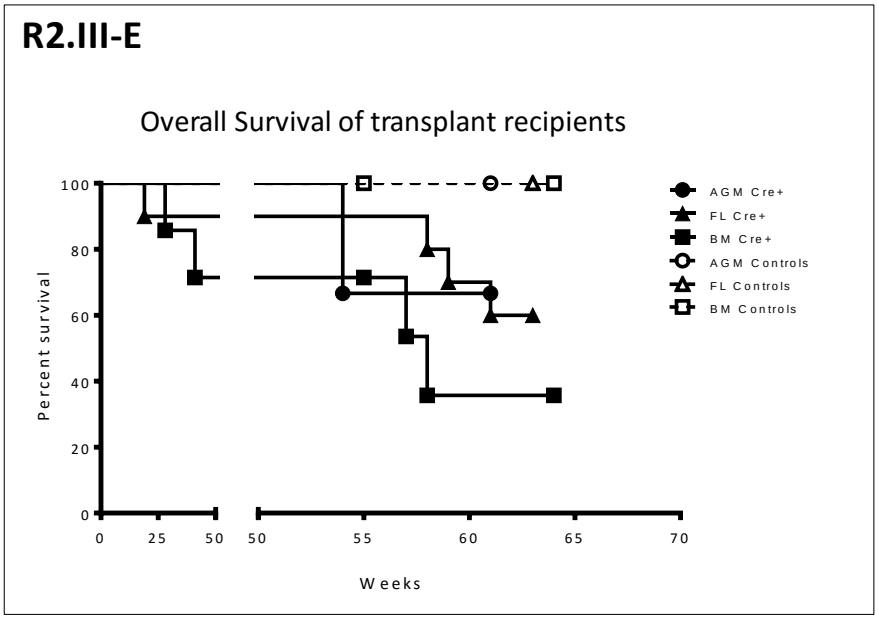

R2. III - E: Kaplan-Meier survival curves of mice transplanted with Cre^+ and control AGM (circle), FL (triangle) and BM (square) tissues are represented. MLL: mixed lineage leukemia, ENL: eleven-nineteen leukemia, YFP: yellow fluorescent protein, AGM: aorta-gonads-mesonephros, FL: fetal liver, BM: bone marrow

Detection of MLL-ENL fusion gene was done by PCR using DNA extracted from BM of all transplant recipients.

Only a subset of the Cre^{+} transplant recipients showed presence of the MLL-ENL fusion gene (Fig. R2.III-F-Upper panel). The recipient mice that did not carry the MLL-ENL fusion gene remained disease free (Fig. R2.III-D,E-Lower panel).

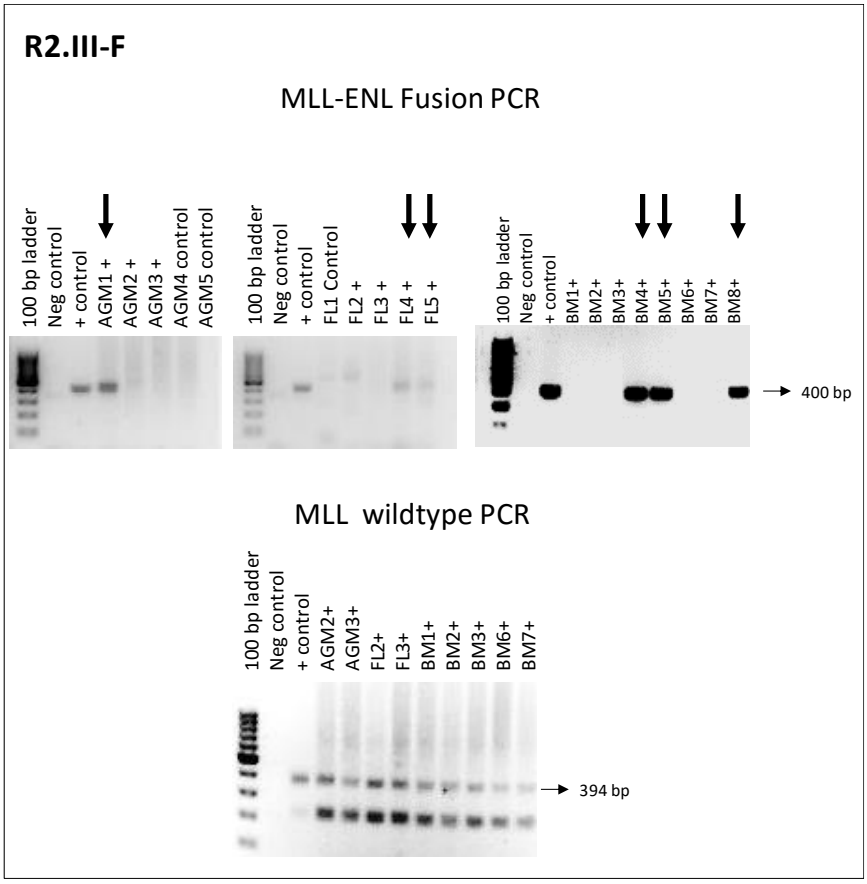

R2. III - F: Translocation detection in diseased/euthanized transplant recipients: DNA was extracted from BM of all transplant recipients. Upper panel- MLL-ENL fusion gene (400bp) was detected by PCR. Lower panel – The MLL-wildtype gene (394 bp) was detected by PCR as a control as it is be present in both Cre^{+} and control tissues (AGM/FL/BM). PCR products were run on 2% agarose gel alongside 100bp DNA ladder. MLL: mixed lineage leukemia, ENL: eleven-nineteen leukemia, AGM: aorta-gonads-mesonephros, FL: fetal liver, BM: bone marrow, DNA: deoxyribonucleic acid, bp: base pairs, PCR: polymerase chain reaction

The recipient mice carrying MLL-ENL fusion gene had disease symptoms only after a year of transplantation, showing a long latency in leukemia development (Fig.R2.III-E).

By comparing results of MLL-ENL translocation detection and survival data of the corresponding mice we deduced that 33%, 50% and 37% of AGM, FL and BM Cre^+ transplant recipients respectively developed an MLL-ENL-driven CML-like disease (Fig. R2.III-F – black arrows are pointed to leukemic mice). Based on these criteria we subdivided the Cre^+ transplant recipients into 'leukemic' and 'non-leukemic' groups.

The majority of BM cells of all transplant recipients were donor-derived (>90%) (Fig. R2.III-G). And, within the donor-derived populations of FL and BM Cre^+ transplant recipients, approximately 50% of cells were YFP^+ (Fig. R2.III-H). High variability in YFP-expression was observed in transplant recipients of the Cre^+ AGM tissue (ranging between 10-90% of YFP^+ cells) (R2.III-E-G).

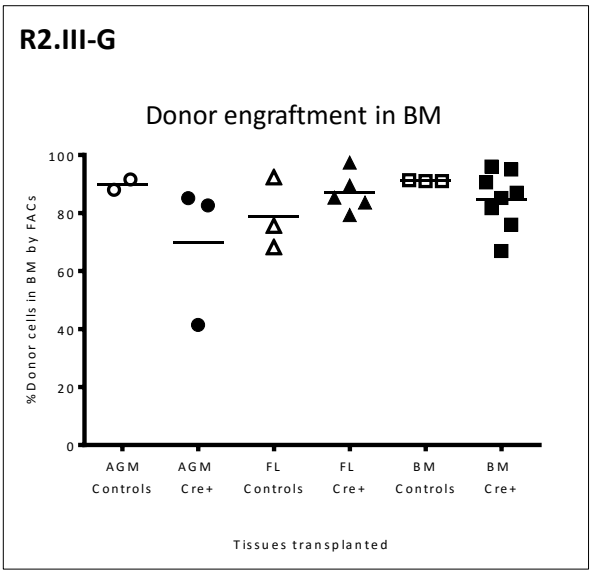

R2. III - G: Donor engraftment in BM cells of euthanized/diseased transplant recipients: Donor derived cells were detected in the BM of diseased/euthanized transplant recipients by staining BM cells with antibodies against CD45.1 and CD45.2 to detect $CD45.2^{+}CD45.1^{-}$ donor population represented in the graph above. MLL: mixed lineage leukemia, ENL: eleven-nineteen leukemia, YFP: yellow fluorescent protein, BM: bone marrow, CD: cluster of differentiation

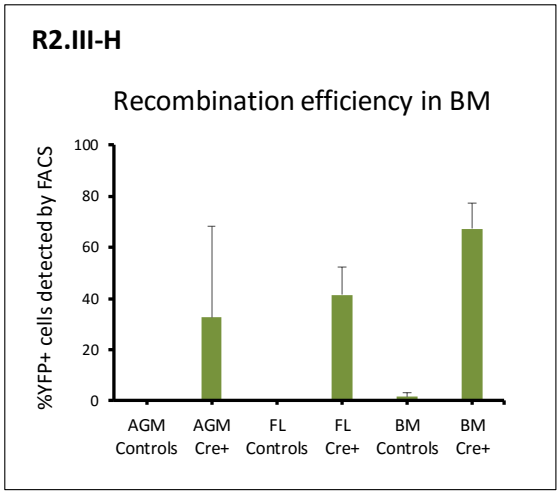

R2. III - H: Detection of YFP-expression within the donor-derived BM cells of euthanized/diseased transplant recipients: YFP-expression within the donor-derived cells were detected in BM of diseased/euthanized transplant recipients as part of the end-point analyses by flow cytometry. YFP^{+} cells were detected in FITC channel. The $CD45.2^{+}YFP^{+}$ cells in all transplant recipients are represented above. Values are represented as Mean±SD. MLL: mixed lineage leukemia, ENL: eleven-nineteen leukemia, YFP: yellow fluorescent protein, BM: bone marrow

The diseased mice carrying MLL-ENL translocation had a significantly higher contribution to $Mac1^{+}Gr1^{+}$ cells when compared to the Cre^{+} 'non-leukemic' and control mice (Fig. R2.III-I).

The BM analyses of 'non-leukemic' and control recipients showed similar contributions to myeloid and lymphocytes (B and T) (Fig. R2.III-I).

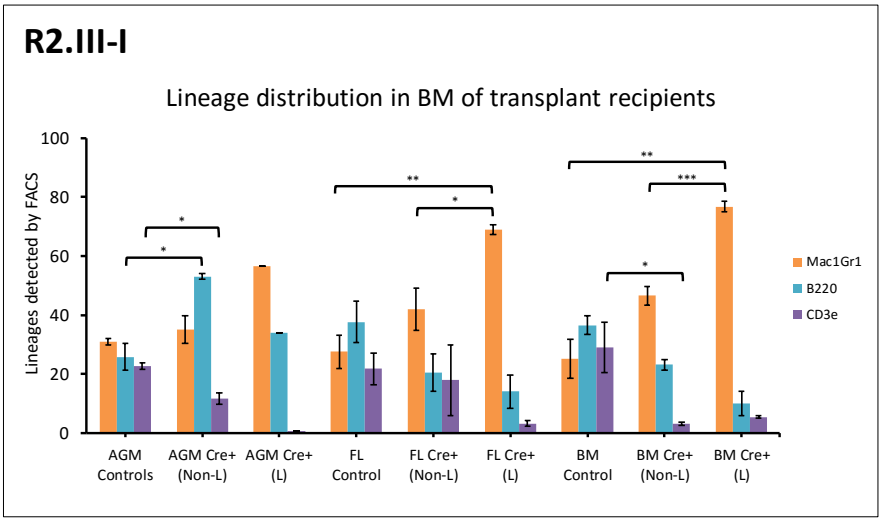

R2. III - I: Lineage distribution analysis of BM cells from all diseased/euthanized transplant recipients: The lineage distribution analysis of BM cells from euthanized transplant recipients (AGM/FL/BM tissues) was performed by FACS. BM cells were stained with antibodies against CD45.1, CD45.2, Mac1, Gr1, B220, CD3e to measure contribution to myeloid, B- and T-lymphocyte lineages within the $CD45.2^{+}$ donor-derived cells in BM of recipient mice. Contribution to myeloid and lymphocyte lineages in Cre^{+} 'Leukemic' (L), Cre^{+} 'Non-leukemic' (Non-L) and control mice are represented as Mean±SD. Student's t-test was performed for statistical analysis (* : $p<0.05$, ** : $p<0.01$, *** : $p<0.001$, ns [not significant]: $p>0.05$). Only one of the Cre^{+} AGM recipients was leukemic and BM analysis of this mouse is represented in the bar graph above as AGM Cre+ (L). MLL: mixed lineage leukemia, ENL: eleven-nineteen leukemia, YFP: yellow fluorescent protein, AGM: aorta-gonads-mesonephros, FL: fetal liver, BM: bone marrow, CD: cluster of differentiation

Organs were collected from diseased/euthanized transplant recipients to perform organ-infiltration analysis. The aspects (size and weight) of spleens were noted (Fig. R2.III-J,K) and histological analysis of all organs (such as spleen, liver and lungs) were performed by Hematoxylin-Eosin staining of paraffin embedded organ sections (Figs. R2.III-L).

We observed significant differences in the appearance of spleens of Cre^+ 'leukemic' versus Cre^+ 'non-leukemic' and control recipients of FL and BM tissues. The Cre^+ 'leukemic' mice showed splenomegaly while spleens of respective Cre^+ 'non-leukemic' mice were normal and comparable to control mice (Fig. R2.III-K).

A tumor was found on the spleen of one of recipient mice of Cre^+ FL tissue that developed chronic myelogenous leukemia-like disease (* in Fig. R2.III-J). And, one of the recipients of Cre^+ AGM also developed splenomegaly as a result of the chronic-like leukemia. However, the other two Cre^+ 'non-leukemic' AGM transplant recipients had normal spleens comparable to control mice (Fig. R2.III-K).

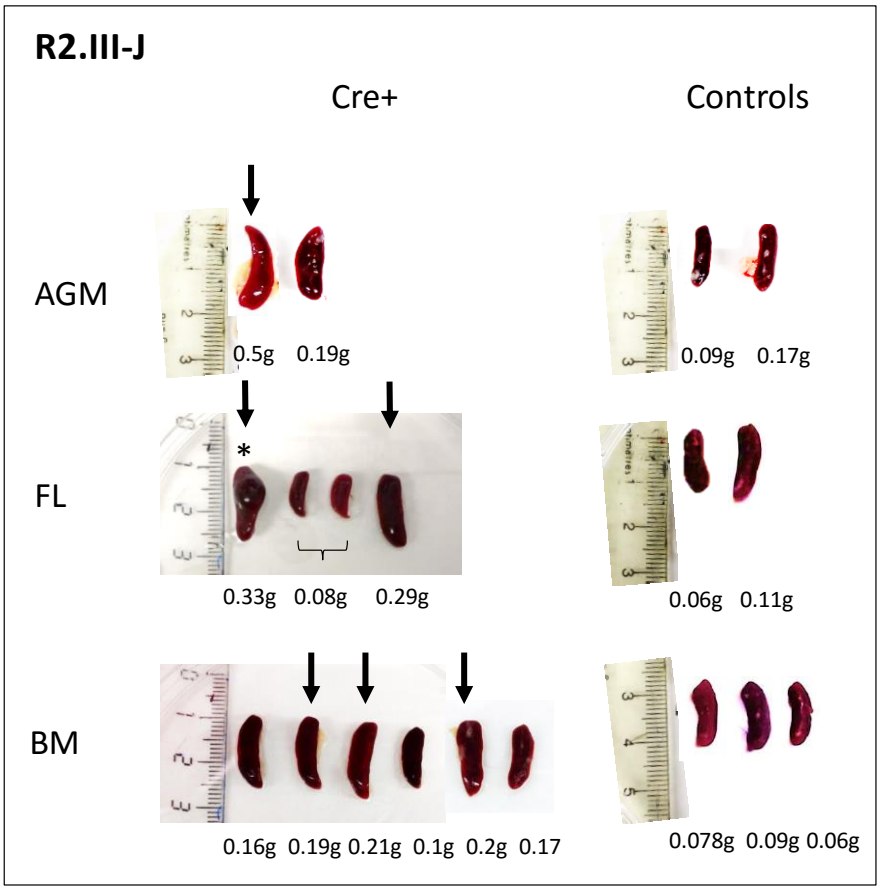

R2. III - J: Spleens from AGM, FL and BM transplant recipients. Black arrows are pointed to spleens of Cre$^+$ 'leukemic' transplant recipients (of AGM/FL/BM tissues) that developed a chronic leukemia-like disease. Spleens of the Cre$^+$ 'non-leukemic' and control recipients had normal aspects. The weights of all spleens are represented below the organs in grams. AGM: aorta-gonads-mesonephros, FL: fetal liver, BM: bone marrow, * : tumor observed in the spleen

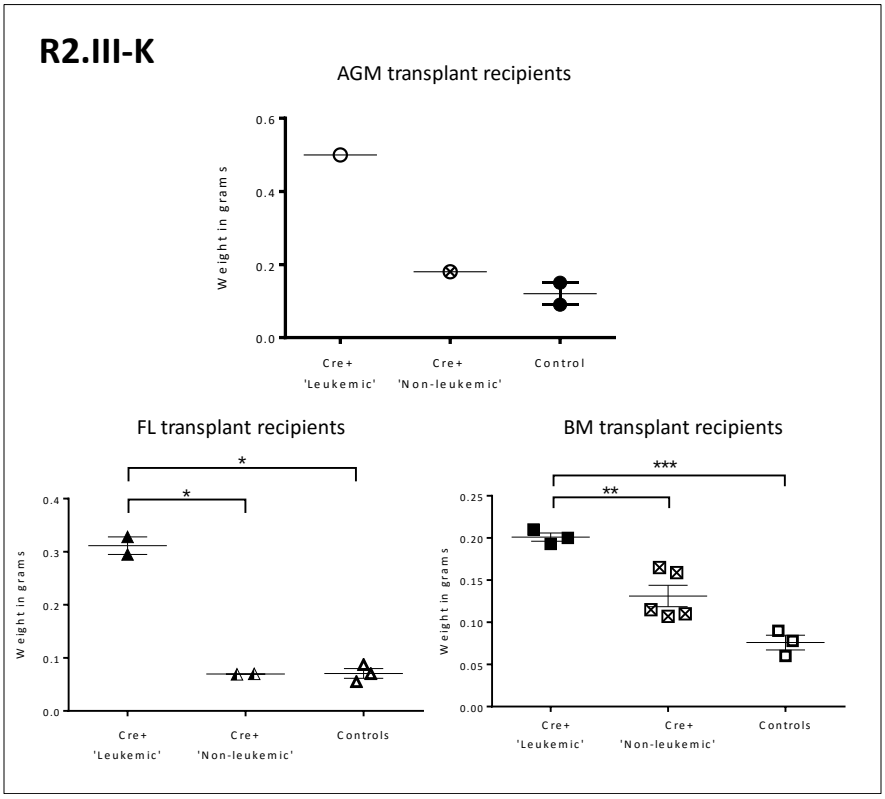

R2. III - K: Overall comparison of splenic aspects of MLL-ENL:R26-YFP:β-actin Cre$^+$ versus control transplant recipients (of AGM/FL/BM tissues): Weights of spleens (in grams) from Cre$^+$ versus control recipients were measured as part of the end-point analyses. Quantifications of spleen weights (in grams) are plotted for Cre$^+$ 'leukemic', Cre$^+$ 'non-leukemic' and control transplant recipients of the AGM, FL and BM tissues. Student's t-test was performed for statistical analysis (* : $p<0.05$, ** : $p<0.01$, *** : $p<0.001$, ns [not significant]:$p>0.05$). MLL: mixed lineage leukemia, ENL: eleven-nineteen leukemia, YFP: yellow fluorescent protein, AGM: aorta-gonads-mesonephros, FL: fetal liver, BM: bone marrow

Leukemic infiltrates were found in the spleens, livers and lungs of all Cre$^+$ 'leukemic' transplant recipients (Fig. R2.III-L). Micro-infiltrations were detected in these mice unlike the extensive infiltrations observed in Vav1-Cre mediated MLL-ENL-driven AML model (Fig. R1-J).

The organs of Cre$^+$ 'non-leukemic' transplant recipients had normal histology, similar to controls (Fig. R2.III-L).

We have encountered recurrent problems in developing MLL-ENL-driven embryonic and adult leukemias using the inducible β-actin Cre^{ERT} line. Inefficient MLL-ENL-recombination has persisted in spite of implementing distinct Cre-induction strategies at embryonic and adult stages. Low efficacy of Cre-mediated translocation in embryonic and adult tissues resulted in development of chronic-like leukemias in <40% of mice.

Therefore, we used the alternative interferon inducible Mx1-Cre mice to improve MLL-ENL-recombination efficiency at embryonic and adult stages.

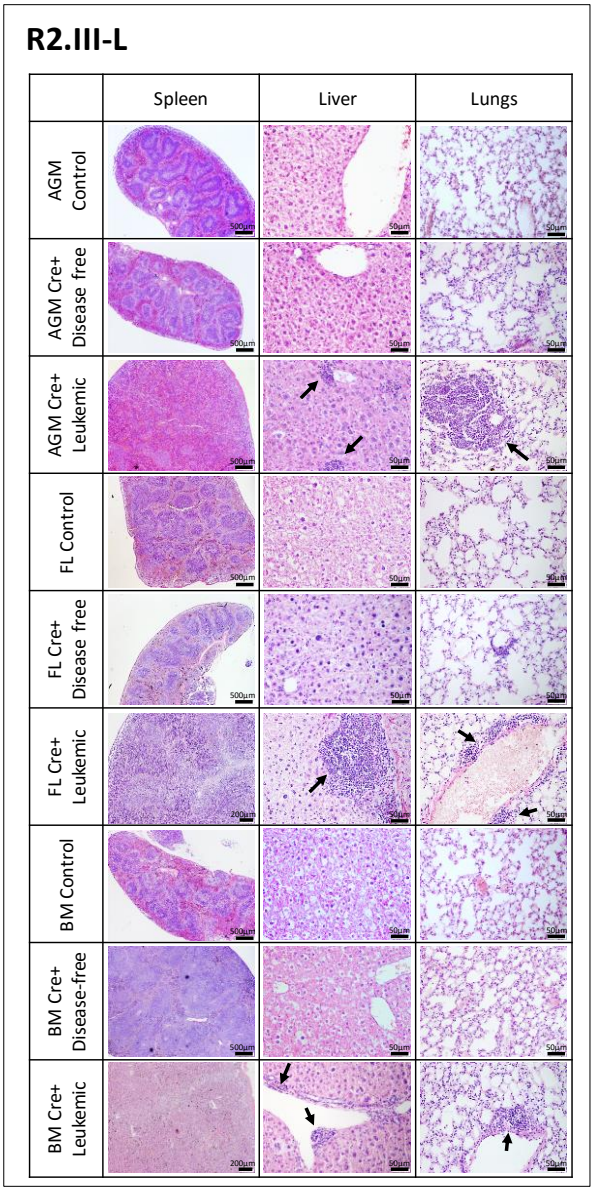

R2. III - L: Histological analysis of organs from diseased/euthanized transplant recipients: Final analysis of all diseased/euthanized transplant recipients included histological analysis of peripheral organs (such as spleen, liver and lungs). Hematoxylin-Eosin staining was performed on paraffin embedded organ sections (10μm thick). Representative images of spleens (2X), livers (20X) and lungs (40X) from Cre^+ 'leukemic', Cre^+ 'Non-leukemic' and control transplant recipients are shown. Leukemic infiltrates were detected only in the organs of Cre^+ 'leukemic' mice (arrows). MLL: mixed lineage leukemia, ENL: eleven-nineteen leukemia, YFP: yellow fluorescent protein, AGM: aorta-gonads-mesonephros, FL: fetal liver, BM: bone marrow

RESULTS PART-3

DEVELOPING T(11;19) INDUCED LEUKEMIA MOUSE MODEL:

RECAPITULATING HUMAN PEDIATRIC AND ADULT LEUKEMIAS

INDUCIBLE MX1-CRE:MLL^{LoxP}ENL^{LoxP} MOUSE MODEL

ADULT LEUKEMIA MODEL: BM-DERIVED

Developing BM-derived adult acute leukemia mouse model carrying t(11;19): Using the Interferon/polyIC inducible Mx1-Cre mice

The tamoxifen-inducible β-actin Cre^{ERT} model was inefficient in inducing the MLL-ENL translocation in both embryonic and adult hematopoietic tissues. To overcome these drawbacks we used an alternative Cre mouse model.

The interferon inducible Mx1-Cre mice were crossed with MLL-LoxP,ENL-LoxP mice to control timing and tissue of recombination (Kühn et al. 1995; Collins et al. 2000). The Mx1 gene is a part of the immune defense system to fight against the Influenza virus. It is silent in healthy mice and its expression can be activated by using interferon or polyIC (synthetic double stranded RNA). Therefore, we could control the initiation of Cre recombination by polyIC induction at different stages of hematopoietic development. The Mx1-Cre mice have been well characterized for their use in targeting the hematopoietic compartment in adult mice (Hall et al. 2003; Li et al. 2011). This Cre model would thus aid in targetting hematopoietic cells more specifically.

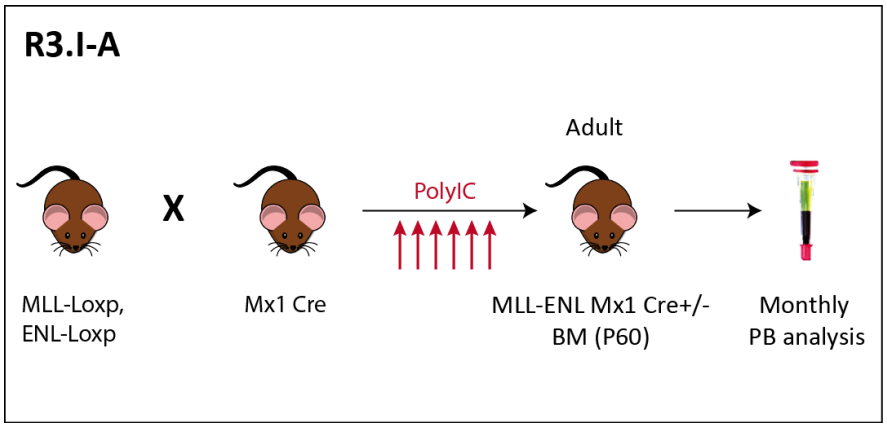

R3.I - A: Experimental scheme of developing adult (BM)-derived MLL-ENL leukemia model using poly IC inducible Mx1-Cre mice: The adult MLL-ENL,Mx1-Cre$^+$/control mice were induced in-vivo with polyIC at 2 months of age (P60). Six doses of polyIC (15 µg/gram body weight/dose) were administered to adult Cre$^+$ and control mice via intraperitoneal injections given every second day. One-month post in-vivo inductions, the Cre$^+$ and control mice were bled from the tail vein and peripheral blood analysis was conducted monthly. MLL: mixed lineage leukemia, ENL: eleven-nineteen, Mx1: Myxovirus, PolyIC: polyinosinic:polycytidylic acid, BM: bone marrow, PB: peripheral blood, P60: postnatal age of mice of 60 days

MLL-LoxP, ENL-LoxP mice (Collins et al. 2000) were crossed with Mx1-Cre$^+$ mice (Kühn et al. 1995)(Fig. R3.1 - A). The progeny from the crossing MLL-ENL,Mx1-Cre$^+$ and Cre negative (controls) littermates were induced in-vivo at 2 months of age (P60). Cre$^+$ and control mice were administered with polyIC using the in-vivo induction protocol as described in methods (See Methods I-ii) (Klinakis et al. 2011). A month post in-vivo inductions, we performed peripheral blood analysis of Cre$^+$ and control mice to detect disease onset (Fig. R3.1 - A).

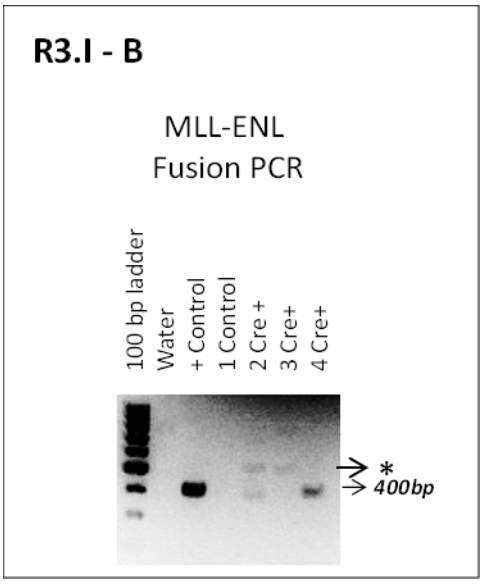

R3.I - B: Recombination detection: MLL-ENL fusion gene (400 bp) detection was performed by PCR as previously described (Cano et al. 2008b). Genomic DNA was extracted from PB of MLL-ENL:Mx1-Cre^{+} and control mice at one-month post in-vivo inductions (See Methods III). PCR products were run on 2% agarose gel alongside the 100bp DNA ladder. * represents an unspecific band. MLL: mixed lineage leukemia, ENL: eleven-nineteen, Mx1: Myxovirus, PolyIC: polyinosinic:polycytidylic acid, BM: bone marrow, PB: peripheral blood, PCR: polymerase chain reaction, DNA: deoxyribonucleic acid, bp: base paris

We first assessed the translocation recombination efficiency of Mx1-Cre model. We extracted DNA from peripheral blood collected from the tail vein of MLL-ENL:Mx1-Cre^{+}/control mice, one month post inductions (Methods III). MLL-ENL fusion PCR was performed and the fusion gene was detected in 60% of Cre^{+} mice at this early time-point (Fig. R3.I - B). This finding indicated the higher efficiency of Cre recombination attained using the Mx1 mice when compared to the β-actin Cre^{ERT}.

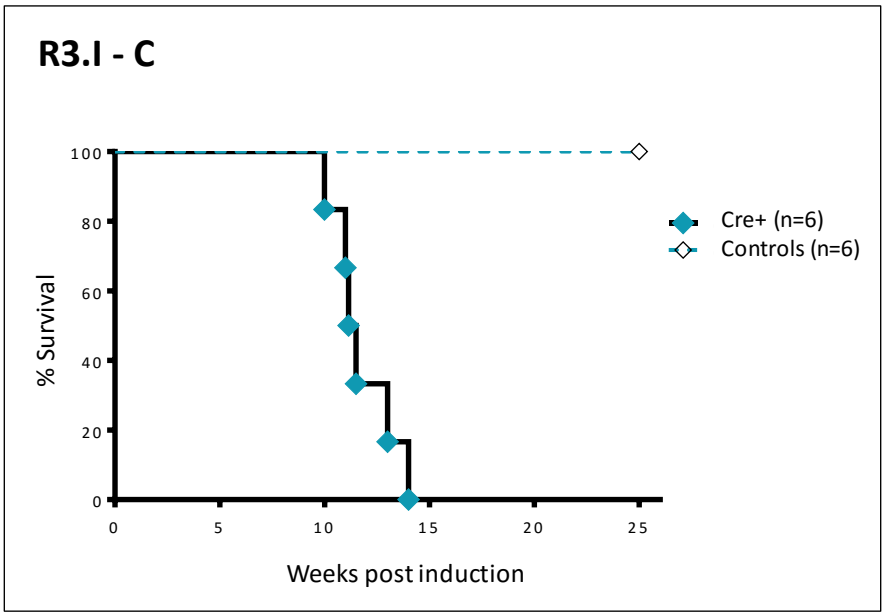

R3.I - C: Survival data of MLL-ENL,Mx1-Cre$^+$ versus control mice: Kaplan-Meier survival curve of MLL-ENL,Mx1-Cre$^+$ and control (cre negative) mice. Median survival of Cre$^+$ mice is 12 weeks post in-vivo inductions. Controls remained disease free. Data is represented of six adult mice (Cre$^+$/controls). MLL: mixed lineage leukemia, ENL: eleven-nineteen, Mx1: Myxovirus

All Cre$^+$ mice carried the MLL-ENL fusion gene and developed a fatal disease within the third month post in-vivo inductions (Fig. R3.I - C). The median survival of Cre$^+$ mice was 12 weeks. The control mice that were also treated with polyIC alongside the Cre$^+$, remained healthy (Fig. R3.I - C). The polyIC inducible Mx1-Cre model resulted in an MLL-ENL driven fatal disease with 100% efficiency. We characterized the disease developed in these mice by peripheral blood analysis, similar to the Vav1-Cre model of MLL-ENL driven disease in mice.

To characterize this BM-derived acute leukemia carrying MLL-ENL fusion genes, we performed several analyses. We began by analyzing the complete and differential peripheral blood counts (Fig R3.I - D).

The complete blood count (CBC) by the second month showed significantly higher (approximately 12 fold higher) white blood cells (WBCs) in the Cre^+ mice when compared to their control counterparts. WBCs of control mice were within the normal range ($2.6x10^9$/l-$13.2x10^9$/l) (Fig R3.I - D). This significant increase in WBCs was the first sign of leukemia onset in Cre^+ mice.

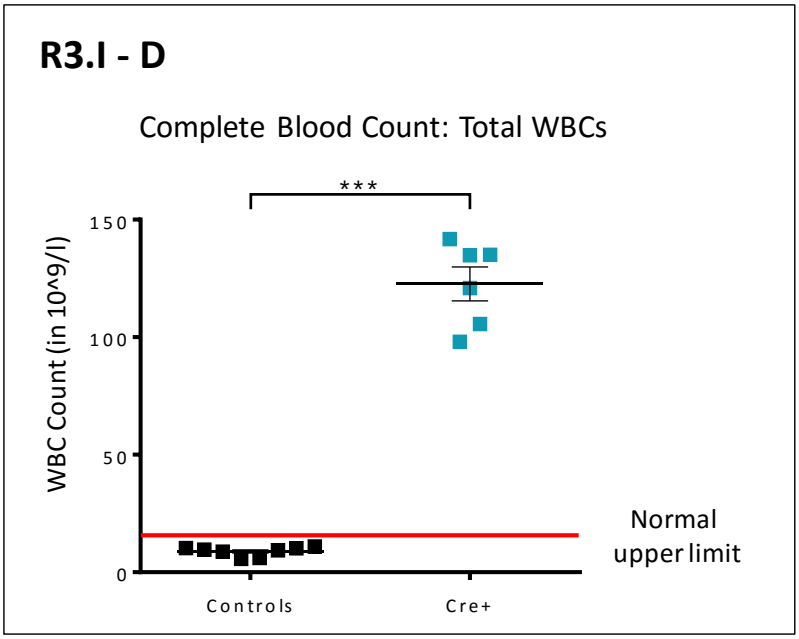

R3.I - D: Disease onset detection by peripheral blood analysis: Complete blood counts were measured from PB samples from MLL-ENL,Mx1-Cre^+/control mice, monthly post-inductions. At two months post-inductions, we detected disease onset, the graph represents total WBCs in Cre^+/control mice at the second month of analysis. The red line marks the normal upper limit of total WBCs found in healthy mice (which is $13x10^9$/liter). Values are represented as Mean±SD of ($n \geq 6$ Cre^+ and control mice). Student's t-test was performed for statistical analysis (*** : $p<0.001$). MLL: mixed lineage leukemia, ENL: eleven-nineteen, Mx1: Myxovirus1, PB: peripheral blood, WBCs: white blood cells

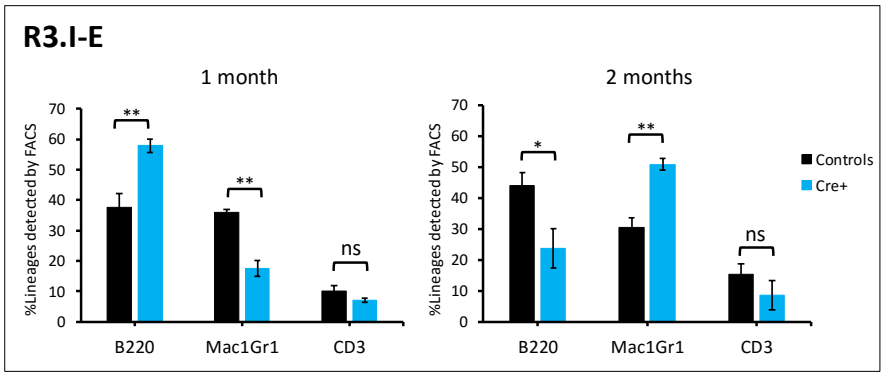

R3.I - E: Disease characterization: MLL-ENL,Mx1-Cre$^+$/control mice were bled monthly from their tail vein. PB was analyzed by flow cytometry to characterize the disease arising in the Cre$^+$ mice. Blood analysis at 1 month (left) and 2 months (right) time-points are represented here. PB cells were stained with antibodies against the surface markers Mac1(CD11b), Gr1, B220, CD3e and Ter119 to detect distribution of PB to myeloid, B- and T-lymphocytes by FACS. PB of Cre$^+$ mice consisted of myeloid cells (Mac1$^+$Gr1$^+$) in majority by the second month post in-vivo inductions. The controls, on the other hand, continued to have normal contributions to all blood cell lineages. Values are represented as Mean±SD. Student's t-test was performed for statistical analysis (* : $p<0.05$, ** : $p<0.01$, ns [not significant]: $p>0.05$). MLL: mixed lineage leukemia, ENL: eleven-nineteen, Mx1: Myxovirus1, PB: peripheral blood, FACS: fluorescence-associated cell sorting

We wanted to characterize the disease further by identifying the leukemia subtype arising in these mice. For this, we analyzed the distinct blood cell lineages in Cre$^+$ versus control mice by flow cytometry analysis on a monthly basis. Blood was collected from the tail vein of Cre$^+$/control mice and stained with antibodies specific to the myeloid and lymphocytes surface markers (Fig. R3.I-E). Initial analysis (at 1 month post-inductions) showed similar contribution to blood cell lineages in Cre$^+$ and control mice. However, by the second month, the Cre$^+$ mice developed leukocytosis and succumbed to an acute myeloid leukemia characterized by Mac$^+$Gr1$^+$ leukemic blasts (Fig. R3.I-E).

By the third month post inductions, all Cre$^+$ mice succumbed to an AML disease driven by MLL-ENL fusion. Control mice were healthy

and had normal contribution to blood cell lineages. The terminally ill mice were euthanized to perform the final analyses. The BM cells from diseased leukemic mice consisted of myeloid cells in majority, concurring with results of blood analysis. The leukemic blasts found in BM were $Mac1^{+}Gr1^{+}$ cells (Fig. R3.I-F).

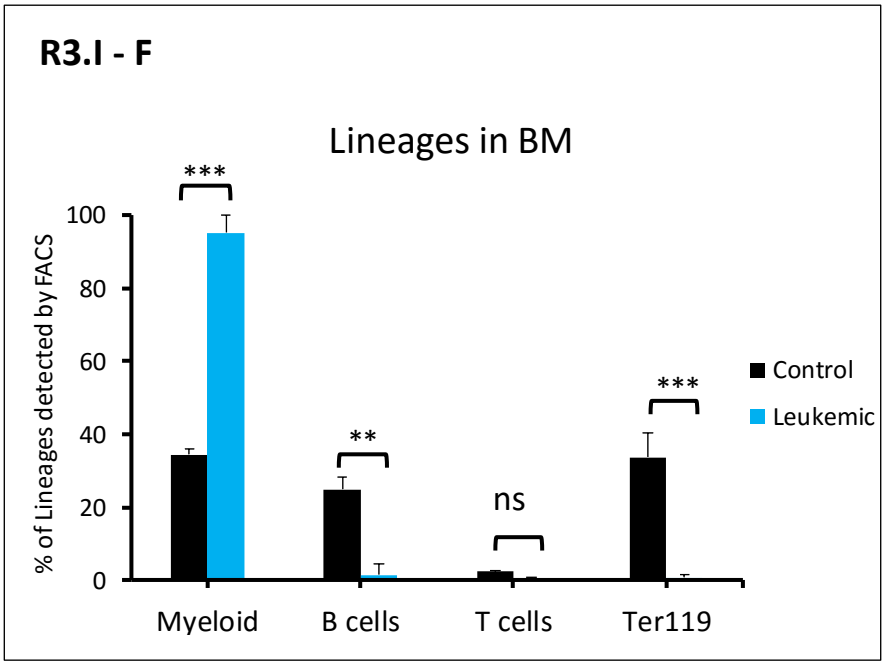

R3.I - F: Identifying leukemic blasts in BM: Bone marrow cells from diseased/euthanized MLL-ENL,Mx1-Cre^{+}/control mice were stained with antibodies against the surface markers for Myeloid(Mac1), granulocytes(Gr1), B-lymphocytes(B220), T-lymphocytes(CD3e) and erythrocytes(Ter119). The BM of Cre^{+} mice were populated in majority with $Mac1^{+}Gr1^{+}$ cells while controls had normal contributions to all BM populations. Values are represented as Mean±SD. Student's t-test was used for statistical analysis (** : $p<0.01$, *** : $p<0.001$, ns [not significant]: $p>0.05$). MLL: mixed lineage leukemia, ENL: eleven-nineteen, Mx1: Myxovirus, BM: bone marrow

We concluded that Mx1-Cre-mediated t(11;19) induction in BM tissue led to the development of acute myeloid leukemia (AML) in mice (Fig.

R3.I-F). The leukemia phenotype was similar to what we had observed with the constitutive Vav1-Cre model of MLL-ENL leukemia.

This was also confirmed by performing Wright-Giemsa staining on BM cytospins from leukemic and control mice (Fig. R3.1-G). We detected majority of BM cells of Cre^+ mice to be 'myeloid-blast like' (Fig. R3.I – G right panel). Whereas BM cells of control mice were a heterogeneous population constituted of myeloid, lymphoid and erythroid populations (Fig. R3.I – G left panel).

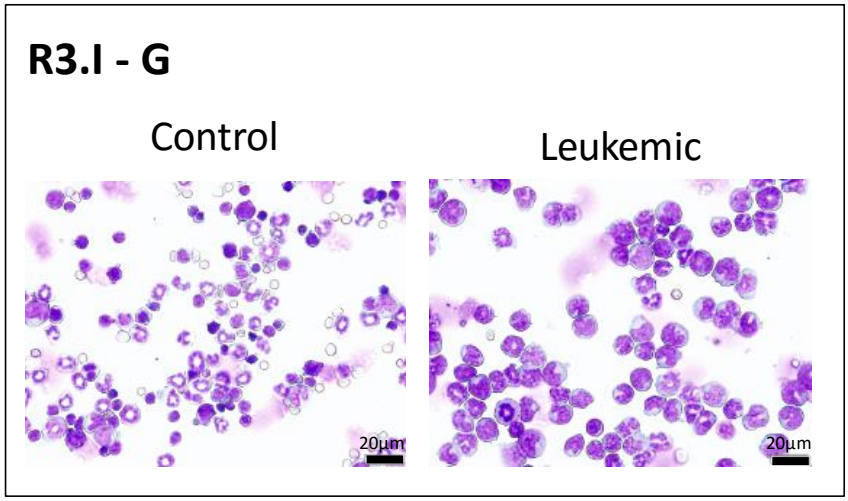

R3.I - G: Representative Wright-Giemsa stained BM cells: Cytospin of bone marrow cells from euthanized control and Cre^+ mice were prepared on slides. Wright-Giemsa staining was performed on the cytospin samples and images were captured at 20X magnification under the bright-field microscope. The control mice had normal contribution to myeloid, T- and B-lymphocytes and erythrocytes. While the BM cells from Cre^+ mice consisted of 'myeloid-blast-like' cells in majority. Scale bar: 20 µm.

The human AML disease leads to infiltration in several peripheral organs including the spleen and liver (Lapidot et al. 1994; Kato et al. 2011; Miraki-Moud et al. 2013). This was also observed in the current

AML mouse model (Fig. R3.I - H). Striking splenomegaly was found in Cre^+ mice (> 3 fold) when compared to controls.

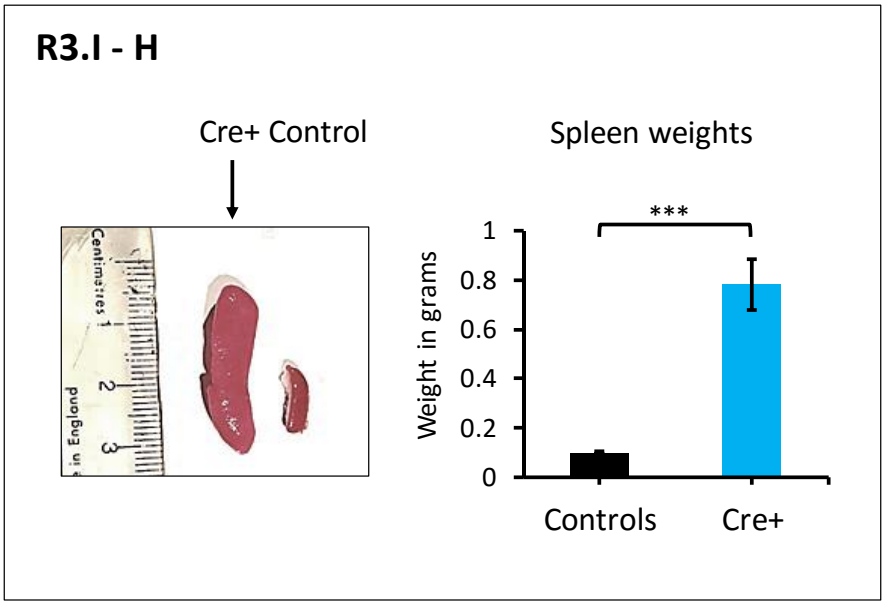

R3.I - H: Splenomegaly was observed in the Cre^+ leukemic mice. Left panel - Representative spleens from control and leukemic (arrow) mice are shown. Right panel - Quantifications of spleen weights (in grams) are also represented. Values are represented as Mean±SD (n=6 mice each of Cre^+ and controls). Student's t-test was performed for statistical analysis (*** : $p<0.001$). MLL: mixed lineage leukemia, ENL: eleven-nineteen, Mx1: Myxovirus1

The peripheral organs taken from Cre^+ and control mice were embedded in paraffin. 10 µm thick sections of the tissues were cut on the microtome and Hematoxylin and Eosin staining was performed to observe histology of organs from Cre^+ versus control mice.

There was substantial infiltration of leukemic cells in liver, lungs and spleens of the diseased Cre^+ mice (Fig R3.I – I lower panel). The red pulp regions of the spleen were disrupted in leukemic mice. Extensive infiltration was found in distinct lobes of the liver, particularly adjacent to vessels. Major areas of the lungs were also affected (Fig.R3.I-I). The

organs of the control mice had normal histology (Fig R3.I – I upper panel).

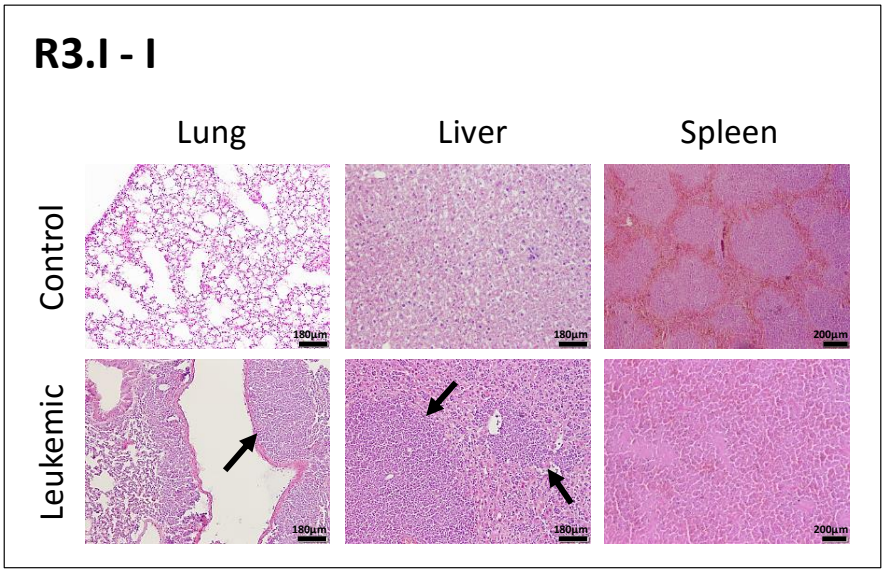

R3.I - I: Infiltration detection in peripheral organs of leukemic mice: Histological analysis of organs (such as liver, lungs and spleen) retrieved from euthanized MLL-ENL,Mx1-Cre^{+}/control mice was performed. 10 µm thick sections of the organs embedded in paraffin were stained with Hematoxylin and Eosin staining to detect leukemic infiltrates. The organs from control mice showed normal histology while leukemic mice had extensive infiltration adjacent to portal vessels of the liver and within the lungs (arrows). The white and red pulp regions of the spleen were completely disrupted with extensive infiltration in this organ in Cre^{+} mice. Representative images are shown here (10X magnification). MLL: mixed lineage leukemia, ENL: eleven-nineteen, Mx1: Myxovirus1

In conclusion, we could successfully develop a (adult BM-derived) mouse model of MLL-ENL driven AML disease using the polyIC inducible Mx1-Cre mice.

EMBRYONIC LEUKEMIA MODEL: FL-DERIVED

Developing an embryo-derived MLL-ENL leukemia model: Using polyIC inducible Mx1-Cre mice

The aim of this thesis has been to develop embryonic and adult MLL-ENL leukemia mice models that can recapitulate the human adult and pediatric diseases respectively.

In humans, infant leukemias arise as a result of chromosomal abnormality occurring prenatally. Thus, by targeting fetal liver hematopoiesis, we aimed at developing an embryo-derived acute leukemia mouse model that could recapitulate the human infant disease.

Despite the extensive use of Mx1-Cre for targeting adult hematopoietic cells, there is not much information on its efficacy in targeting embryonic cells. Most studies refer mainly to Mx1 gene expression post E16.5 stage in mice. Post E16.5 stage the Mx1 gene expression is found to be comparable to expression in adults (Arrode-Brusés & Brusés 2012; Kühn et al. 1995).

MLL-LoxP, ENL-LoxP mice (Collins et al. 2000) were crossed with the Mx1-Cre mice (Kühn et al. 1995) (Fig. R3.II - A) and Cre-induction was performed in-vivo in pregnant mice.

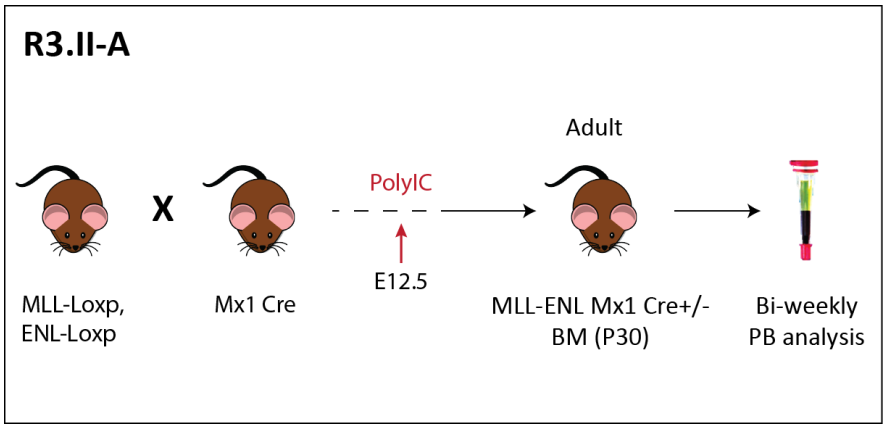

R3.II - A: Experimental strategy used to establish an embryo derived MLL-ENL leukemia mouse model using polyIC inducible Mx1-Cre: The MLL-LoxP, ENL-LoxP mice were crossed with Mx1-Cre^{+} mice and 20μg/g of polyIC was administered via an intraperitoneal injection in pregnant mice at E12.5 stage. The progeny from the crossing (MLL-ENL:Mx1Cre^{+}/controls) were bled post-weening (P30) and bi-weekly thereafter to detect disease onset and follow its progression. MLL: mixed lineage leukemia, ENL: eleven-nineteen, Mx1: Myxovirus1, PolyIC: polyinosinic:polycytidylic acid, E12.5: embryonic age of 12.5 (days post-coitus), PB: peripheral blood, P30: 30 days post-birth (postnatal age of mice), FL: fetal liver

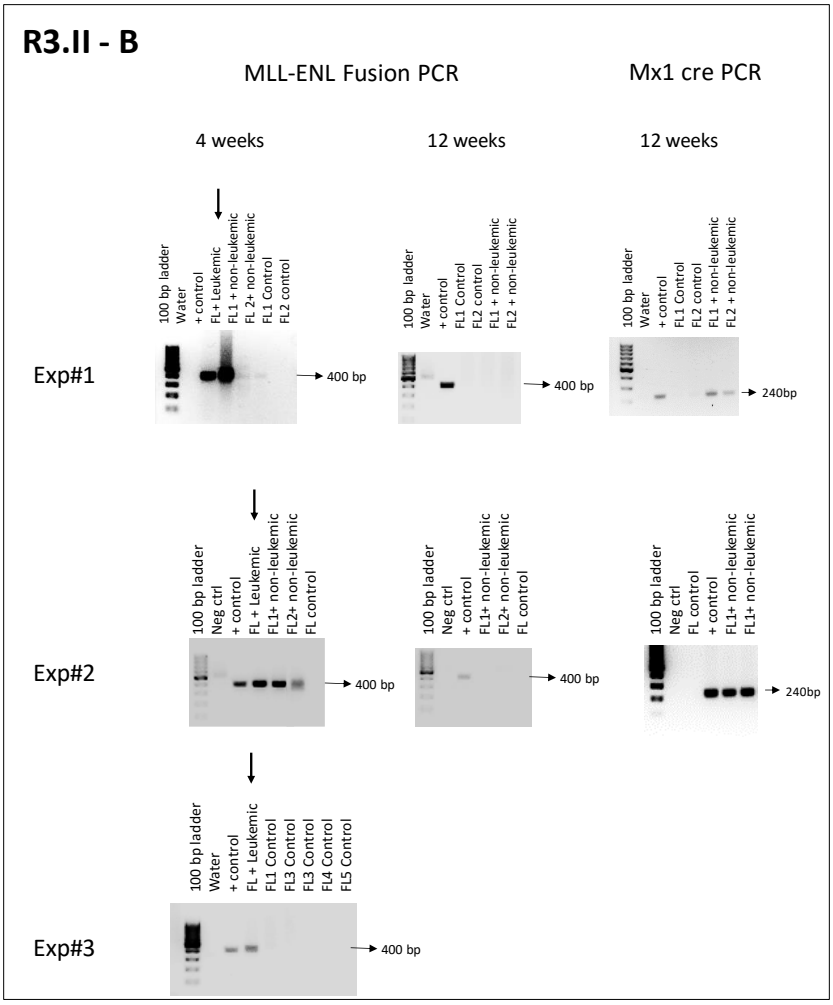

R3.II - B: Detecting translocation in circulation in MLL-ENL:Mx1-Cre^{+}/control mice induced in FL in-vivo: DNA was extracted from PB of MLL-ENL:Mx1-Cre^{+}/control mice that were induced in-vivo at E12.5 stage of development. Left and middle panels illustrate detection of MLL-ENL fusion gene (400bp) by PCR as previously described (Cano et al. 2008b). This was done using DNA extracted from PB of Cre^{+} and control mice at four weeks (P30) and twelve weeks (P90) respectively. Right panel - Mx1-Cre genotyping PCR was performed to detect the Cre gene (240 bp). PCR products were run on 2% agarose gel alongside 100 bp DNA ladder. Black arrows indicate the Cre^{+} mice that went on to develop the disease. Exp1, 2 and 3 represent three independent experiments with each experiment constutiting one pregnant mouse induced in-vivo at E12.5. MLL: mixed lineage leukemia, ENL: eleven-nineteen, Mx1: Myxovirus1, PolyIC: Polyinosinic:polycytidylic acid, E12.5: mouse embryonic stage (12.5 days post-coitus), PCR: polymerase chain reaction, bp: base pairs, DNA: deoxyribonucleic acid, PB: peripheral blood, P30/90: 30/90 days post-birth (postnatal age of mice), FL: fetal liver

PolyIC was administered at 20μg/g concentration, via intraperitoneal injection in the pregnant mice at 12.5 dpc as in Arrode-Brusés & Brusés 2012 (Fig. R3.II - A). The newborns had a normal survival rate and development.

Peripheral blood was collected at P30 by bleeding MLL-ENL:Mx1-Cre^{+} and control mice from their tail vein. Blood analyses were performed as described for previous models (See Methods VI) to detect disease onset (Fig. R3.II - A). The MLL-ENL fusion gene was detected by PCR in all Cre^{+} mice at 30 days of age (P30). However, a subset of Cre^{+} mice lost the MLL-ENL fusion gene by the age of 90 days (P90) and they were disease free.

Only 43% of in-vivo induced MLL-ENL:Mx1-Cre^{+} developed an aggressive disease resulting from MLL-ENL translocation formation. The median survival of these mice was seven weeks (Fig. R3.II-C-a). These mice were termed as Cre^{+} 'leukemic'.

Although we did detect the MLL-ENL fusion gene in all Cre^{+} mice at one month of age (P30), 57% of Cre^{+} mice lost the MLL-ENL fusion gene by 12th week of age (Fig.R3.II-B). This resulted in lack of disease development in these Cre^{+} mice (termed Cre^{+} 'non-leukemic').

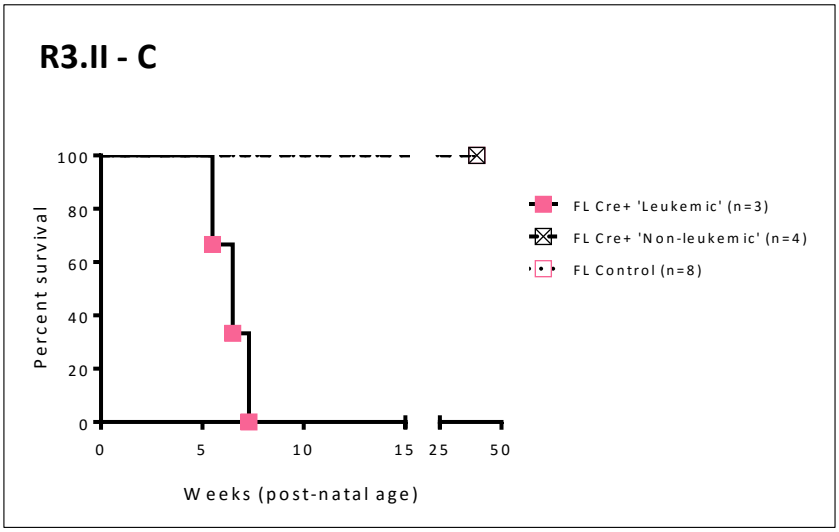

R3.II - C-a: Survival curve of Cre$^+$ versus controls in the embryonic (FL-derived) model of MLL-ENL leukemia: Kaplan-Meier survival curves are represented of MLL-ENL:Mx1-Cre$^+$ (leukemic versus non-leukemic) and control mice. In this graph, we have divided the Cre$^+$ mice into two subgroups based on their survival status and detection of MLL-ENLfusion gene by P90 (Fig.R3.II-B). The Cre$^+$ 'leukemic' mice succumbed to a fatal disease by week 7 (P49). Whereas, the Cre$^+$ 'non-leukemic' mice did not carry the MLL-ENL fusion gene post P90 stage and remained healthy like the controls. Pool of three independent experiments performed are shown. MLL: mixed lineage leukemia, ENL: eleven-nineteen, Mx1: Myxovirus1, PolyIC: polyinosinic:polycytidylic acid, E12.5: embryonic age of 12.5 (days post-coitus), P30/90: postnatal age of mice of 30/90 days, FL: fetal liver, PCR: polymerase chain reaction

Results are summarized in fig. R3.II-C-b

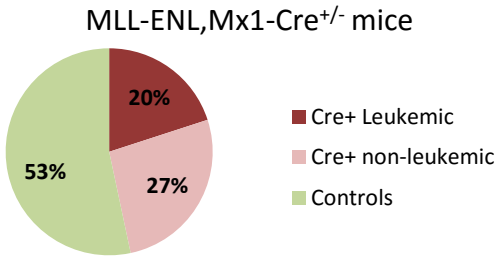

R3.II-C-b: Pie-chart representing the MLL-ENL:Mx1-Cre$^+$ and control mice induced at E12.5 from three independent experiments. Cre$^+$ mice are further subdivided into 'leukemic' versus 'non-leukemic'. 'Non-leukemic' mice did not carry the MLL-ENL fusion after P90 and remained disease free, while 'leukemic' mice succumbed to the disease driven by the MLL-ENL fusion gene.

The median survival of leukemic mice in the embryonic model of leukemia (seven weeks) was significantly shorter when compared to the adult leukemia (twelve weeks) (Fig.R3.II-D) suggesting a more aggressive embryo-derived disease when compared to the adult. This concurs with the more aggressive nature of human infant leukemias when compared to adult leukemias. This finding also suggests that an embryonic (FL) population has a greater leukemogenic potential when compared to an adult tissue (BM).

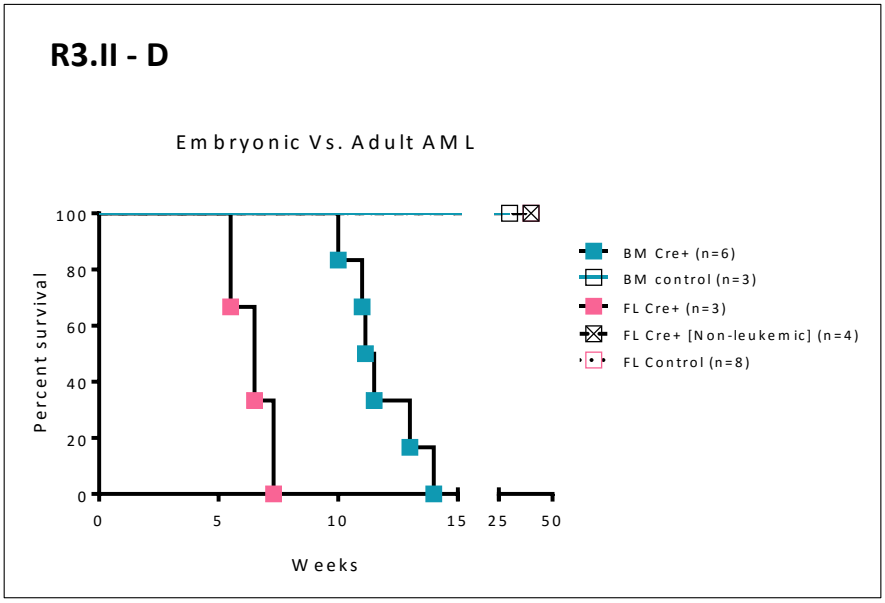

R3.II - D: Comparing survival of adult versus embryonic leukemias: Kaplan-Meier survival curves are represented of MLL-ENL:Mx1-Cre^{+}/control mice induced in adults versus embryonic tissues. In blue are mice from the adult (BM-derived) model of MLL-ENL disease that have a median survival of 12 weeks. In pink are the mice from the embryonic (FL-derived) model wherein a subset of Cre^{+} mice developed an MLL-ENL driven disease with a median survival of 7 weeks. Number of mice per group are mentioned within parenthesis in the graph. Three independent experiments were conducted for the embryonic model, by injecting three distinct pregnant mice during gestation at E12.5. And, six adult Cre^{+} and control mice each were induced in-vivo for the adult model. MLL: mixed lineage leukemia, ENL: eleven-nineteen, Mx1: Myxovirus1, PolyIC: polyinosinic:polycytidylic acid, E12.5: embryonic age of 12.5 (days post-coitus), P30/90: postnatal age of mice of 30/90 days, FL: fetal liver, BM: bone marrow

Disease onset was detected at the first time-point of blood analysis (at P30 stage) in Cre^{+} 'leukemic' mice with a significantly higher (>10 fold) total WBCs when compared to the remaining Cre^{+} 'non-leukemic' and control mice that remained healthy (Fig. R3.II-E).

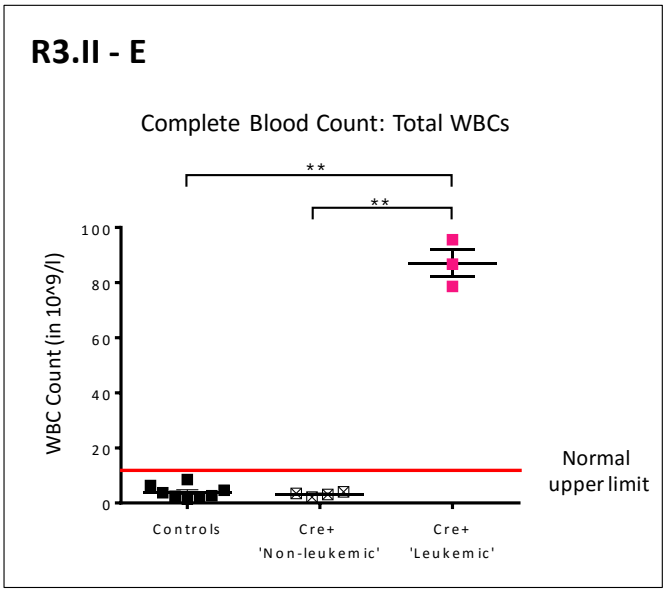

R3.II - E: Disease onset detection by peripheral blood analysis: Complete blood counts were measured of MLL-ENL:Mx1-Cre^{+} (Non-leukemic and leukemic) and control mice at one month of age (P30). These mice were induced in-vivo at E12.5. Leukocytosis was detected in the Cre^{+} 'leukemic' mice at this stage. The graph represents total WBCs in Cre^{+} versus control mice at one-month of age. The red line marks the normal upper limit of total WBCs found in healthy mice (which is $13x10^{9}$/liter). Values are represented as Mean$\pm$SD. Student's t-test was performed for statistical analysis (** : $p<0.01$). MLL: mixed lineage leukemia, ENL: eleven-nineteen, Mx1: Myxovirus1, PB: peripheral blood, WBCs: white blood cells, FL: fetal liver, E12.5: embryonic age of 12.5 (days post-coitus)

Disease characterization analysis was performed in a similar manner to the previous models. PB of Cre^{+} and control mice was analyzed by flow cytometry to detect contribution to myeloid and lymphocyte lineages at one month of age (P30) (Fig.R3.II-F). We found higher contribution to

the myeloid compartment in the Cre$^+$ 'leukemic' mice with up to 80% of Mac1$^+$Gr1$^+$ cells found in circulation.

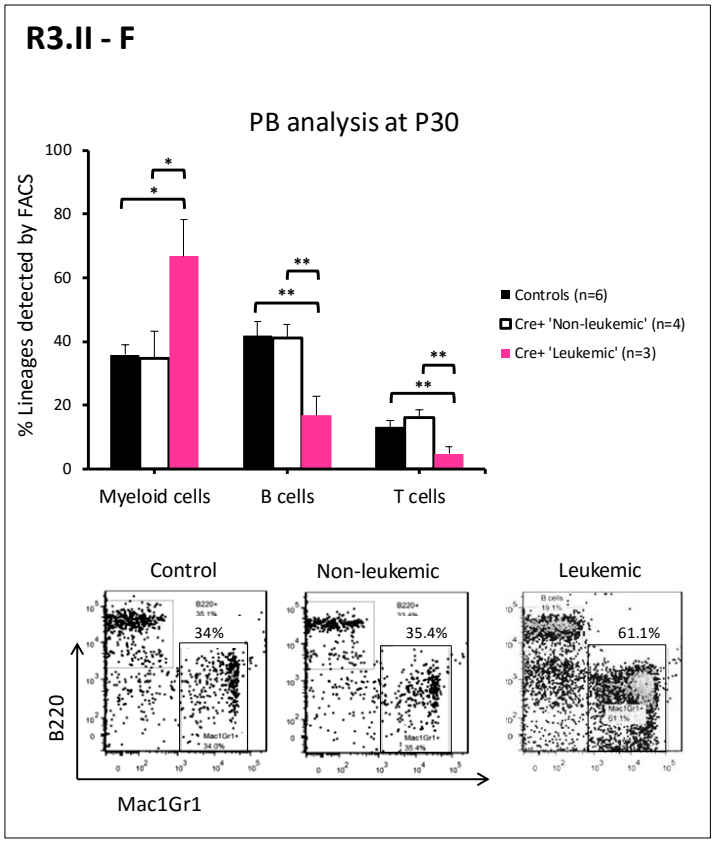

R3.II - F: Characterizing embryonic disease model driven by Mx1-Cre-mediated MLL-ENL fusion: Upper panel - The MLL-ENL:Mx1-Cre$^+$/control mice that were induced in-vivo at E12.5 by polyIC administration were bled post-weening (P30). Quantification of blood cell lineages in Cre$^+$ (Non-leukemic and leukemic) and control mice are represented. Contribution to Myeloid, T- and B-lymphocytes were measured by flow cytometry analysis by staining PB cells with antibodies against surface markers Mac1, Gr1, B220 and CD3e respectively. The number of mice per group is mentioned in graph within parentheses. Values are represented as Mean±SD. Student's t-test was performed for statistical analysis (* : $p<0.05$, **: $p<0.01$). Lower panel - Representative flow cytometry plots of Cre$^+$ 'Non-leukemic', Cre$^+$ 'leukemic' and control mice are shown. The FACS plots highlight the Mac1$^+$Gr1$^+$ cells in circulation at one-month of age (P30) in these mice. This population constitutes the leukemic blast population in the current AML model. MLL: mixed lineage leukemia, ENL: eleven-nineteen, Mx1: Myxovirus1, PolyIC: polyinosinic:polycytidylic acid, E12.5: embryonic age of 12.5 (days post-coitus), P30: postnatal age of mice of 30 days, FL: fetal liver, BM: bone marrow, PB: peripheral blood

The disease progressed rapidly hereafter and was lethal by P42 (Fig. R3.II - E). Leukemic mice also had infiltrations in peripheral organs similar to what was observed in the adult model of leukemic. Splenomegaly was observed only in the leukemic mice, as expected, while the splenic aspects of Cre^+ 'non-leukemic' mice were normal and comparable to control mice (Fig. R3.II – G, H).

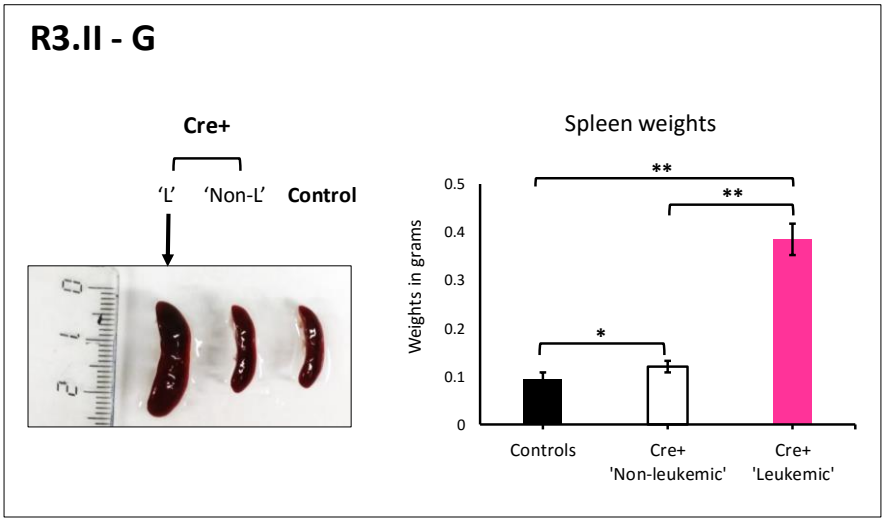

R3.II - G: Splenomegaly observed in mice that developed AML: Comparisons were drawn between splenic aspects of MLL-ENL:Mx1-Cre^+ leukemic ('L'), Cre^+ 'non-leukemic' ('Non-L') and control mice. Upper panel - Representative spleens are shown. Right panel - Quantifications of spleen weights (in grams) are represented in the bar graph. Values are represented as Mean±SD. Student's t-test was performed for statistical analysis (* : $p<0.05$, ** :$p<0.01$). MLL: mixed lineage leukemia, ENL: eleven-nineteen, Mx1: Myxovirus1, 'L': leukemic, 'Non-L': non-leukemic

Both embryonic and adult models of Mx1-Cre-mediated MLL-ENL leukemia were AMLs as suggested by FACS analysis. However, the embryo-derived leukemia was more aggressive when compared to the adult leukemia as was evident by disease onset, progression and median survival data of mice in the two models (Fig. R3.II-C,D).

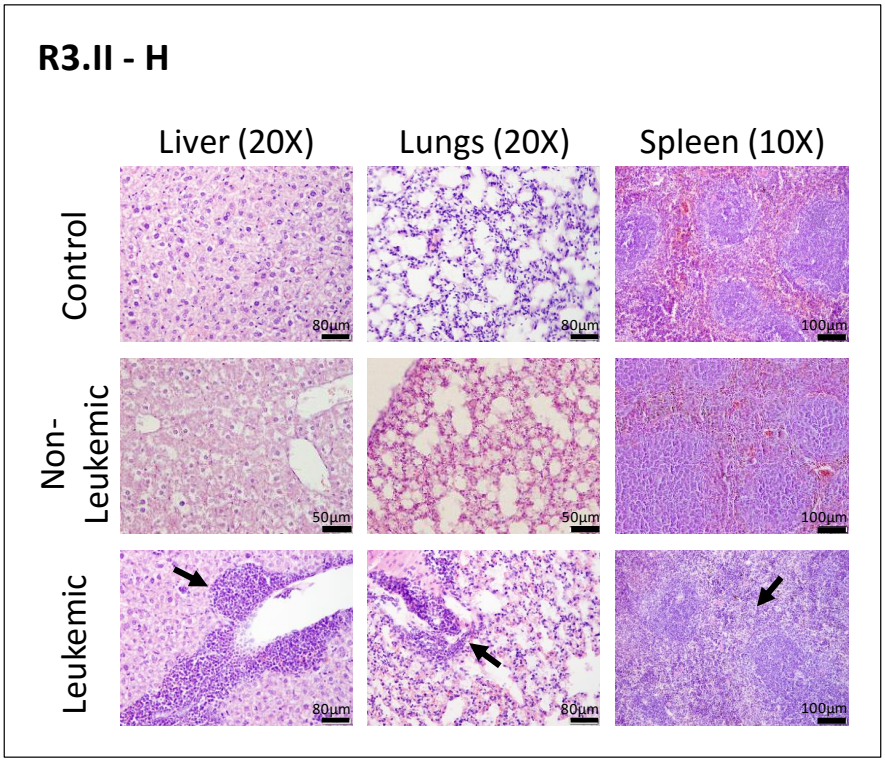

R3.II - H: Histologic analysis of leukemic infiltrates: Histological analysis was performed of organs collected from disease/euthanized MLL-ENL:Mx1-Cre^{+} and control mice. Hematoxylin-Eosin staining was performed on paraffin embedded organ sections (10 µm thick sections). Representative images are illustrated here. The organs from control and Cre^{+} 'non-leukemic' mice had normal histology while the leukemic mice showed infiltrations in multiple peripheral organs (such as liver, lungs and spleen) (black arrow). MLL: mixed lineage leukemia, ENL: eleven-nineteen, Mx1: Myxovirus1

The Cre+ 'Leukemic' mice

After characterizing the embryonic disease, we assessed its transplantability in-vivo by performing competitive transplantation of the primary leukemia cells into adult irradiated recipients (Fig. R3.II-I).

BM cells were collected from femurs of euthanized primary leukemic mice and transplanted retro-orbitally into recipient mice with competitor cells.

Two weeks' post-transplantations, we performed the first blood analysis of transplant recipients, to detect donor reconstitution as well as disease onset (Fig. R3.II - I).

PB samples were collected from transplant recipients to perform donor engraftment and lineage contribution analyses by FACS (Fig. R3.II – L, M).

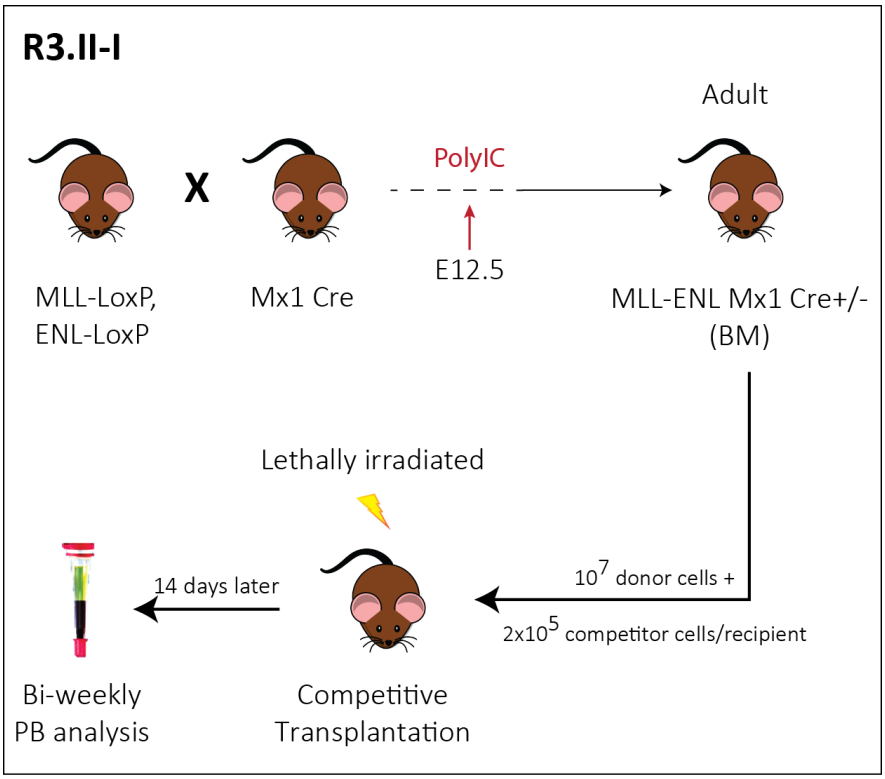

R3.II - I: Assessing leukemia initiation capacity of FL-derived AML in-vivo: Competitive transplantations of 10 million CD45.2 control or primary leukemic BM cells was performed per transplant recipient. The competitor cells were 200,000 whole BM cells/recipient taken from CD45.1-45.2 mice. Transplantation of donor and competitor cells were performed retro-orbitally in CD45.1 adult lethally irradiated recipients (2 doses of 4Gy each). Three mice each were transplanted with controls or primary leukemic BM cells. Two weeks post transplantations, the recipient mice were bled from the tail vein to detect engraftment and disease onset by performing PB analysis. MLL: mixed lineage leukemia, ENL: eleven-nineteen leukemia, FL: fetal liver, BM: bone marrow, PB: peripheral blood, CD: cluster of differentiation

Also, DNA was extracted from PB cells to perform MLL-ENL fusion PCR in control versus primary leukemia recipients. At this early analysis we were able to detect MLL-ENL fusion gene in mice transplanted with primary leukemic BM cells (Fig. R3.II – J).

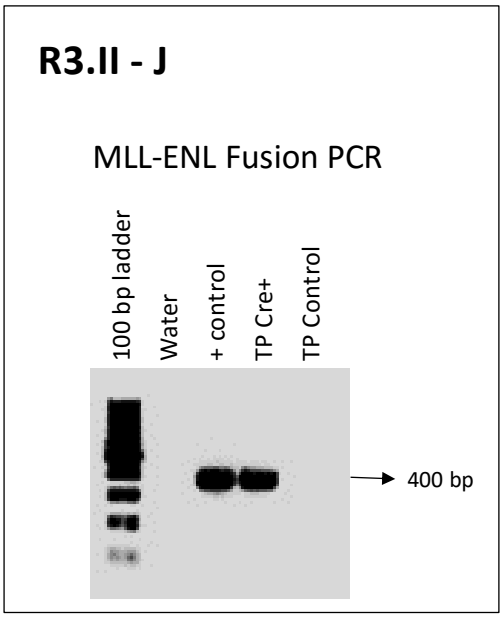

R3.II - J: Translocation PCR in transplant recipients: DNA was extracted from PB of transplant recipients (of primary leukemia/control BM cells) at two weeks post-transplantation. MLL-ENL fusion gene (400bp) was detected by performing PCR as previously described (Cano et al. 2008b). MLL: mixed lineage leukemia, ENL: eleven-nineteen leukemia, PB: peripheral blood, PCR: polymerase chain reaction, bp: base pair, +: positive, TP: transplant recipients

Within the week that followed all of the transplant recipients died. The median survival resulting from the secondary leukemia was 19 days while that from the primary disease was 44 days (Fig. R3.II - K).

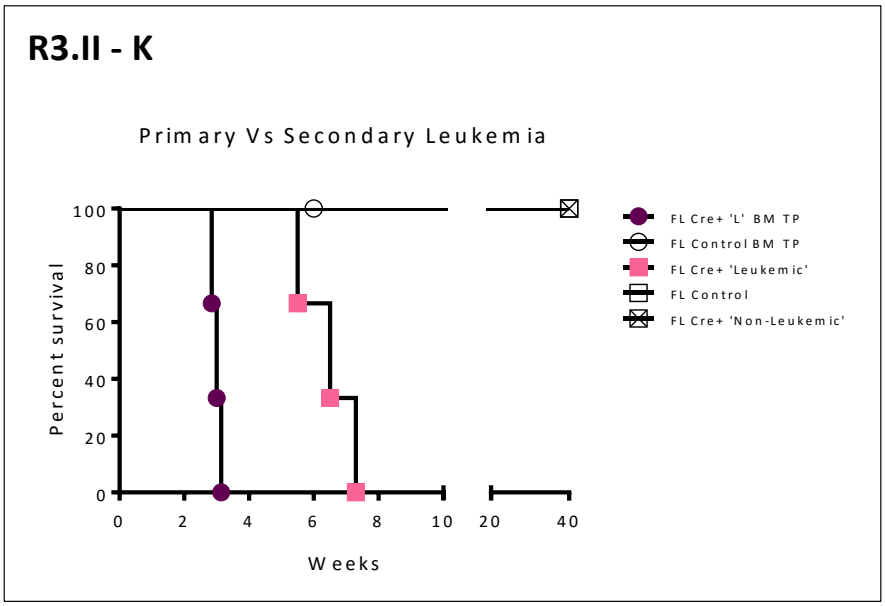

R3.II - K: Survival of primary versus secondary leukemia: Kaplan-Meier survival curves of primary FL-derived leukemic mice (pink) alongside that of transplant recipients of the primary leukemia (red) have been plotted together. Controls from both experiments are plotted together. Number of mice per group are specified within parentheses in the graph. MLL: mixed lineage leukemia, ENL: eleven-nineteen leukemia, FL: fetal liver, Cre^+/Control: primary leukemic/control mice; TP: transplant recipients

The control transplant recipients remained healthy and disease-free. Donor engraftment, as measured by flow cytometry analysis of PB was >75% in all transplant recipients (controls and leukemic) (Fig. R3.II – L).

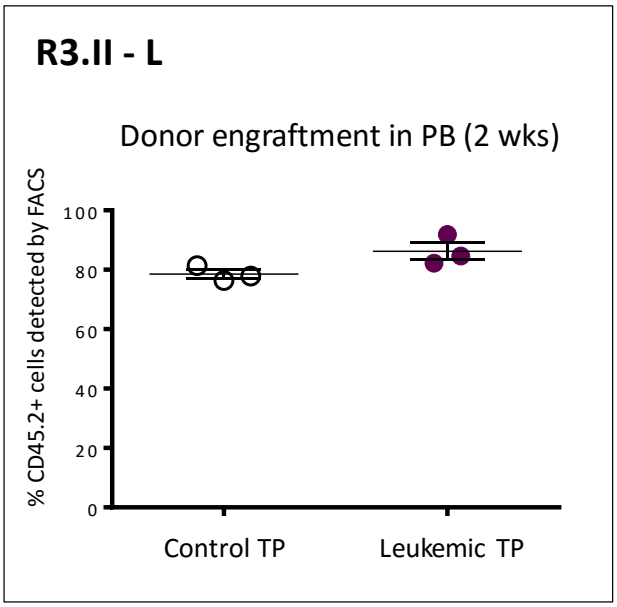

R3.II - L: Donor reconstitution in peripheral blood of transplant recipients: Two weeks post-transplantation, the recipient mice were bled from the tail vein. PB analysis was performed by flow cytometry. To detect donor reconstitution PB cells were stained with antibodies against CD45.1 and CD45.2 to distinguish the donor ($CD45.2^+$), competitor ($CD45.1^+CD45.2^+$) and endogenous recipient populations ($CD45.1^+$). The $CD45.2^+$ donor engraftment in recipients of leukemia/control cells are plotted. Values are represented as Mean±SD with three transplant recipients per group. MLL: mixed lineage leukemia, ENL: eleven-nineteen leukemia, PB: peripheral blood, TP: transplant recipients

Lineage distribution analysis of donor cells in recipient mice was measured by flow cytometry analysis of PB. A significant increase in the myeloid compartment was observed in recipients of primary leukemia when compared to controls.

Rapid accumulation of $Mac1^+Gr1^+$ leukemic blasts led to lethality in recipients of primary leukemia by three weeks post-transplantation (Fig. R3.II - M).

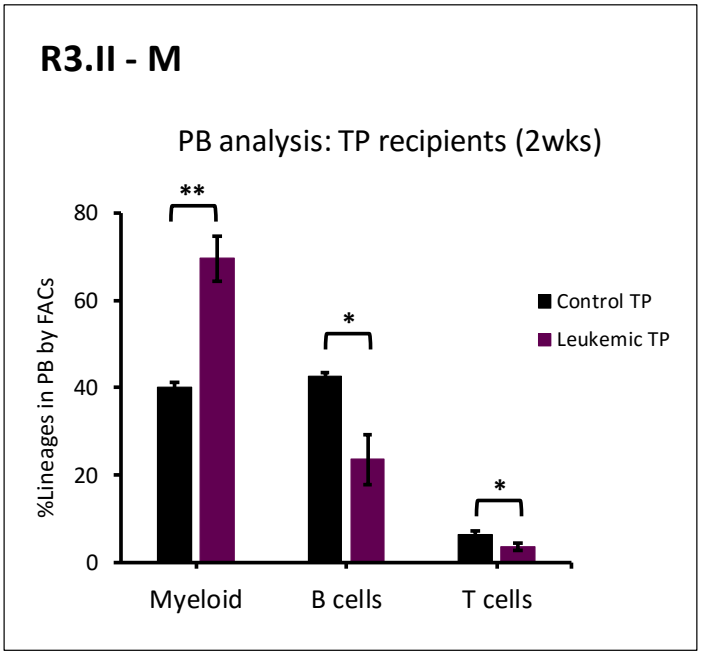

R3.II - M: Lineage contribution analysis in peripheral blood of transplant recipients: Flow cytometry analysis of PB cells stained with antibodies against CD11b (Mac1), Gr1, B220 and CD3e surface markers was performed to detect myeloid, B- and T-lymphocyte populations respectively. Values are represented as Mean±SD of n=3 recipients per group. Student's t-test was used for statistical analysis (* : $p<0.05$, **: $p<0.01$). FL: fetal liver, TP: transplant recipients, PB: peripheral blood

The secondary leukemia, similar to the primary and adult model of MLL-ENL leukemia, was an acute myeloid leukemia (AML) driven by MLL-ENL fusion.

Splenomegaly as well as multiple organs infiltration was observed resulting from the secondary leukemia as well (Fig. R3.II – N,O).

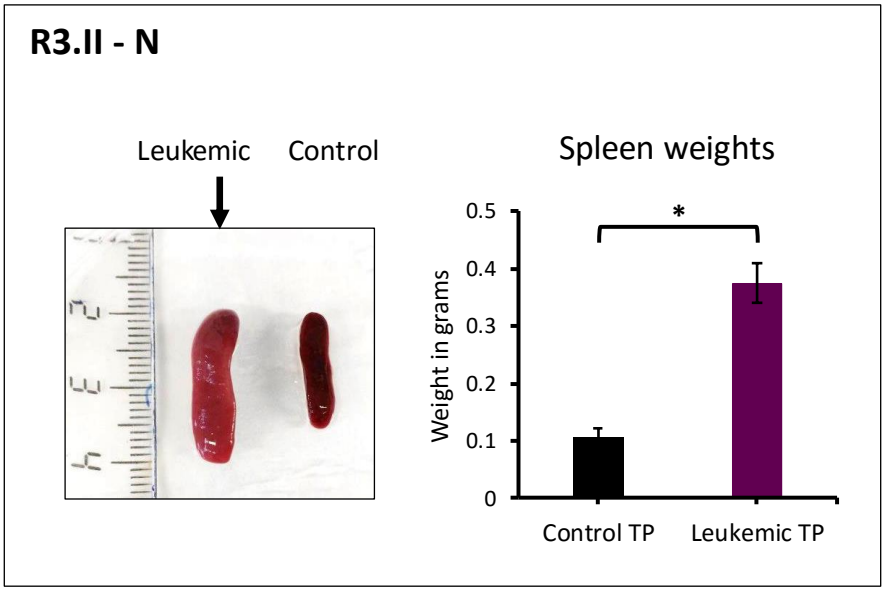

R3.II - N: Splenomegaly in secondary leukemic mice: The secondary AML disease arising in transplant recipients of MLL-ENL-driven primary embryonic AML disease also resulted in splenomegaly. While the control recipients had normal spleens. Left panel - Representative spleens are shown. Right panel - Quantifications of spleen weights (in grams) are represented in the bar graph. Values are represented as Mean±SD. Student's t-test was performed for statistical analysis (* : $p<0.05$). MLL: mixed lineage leukemia, ENL: eleven-nineteen leukemia, AML: acute myeloid leukemia, TP: transplant recipients.

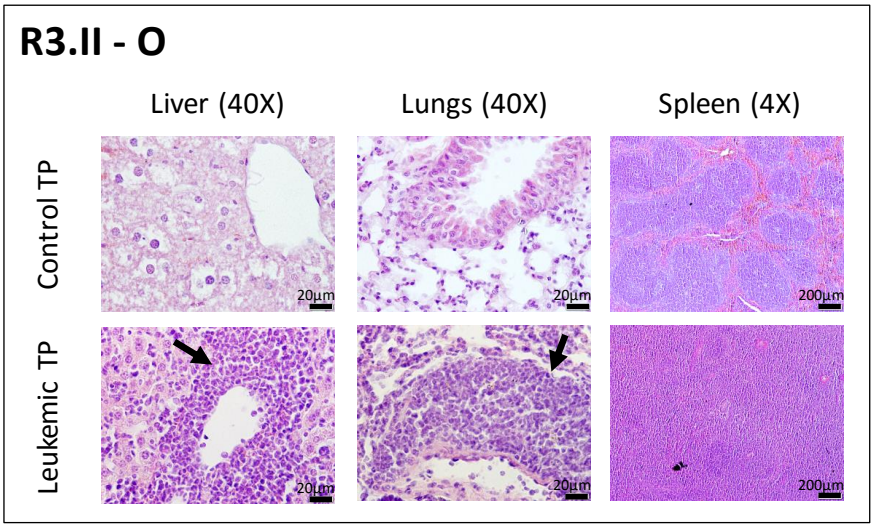

R3.II - O: Leukemia infiltration detection: The secondary AML disease, arising in transplant recipients of primary embryonic MLL-ENL driven AML disease, led to extensive infiltration in multiple peripheral organs (such as liver, spleen and lungs). This was observed by Hematoxylin-Eosin staining of organ sections (10 µm thick sections). Leukemic blasts (black arrows) were found around vessels in the liver as well as in the lungs and the white and red pulp regions of the spleen were disrupted in the Cre^+ (leukemic) mice. Histology of organs from control mice was normal. Representative images of infiltrations are shown. MLL: mixed lineage leukemia, ENL: eleven-nineteen leukemia, AML: acute myeloid leukemia, TP: transplant recipients

The Cre+ 'Non-leukemic' mice

Surprisingly, a subset of MLL-ENL:Mx1-Cre^{+} mice that were induced at E12.5 did not develop any disease in spite of carrying an MLL-ENL fusion gene until 11 weeks of age (Fig. R3.II-C). The 57% of Cre^{+} mice that were disease-free were analyzed once every two weeks for up to 6 months in case they develop a latent disease, as was observed with the β-actin Cre^{ERT} model. Bi-weekly bleedings were conducted to detect any sign of disease.

The lineage distribution analysis of PB by flow cytometry showed presence of a distinct B220 population at 12th week. This population expressed lower intensity of the B220 marker and so we refer to this population as B220^{low}. This B220^{low} population was specifically found in Cre^{+} mice and was absent in PB of all control mice (Fig. R3.II - P upper panel). Moreover, we found this population to be transitory as it was lost by the 16th week (Fig. R3.II - P lower panel).

A few studies within the past decade have described an immature natural killer cells population termed as 'pre-mNK cells' (premature natural killer cells) (Guimont-Desrochers et al. 2012; Taieb et al. 2006; Himoudi et al. 2008). These studies stated that pre-mNKs express B220 surface marker. They characterized 'pre-mNK' population as CD3^{-} CD122^{+}CD244^{+}NK1.1^{+}CD49b^{+}B220^{+}. They also described that these pre-mNK cells possess a prominent anti-tumoral potential.

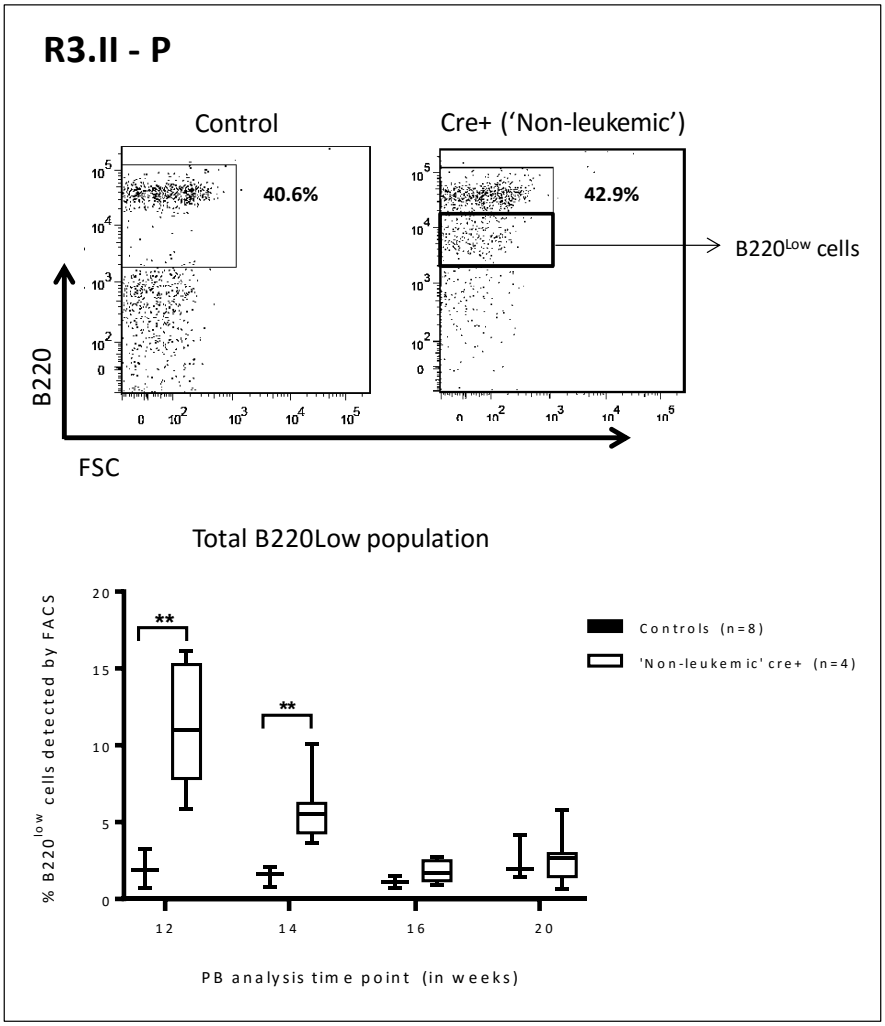

R3.II - P: Comparing B220^{low} population in control versus Cre^{+} 'non-leukemic' mice : PB analysis at the 12th week (P94) showed presence of a B220^{Low} population that appeared specifically in Cre^{+} 'non-leukemic' mice and not in the controls. Upper panel - Representative FACS plots of B220^{+} cells in control and Cre^{+} 'non-leukemic' mice are shown. Lower panel - Quantifications of B220^{Low} cells (population within the black box) in control versus Cre^{+} mice during bi-weekly analysis is shown from week 12 to 20. Values are represented as Mean±SD. Student's t-test was performed for statistical analysis (** : $p<0.01$, ns [not significant]: $p>0.05$). MLL: mixed lineage leukemia, ENL: eleven-nineteen, Mx1: Myxovirus1, P94: postnatal age of mice of 94 days, PB: peripheral blood, FACS: fluorescence associated cell sorting

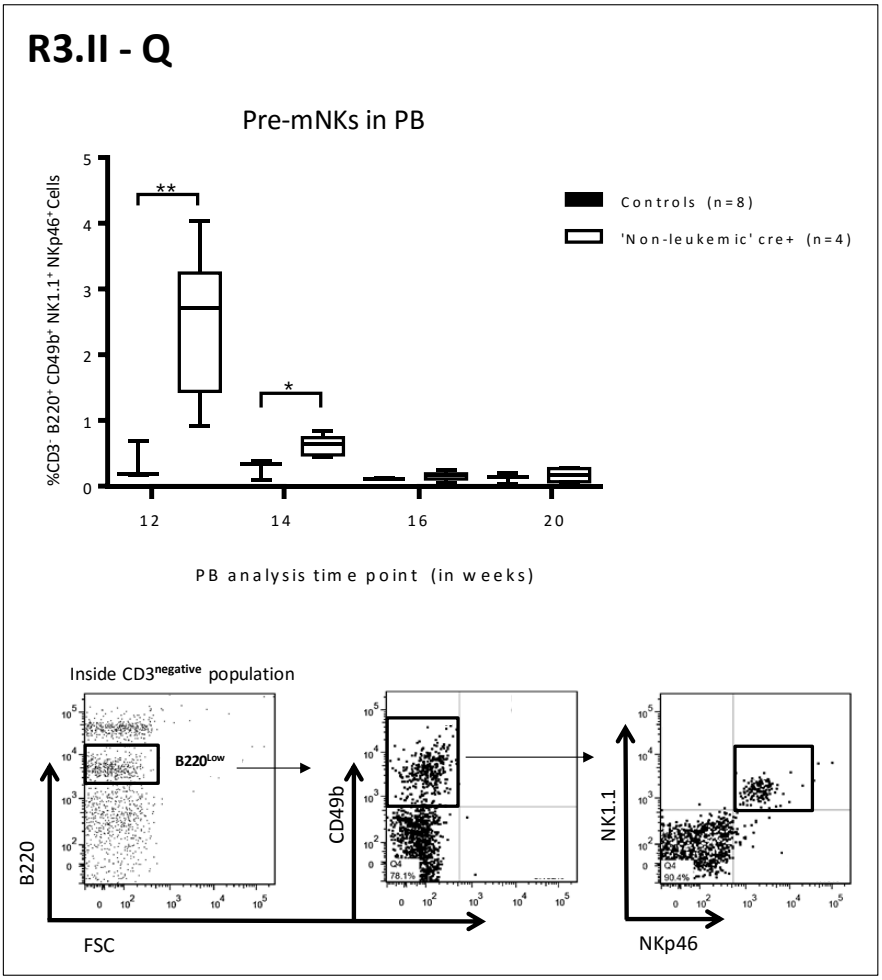

R3.II - Q: Identifying 'pre-mNKs': Pre-mNK cells were detected in PB of MLL-ENL:Mx1-Cre^{+} 'non-leukemic' and control mice by flow cytometry. The pre-mNK population was detected as CD3^{-}B220^{Low}CD49b^{+}NK1.1^{+}NKp46^{+}. Upper panel - Quantification of pre-mNK population in PB is represented. Significantly higher pre-mNKs were found in Cre^{+} 'non-leukemic' mice when compared to controls at 12th week. Lower panel - Gating strategy implemented to gate pre-mNK cells is represented. Values are represented as Mean±SD. Student's t-test was performed for statistical analysis (* : $p<0.05$, ** : $p<0.01$, ns[not significant]: $p>0.05$). MLL: mixed lineage leukemia, ENL: eleven-nineteen, Mx1: Myxovirus1, P94: postnatal age of mice of 94 days, PB: peripheral blood, FACS: fluorescence associated cell sorting, premNK: premature natural killer cells

We were able to detect these immature natural killer cells that express the B220 marker, within the PB of Cre^+ 'non-leukemic' mice by flow cytometry (Fig. R3.II - Q).

This population was specifically found in Cre^+ 'non-leukemic' mice and was absent from Cre^+ 'leukemic' and control mice. The Cre^+ 'leukemic' mice had no $B220^{Low}$ cells at one-month analysis and they died of leukemia by P49.

This $B220^{Low}$ population in Cre+ 'non-leukemic' mice was lost after P98 (14^{th} week), at which point the MLL-ENL fusion gene was also lost in these mice (Fig. R3.II - B).

Thereafter, the Cre^+ 'non-leukemic' and control mice had comparable contribution to the myeloid and lymphoid lineages as observed in PB analyses by FACS (Fig. R3.II - R).

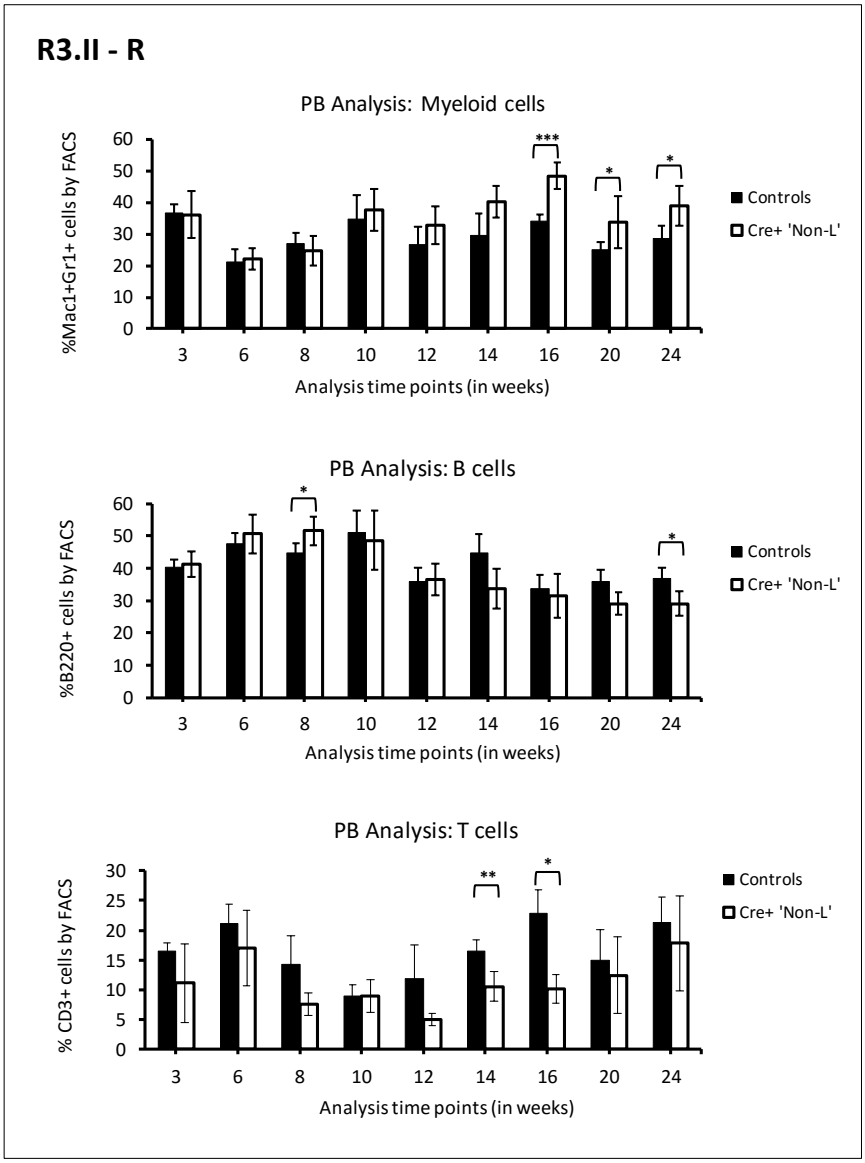

R3.II - R: Bi-weekly PB analysis: MLL-ENL:Mx1-Cre^{+} 'non-leukemic' and control mice were bled bi-weekly to measure contribution to myeloid and lymphocyte lineages by flow cytometry analysis. PB cells were stained with antibodies against surface markers. Values are represented as Mean$\pm$SD. Student's t-test was performed for statistical analysis (* : $p<0.05$, ** : $p<0.01$, *** : $p<0.001$). The rest of differences were not significant (ns): $p>0.05$. MLL: mixed lineage leukemia, ENL: eleven-nineteen, Mx1: Myxovirus1, PB: peripheral blood, FACS: fluorescence associated cell sorting. PB: peripheral blood

Discussion

DISCUSSION

Infant leukemias are an aggressive disease with unique clinical and biological characteristics such as prenatal origin, short latency and extremely poor prognosis. Infant leukemias are a rare disease and majority of them carry MLL-gene rearrangements. Conventional chemo and radiation therapies fail to effectively reduce leukemia burden in neonates, and therapy-related toxicity (such as neurotoxicity) is a constant risk while treating these patients. The prenatal origin of infant leukemias limits the scope of understanding the disease development mechanisms. Therefore, it remains a poorly characterized disease.

The human infant, childhood and adult leukemias driven by t(11;19) are either AML, ALL or mixed lineage leukemias (Jung et al. 2010). The molecular reasons behind difference in infant versus adult leukemias are largely unclear. There is a need for disease models that can efficiently retrace the human infant leukemia development and my thesis is focused on developing mice models driven by t(11;19) which are implicated in leukemia patients of all age groups.

The hematopoietic specific, constitutively active Vav1-Cre line was an efficient means to develop t(11;19) leukemia in mice. The resulting AML disease was similar to that of the Lmo2-Cre mediated MLL-ENL disease (Cano et al. 2008b). The Cre activation was confirmed in E11 MLL-ENL:Vav1-Cre^{+} embryos by detection of the MLL-ENL fusion gene in distinct hematopoietic tissues (AGM and FL) (Fig. R1-B). However, it was difficult to know with certainty at which stage of hematopoietic development the leukemia was initiated.

Therefore, transgenic $MLL^{LoxP}ENL^{LoxP}$ mice were crossed with different inducible Cre mice to initiate translocation at embryonic or adult stages to develop, study and compare MLL-ENL leukemias that can recapitulate human infant and adult diseases.

Tamoxifen inducible β-actin Cre^{ERT} mice were used to induce MLL-ENL translocation in distinct hematopoietic tissues at different stages of development. However, the tamoxifen inducible R26-YFP;β-actin Cre^{ERT} mice failed to reproduce the MLL-ENL driven human diseases due to inefficient MLL-ENL-recombination. This was concluded after several attempts of mediating Cre-induction using different strategies (in-vitro and in-vivo). Although we obtained low to average levels of YFP recombination (>50% in embryonic tissues and approximately 20% in the adult tissue Fig. R2.I-B), the MLL-ENL-recombination efficiency was consistently low in all three hematopoietic tissues i.e., E10.5 AGMs, E12.5 fetal livers and P60 bone marrow.

One possibility of inefficient Cre-mediated recombination could be the distant LoxP sites in MLL and ENL genes when compared to the nearby LoxP sites in the Rose26YFP promoter. It has been previously described in Coppoolse et al. 2005; Zheng et al. 2000; Wang et al. 2009 that Cre-mediated recombination is less efficient when the lox sites are separated over larger distances. This would explain YFP-expression in induced AGM/FL/BM cells that did not carry the MLL-ENL fusion gene.

With the in-vivo induction strategy (Strategy III) we achieved MLL-ENL fusion-driven leukemia in <40% of mice transplanted with transformed AGM, FL and BM cells. In this case, the disease developed at a slow pace or after a long latency (12 months post-transplantation

Fig. R2.III-E). It is possible that transformed cells became quiescent as is observed with some dormant leukemic stem cells (LSCs) (Essers et al. 2010), as we could not detect leukemic blast load accumulation during the monthly analyses performed for 365 days post-transplantation. However, it is still probable that the disease showed similarities to human chronic leukemias that are asymptomatic for a long period (Amikam et al. 1994; Kalil & Cheson 1999; Abbott 2006). This chronic phenotype did not reflect the acute leukemias that are found in human infant and adult patients carrying an MLL-gene rearrangement.

The inefficient MLL-ENL-recombination achieved with this Cre line probably hindered targeting the subset of hematopoietic stem/progenitor cell that carry leukemogenic potential.

Even with implementation of maximal induction protocols, we could not develop the desired disease models using tamoxifen inducible β-actin Cre^{ERT} mice. Therefore, we used an alternative Cre/LoxP line that would yield better translocation recombination.

The interferon inducible Mx1-Cre mice were used to target embryonic and adult hematopoietic cells with MLL-ENL translocation. Cre-inductions were performed in-vivo:

- In pregnant mice (at E12.5) to mimic the prenatal origin of human infant leukemias, and
- in adult mice (P60) to mimic postnatal translocation in adult leukemias

PolyIC inductions were performed in-vivo in adult MLL-ENL:Mx1-Cre^{+} mice based on the maximal induction strategy as previously

described (Klinakis et al. 2011). MLL-ENL translocation was detected in all Cre^+ mice (100% recombination efficiency), it led to an aggressive AML disease which was lethal within three months. The disease was characterized by $Mac1^+Gr1^+$ leukemic blasts.

The $Mac1^{High}Gr1^{High}$ cells have been previously described as leukemic blast populations in other AML mice models such as the Lmo2-Cre mediated MLL-ENL translocation driven AML disease in mice that was lethal within 15 weeks (Forster, Pannell, Lesley F. Drynan, et al. 2003). Similar results were also obtained in mice with a different MLL-rearrangement, the MLL-AF9 wherein retroviral transduction of MLL-AF9 fusion oncogene in BM-derived HSCs drove an AML disease in transplant recipients with lethality in these mice within 10 weeks post-transplantation (Somervaille & Cleary 2006). Similarly, these leukemic blasts were also found in the MLL-AF9-knock-in model of AML disease, amongst others (Taggart et al. 2016; Zuber et al. 2009a; Somervaille et al. 2009; Horton et al. 2009; Chen et al. 2008).

A reproducible adult-BM-derived MLL-ENL-driven acute leukemia model was successfully developed using the inducible Mx1-Cre mice. The resulting disease also shared similar characteristics to the MLL-ENL-driven AML model developed using the constitutive Vav1-Cre line.

Mx1-Cre mice are not well characterized for targeting hematopoietic cells within embryonic tissues, unlike the adult BM tissue. To test the efficacy of MLL-ENL-recombination during embryonic development, we performed in-vivo induction by injecting pregnant mice with polyIC at E12.5 to target embryonic hematopoietic cells within the fetal liver.

With this approach, the embryonic model of acute leukemia was developed (with 43% efficacy Fig.R3.II-Cb) resulting from a prenatal MLL-ENL translocation, similar to the human infant disease.

The embryonic (FL-derived) leukemia:

- had a short latency (disease onset observed by P27) similar to human infant leukemias that arise within the first year of birth,
- was lethal by P49, concurring with the poor prognosis of infant leukemia patients (<40% of infant leukemia patients have a 5-year EFS) (Fig.R3.II-Ca)
- was transplantable, and secondary AML disease arising in transplant recipients was lethal within two weeks, being more aggressive than the primary leukemia
- resulted in multiple organ infiltration (in spleen, liver and lungs) similar to the human infant disease (Fig.R3.II-H)
- was the AML-subtype but not B-ALL and mixed leukemias. t(11;19) can drive either AML, ALL or mixed leukemias in infants.

It has also been difficult to develop a disease model for MLL-AF4-driven B-ALLs. It is the most common MLL-partner and it is implicated in majority of human infant B-cell ALLs. Several attempts have been made in the past (using retroviral transduction of MLL-AF4 alone or its reciprocal fusion AF4-MLL alone or both MLL-AF4 and AF4-MLL together; and other strategies such as MLL-AF4-knock-in mice) but no model has been able to reproduce the disease phenotype and latency (Kowarz et al. 2007; Kumar et al. 2011; Bursen et al. 2010; Sanders et al. 2011). There are conflicting results regarding the role of its reciprocal fusion gene AF4-MLL in disease development process. Some studies

suggest that the MLL-AF4 fusion is required for leukemic cells proliferation and its reverse fusion gene the AF4-MLL is necessary for the early transformation process. Various other factors such as the target cell (developmental stage and type) that undergoes transformation adds to the variations in disease phenotype and latency in these models (Kumar et al. 2011; Montes et al. 2011; Bursen et al. 2010; Bueno et al. 2012; Sanjuan-Pla et al. 2015). It is important to identify the developmental stage and subset of hematopoietic cells that upon undergoing transformation can give rise to leukemias more comparable to humans.

The Mx1-Cre-mediated MLL-ENL translocation led to development of both embryonic (FL-derived) and adult (BM-derived) leukemias in mice. The embryonic mouse model was more aggressive (median survival of 7 weeks) when compared to the adult model (median survival of 12 weeks), similar to what is found in human infant versus adult leukemia patients carrying an MLL-rearrangement.

The distinctions in the embryonic versus adult leukemia models that we have developed, could be accounted to the exponential expansion of HSCs and progenitors in the fetal liver (from E12.5 – E16.5 in mice), which does not occur in the BM. The majority of HSCs in the adult BM are in a quiescent state (in G0 phase of cell cycle). However, this needs to be further investigated. The embryonic and adult leukemia models that we have developed can be used to assess whether these hematopoietic tissues hold distinct leukemogenic potentials. It could be done by performing Cre-induction using the same dose of polyIC at embryonic and adult stages and transplanting a particular population of hematopoietic cells (HSCs or progenitors) from the two tissues (FL and

BM) into adult irradiated recipients to assess onset, progression and subtype of disease arising in the recipient mice.

Open debate in the field of infant leukemia research attempts to address reasons behind its unique characteristics. Several attempts have been made in the past to develop mice models of the human infant or childhood or adult leukemias carrying MLL-gene rearrangements (Doty et al. 2002; Cano et al. 2008; Forster et al. 2003; Ugale et al. 2014; Lavau et al. 1997; Barrett et al. 2016). In Zuber et al. 2009b and Zeisig et al. 2003 MLL-ENL oncogene was co-transduced with co-operating mutations (such as Ras and flt3) into murine HSCs to develop AML and B-ALL diseases. However, these models resembled 'non-infant' childhood leukemias as infant leukemias rarely carry secondary mutations. Similarly, Juge et al. 2013 mentions using doxycycline inducible transgenic mice to induce MLL-ENL oncogene postnatally, in newborn and adult mice which they claim resulted in B-ALL and mixed leukemias but not the AML-subtype that we have found in our models of MLL-ENL-driven disease developed using Mx1-Cre line. MLL-ENL-oncogene can result in AML, ALL or mixed leukemias. These distinctions in leukemia subtypes might be a result of the differentiation state and specific type of cells undergoing transformation (Cano et al. 2008a). However, in Juge et al. 2013 generation of an infant leukemia model from a prenatal induction of MLL-ENL fusion is not mentioned, they only claim to assess the clonogenic potential of embryonic (FL-derived) cells in in-vitro assays.

In another study, Ugale et al. 2014 used transgenic mice to induce MLL-ENL fusion gene in distinct hematopoietic cells. Surprisingly, the induced BM or fetal liver derived (at E14.5) HSCs showed no

leukemogenic potential. But the GMLPs or CLPs from BM of adult mice gave rise to AML upon MLL-ENL induction, with lethality in mice by 15 weeks. This result concurs with the adult leukemia model that we have developed using the Mx1-Cre line. In our model, AML-subtype is observed as well, with median survival of 12 weeks. However, Ugale et al. 2014 did not develop an infant leukemia model. While they demonstrated that FL-derived HSCs were unable to give rise to leukemias upon MLL-ENL induction, they did not explore the leukemogenic potential of other hematopoietic cells in the FL (such as GMLPs or CLPs).

Chen et al. 2011 performed a study similar to ours wherein they investigated differences in an embryonic (FL-derived) leukemia versus an adult (BM-derived) leukemia, except they performed retroviral transduction of murine cells with the MLL-AF9 fusion oncogene. Contrary to our finding, they observed a longer latency in the embryonic disease when compared to the adult. Moreover, the latency in disease development was >150 days post-induction, suggesting inability to recapitulate the MLL-AF9-driven acute leukemias that are found in humans. In our study, the Mx1-Cre mediated MLL-ENL recombination in embryonic and adult tissues resulted in acute leukemias with a shorter latency in the embryo-derived (FL-derived) disease.

The MLL-ENL translocation-driven embryonic leukemia that we have developed demonstrates a greater leukemogenic potential of FL tissue when compared to the adult BM-tissue. The recent study by Barrett et al. 2016 has demonstrated this enhanced leukemogenic potential of FL cells between E12.5-E14 carrying a different MLL-fusion, the MLL-AF4 (the most common MLL-fusion found in human infant B-ALLs).

These studies have demonstrated leukemogenic potential of murine embryonic stem and progenitor cells but an efficient model for studying infant leukemias was still required. These studies also aimed at characterizing leukemic initiating cells (LICs) containing population in MLL-rearranged leukemias (Ugale et al. 2014; Chen et al. 2011; Zuber et al. 2009b; Zeisig et al. 2003; Saito et al. 2015; Somervaille & Cleary 2006).

Leukemia initiating cells (LICs) are a subset of hematopoietic cells that possess leukemogenic potential upon undergoing genetic transformation. One of the hypotheses regarding LICs is that HSCs are likely to transform into LICs as they possess similar properties such as self-renewal ability, multipotency and semi-quiescence which makes them refractory to conventional therapies that only target dividing cells (such as chemo- and radiation therapies) (Bhatia et al. 1997; Jordan 2007). But, it has been demonstrated by several recent studies that a potent oncogene such as an MLL-rearrangement which is rarely accompanied by secondary mutations, can transform lineage committed progenitors into LICs (Ugale et al. 2014; McKenzie 2005; Taussig et al. 2008). It remains unclear whether the LIC-containing populations are different in human infant, childhood and adult leukemias. Therefore, it is crucial to be able to identify this population in each type of leukemia.

LICs are different from the leukemic blast population. There are several examples of this such as, the Notch1-driven T-ALL in mice wherein the LIC-containing population were LSK cells while the leukemic blast load comprised of $CD4^{+}CD8^{+}$ cells (Gekas et al. 2016), retroviral transduction of MLL-AF9 oncogene in BM LSK cells gave rise to AML with $Mac1^{+}Gr1^{+}$c-Kit^{+} leukemic blasts (Somervaille & Cleary 2006).

Similarly, retroviral transduction of MLL-ELL in Lin^- BM cells gave rise to an AML disease in transplant recipients characterized by $Mac1^+F4/80^+Gr1^+$ leukemic blasts (Lavau et al. 2000). The characterization of LICs in infant leukemias should help develop novel targeted therapies that can be used in combination with conventional chemo/radiation-therapies to achieve complete remission in these patients.

LICs survive in human leukemias based on cell intrinsic and extrinsic properties. While chromosomal aberrations alter cell intrinsic properties of hematopoietic cells, the cell extrinsic components are provided by the microenvironment (Konopleva & Jordan 2011; Sison & Brown 2011; Isidori et al. 2014; Bakker et al. 2016). Cancer microenvironment plays a crucial role in disease progression and resistance to therapy (Chen et al. 2015; Sun 2016; Fokas et al. 2012; Sounni & Noel 2013).

The MLL-ENL-driven embryonic and adult leukemias that we have developed using Mx1-Cre line allows disease development to occur within its natural microenvironment with minimal manipulations. It would be interesting to investigate the role of FL and BM microenvironments in these disease models.

Further characterization of these models need to be done by:

- identifying LIC-containing population and frequency of LICs in the infant versus adult diseases; and
- identifying set of candidate genes that are specifically deregulated in the two models, to find druggable targets (by RNA-sequencing of identified LICs)

- comparing the transcriptome of embryonic and adult models of MLL-ENL leukemia with the human infant and adult diseases respectively, to confirm clinical relevance of these models

The development of an embryonic (FL-derived) model of MLL-ENL leukemia using the Mx1-Cre line led to disease development in only 43% of MLL-ENL:Mx1-Cre^{+} mice. The remaining 57% of Cre^{+} mice remained disease free (Fig. R3.II-C).

Likely explanations for this variation might include:

- inefficient Cre-induction, since a single pulse of polyIC was administered;
- inability to efficiently target the subset of fetal liver cells that possess leukemogenic potential. Similarly, recombination in cells that do not possess leukemogenic potential would also result in lack of disease. This is supported by findings of Cano et al. 2008a wherein MLL-ENL-recombination in B-cell progenitors using the constitutive CD19-Cre mice led to lack of disease development in all mice. They stated that MLL-ENL fusion might only play a tumorigenic role in specific cell types or at specific differentiation states.

To investigate why this variation was consistently observed (in three independent experiments), we performed bi-weekly peripheral blood analyses of the Cre^{+} 'non-leukemic' mice. Interestingly, these mice carried the MLL-ENL fusion at P30 but it could no longer be detected post P84.

During the bi-weekly analyses, we observed presence of a distinct $B220^{Low}$ population specifically in the Cre^+ 'non-leukemic' mice while it was absent from control mice. Further investigation of the nature of $B220^{Low}$ cells led to the identification of a pre-natural killer phenotype in those cells. These cells have been described by Guimont-Desrochers et al. 2012 as an immature natural killer cell population that expresses the B220 surface marker and possesses anti-tumoral potential (Guimont-Desrochers et al. 2012; Taieb et al. 2006; Himoudi et al. 2008).

It is known that interferon or polyIC administration in mice does alter their immune system by producing more mature natural killer cells in the body, but we found equal percentages of mature natural killer cells in both Cre^+ and control mice. It was only the premature NK population that was significantly higher in the Cre^+ mice and negligible in the control mice.

This pre-mNK population was lost after P84 (12 weeks) at which point the MLL-ENL fusion gene could also no longer be detected. It is tempting to speculate that transformed cells were perhaps killed by the premature-natural killer cells in these Cre^+ 'non-leukemic' mice resulting in their disease-free state. Further investigations are necessary to confirm this preliminary finding.

Transplanting sorted 'non-pre-mNK' BM cells from Cre^+ 'non-leukemic' mice prior to P27 (at which point the translocation was still detectable) into immunosuppressed NK-cell deficient mice would help in understanding the function of pre-mNKs and other immune cells.

Importantly, the anti-tumoral potential of 'pre-mNK' cells might make them a promising therapeutic strategy for these leukemias. The mature NK cells have a known function that is analogous to cytotoxic T cells, and pre-mNKs are able to produce a vast number of mNKs. Therefore, pre-mNKs have a more effective anti-tumoral potential on a per cell basis when compared to mNKs (Taieb et al. 2006). However, there are some challenges that need to be overcome to use it for therapy as no known factors are able to uniquely promote number of pre-mNK cells in-vivo (Guimont-Desrochers et al. 2012). Moreover, pre-mNKs are a very small population which are difficult to isolate and maintain in-vitro.

Having established the FL-derived MLL-ENL leukemia model using the Mx1-Cre line, we made several attempts at developing another embryonic model of infant leukemia to compare the transformation capacity of AGM-derived cells with those of FL and BM cells. However, we encountered several problems in developing the AGM-disease model. PolyIC administration in pregnant mice at E9.5 led to abortions (in three independent experiments). Further investigations are required to identify cause of lethality.

In a case-report by (Hunger et al. 1998), in-utero death of a human conceptus was found resulting from an MLL-rearranged leukemia towards the end of gestation period. Hepatosplenomegaly was observed in the fetus and leukemic infiltrates were observed in the organs. This is the only case report that has described the possibility of in-utero death caused by a pre-natal chromosomal aberration. The possibility that this might be occurring in the AGM-derived MLL-ENL leukemia model using the Mx1-Cre line cannot yet be discarded.

It would be interesting to investigate whether MLL-ENL-recombination at early stages of embryonic development (prior to E10) is lethal.

The possible approaches to develop an AGM-derived leukemia are:

- transplanting transformed AGM tissues (polyIC induction at E9.5) into adult irradiated mice,
- administering lower dosage of polyIC in-vivo in pregnant mice at E9.5,
- administering polyIC in pregnant mice at a later stage of embryonic development i.e., E10 or E10.5

It would also be interesting to use the Mx1-Cre line to assess the leukemogenic potential of other embryonic hematopoietic tissues alongside AGM (such as the placenta, yolk sac and vitelline arteries) at early stages of development.

From our efforts in this project, we have been able to develop acute leukemias in mice from embryonic and adult hematopoietic tissues carrying the MLL-ENL translocation. These disease models have shown some similar characteristics to the corresponding human infant and adult leukemias. Further characterization of these disease models are required to have applications in understanding infant leukemia ontogeny and in finding optimal treatment strategies for infant leukemia patients.

CONCLUSIONS

CONCLUSIONS

1. Vav1-Cre-mediated MLL-ENL translocation led to development of AML disease in mice with a median survival of 12 weeks.
2. The tamoxifen inducible β-actin Cre^{ERT} model was inefficient in mediating MLL-ENL translocation in embryonic and adult hematopoietic tissues by in-vitro and in-vivo induction strategies.
3. β-actin Cre^{ERT} mediated MLL-ENL translocation in embryonic and adult tissues led to development of chronic myeloid leukemia-like disease in <40% of mice and it failed to recapitulate the acute leukemias found in human infant and adult patients.
4. The hematopoietic specific, polyIC inducible Mx1-Cre line led to efficient MLL-ENL translocation formation in the adult hematopoietic tissue (BM) resulting in development of a reproducible AML mouse model carrying MLL-ENL translocation. Median survival of leukemic mice was twelve weeks.
5. Mx1-Cre-mediated MLL-ENL recombination in embryonic tissues (FL) led to development of an AML disease in 43% of mice with median survival of seven weeks.
6. The embryonic leukemia was transplantable and the secondary AML disease was more aggressive than the primary leukemia with median survival of mice being two weeks.
7. The embryonic AML disease arising from the prenatal MLL-ENL translocation in mice had a short latency similar to human infant leukemias.

8. The MLL-ENL translocation-driven embryonic (FL-derived) AML disease was more aggressive compared to the adult (BM-derived) AML disease in mice, similar to what is found in human infant versus adult leukemias.
9. The lack of disease development in 53% of mice in the embryonic model might result from low recombination efficiency or loss of recombined cells in-vivo or inefficient targeting of the cells with leukemogenic potential.

BIBILOGRAPHY

BIBILOGRAPHY

Abbott, B.L., 2006. Chronic lymphocytic leukemia: recent advances in diagnosis and treatment. *The oncologist*, 11(1), pp.21–30.

Adams, G.B. et al., 2007. Therapeutic targeting of a stem cell niche. *Nature biotechnology*, 25(2), pp.238–43.

Akashi, K. et al., 2000. A clonogenic common myeloid progenitor that gives rise to all myeloid lineages. *Nature*, 404(6774), pp.193–7.

Alvarez-Silva, M. et al., 2003. Mouse placenta is a major hematopoietic organ. *Development*, 130(22), pp.5437–5444.

Amikam, D. et al., 1994. Molecular analysis of an asymptomatic Ph-positive CML patient with 27 years of prolonged remission. *American Journal of Hematology*, 46(4), pp.358–362.

Anon, 1978. An anatomical disputation concerning the movement of the heart and blood in living creatures. *Medical History*, 22(1), p.102.

Argiropoulos, B., Yung, E. & Humphries, R.K., 2007. Unraveling the crucial roles of Meis1 in leukemogenesis and normal hematopoiesis. *Genes and Development*, 21(22), pp.2845–2849.

Arinobu, Y. et al., 2005. Developmental checkpoints of the basophil/mast cell lineages in adult murine hematopoiesis. *Proceedings of the National Academy of Sciences of the United States of America*, 102(50), pp.18105–10.

Arrode-Brusés, G. & Brusés, J.L., 2012. Maternal immune activation by poly I:C induces expression of cytokines IL-1β and IL-13,

chemokine MCP-1 and colony stimulating factor VEGF in fetal mouse brain. *Journal of neuroinflammation*, 9, p.83.

Auerbach, R., Huang, H. & Lu, L., 1996. Hematopoietic stem cells in the mouse embryonic yolk sac. *Stem cells (Dayton, Ohio)*, 14(3), pp.269–80.

Auffray, C. & Noble, D., 2009. Origins of Systems Biology in William Harvey's Masterpiece on the Movement of the Heart and the Blood in Animals. *International Journal of Molecular Sciences*, 10(4), pp.1658–1669.

Bakker, E. et al., 2016. The role of microenvironment and immunity in drug response in leukemia. *Biochimica et Biophysica Acta (BBA) - Molecular Cell Research*, 1863(3), pp.414–426.

Barabé, F. et al., 2007. Modeling the initiation and progression of human acute leukemia in mice. *Science (New York, N.Y.)*, 316(5824), pp.600–4.

Baron, M.H. & Mohn, D., 2005. Mouse embryonic explant culture system for analysis of hematopoietic and vascular development. *Methods in molecular medicine*, 105, pp.231–56.

Barrett, N.A. et al., 2016. Mll-AF4 Confers Enhanced Self-Renewal and Lymphoid Potential during a Restricted Window in Development. *Cell reports*, 16(4), pp.1039–54.

Bassan, R. & Hoelzer, D., 2011. Modern Therapy of Acute Lymphoblastic Leukemia. *Journal of Clinical Oncology*, 29(5), pp.532–543.

Beer, P.A. et al., 2015. Modeling Normal and Disordered Human

Hematopoiesis. *Trends in Cancer*, 1(3), pp.199–210.

Behm, B.F. et al., 1996. Rearrangement of the MLL Gene Confers a Poor Prognosis in Childhood Acute Lymphoblastic Leukemia, Regardless of Presenting Age.

Belizário, J.E. et al., 2012. New routes for transgenesis of the mouse. *Journal of Applied Genetics*, 53(3), pp.295–315.

Bennett, J.M. et al., 1976. Proposals for the Classification of the Acute Leukaemias French-American-British (FAB) Co-operative Group. *British Journal of Haematology*, 33(4), pp.451–458.

Bhatia, M. et al., 1997. Quantitative analysis reveals expansion of human hematopoietic repopulating cells after short-term ex vivo culture. *The Journal of experimental medicine*, 186(4), pp.619–24.

Bigas, A., D'Altri, T. & Espinosa, L., 2012. The Notch Pathway in Hematopoietic Stem Cells. In Springer Berlin Heidelberg, pp. 1–18.

Biondi, a et al., 2000. Biological and therapeutic aspects of infant leukemia. *Blood*, 96(1), pp.24–33.

Bowie, M.B. et al., 2006. Hematopoietic stem cells proliferate until after birth and show a reversible phase-specific engraftment defect. *The Journal of clinical investigation*, 116(10), pp.2808–16.

De Braekeleer, M. et al., 2005. The MLL gene and translocations involving chromosomal band 11q23 in acute leukemia. *Anticancer Research*, 25(3 B), pp.1931–1944.

Breen, T.R. & Harte, P.J., 1993. Trithorax regulates multiple homeotic

genes in the bithorax and Antennapedia complexes and exerts different tissue-specific, parasegment-specific and promoter-specific effects on each. *Development (Cambridge, England)*, 117(1), pp.119–34.

Bresnick, E.H. et al., 2010. GATA Switches as Developmental Drivers. *Journal of Biological Chemistry*, 285(41), pp.31087–31093.

Broeker, P.L. et al., 1996. Distribution of 11q23 breakpoints within the MLL breakpoint cluster region in de novo acute leukemia and in treatment-related acute myeloid leukemia: correlation with scaffold attachment regions and topoisomerase II consensus binding sites. *Blood*, 87(5), pp.1912–22.

de Bruijn, M.F.T.R. et al., 2000. Definitive hematopoietic stem cells first develop within the major arterial regions of the mouse embryo. *The EMBO Journal*, 19(11), pp.2465–2474.

Bueno, C. et al., 2012. A human ESC model for MLL-AF4 leukemic fusion gene reveals an impaired early hematopoietic-endothelial specification. *Cell research*, 22(6), pp.986–1002.

Bursen, A. et al., 2010. The AF4.MLL fusion protein is capable of inducing ALL in mice without requirement of MLL.AF4. *Blood*, 115(17), pp.3570–9.

Bustelo, X.R. et al., 1993. Developmental expression of the vav protooncogene. *Cell growth & differentiation : the molecular biology journal of the American Association for Cancer Research*, 4(4), pp.297–308.

Byrd, J.C., 2015. Introduction to a series of reviews on chronic

lymphocytic leukemia. *Blood*, 126(4), p.427.

Canaani, E. et al., 2004. ALL-1/MLL1, a homologue of Drosophila TRITHORAX, modifies chromatin and is directly involved in infant acute leukaemia. *British journal of cancer*, 90(4), pp.756–60.

Cano, F. et al., 2008a. Leukaemia lineage specification caused by cell-specific Mll-Enl translocations. *Oncogene*, 27(13), pp.1945–1950.

Cano, F. et al., 2008b. Leukaemia lineage specification caused by cell-specific Mll-Enl translocations. *Oncogene*, 27(13), pp.1945–1950.

Caprioli, A. et al., 1998. Blood-borne seeding by hematopoietic and endothelial precursors from the allantois. *Proceedings of the National Academy of Sciences* , 95(4), pp.1641–1646.

Chagraoui, J. et al., 2003. Fetal liver stroma consists of cells in epithelial-to-mesenchymal transition. *Blood*, 101(8), pp.2973–82.

Chan, I.T. et al., 2004. Conditional expression of oncogenic K-ras from its endogenous promoter induces a myeloproliferative disease. *The Journal of clinical investigation*, 113(4), pp.528–38.

Chen, F. et al., 2015. New horizons in tumor microenvironment biology: challenges and opportunities. *BMC Medicine*, 13(1), p.45.

Chen, W. et al., 2008. Malignant transformation initiated by Mll-AF9: gene dosage and critical target cells. *Cancer cell*, 13(5), pp.432–40.

Chen, W. et al., 2011. Modeling human infant MLL leukemia in mice: leukemia from fetal liver differs from that originating in postnatal marrow. *Blood*, 117(12), pp.3474–5.

Cheshier, S.H. et al., 1999. In vivo proliferation and cell cycle kinetics

of long-term self-renewing hematopoietic stem cells. *Proceedings of the National Academy of Sciences of the United States of America*, 96(6), pp.3120–5.

Chou, S. & Lodish, H.F., 2010. Fetal liver hepatic progenitors are supportive stromal cells for hematopoietic stem cells. *Proceedings of the National Academy of Sciences of the United States of America*, 107(17), pp.7799–804.

Collins, E.C. et al., 2000. Inter-chromosomal recombination of Mll and Af9 genes mediated by cre-loxP in mouse development. *EMBO reports*, 1(2), pp.127–32.

Cook, G.J. and & Pardee, T.S., 2013. Animal models of leukemia: any closer to the real thing? *Cancer metastasis reviews*, 32(1–2), pp.63–76.

Coppoolse, E.R. et al., 2005. Size does matter: cre-mediated somatic deletion efficiency depends on the distance between the target lox-sites. *Plant molecular biology*, 58(5), pp.687–98.

Corral, J. et al., 1996. An Mll-AF9 fusion gene made by homologous recombination causes acute leukemia in chimeric mice: a method to create fusion oncogenes. *Cell*, 85(6), pp.853–61.

Coşkun, S. et al., 2014. Development of the fetal bone marrow niche and regulation of HSC quiescence and homing ability by emerging osteolineage cells. *Cell reports*, 9(2), pp.581–90.

Cumano, A. et al., 2001. Intraembryonic, but Not Yolk Sac Hematopoietic Precursors, Isolated before Circulation, Provide Long-Term Multilineage Reconstitution. *Immunity*, 15(3), pp.477–485.

Cumano, A. & Godin, I., 2007. Ontogeny of the Hematopoietic System. *Annual Review of Immunology*, 25(1), pp.745–785.

Cutts, B.A. et al., 2009. Nf1 deficiency cooperates with oncogenic K-RAS to induce acute myeloid leukemia in mice. *Blood*, 114(17), pp.3629–32.

Dakic, A. et al., 2005. PU.1 regulates the commitment of adult hematopoietic progenitors and restricts granulopoiesis. *The Journal of Experimental Medicine*, 201(9), pp.1487–1502.

Danielian, P.S. et al., 1998. Modification of gene activity in mouse embryos in utero by a tamoxifen-inducible form of Cre recombinase. *Current biology : CB*, 8(24), pp.1323–6.

Daser, A. & Rabbitts, T.H., 2004. Extending the repertoire of the mixed-lineage leukemia gene MLL in leukemogenesis. *Genes and Development*, 18(9), pp.965–974.

Doty, R.T. et al., 2002. The leukemia-associated gene Mllt1/ENL: characterization of a murine homolog and demonstration of an essential role in embryonic development. *Blood cells, molecules & diseases*, 28(3), pp.407–417.

Doulatov, S. et al., 2013. Induction of multipotential hematopoietic progenitors from human pluripotent stem cells via respecification of lineage-restricted precursors. *Cell stem cell*, 13(4), pp.459–70.

Dzierzak, E., 2002. Hematopoietic stem cells and their precursors: developmental diversity and lineage relationships. *Immunological Reviews*, 187(1), pp.126–138.

Ema, H. & Nakauchi, H., 2000. Expansion of hematopoietic stem cells

in the developing liver of a mouse embryo. *Blood*, 95(7), pp.2284–8.

Erfurth, F. et al., 2004. MLL fusion partners AF4 and AF9 interact at subnuclear foci. *Leukemia*, 18(1), pp.92–102.

Essers, M.A.G. et al., 2010. Targeting leukemic stem cells by breaking their dormancy. *Molecular oncology*, 4(5), pp.443–50.

Estey, E. et al., 2006. Acute myeloid leukaemia. *Lancet (London, England)*, 368(9550), pp.1894–907.

Faderl, S. et al., 1999. Chronic myelogenous leukemia: biology and therapy. *Annals of internal medicine*, 131(3), pp.207–19.

Felix, C.A. & Lange, B.J., 1999. Leukemia in infants. *The oncologist*, 4(3), pp.225–40.

Fiedler, K. & Brunner, C., 2012. Mechanisms Controlling Hematopoiesis. *Hematology - Science and Practice*, pp.3–46.

Fokas, E., McKenna, W.G. & Muschel, R.J., 2012. The impact of tumor microenvironment on cancer treatment and its modulation by direct and indirect antivascular strategies. *Cancer metastasis reviews*, 31(3–4), pp.823–42.

Forster, A., Pannell, R., Drynan, L.F., et al., 2003. Engineering de novo reciprocal chromosomal translocations associated with Mll to replicate primary events of human cancer. *Cancer Cell*, 3(5), pp.449–458.

Forster, A., Pannell, R., Drynan, L.F., et al., 2003. Engineering de novo reciprocal chromosomal translocations associated with Mll to

replicate primary events of human cancer. *Cancer cell*, 3(5), pp.449–58.

Freireich, E.J., Wiernik, P.H. & Steensma, D.P., 2014. The Leukemias: A Half-Century of Discovery. *Journal of Clinical Oncology*, 32(31), pp.3463–3469.

Friend, C., 1957. Cell-free transmission in adult Swiss mice of a disease having the character of a leukemia. *The Journal of experimental medicine*, 105(4), pp.307–18.

Fujiwara, Y. et al., 1996. Arrested development of embryonic red cell precursors in mouse embryos lacking transcription factor GATA-1. *Proceedings of the National Academy of Sciences of the United States of America*, 93(22), pp.12355–12358.

Gale, K.B. et al., 1997. Backtracking leukemia to birth: identification of clonotypic gene fusion sequences in neonatal blood spots. *Proceedings of the National Academy of Sciences of the United States of America*, 94(25), pp.13950–4.

Gama Sosa, M.A., De Gasperi, R. & Elder, G.A., 2010. Animal transgenesis: an overview. *Brain Structure and Function*, 214(2–3), pp.91–109.

Gama-Norton, L. et al., 2015. Notch signal strength controls cell fate in the haemogenic endothelium. *Nature Communications*, 6, p.8510.

Gan, T. et al., 2010a. Developmentally induced Mll1 loss reveals defects in postnatal haematopoiesis. *Leukemia*, 24(10), pp.1732–41.

Gan, T. et al., 2010b. Developmentally induced Mll1 loss reveals defects in postnatal haematopoiesis. *Leukemia*, 24(10), pp.1732–41.

Garcia-Porrero, J., Godin, I. & Dieterlen-Lievre, F., 1995. Potential intraembryonic hemogenic sites at pre-liver stages in the mouse. *Anatomy and Embryology*, 192(5), pp.425–435.

Gekas, C. et al., 2005. The Placenta Is a Niche for Hematopoietic Stem Cells. *Developmental Cell*, 8(3), pp.365–375.

Gekas, C. et al., 2016. β-Catenin is required for T-cell leukemia initiation and MYC transcription downstream of Notch1. *Leukemia*.

Goardon, N. et al., 2011. Coexistence of LMPP-like and GMP-like leukemia stem cells in acute myeloid leukemia. *Cancer cell*, 19(1), pp.138–52.

Godin, I.E. et al., 1993. Para-aortic splanchnopleura from early mouse embryos contains B1a cell progenitors. *Nature*, 364(6432), pp.67–70.

Gordon, A.S., 1972. Haemopoietic Cells. D. Metcalf and M. A. S. Moore. North-Holland, Amsterdam, and Elsevier, New York, 1971. xiv, 550 pp., illus. $41.50. Frontiers of Biology, vol. 24. *Science*, 178(4064), pp.974–975.

Gordon-Keylock, S. et al., 2013. Mouse extraembryonic arterial vessels harbor precursors capable of maturing into definitive HSCs. *Blood*, 122(14), pp.2338–45.

Göthert, J.R. et al., 2005. In vivo fate-tracing studies using the Scl stem cell enhancer: embryonic hematopoietic stem cells significantly contribute to adult hematopoiesis. *Blood*, 105(7), pp.2724–32.

Greaves, 2000. *Cancer: The Evolutionary Legacy - Mel Greaves - Google Books*, Oxford University Press.

Greaves, M.F. et al., 2003. Leukemia in twins: lessons in natural history. *Blood*, 102(7), pp.2321–33.

Greenblatt, S. et al., 2012. Knock-in of a FLT3/ITD mutation cooperates with a NUP98-HOXD13 fusion to generate acute myeloid leukemia in a mouse model. *Blood*, 119(12), pp.2883–94.

Guimont-Desrochers, F. et al., 2012. Redefining interferon-producing killer dendritic cells as a novel intermediate in NK-cell differentiation.

Hahn, H.K., Georg, M. & Peitgen, H.-O., 2005. Fractal Aspects of Three-Dimensional Vascular Constructive Optimization. In *Fractals in Biology and Medicine*. Basel: Birkhäuser-Verlag, pp. 55–66.

Hall, M.A. et al., 2003. The critical regulator of embryonic hematopoiesis, SCL, is vital in the adult for megakaryopoiesis, erythropoiesis, and lineage choice in CFU-S12. *Proceedings of the National Academy of Sciences of the United States of America*, 100(3), pp.992–7.

Hayashi, S. & McMahon, A.P., 2002. Efficient recombination in diverse tissues by a tamoxifen-inducible form of Cre: a tool for temporally regulated gene activation/inactivation in the mouse. *Developmental biology*, 244(2), pp.305–18.

Heim, S., Mandahl, N. & Mitelman, F., 1988. Genetic convergence and divergence in tumor progression. *Cancer research*, 48(21), pp.5911–6.

Hess, J.L. et al., 1997. Defects in yolk sac hematopoiesis in Mll-null embryos. *Blood*, 90, pp.1799–1806.

Heyer, W.-D., Ehmsen, K.T. & Liu, J., 2010. Regulation of homologous recombination in eukaryotes. *Annual review of genetics*, 44, pp.113–39.

Hilden, J.M. et al., 1995. Molecular analysis of infant acute lymphoblastic leukemia: MLL gene rearrangement and reverse transcriptase-polymerase chain reaction for t(4; 11)(q21; q23). *Blood*, 86(10), pp.3876–82.

Himoudi, N. et al., 2008. Activity of Unpulsed Dendritic Cells Dendritic Cells Account for the Tumoricidal Bone Marrow-Derived IFN-Producing Killer Bone Marrow-Derived IFN-Producing Killer Dendritic Cells Account for the Tumoricidal Activity of Unpulsed Dendritic Cells 1. *J Immunol References*, 1816654(9), pp.6654–6663.

Hirschi, K.K., 2012. Hemogenic endothelium during development and beyond. *Blood*, 119(21), pp.4823–7.

Hock, H. et al., 2004. Tel/Etv6 is an essential and selective regulator of adult hematopoietic stem cell survival. *Genes & development*, 18(19), pp.2336–41.

Hoffman, R., 2013. *Hematology basic principles and practice*, Saunders/Elsevier.

Hong, D. et al., 2008. Initiating and cancer-propagating cells in TEL-AML1-associated childhood leukemia. *Science (New York, N.Y.)*, 319(5861), pp.336–9.

Horton, S.J. et al., 2009. Acute myeloid leukemia induced by MLL-ENL is cured by oncogene ablation despite acquisition of complex genetic abnormalities. *Blood*, 113(20), pp.4922–9.

Hunger, S.P. et al., 1998. Oncogenesis in utero: Fetal death due to acute myelogenous leukaemia with an MLL translocation. *British Journal of Haematology*, 103(2), pp.539–542.

Isidori, A. et al., 2014. The role of the immunosuppressive microenvironment in acute myeloid leukemia development and treatment. *Expert Review of Hematology*, 7(6), pp.807–818.

Iwasaki, H. et al., 2005. The order of expression of transcription factors directs hierarchical specification of hematopoietic lineages.

Jaffredo, T. et al., 2003. Avian HSC emergence, migration, and commitment toward the T cell lineage. *FEMS immunology and medical microbiology*, 39(3), pp.205–12.

Jaffredo, T. et al., 2000. Tracing the Progeny of the Aortic Hemangioblast in the Avian Embryo. *Developmental Biology*, 224(2), pp.204–214.

Jansen, M.W.J.C. et al., 2007. Immunobiological diversity in infant acute lymphoblastic leukemia is related to the occurrence and type of MLL gene rearrangement. *Leukemia : official journal of the Leukemia Society of America, Leukemia Research Fund, U.K*, 21(4), pp.633–641.

de Jong, J.L.O. & Zon, L.I., 2005. Use of the zebrafish system to study primitive and definitive hematopoiesis. *Annual review of genetics*, 39, pp.481–501.

Jordan, C.T., 2007. The leukemic stem cell. *Best practice & research. Clinical haematology*, 20(1), pp.13–8.

Juge, S. et al., 2013. A Novel Conditional Mouse Model For MLL-ENL Induced Acute Leukemia. *Blood*, 122(21), pp.1277–1277.

Jung, R. et al., 2010. Bimodal distribution of genomic MLL breakpoints in infant acute lymphoblastic leukemia treatment. *Leukemia*, 24(4), pp.903–907.

Kalil, N. & Cheson, B., 1999. Chronic Lymphocytic Leukemia. *The Oncologist*, (4), pp.352–369.

Kampen, K.R., 2012. The discovery and early understanding of leukemia. *Leukemia Research*, 36(1), pp.6–13.

Karsunky, H. et al., 2008. Flk2+ common lymphoid progenitors possess equivalent differentiation potential for the B and T lineages. *Blood*, 111(12), pp.5562–70.

Kato, I. et al., 2011. Identification of hepatic niche harboring human acute lymphoblastic leukemic cells via the SDF-1/CXCR4 axis. *PloS one*, 6(11), p.e27042.

Kaufman, 1994. The atlas of mouse development. *Molecular Reproduction and Development*, 37(1), p.120.

Kebriaei, P. et al., 2002. Acute lymphoblastic leukaemia: diagnosis and classification. *Best Practice & Research Clinical Haematology*, 15(4), pp.597–621.

Khan, J.A. et al., 2016. Fetal liver hematopoietic stem cell niches associate with portal vessels. *Science (New York, N.Y.)*, 351(6269), pp.176–80.

Kim, I. et al., 2006. Enhanced purification of fetal liver hematopoietic stem cells using SLAM family receptors. *Blood*, 108(2), pp.737–44.

Klinakis, A. et al., 2011. A novel tumour-suppressor function for the

Notch pathway in myeloid leukaemia. *Nature*, 473(7346), pp.230–3.

Kondo, E. et al., 2003. A yeast two-hybrid assay provides a simple way to evaluate the vast majority of hMLH1 germ-line mutations. *Cancer research*, 63(12), pp.3302–8.

Kondo, M. et al., 1997. Identification of clonogenic common lymphoid progenitors in mouse bone marrow. *Cell*, 91(5), pp.661–72.

Konopleva, M.Y. & Jordan, C.T., 2011. Leukemia Stem Cells and Microenvironment: Biology and Therapeutic Targeting. *Journal of Clinical Oncology*, 29(5), pp.591–599.

Kowarz, E. et al., 2007. Complex MLL rearrangements in t(4;11) leukemia patients with absent AF4.MLL fusion allele. *Leukemia*, 21(6), pp.1232–8.

Krivtsov et al., 2008. H3K79 methylation profiles define murine and human MLL-AF4 leukemias. *Cancer Cell*, 14, pp.355–368.

Krivtsov, A. V. et al., 2006. Transformation from committed progenitor to leukaemia stem cell initiated by MLL–AF9. *Nature*, 442(7104), pp.818–822.

Krivtsov, A. V & Armstrong, S. a, 2007. MLL translocations, histone modifications and leukaemia stem-cell development. *Nature reviews. Cancer*, 7(11), pp.823–33.

Krumlauf, R. et al., 1994. Hox genes in vertebrate development. *Cell*, 78(2), pp.191–201.

Kühn, R. et al., 1995. Inducible gene targeting in mice. *Science (New York,*

N.Y.), 269(5229), pp.1427–9.

Kumar, A.R. et al., 2009. A role for MEIS1 in MLL-fusion gene leukemia. *Blood*, 113(8), pp.1756–8.

Kumar, A.R. et al., 2011. t(4;11) leukemias display addiction to MLL-AF4 but not to AF4-MLL. *Leukemia research*, 35(3), pp.305–9.

Kumaravelu, P. et al., 2002. Quantitative developmental anatomy of definitive haematopoietic stem cells/long-term repopulating units (HSC/RUs): role of the aorta-gonad-mesonephros (AGM) region and the yolk sac in colonisation of the mouse embryonic liver. *Development (Cambridge, England)*, 129(21), pp.4891–9.

Kunisaki, Y. et al., 2013. Arteriolar niches maintain haematopoietic stem cell quiescence. *Nature*, 502(7473), pp.637–43.

Kuntimaddi, A. et al., 2014. Degree of Recruitment of DOT1L to MLL-AF9 Defines Level of H3K79 Di- and Tri-methylation on Target Genes and Transformation Potential. *Cell Reports*, 11(5), pp.808–820.

Lapidot, T. et al., 1994. A cell initiating human acute myeloid leukaemia after transplantation into SCID mice. *Nature*, 367(6464), pp.645–648.

Laslo, P. et al., 2008. Gene regulatory networks directing myeloid and lymphoid cell fates within the immune system. *Seminars in Immunology*, 20, pp.228–235.

Lassila, O. et al., 1982. Erythropoiesis and lymphopoiesis in the chick yolk-sac-embryo chimeras: contribution of yolk sac and intraembryonic stem cells. *Blood*, 59(2), pp.377–81.

Lavau, C. et al., 1997. Immortalization and leukemic transformation of a myelomonocytic precursor by retrovirally transduced HRX-ENL. *EMBO Journal*, 16(14), pp.4226–4237.

Lavau, C. et al., 2000. Retrovirus-mediated gene transfer of MLL-ELL transforms primary myeloid progenitors and causes acute myeloid leukemias in mice. *Proceedings of the National Academy of Sciences of the United States of America*, 97(20), pp.10984–9.

Lawrence, H.J. et al., 1999. Frequent co-expression of the HOXA9 and MEIS1 homeobox genes in human myeloid leukemias. *Leukemia*, 13(12), pp.1993–9.

Leach, B.I. et al., 2013. Leukemia fusion target AF9 is an intrinsically disordered transcriptional regulator that recruits multiple partners via coupled folding and binding. *Structure (London, England : 1993)*, 21(1), pp.176–83.

Lebert-Ghali, C.-E. et al., 2010. HoxA cluster is haploinsufficient for activity of hematopoietic stem and progenitor cells. *Experimental hematology*, 38(11), pp.1074-1086–5.

Lemischka, I.R., 1991. Clonal, in vivo behavior of the totipotent hematopoietic stem cell. *Seminars in immunology*, 3(6), pp.349–355.

Li, Q. et al., 2011. Hematopoiesis and leukemogenesis in mice expressing oncogenic NrasG12D from the endogenous locus. *Blood*, 117(6), pp.2022–32.

Lie, S.O. et al., 1996. A population-based study of 272 children with acute myeloid leukaemia treated on two consecutive protocols with different intensity: best outcome in girls, infants, and children

with Down's syndrome. *British Journal of Haematology*, 94(1), pp.82–88.

Lieu, Y.K. & Reddy, E.P., 2012. Impaired adult myeloid progenitor CMP and GMP cell function in conditional c-myb-knockout mice. *Cell cycle (Georgetown, Tex.)*, 11(18), pp.3504–12.

Little, J.B., 2000. Radiation carcinogenesis. *Carcinogenesis*, 21(3), pp.397–404.

Mackie, E.J. et al., 2008. Endochondral ossification: How cartilage is converted into bone in the developing skeleton. *The International Journal of Biochemistry & Cell Biology*, 40(1), pp.46–62.

Maillard, I. et al., 2008. Canonical notch signaling is dispensable for the maintenance of adult hematopoietic stem cells. *Cell stem cell*, 2(4), pp.356–66.

Mak, K.S. et al., 2011. PU.1 and Haematopoietic Cell Fate: Dosage Matters. *International journal of cell biology*, 2011, p.808524.

Martinez-Climent, J.A. et al., 1995. Clinical and prognostic significance of chromosomal abnormalities in childhood acute myeloid leukemia de novo. *Leukemia*, 9(1), pp.95–101.

Maximow, A., 1909. Der Lymphozyt als gemeinsame Stammzelle der verschiedenen Blutelemente in der embryonalen Entwicklung und im postfetalen Leben der Säugetiere. *Folia Haematologica*, 8, pp.125–134.

McCormack, E., Bruserud, O. & Gjertsen, B.T., 2005. Animal models of acute myelogenous leukaemia - development, application and future perspectives. *Leukemia*, 19(5), pp.687–706.

McKenzie, S.B., 2005. Advances in Understanding the Biology and Genetics of Acute Myelocytic Leukemia. *Clinical Laboratory Science18.1*, 18.1, pp.28–37.

McKinney-Freeman, S.L. et al., 2009. Surface antigen phenotypes of hematopoietic stem cells from embryos and murine embryonic stem cells. *Blood*, 114(2), pp.268–78.

McMahon, K.A. et al., 2007. Mll has a critical role in fetal and adult hematopoietic stem cell self-renewal. *Cell stem cell*, 1(3), pp.338–45.

Medvinsky, A. & Dzierzak, E., 1996. Definitive Hematopoiesis Is Autonomously Initiated by the AGM Region. *Cell*, 86(6), pp.897–906.

Medvinsky, A.L. et al., 1993. An early pre-liver intraembryonic source of CFU-S in the developing mouse. *Nature*, 364(6432), pp.64–7.

Metzler, M. et al., 2006. A conditional model of MLL-AF4 B-cell tumourigenesis using invertor technology. *Oncogene*, 25(22), pp.3093–3103.

Meyer, C. et al., 2009. New insights to the MLL recombinome of acute leukemias. *Leukemia : official journal of the Leukemia Society of America, Leukemia Research Fund, U.K*, 23(8), pp.1490–1499.

Mikkola, H.K.A. & Orkin, S.H., 2006. The journey of developing hematopoietic stem cells. *Development*, 133(19), pp.3733–3744.

Milne, T.A. et al., 2005. Menin and MLL cooperatively regulate expression of cyclin-dependent kinase inhibitors. *Proceedings of the National Academy of Sciences of the United States of America*, 102(3), pp.749–54.

Miraki-Moud, F. et al., 2013. Acute myeloid leukemia does not deplete normal hematopoietic stem cells but induces cytopenias by impeding their differentiation. *Proceedings of the National Academy of Sciences*, 110(33), pp.13576–13581.

Mohan, M. et al., 2010. Linking H3K79 trimethylation to Wnt signaling through a novel Dot1-containing complex (DotCom). *Genes and Development*, 24(6), pp.574–589.

Montes, R. et al., 2011. Enforced expression of MLL-AF4 fusion in cord blood CD34+ cells enhances the hematopoietic repopulating cell function and clonogenic potential but is not sufficient to initiate leukemia. *Blood*, 117(18), pp.4746–58.

Moore, K.A., Ema, H. & Lemischka, I.R., 1997. In vitro maintenance of highly purified, transplantable hematopoietic stem cells. *Blood*, 89(12), pp.4337–47.

MORCEAU, F. et al., 2004. GATA-1: Friends, Brothers, and Coworkers. *Annals of the New York Academy of Sciences*, 1030(1), pp.537–554.

Morgan, K. et al., 2008. Isolation of early hematopoietic stem cells from murine yolk sac and AGM. *Journal of visualized experiments : JoVE*, (16).

Morrison, S.J. et al., 1994. The long-term repopulating subset of hematopoietic stem cells is deterministic and isolatable by phenotype. *Immunity*, 1(8), pp.661–73.

Morrissey, J. et al., 1993. A serine/proline-rich protein is fused to HRX in t(4;11) acute leukemias. *Blood*, 81(5), pp.1124–31.

Müller, A.M. et al., 1994. Development of hematopoietic stem cell activity in the mouse embryo. *Immunity*, 1(4), pp.291–301.

Muntean, A.G. & Hess, J.L., 2012. The pathogenesis of mixed-lineage leukemia. *Annual review of pathology*, 7, pp.283–301.

Nagy, S. et al., 2014. *Manipulating the Mouse Embryo: A Laboratory Manual, Fourth Edition* 4th ed., Cold Spring Harbor Laboratory Press.

Nakamura, E., Nguyen, M.-T. & Mackem, S., 2006. Kinetics of tamoxifen-regulated Cre activity in mice using a cartilage-specific CreERT to assay temporal activity windows along the proximodistal limb skeleton. *Developmental Dynamics*, 235(9), pp.2603–2612.

Nakamura, H. et al., 1997. Morphological subtyping of acute myeloid leukemia with maturation (AML-M2): homogeneous pink-colored cytoplasm of mature neutrophils is most characteristic of AML-M2 with t(8;21). *Leukemia*, 11(5), pp.651–655.

Nemeth, M.J., Kirby, M.R. & Bodine, D.M., 2006. Hmgb3 regulates the balance between hematopoietic stem cell self-renewal and differentiation. *Proceedings of the National Academy of Sciences of the United States of America*, 103(37), pp.13783–8.

North, T. et al., 1999. Cbfa2 is required for the formation of intra-aortic hematopoietic clusters. *Development*, 126(11), pp.2563–2575.

North, T.E. et al., 2002. Runx1 expression marks long-term repopulating hematopoietic stem cells in the midgestation mouse embryo. *Immunity*, 16(5), pp.661–72.

Osawa, M. et al., 1996. Long-term lymphohematopoietic reconstitution

by a single CD34-low/negative hematopoietic stem cell. *Science (New York, N.Y.)*, 273(5272), pp.242–5.

Ottersbach, K. & Dzierzak, E., 2005. The Murine Placenta Contains Hematopoietic Stem Cells within the Vascular Labyrinth Region. *Developmental Cell*, 8(3), pp.377–387.

Palis, J. et al., 1999. Development of erythroid and myeloid progenitors in the yolk sac and embryo proper of the mouse. *Development*, 126(22), pp.5073–5084.

Park, I. et al., 2003. Bmi-1 is required for maintenance of adult self-renewing haematopoietic stem cells. *Nature*, 423(6937), pp.302–305.

Passegué, E. et al., 2003. Normal and leukemic hematopoiesis: are leukemias a stem cell disorder or a reacquisition of stem cell characteristics? *Proceedings of the National Academy of Sciences of the United States of America*, 100 Suppl, pp.11842–9.

Paul, F. et al., 2015. Transcriptional Heterogeneity and Lineage Commitment in Myeloid Progenitors. *Cell*, 163(7), pp.1663–77.

PÉAULT, B. & TAVIAN, M., 2003. Hematopoietic Stem Cell Emergence in the Human Embryo and Fetus. *Annals of the New York Academy of Sciences*, 996(1), pp.132–140.

Pereira, C.-F. et al., 2016. Hematopoietic Reprogramming In Vitro Informs In Vivo Identification of Hemogenic Precursors to Definitive Hematopoietic Stem Cells. *Developmental Cell*, 36(5), pp.525–539.

Pietras, E.M. et al., 2015. Functionally Distinct Subsets of Lineage-

Biased Multipotent Progenitors Control Blood Production in Normal and Regenerative Conditions. *Cell stem cell*, 17(1), pp.35–46.

Prasad, R. et al., 1995. Domains with transcriptional regulatory activity within the ALL1 and AF4 proteins involved in acute leukemia. *Proceedings of the National Academy of Sciences of the United States of America*, 92(26), pp.12160–4.

Pui, C.H. et al., 1994. 11q23/MLL rearrangement confers a poor prognosis in infants with acute lymphoblastic leukemia. *Journal of clinical oncology : official journal of the American Society of Clinical Oncology*, 12(5), pp.909–15.

Pui, C.-H. et al., 2008. Acute lymphoblastic leukaemia. *Lancet (London, England)*, 371(9617), pp.1030–43.

Pui, C.-H., 1995. Childhood Leukemias. *New England Journal of Medicine*, 332(24), pp.1618–1630.

Pui, C.H. & Evans, W.E., 1999. Acute lymphoblastic leukemia in infants. *Journal of clinical oncology : official journal of the American Society of Clinical Oncology*, 17(2), pp.438–40.

Reaman, G. et al., 1985. Acute lymphoblastic leukemia in infants less than one year of age: a cumulative experience of the Children's Cancer Study Group. *Journal of clinical oncology : official journal of the American Society of Clinical Oncology*, 3(11), pp.1513–21.

Robert-Moreno, A. et al., 2008. Impaired embryonic haematopoiesis yet normal arterial development in the absence of the Notch ligand Jagged1. *The EMBO journal*, 27(13), pp.1886–95.

Robert-Moreno, A. et al., 2005. RBPjkappa-dependent Notch function regulates Gata2 and is essential for the formation of intra-embryonic hematopoietic cells. *Development (Cambridge, England)*, 132(5), pp.1117–26.

Robin, C. et al., 2009. Human placenta is a potent hematopoietic niche containing hematopoietic stem and progenitor cells throughout development. *Cell stem cell*, 5(4), pp.385–95.

Rosenbauer, F. & Tenen, D.G., 2007. Transcription factors in myeloid development: balancing differentiation with transformation. *Nature reviews. Immunology*, 7(2), pp.105–17.

Rozovskaia, T. et al., 2001. Upregulation of Meis1 and HoxA9 in acute lymphocytic leukemias with the t(4 : 11) abnormality. *Oncogene*, 20(7), pp.874–878.

Rubnitz, B.J.E. et al., 1999. Childhood Acute Lymphoblastic Leukemia With the MLL-ENL F u s i o n a n d t (1 1 ; 1 9) (q 2 3 ; p 1 3 . 3) T r a n s l o c a t i o n Patients and Methods : A retrospective analysis of leukemic cell karyotypes obtained from patients with Conclusion : . , 17(1), pp.191–196.

Rubnitz, J.E. et al., 1994. ENL, the gene fused with HRX in t(11;19) leukemias, encodes a nuclear protein with transcriptional activation potential in lymphoid and myeloid cells. *Blood*, 84(6), pp.1747–52.

Rugh, R., 1968. The mouse. Its reproduction and development. *The mouse. Its reproduction and development.*

Rytting, 2014. *Acute Leukemia Overview - Hematology and Oncology - Merck*

Manuals Professional Edition,

Saito, Y. et al., 2015. AMPK Protects Leukemia-Initiating Cells in Myeloid Leukemias from Metabolic Stress in the Bone Marrow. *Cell Stem Cell*, 17(5), pp.585–596.

Samokhvalov, I.M., Samokhvalova, N.I. & Nishikawa, S., 2007. Cell tracing shows the contribution of the yolk sac to adult haematopoiesis. *Nature*, 446(7139), pp.1056–1061.

Sanders, D.S., Muntean, A.G. & Hess, J.L., 2011. Significance of AF4-MLL reciprocal fusion in t(4;11) leukemias? *Leukemia research*, 35(3), pp.299–300.

Sandler, D.P. & Ross, J.A., 1997. Epidemiology of acute leukemia in children and adults. *Seminars in oncology*, 24(1), pp.3–16.

Sanjuan-Pla, A. et al., 2015. Revisiting the biology of infant t(4;11)/MLL-AF4+ B-cell acute lymphoblastic leukemia. *Blood*, 126(25), pp.2676–85.

Schmitt, C.A., Rosenthal, C.T. & Lowe, S.W., 2000. Genetic analysis of chemoresistance in primary murine lymphomas. *Nature medicine*, 6(9), pp.1029–35.

Schnabel, C.A., Jacobs, Y. & Cleary, M.L., 2000. HoxA9-mediated immortalization of myeloid progenitors requires functional interactions with TALE cofactors Pbx and Meis. *Oncogene*, 19(5), pp.608–16.

Seita, J. & Weissman, I.L., 2010. Hematopoietic stem cell: self-renewal versus differentiation. *Wiley interdisciplinary reviews. Systems biology and medicine*, 2(6), pp.640–53.

Serwold, T., Ehrlich, L.I.R. & Weissman, I.L., 2009. Reductive isolation from bone marrow and blood implicates common lymphoid progenitors as the major source of thymopoiesis. *Blood*, 113(4), pp.807–15.

Shen, W.F. et al., 1999. HOXA9 forms triple complexes with PBX2 and MEIS1 in myeloid cells. *Molecular and cellular biology*, 19(4), pp.3051–61.

Shilatifard, A., 2006. Chromatin Modifications by Methylation and Ubiquitination: Implications in the Regulation of Gene Expression. *Annual Review of Biochemistry*, 75(1), pp.243–269.

Sison, E.A.R. & Brown, P., 2011. The bone marrow microenvironment and leukemia: biology and therapeutic targeting. *Expert review of hematology*, 4(3), pp.271–83.

Skipper, H.E. & Perry, S., 1970. Kinetics of normal and leukemic leukocyte populations and relevance to chemotherapy. *Cancer research*, 30(6), pp.1883–97.

Slany, R.K., 2009. The molecular biology of mixed lineage leukemia. *Haematologica*, 94(7), pp.984–993.

Slany, R.K. et al., 2009. The molecular biology of mixed lineage leukemia. *Haematologica*, 94(7), pp.984–93.

Somervaille, T.C.P. et al., 2009. Hierarchical maintenance of MLL myeloid leukemia stem cells employs a transcriptional program shared with embryonic rather than adult stem cells. *Cell stem cell*, 4(2), pp.129–40.

Somervaille, T.C.P. & Cleary, M.L., 2006. Identification and

characterization of leukemia stem cells in murine MLL-AF9 acute myeloid leukemia. *Cancer cell*, 10(4), pp.257–68.

Sorensen, P.H. et al., 1994. Molecular rearrangements of the MLL gene are present in most cases of infant acute myeloid leukemia and are strongly correlated with monocytic or myelomonocytic phenotypes. *The Journal of clinical investigation*, 93(1), pp.429–37.

Sounni, N.E. & Noel, A., 2013. Targeting the Tumor Microenvironment for Cancer Therapy. *Clinical Chemistry*, 59(1).

Spangrude, G.J. et al., 1991. Mouse hematopoietic stem cells. *Blood*, 78(6), pp.1395–1402.

Stadtfeld, M. & Graf, T., 2005. Assessing the role of hematopoietic plasticity for endothelial and hepatocyte development by non-invasive lineage tracing. *Development (Cambridge, England)*, 132(1), pp.203–13.

Stam, R.W. et al., 2014. Gene expression profiling − based dissection of MLL translocated and MLL germline acute lymphoblastic leukemia in infants Gene expression profiling – based dissection of MLL translocated and MLL germline acute lymphoblastic leukemia in infants. , 115(14), pp.2835–2844.

Stanulla, M. et al., 1997. DNA cleavage within the MLL breakpoint cluster region is a specific event which occurs as part of higher-order chromatin fragmentation during the initial stages of apoptosis. *Molecular and cellular biology*, 17(7), pp.4070–9.

Sun, Y., 2016. Tumor microenvironment and cancer therapy resistance. *Cancer letters*, 380(1), pp.205–15.

Taggart, J. et al., 2016. MSI2 is required for maintaining activated myelodysplastic syndrome stem cells. *Nature communications*, 7, p.10739.

Taichman, R.S., 2005. Blood and bone: two tissues whose fates are intertwined to create the hematopoietic stem-cell niche. *Blood*, 105(7), pp.2631–9.

Taieb, J. et al., 2006. A novel dendritic cell subset involved in tumor immunosurveillance. *Nature Medicine*, 12(2), pp.214–219.

Tam, P.P.. & Behringer, R.R., 1997. Mouse gastrulation: the formation of a mammalian body plan. *Mechanisms of Development*, 68(1), pp.3–25.

Taussig, D.C. et al., 2008. Anti-CD38 antibody-mediated clearance of human repopulating cells masks the heterogeneity of leukemia-initiating cells. *Blood*, 112(3), pp.568–75.

Teicher, B.A., 2006. Tumor models for efficacy determination. *Molecular cancer therapeutics*, 5(10), pp.2435–43.

Thirman, M.J. et al., 1993. Rearrangement of the MLL Gene in Acute Lymphoblastic and Acute Myeloid Leukemias with 11q23 Chromosomal Translocations. *New England Journal of Medicine*, 329(13), pp.909–914.

Till, J.E. & McCULLOCH, E. a, 1961. A direct measurement of the radiation sensitivity of normal mouse bone marrow cells. *Radiation research*, 14(2), pp.213–222.

Tkachuk, D.C., Kohler, S. & Cleary, M.L., 1992. Involvement of a Homolog of Drosophila-Trithorax By 11Q23 Chromosomal

Translocations in Acute Leukemias. *Cell*, 71(4), pp.691–700.

Ugale, A., Norddahl, G.L., et al., 2014. Hematopoietic Stem Cells Are Intrinsically Protected against MLL-ENL-Mediated Transformation. *Cell Reports*, 9(4), pp.1246–1255.

Ugale, A., Norddahl, G.L., et al., 2014. Hematopoietic stem cells are intrinsically protected against MLL-ENL-mediated transformation. *Cell reports*, 9(4), pp.1246–55.

Upton, A.C., 1975. Physical Carcinogenesis: Radiation—History and Sources. In *Cancer. A Comprehensive Treatise*. Boston, MA: Springer US, pp. 387–403.

Vardiman, J.W. et al., 2002. The World Health Organization (WHO) classification of the myeloid neoplasms. *Blood*, 100(7), pp.2292–302.

Wang, J.C.Y. and & Dick, J.E., 2005. Cancer stem cells: lessons from leukemia. *Trends in cell biology*, 15(9), pp.494–501.

Wang, S.-Z. et al., 2009. A genetic strategy for stochastic gene activation with regulated sparseness (STARS). *PloS one*, 4(1), p.e4200.

Wei, J. et al., 2008. Microenvironment determines lineage fate in a human model of MLL-AF9 leukemia. *Cancer cell*, 13(6), pp.483–95.

Weissman, I.L. & Shizuru, J.A., 2008. The origins of the identification and isolation of hematopoietic stem cells, and their capability to induce donor-specific transplantation tolerance and treat autoimmune diseases. *Blood*, 112(9), pp.3543–53.

Wilson, A. et al., 2004. c-Myc controls the balance between

hematopoietic stem cell self-renewal and differentiation. *Genes & development*, 18(22), pp.2747–63.

WILSON, A. et al., 2007. Dormant and Self-Renewing Hematopoietic Stem Cells and Their Niches. *Annals of the New York Academy of Sciences*, 1106(1), pp.64–75.

Wilson, A. & Trumpp, A., 2006. Bone-marrow haematopoietic-stem-cell niches. *Nature reviews. Immunology*, 6(2), pp.93–106.

Wright, D.E. et al., 2002. Hematopoietic stem cells are uniquely selective in their migratory response to chemokines. *The Journal of experimental medicine*, 195(9), pp.1145–54.

Yamamoto, K. et al., 1993. Two distinct portions of LTG19/ENL at 19p13 are involved in t(11;19) leukemia. *Oncogene*, 8(10), pp.2617–25.

Yamasaki, S. et al., 2011. Identification of a yolk sac cell population with hematopoietic activity in view of CD45/c-Kit expression. *Development, growth & differentiation*, 53(7), pp.870–7.

Yu, B.D. et al., 1995. Altered Hox expression and segmental identity in Mll-mutant mice. *Nature*, 378(6556), pp.505–8.

Yu, H. et al., 2010. Relevant mouse model for human monocytic leukemia through Cre/lox-controlled myeloid-specific deletion of PTEN. *Leukemia*, 24(5), pp.1077–80.

Zeigler, B.M. et al., 2006. The allantois and chorion, when isolated before circulation or chorio-allantoic fusion, have hematopoietic potential. *Development*, 133(21), pp.4183–4192.

Zeisig, B.B. et al., 2004. Hoxa9 and Meis1 Are Key Targets for MLL-ENL-Mediated Cellular Immortalization. *Molecular and Cellular Biology*, 24(2), pp.617–628.

Zeisig, B.B. et al., 2003. The Oncoprotein MLL–ENL disturbs hematopoietic lineage determination and transforms a biphenotypic lymphoid/myeloid cell. *Oncogene*, 22(11), pp.1629–1637.

Zhang, D.E. et al., 1997. Absence of granulocyte colony-stimulating factor signaling and neutrophil development in CCAAT enhancer binding protein alpha-deficient mice. *Proceedings of the National Academy of Sciences of the United States of America*, 94(2), pp.569–74.

Zhang, J. et al., 2003. Identification of the haematopoietic stem cell niche and control of the niche size. *Nature*, 425(6960), pp.836–41.

Zhang, P. et al., 2004. Enhancement of hematopoietic stem cell repopulating capacity and self-renewal in the absence of the transcription factor C/EBP alpha. *Immunity*, 21(6), pp.853–63.

Zhang, P. et al., 2015. G protein-coupled receptor 183 facilitates endothelial-to-hematopoietic transition via Notch1 inhibition. *Cell Research*, 25(10), pp.1093–1107.

Zhang, P. et al., 1999. Negative cross-talk between hematopoietic regulators: GATA proteins repress PU.1. *Proceedings of the National Academy of Sciences of the United States of America*, 96(15), pp.8705–10.

Zhen, F. et al., 2013. Hemogenic endothelium specification and hematopoietic stem cell maintenance employ distinct Scl isoforms. *Development (Cambridge, England)*, 140(19), pp.3977–85.

Zheng, B. et al., 2000. Engineering mouse chromosomes with Cre-loxP: range, efficiency, and somatic applications. *Molecular and cellular biology*, 20(2), pp.648–55.

Zou, Y.R. et al., 1998. Function of the chemokine receptor CXCR4 in haematopoiesis and in cerebellar development. *Nature*, 393(6685), pp.595–9.

Zuber, J. et al., 2009a. Mouse models of human AML accurately predict chemotherapy response. *Genes & development*, 23(7), pp.877–89.

Zuber, J. et al., 2009b. Mouse models of human AML accurately predict chemotherapy response. *Genes & development*, 23(7), pp.877–89.

ANNEX: CV

Roshani Sinha

EDUCATION:

2012–Present

Pursuing PhD in Biomedicine at the University of Pompeu Fabra, and pursuing research on the "**Understanding the development of MLL-rearranged Leukemias:** *Developing disease models*" at Institut Hospital del Mar d'Investigacions Mèdiques in the lab of Cancer and Stem Cell Research under the guidance of my PhD supervisors Dr. Anna Bigas Salvans and Dr. Cristina Porcheri.

I participated in poster presentation at the 45th annual scientific meeting of International Society for Experimental hematology conducted in August 2016 where I presented results of my doctoral research (Sinha et al. 2016)

I have also worked on other projects apart from my doctoral research topic which is the post-doctoral research of Dr. Cristina Porcheri in the lab of Cancer and Stem Cell Research at Institut Hospital del Mar d'Investigacions Mèdiques. Dr. Porcheri presented a poster on her research entitled "Visualizing the hematopoietic emergence in the mouse embryo" at the 45th annual scientific meeting of International Society for Experimental hematology conducted in August 2016 (Porcheri et al. 2016).

This project is directed towards studying the influence of the niche on hematopoitic stem cells (HSCs) emergence. Dr.Porcheri has performed advanced imaging techniques to visualize the 3D-organization of hemogenic clusters and their maturation over time to identify initial events of hemogenesis. We also observed occasional cell division within the cluster. Using classical proliferation markers such as Ki67 and BrdU pulses, we could conclude that all cellular components of the cluster are actively cycling even though mitosis remains an elusive event involving a rare cohort of cells. In this project my contribution has been in performing flow cytometry analysis to study kinetics of endothelilal and hematopoietic populations by detecting proliferation markers such as Ki67 and BrdU within the intra-aortic clusters in a mouse embryo at E10.5 stage (embryonic age in days post-coitus).

Nov – Dec 2012

Successfully completed Level C (Researcher's level) of: **"Curso de formación de personal investigador usuario de animales de experimentación curso 2012-2013"** at the University of Barcelona, Faculty of Medicine in Barcelona, Spain

February 2012

Graduated Master's in Cancer Biology at Kingston University, London, UK

2010 –2011

Completed MSc Cancer biology, First class with commendation from Kingston University, Surrey, London, UK

2006 – 2010

Bachelor of Technology (B. Tech), Biotechnology from Jawaharlal Nehru Technological University, Hyderabad, India
I completed my undergraduate degree with Distinction (78%) and Held 2nd rank in College and 11th rank in State of Andhra Pradesh, India

2004 – 2006

Completed high school with Distinction (75%)
Andhra Pradesh Board Senior School Certificate Examination - 2006 from Narayana Junior college, Hyderabad, India

2003 - 2004

Completed All India Secondary School Examination (AISSE) from Kendriya Vidyalaya Kanchanbagh, Hyderabad with distinction (84.3%)

AWARDS

- Awarded the FI-AGAUR Fellowship from 2013 – 2016 by Generalitat de Catalunya for pursuing my doctoral research on the topic "Understanding the development of MLL-rearranged leukemias: *Developing disease models*" at University of Pompeu Fabra and IMIM-Hospital del Mar in the institute of PRBB (Barcelona Biomedical Research Park).

- Awarded First Prize for "The Researchers Award" as the most promising researcher in the Faculty of Science 2010-2011 for my Master's Thesis at Kingston University entitled "Assessing changes in expression of pancreatic cancer stem cell markers CD24, CD133 & intracellular proteins involved in Notch and Hedgehog signalling pathways"

- Awarded Silver medal and certificate for 2nd position in the state of Andhra Pradesh in my 3rd year of B.Tech in Biotechnology by Jawaharlal Nehru Technological University.

PUBLICATIONS AND PRESENTATIONS

- Participated in poster presentations at the 45th Annual Scientific Meeting of International Society for Experimental Hematology conference held in San Diego in august 2016.

    - 1st author in: Sinha, R. et al., 2016. Understanding the development of MLL rearranged leukemias. *Experimental Hematology*, 44(9), p.S99.

    - 2nd author in: Porcheri, C. et al., 2016. Visualizing the hematopoietic emergence in the mouse embryo. *Experimental Hematology*, 44(9), p.S96.

- Presented a poster on Micro-propagation (Plant Tissue culture) from rice seeds at the Annual College Technical Fest in 2009 during my undergraduate course at JNTU-Hyderabad, India. Embryos were grown after sterilization of seeds, incubation overnight. Grown embryos were cut using scalpel and inoculated in laminar air flow in MS medium, incubated in highly sterile area for about 5 days until callus development became visible.

SKILLS AND TECHNIQUES

In-vivo based techniques:

Competent in working with mice and designing experiments independently and skilled in performing:

- Intravenous and retro-orbital injections for performing transplantations in mice
- Intraperitoneal injections in mice: Treatments with drugs or compounds for Cre-inductions in-vivo
- Blood extractions from: Tail vein, retro-orbital vein
- Anesthetizing mice (using isoflurane)
- Dissection: Retrieving organs, embryos and embryonic tissues

In-vitro based techniques:

Culture-based techniques:

- Cell culture and plating
- Clonogenic assay
- Cre-inductions
- AGM explant cultures
- PEEI Transfections and Viral infections
- Treatment with drugs

Molecular Biology Techniques:

- RNA and DNA isolation
- DNA sequencing
- EMSA
- Sulforhodamide B assay
- cDNA synthesis
- QRT-PCR
- Cloning
- Retrovirus and Lentivirus production
- Luciferase assay
- Embedding in paraffin
- Embedding in OCT
- Cutting organs sections in microtome or criostat
- Light microscopy
- Fluorescent microscopy
- DNA extraction, purification

Protein Biochemistry Techniques:

- Flow cytometry, cell sorting
- Protein gel electrophoresis
- Western blotting
- Immunofluorescence

Biochemical engineering techniques:

- Ultrafiltration
- Reverse osmosis
- Microfiltration
- Preparing ultrafiltration membrane

Bioinformatics:

- GenBank searching: BLAST, FASTA
- Multiple sequence alignments
- Primer3 software
- Rasmol software

Computer Skills:

Softwares: Flowjo, Graphpad prism, Analysis of QRT-PCR data

AFFILIATIONS

- IMIM - Institut Hospital del Mar d'Investigacions Mèdiques at PRBB (Parc de Recerca Biomèdica de Barcelona)
- University of Pompeu Fabra
- Kingston University, London UK
- Jawaharlal Nehru Technological University, JNTU: Sri Indu College of Engineering and Technology
- Kamineni Hospitals
- Indian Institute of Chemical Technology (IICT)
- CMR College of Engineering; Sri Nidhi COET; TKR College of Engineering & Tech.